

**INVESTIGATING THE STABILITY OF SUPEROXIDE
ION GENERATED IN IONIC LIQUIDS AND THE
CONVERSION OF SULFUR COMPOUNDS**

MUNA HASSAN AHMED IBRAHIM

**DISSERTATION SUBMITTED IN FULFILMENT OF THE
REQUIREMENTS FOR THE DEGREE OF MASTER OF
ENGINEERING SCIENCE**

**FACULTY OF ENGINEERING
UNIVERSITY OF MALAYA
KUALA LUMPUR**

2016

UNIVERSITY OF MALAYA
ORIGINAL LITERARY WORK DECLARATION

Name of Candidate: Muna Hassan Ahmed Ibrahim

Registration/Matric No.: KGA130009

Name of Degree: Master of Engineering Science

Title of Project Paper/Research Report/Dissertation/Thesis (“this Work”):

**INVESTIGATING THE STABILITY OF SUPEROXIDE ION GENERATED IN
IONIC LIQUIDS AND THE CONVERSION OF SULFUR COMPOUNDS**

Field of Study: Reaction Engineering (Chemical Process)

I do solemnly and sincerely declare that:

- (1) I am the sole author/writer of this Work;
- (2) This Work is original;
- (3) Any use of any work in which copyright exists was done by way of fair dealing and for permitted purposes and any excerpt or extract from, or reference to or reproduction of any copyright work has been disclosed expressly and sufficiently and the title of the Work and its authorship have been acknowledged in this Work;
- (4) I do not have any actual knowledge nor ought I reasonably to know that the making of this work constitutes an infringement of any copyright work;
- (5) I hereby assign all and every rights in the copyright to this Work to the University of Malaya (“UM”), who henceforth shall be owner of the copyright in this Work and that any reproduction or use in any form or by any means whatsoever is prohibited without the written consent of UM having been first had and obtained;
- (6) I am fully aware that if in the course of making this Work I have infringed any copyright whether intentionally or otherwise, I may be subject to legal action or any other action as may be determined by UM.

Candidate’s Signature

Date:

Subscribed and solemnly declared before,

Witness’s Signature

Date:

Name:

Designation:

**University of Malaya,
Kuala Lumpur 50603,
Malaysia**

ABSTRACT

Superoxide ion ($O_2^{\bullet-}$) is a reactive oxygen species which plays a primary role in numerous applications. This radical anion has not received much interest for industrial use due to its reactivity with most solvents. In the last decade, $O_2^{\bullet-}$ was found to be stable in ionic liquids (ILs), which have many benefits over conventional aprotic solvents. Nevertheless, the stability of $O_2^{\bullet-}$ with ILs has not been well studied in the long term which is essential for industrial applications.

In the present work, $O_2^{\bullet-}$ stability and kinetics were examined with various ILs based on morpholinium, ammonium, imidazolium, piperidinium, pyrrolidinium and sulfonium cations, paired with anions such as bis(trifluoromethylsulfonyl)imide [TFSI], octylsulfate, tetracyanoborate and tris(pentafluoroethyl)trifluorophosphate. Stable ILs were used as media for the reaction of $O_2^{\bullet-}$ with sulfur compounds. The physical properties of some stable ILs were determined as another key factor for their industrial use as media for $O_2^{\bullet-}$ generation.

Cyclic voltammetry (CV) was used to electrochemically generate $O_2^{\bullet-}$ and to investigate the ion's short term stability in ILs; the observations were successful generation of $O_2^{\bullet-}$ and short term stability of $O_2^{\bullet-}$ in the ILs. However, the small oxidation peak obtained for triethylsulfoniumbis(trifluoromethylsulfonyl)imide at 9 mV/s suggested $O_2^{\bullet-}$ might be unstable in this IL. The electrochemical generation of $O_2^{\bullet-}$ in the studied ILs was a quasi-reversible process.

Subsequently, ultraviolet-visible spectrophotometry was employed to investigate the long term stability of $O_2^{\bullet-}$ and to study the kinetics of $O_2^{\bullet-}$ reactions. The rate constant of the reaction of $O_2^{\bullet-}$ generated in dimethyl sulfoxide containing ILs was calculated based on pseudo 1st order (k_1) and pseudo 2nd order (k_2). The value of k_1 ranged from 7.049×10^{-6} to $2.645 \times 10^{-3} \text{ s}^{-1}$ while k_2 ranged from 4.732×10^{-3} to $3.547 \text{ M}^{-1} \text{ s}^{-1}$. The generated $O_2^{\bullet-}$ stability was found to be dominated by the type of cation in the order

morpholinium>ammonium>piperidinium≈pyrrolidinium>>imidazolium>>sulfonium.

The $O_2^{\bullet-}$ was unstable in triethylsulfoniumbis(trifluoromethylsulfonyl)imide, 1-butyl-3-methyl-imidazoliumoctylsulfate and 1-butyl-3-methylimidazoliumhexafluorophosphate.

Chemically generated $O_2^{\bullet-}$ in 1-butyl-1-methylpyrrolidiniumbis(trifluoromethylsulfonyl)imide, N-methoxyethyl-N-methylmorpholiniumbis(trifluoromethylsulfonyl)imide, 1-(2-methoxyethyl)-1-methylpiperidiniumtris(pentafluoroethyl)trifluorophosphate, 4-(2-methoxyethyl)-4-methylmorpholiniumtris(pentafluoroethyl)trifluorophosphate and ethyl-dimethyl-propylammoniumbis(trifluoromethylsulfonyl)imide was utilized for the conversion of two types of sulfur compounds, thiophene (TH) and 2-methylthiophene (2-MTH). The conversion percentage and formation of by-products were analyzed using both HPLC and GC/MS. The conversion percentage ranged from 35 to 99% for TH and from 20 to 96% for 2-MTH. A mechanism was proposed for this conversion. The products of the conversion were identified as H_2O , CO_2 , and SO_3 . Furthermore, the effect of temperature on this reaction was studied. The ILs did not only behave as media for the generation of $O_2^{\bullet-}$ but also possessed catalytic activity to accelerate the reaction rate between $O_2^{\bullet-}$ and substrates.

The physical properties, namely density, viscosity, conductivity and surface tension of five stable ILs containing [TFSI] anion paired with 1-(2-methoxyethyl)-1-methylpiperidinium, 1-(2-methoxyethyl)-1-methylpyrrolidinium, N-methoxyethyl-N-methylmorpholinium, N-ethyl-N,N-dimethyl-2-methoxyethylammonium and ethyl-dimethyl-propylammonium respectively were determined between 25 to 80 °C. The ILs followed Arrhenius behavior for conductivity and viscosity while a linear trend was observed for surface tension and density.

ABSTRAK

Ion superoxide ($O_2^{\bullet-}$) adalah spesies oksigen reaktif yang memainkan peranan utama dalam pelbagai aplikasi. Anion radikal ini tidak mendapat banyak perhatian untuk kegunaan industri disebabkan kereaktifannya dengan kebanyakan pelarut. Pada dekad yang lalu, $O_2^{\bullet-}$ didapati stabil dalam cecair ionik (ILs), yang mempunyai banyak kelebihan berbanding pelarut-pelarut aprotic konvensional. Walau bagaimanapun, kestabilan $O_2^{\bullet-}$ dengan ILs tidak dikaji dengan baik dalam jangka masa panjang, sedangkan ianya penting untuk aplikasi dalam industri. Dalam kajian ini, kestabilan dan kinetik $O_2^{\bullet-}$ telah diuji dengan pelbagai ILs yang berasaskan kation morpholinium, ammonium, imidazolium, piperidinium, pyrrolidinium dan sulfonium, serta berpasangan dengan anion seperti bis (trifluoromethylsulfonyl) imide [TFSI], octyl sulfate, tetracyanoborate dan tris (pentafluoroethyl)trifluorophosphate. ILs yang stabil telah digunakan sebagai media untuk reaksi antara $O_2^{\bullet-}$ dengan sebatian sulfur. Sifat-sifat fizikal ILs yang stabil juga telah ditentukan, di mana ianya merupakan faktor utama untuk proses di peringkat industri. Voltametri berkitar (CV) telah digunakan untuk menghasilkan $O_2^{\bullet-}$ secara elektrokimia dan menyiasat kestabilan jangka pendek ion ini dalam ILs; penghasilan $O_2^{\bullet-}$ didapati berjaya dan ion ini juga didapati stabil dalam ILs untuk jangka pendek. Walau bagaimanapun, puncak pengoksidaan kecil telah diperolehi untuk triethylsulfoniumbis(trifluoromethylsulfonyl)imide pada 9 mV/s, dan ini mencadangkan bahawa $O_2^{\bullet-}$ mungkin tidak stabil di dalam IL ini. Penghasilan $O_2^{\bullet-}$ secara elektrokimia adalah merupakan suatu proses yang hampir boleh-balik (*quasi-reversible*). Seterusnya, spektrofotometri nyata ultra-ungu telah digunakan untuk menyiasat $O_2^{\bullet-}$ dari segi kestabilan jangka panjang dan tindak balas kinetik. Pemalar untuk kadar tindak balas bagi $O_2^{\bullet-}$ terhasil dalam dimethyl sulfoksida yang mengandungi IL telah dikira berdasarkan pseudo pertama (k_1) dan pseudo kedua (k_2). Nilai k_1 adalah di antara 7.049×10^{-6} hingga $2.645 \times 10^{-3} \text{ s}^{-1}$, sementara nilai k_2 pula di

antara 4.732×10^{-3} hingga $3.547 \text{ M}^{-1} \text{ s}^{-1}$. Didapati kestabilan $\text{O}_2^{\bullet-}$ yang dihasilkan ini didominasi oleh jenis kation pada urutan morpholinium > ammonium > piperidinium \approx pyrrolidinium \gg imidazolium \gg sulfonium. $\text{O}_2^{\bullet-}$ adalah tidak stabil di dalam triethylsulfoniumbis(trifluoromethylsulfonyl)imide, 1-butyl-3-methylimidazoliumoctylsulfate dan 1-butyl-3-methylimidazoliumhexafluorophosphate. $\text{O}_2^{\bullet-}$ yang terhasil secara kimia di dalam 1-butyl-1-methylpyrrolidiniumbis(trifluoromethylsulfonyl)imide, N-methoxyethyl-N-methylmorpholiniumbis(trifluoromethylsulfonyl)imide, 1-(2-methoxyethyl)-1-methylpiperidiniumtris(pentafluoroethyl)trifluorophosphate, 4-(2-methoxyethyl)-4-methylmorpholiniumtris(pentafluoroethyl)trifluorophosphate dan ethyl-dimethyl-propylammoniumbis(trifluoromethylsulfonyl)imide telah digunakan untuk penukaran dua jenis sebatian sulfur, iaitu thiophene (TH) and 2-methylthiophene (2-MTH). Peratus penukaran dan pembentukan produk sampingan telah dianalisis melalui HPLC dan GC/MS. Peratus penukaran adalah antara 35 hingga 99% untuk TH, dan antara 20 hingga 96% untuk 2-MTH. Satu mekanisme telah dicadangkan untuk penukaran ini. Hasil-hasil penukaran ini telah dikenalpasti iaitu H_2O , CO_2 , and SO_3 . Tambahan pula, kesan suhu terhadap tindak balas ini juga telah dikaji. ILs bukan sahaja bertindak sebagai media untuk penghasilan $\text{O}_2^{\bullet-}$, malahan juga mempunyai aktiviti pemangkinan untuk mempercepatkan kadar tindak balas antara $\text{O}_2^{\bullet-}$ dan substrat. Ciri-ciri fizikal, iaitu ketumpatan, kelikatan, kekonduksian dan ketegangan permukaan pada suhu 25 hingga 80 °C telah ditentukan bagi lima ILs yang mengandungi [TFSI] anion bersama dengan 1-(2-methoxyethyl)-1-methylpiperidinium, 1-(2-methoxyethyl)-1-methylpyrrolidinium, N-methoxyethyl-N-methylmorpholinium, N-ethyl-N,N-dimethyl-2-methoxyethylammonium dan ethyl-dimethyl-propylammonium. ILs didapati mengikut kelakuan Arrhenius untuk kekonduksian dan kelikatan, sementara trend yang linear diperhatikan untuk ketegangan permukaan dan kepadatan.

ACKNOWLEDGMENTS

First, I would like to extend my sincere appreciation to my main supervisor, Prof. Dr. Mohd Ali bin Hashim, Head of the University of Malaya Centre for Ionic Liquids (UMCiL). I am grateful to Prof. Ali for allowing me the privilege to join the UMCiL group, and for his kindness, valuable advice and indispensable support during my time as his Research Assistant and student.

I would like to express my deepest gratitude to my co-supervisor, Dr. Maan Hayyan, for guiding me as his student. I am grateful for his continuous generous support and patience despite his hectic schedule and growing responsibilities.

I am immeasurably grateful to Dr. Adeb Hayyan for his pivotal role in the completion of this work. I have greatly benefited from his invaluable guidance and talent for organizing ideas and simplifying complicated practical difficulties. I am also thankful to him for his encouragement, as well as for patiently reading my work and providing valuable feedback and advice. My profound appreciation also goes to Prof. Dr. Mohamed Elwathig Saeed Mirghani.

I would also like to thank my fellow members of UMCiL who provided useful assistance, training and advice. I further extend my appreciation to other UM staff and anyone I have not named who has supported this work. I also express my thanks to University of Malaya HIR-MOHE (D000003-16001).

Most importantly, none of this would have been possible without the support of my family. I am particularly grateful to my parents, for their unwavering encouragement, prayers and advice throughout my ups and downs in completing this work.

TABLE OF CONTENTS

Abstract.....	iii
Abstrak.....	v
Acknowledgments.....	vii
Table of Contents.....	viii
List of Figures.....	xi
List of Tables.....	xi
List of Symbols and Abbreviations.....	xv
List of Appendices.....	xviii
CHAPTER 1: INTRODUCTION.....	1
1.1 Overview.....	1
1.2 Problem Statement and Significance of Study.....	3
1.3 Research Objectives.....	4
1.4 Research Methodology.....	5
1.5 Outline of the Thesis.....	5
CHAPTER 2: LITERATURE REVIEW.....	6
2.1 Desulfurization of fuels.....	6
2.1.1 Hydrodesulfurization (HDS).....	7
2.1.2 Biodesulfurization (BDS).....	10
2.1.3 Adsorption.....	12
2.1.4 Extraction.....	13
2.1.5 Oxidative Desulfurization (ODS).....	14
2.2 Ionic Liquids (ILs).....	16
2.2.1 Structure of ILs.....	18
2.2.1.1 Cations.....	18
2.2.1.2 Anions.....	19
2.2.2 Effect of structure on physiochemical properties of ILs.....	20
2.2.3 Toxicity of ILs and Impact on the Environment.....	21
2.2.4 Impurities.....	22
2.2.5 ILs Applications.....	22
2.2.6 Desulfurization of Fuels using ILs.....	23

2.2.7	Desulfurization of Fuels using ILs by ODS.....	32
2.3	Superoxide Ion ($O_2^{\bullet-}$).....	35
2.3.1	Superoxide Salts.....	35
2.3.2	Superoxide in Aprotic Solvents	36
2.4	Generation of $O_2^{\bullet-}$ in ILs	38
2.4.1	Stability of $O_2^{\bullet-}$ in ILs	38
2.4.1.1	Short Term Stability of $O_2^{\bullet-}$ in ILs	38
2.4.1.2	Long Term Stability of $O_2^{\bullet-}$ in ILs	43
2.4.2	Destruction of Chlorinated Hydrocarbons Using $O_2^{\bullet-}$	52
2.4.3	Conversion of Sulfur Compounds Using $O_2^{\bullet-}$	53
CHAPTER 3: EXPERIMENTAL METHODOLOGY.....		55
3.1	Instruments, Accessories, Gases, Chemicals and Ionic Liquids Used.....	55
3.1.1	Instruments.....	55
3.1.2	Equipment	55
3.1.3	Accessories.....	55
3.1.3.1	Electrodes	55
3.1.3.2	Polishing Kit (BASi PK-4).....	56
3.1.4	Gases	56
3.1.5	Chemicals.....	56
3.1.6	Sulfur Compounds	56
3.1.7	Ionic Liquids	57
3.2	Experimental Procedures	62
3.2.1	Preparation for Experiments	62
3.2.1.1	Drying of ILs.....	62
3.2.1.2	Acidity of ILs	62
3.2.2	Electrochemical Generation of Superoxide Ion	62
3.2.2.1	Cleansing of the Electrochemical Cell.....	62
3.2.2.2	Polishing of Electrodes	62
3.2.2.3	Electrochemical Procedure.....	63
3.2.3	Chemical Generation of $O_2^{\bullet-}$	63
3.2.3.1	Calibration of $O_2^{\bullet-}$ in DMSO Using UV-vis Spectrophotometer	64
3.2.4	Conversion of Sulfur Compound	64
3.2.5	Physical Properties	65
3.2.6	GC/MS Analysis	65

3.2.7 Solubilities of Sulfur Compounds in ILs	66
CHAPTER 4: RESULTS AND DISCUSSION	67
4.1 Superoxide Ion Generation	67
4.1.1 Electrochemical Generation of $O_2^{\bullet-}$	67
4.1.1.1 Cyclic Voltammetry (Short Term Stability Test).....	67
4.1.2 Chemical Generation of $O_2^{\bullet-}$	85
4.1.2.1 Long Term Stability of $O_2^{\bullet-}$	85
4.1.2.2 Kinetics Study	88
4.2 Conversion of Sulfur compounds by $O_2^{\bullet-}$	98
4.2.1.1 Conversion of Thiophene by $O_2^{\bullet-}$	98
4.2.1.2 Conversion of 2-Methylthiophene by $O_2^{\bullet-}$	101
4.2.1.3 Effect of Temperature on Conversion of Thiophene and 2- Methylthiophene by $O_2^{\bullet-}$	102
4.2.1.4 Mechanism of Reaction.....	104
4.2.2 Solubilities of Sulfur Compounds in ILs	107
4.3 Physical Properties of ILs	108
4.3.1.1 Density	108
4.3.1.2 Viscosity.....	111
4.3.1.3 Conductivity.....	114
4.3.1.4 Surface Tension.....	116
CHAPTER 5: CONCLUSIONS AND RECOMMENDATIONS.....	119
5.1 Conclusions	119
5.2 Recommendations	123
References.....	124
List of Publications and Papers Presented	150
Appendices.....	153
APPENDIX A	153
APPENDIX B	161
APPENDIX C	167

LIST OF FIGURES

Figure 2.1: Refining flowsheet of a typical oil refinery, adapted from Wauquier (2001).	7
Figure 2.2: The structure of CoMo catalyst in hydrodesulfurization (Mochida & Choi, 2006).....	8
Figure 2.3: Extractive desulfurization (EDS) using ionic liquids	25
Figure 2.4: The first reported voltammetry of dioxygen in IL, a) Cyclic staircase voltammogram and b) Normal pulse voltammogram, a single cathodic peak was observed (Carter et al., 1991).	39
Figure 2.5: The first report of stable $O_2^{\bullet-}$ in ILs. CVs at 37°C of an IL in which $O_2^{\bullet-}$ is stable (3) [BMIm][PF ₆] and unstable (1) 1,2-dimethyl-3-n-butylimidazolium hexafluorophosphate. (2) and (4) are the background voltammograms of the ILs with Nitrogen The working electrode was glassy carbon and the reference electrode was Ag/AgCl(AlNashef et al., 2001).	40
Figure 2.6: Long term stability of [BMIm][PF ₆] measured by UV-vis, maximum absorbance is proportional to $O_2^{\bullet-}$ concentration (AlNashef et al., 2001).....	44
Figure 4.1: CVs in [EDMPAm][TFSI] after sparging with oxygen and nitrogen (background) at 25 °C for scan rates of 9 and 100 mV/s.	67
Figure 4.2: Cyclic voltammetry of O ₂ in [EDMPAm][TFSI] at scan rate of 100 mV/s.	71
Figure 4.3: CVs in [BMIm][OctSO ₄] after sparging with oxygen and nitrogen (background) at 25 °C for scan rates of 9 and 100 mV/s.	76
Figure 4.4: CVs in [EDMOEAm][TPTP] (0 to -1.2 V), after sparging with oxygen and nitrogen (background) at 25 °C for scan rates of 9 and 100 mV/s.	79
Figure 4.5: CVs in [EDMOEAm][TPTP] (0.2 to -1.7V), after sparging with oxygen and nitrogen (background) at 25 °C for scan rates of 9 and 100 mV/s.	80
Figure 4.6: CVs of a Au electrode in in trimethyl-n-hexylammonium bis(trifluoromethylsulfonyl)imide [TMHA][TFSI] before and after saturation with O ₂ at 25 °C. Scan rate 50 mV/s (IUPAC voltammogram convention) (Katayama et al., 2004).....	82
Figure 4.7: CVs in [BMPyrr][TFSI], after sparging with oxygen and nitrogen (background) at 25 °C for scan rates of 9 and 100 mV/s.	83

Figure 4.8: CVs of O ₂ in [BMPyrr][TFSI] at 25°C using scan rate of 50 mV/s. a) Au electrode (Katayama et al., 2004) and b) Pt electrode (Katayama et al., 2005).....	83
Figure 4.9: CVs in [S222][TFSI], after sparging with oxygen and nitrogen (background) at 25 °C for scan rates of 9 and 100 mV/s.	84
Figure 4.10: The change of O ₂ ^{•-} absorbance peak with time for [BMPyrr][TFSI], [N112,1O2][TFSI] and [MOPMPip][TFSI] in DMSO.	88
Figure 4.11: The change of O ₂ ^{•-} ln(concentration) and 1/ concentration with time for [MOEMPyrr][TPTP] in DMSO.	89
Figure 4.12: The change of O ₂ ^{•-} absorbance peak with time for [S222][TFSI] in DMSO.	97
Figure 4.13: HPLC chromatograms of TH in [EDMPAmm][TFSI] (a) before KO ₂ addition (b) after KO ₂ addition.....	99
Figure 4.14: HPLC chromatograms of TH in [MOEMMMor][TFSI] (a) before KO ₂ addition (b) after KO ₂ addition.	108
Figure 4.15: HPLC chromatograms of 2-MTH in [MOEMMMor][TFSI] (a) before KO ₂ addition (b) after KO ₂ addition.....	103
Figure 4.16: Densities of ILs as a function of temperature.....	110
Figure 4.17: Viscosities of ILs as a function of temperature	113
Figure 4.18: ln (η) of ILs as a function of (1/T) temperature.....	113
Figure 4.19: Conductivities of ILs as a function of temperature	115
Figure 4.20: ln (γ) of ILs as a function of (1/T) temperature.....	116
Figure 4.21: Surface tensions of ILs as a function of temperature	118

LIST OF TABLES

Table 2.1: Summary of advantages and disadvantages of hydrodesulfurization technology (HDS)	9
Table 2.2: Summary of advantages and disadvantages of biodesulfurization technology (BDS).....	11
Table 2.3: Summary of advantages and disadvantages of desulfurization by adsorption	13
Table 2.4: Summary of advantages and disadvantages of desulfurization by extraction.....	14
Table 2.5: Summary of advantages and disadvantages of oxidative desulfurization (ODS)	16
Table 2.6: ILs that have been used for extractive desulfurization (EDS) of sulfur compounds.	25
Table 2.7: $O_2/O_2^{\bullet-}$ formal potentials for different electrode materials (Song & Zhang, 2008).....	41
Table 2.8: $O_2/O_2^{\bullet-}$ redox potential in varying solvents (1 atm O_2) (Song & Zhang, 2008).....	41
Table 2.9: Summary of studied ILs for $O_2^{\bullet-}$ generation.....	45
Table 2.10: Destruction of chlorinated hydrocarbons using $O_2^{\bullet-}$ generated in ionic liquids.	52
Table 3.1: Sulfur compounds used in this work.....	57
Table 3.2: Ionic liquids specifications.	58
Table 3.3: HPLC specifications and analytical conditions.	65
Table 3.4: GC/MS specifications and analytical conditions.	66
Table 4.1: List of ILs in which CV was used to electrochemically generate $O_2^{\bullet-}$ from reduction of O_2	68
Table 4.2: CVs of O_2 in ILs studied in this work (Excluding [BMIm][OctSO ₄], [EDMOEAm][TPTP]and [MOEMPip][TFSI])	74
Table 4.3: The CV of 1-butyl-3-methylimidazolium ILs with different anions.	77
Table 4.4: Comparison of redox peaks for ILs with 1-butyl-3-methylimidazolium cation and different anions. Working electrode, GC, reference electrode Ag/AgCl.....	78
Table 4.5: Examined ILs as media for the long term stability of $O_2^{\bullet-}$	86

Table 4.6: Rate constant of $O_2^{\bullet-}$ in DMSO containing [MOEMPyrr][TPTP]	89
Table 4.7: Pseudo 2 nd order rate constants (k_2 in $M^{-1} s^{-1}$) for reaction of $O_2^{\bullet-}$ with ILs in DMSO, in order of decreasing stability of $O_2^{\bullet-}$	91
Table 4.8: Rate constant of $O_2^{\bullet-}$ in DMSO containing ammonium based ILs.....	93
Table 4.9: Rate constant of $O_2^{\bullet-}$ in DMSO containing pyrrolidinium based ILs.....	94
Table 4.10: Rate constant of $O_2^{\bullet-}$ in DMSO containing imidazolium based ILs.....	95
Table 4.11: Conversion of TH by $O_2^{\bullet-}$ at RT.....	99
Table 4.12: Experimental conditions comparison between Chan <i>et al.</i> (2008) and this study.	100
Table 4.13: Conversion of 2-MTH by $O_2^{\bullet-}$ at RT.....	102
Table 4.14: Conversion of TH and 2-MTH by $O_2^{\bullet-}$ at different temperatures.	103
Table 4.15: Solubilities of the sulfur compounds in ILs.....	107
Table 4.16: Calculated parameters for a and b of density of [TFSI]-based ILs using Eq 4.8.	110
Table 4.17: Calculated parameters for $-(E\eta/R)$ and η_0 of viscosity of [TFSI]-based ILs using 4.9.....	112
Table 4.18: Calculated parameters for $-(E\gamma/R)$ and γ_0 of conductivity of [TFSI]-based ILs using Eq 4.9	115
Table 4.19: Calculated parameters for a and b of surface tension [TFSI]-based ILs using Eq 4.11.....	118

LIST OF SYMBOLS AND ABBREVIATIONS

List of Symbols

[AMIm][BF ₄]	1- <i>n</i> -alkyl-3-methylimidazolium tetrafluoroborate
[BDMIm][TFSI]	1- <i>n</i> -butyl-2,3-dimethylimidazolium bis(trifluoromethylsulfonyl)imide
[BDMIm] ⁺ [BF ₄] ⁻	1- <i>n</i> -butyl-2,3-dimethylimidazolium Tetrafluoroborate
[BMIm][BF ₄]	1- <i>n</i> -butyl-3-methylimidazolium tetrafluoroborate
[BMIm][PF ₆]	1-butyl-3-methylimidazolium hexafluorophosphate
[BMIm] ⁺	1- <i>n</i> -butyl-3-methylimidazolium
[BMPyrr][TFSI]	1-butyl-1-methylpyrrolidinium bis(trifluoromethylsulfonyl) imide
[BMPyrr] ⁺	1-butyl-1-methylpyrrolidinium
[DCA] ⁻	Dicyanamide
[DMPIIm] ⁺	1,2-dimethyl-3-propylimidazolium
[EMIm][BF ₄]	1-ethyl-3-methylimidazolium tetrafluoroborate
[EMIm][TFSI]	1-ethyl-3-methylimidazolium bis[(trifluoromethyl)sulfonyl]imide
[FAP] ⁻	Trifluorotris (pentafluoroethyl) phosphate
[Im] ⁺	Imidazolium
[Mor] ⁺	Morpholinium
[N6222][TFSI]	triethyl- <i>n</i> -hexylammonium bis(trifluoromethylsulfonyl) imide
[N6222] ⁺	Triethyl- <i>n</i> -hexylammonium
[OctSO ₄] ⁻	Octylsulfate
[OMIm] ⁺	1- <i>n</i> -octyl-3-methyl imidazolium
[P14,666] ⁺	Tris(<i>n</i> -hexyl)tetradecylphosphonium
[P14,666][FAP]	tris(<i>n</i> -hexyl)tetradecylphosphonium trifluoro tris (pentafluoroethyl) phosphate
[PF ₆] ⁻	Hexafluorophosphate
[Pip] ⁺	Piperidinium
[PMIm][BF ₄]	1- <i>n</i> -propyl-3-methylimidazolium tetrafluoroborate
[Py] ⁺	Pyridinium
[Pyrr] ⁺	Pyrrolidinium
[S] ⁺	Sulfonium
[TFA] ⁻	Trifluoroacetate
[TfO] ⁻	Trifluoromethanesulfonate
[TFSI] ⁻	Bis(trifluoromethylsulfonyl)imide
[TMHAm] ⁺	Trimethyl- <i>n</i> -hexylammonium
[TPTP] ⁻	Tris (pentafluoroethyl)trifluorophosphate
AcN	Acetonitrile
BT	Benzothiophene
Brønsted acidic ionic liquid	BAIL
Ca(O ₂) ₂	Calcium superoxide
CsO ₂	Cesium superoxide
CV	Cyclic voltammetry
DBT	Dibenzothiophene
DEE	Diethyl ether

DMF	Dimethyl formamide
DMSO	Dimethyl sulfoxide
$E^{0'}$	Formal potential
ΔE_p	Peak potential separation (separation between the oxidative and reductive peaks)
E_{Pred}	Potential of the reduction peak
E_{Pox}	Potential of the oxidation peak
ESR	Electron spin resonance
EW	Electrochemical window
GC	Glassy carbon
GC/MS	Gas Chromatography-Mass Spectrophotometer
H_2O_2	Hydrogen peroxide
HDS	Hydrodesulfurization
HM	Hazardous materials
HMDE	Hanging mercury drop electrode
HO_2^{\bullet}	Hydroperoxyl radical
HPLC	High Performance Liquid Chromatography
ILs	Ionic liquids
j_p^a / j_p^c	ratio of anodic current density to cathodic one
k_1	Rate constant of pseudo-first-order
k_2	Rate constant of pseudo-second-order
KO_2	Potassium superoxide
L	Liquid
LSV	Linear sweep voltammetry
2-MTH	2-Methylthiophene
N	Number of electrons transferred
Na	Sodium
NaO_2	Sodium superoxide
O_2	Dioxygen
$O_2^{\bullet-}$	Superoxide ion
$O_2^{\bullet+}$	Dioxygen cation
O_2^1	Singlet oxygen
O_2^{2-}	Peroxide dianion
O_3	Ozone
ODS	Oxidative desulfurization
Pt	Platinum
Rb	Rubidium
RbO_2	Rubidium superoxide
ROS	Reactive oxygen species
SO_2	Sulfur dioxide
SOD	Superoxide dismutase
TH	Thiophene
UV-vis	Ultraviolet-visible spectrophotometry
UAOD	Ultrasound-assisted oxidative desulfurization
VOCs	Volatile organic compounds

Subscripts

P	Peak
a	Anodic

c	Cathodic
<i>oxdn</i>	Oxidation
<i>redn</i>	Reduction

Greek letters

γ	Conductivity
η	Viscosity
ρ	Density
σ	Surface tension

University of Malaya

LIST OF APPENDICES

APPENDIX A: Cyclic Voltammograms of $O_2^{\bullet-}$ in ILs	153
APPENDIX B: The Long Term Stability Experiments of $O_2^{\bullet-}$	161
APPENDIX C: Derivation of Equations Used to Obtain Pseudo 1 st Order and Pseudo 2 nd Order Models	167

University of Malaya

CHAPTER ONE

INTRODUCTION

1.1 Overview

The electroreduction of oxygen is an important reaction in numerous applications such as fuel cells, metal-air batteries and electrosynthesis. Recently, the unique solvents known as ionic liquids (ILs) have become increasingly popular for these applications (Barnes et al., 2008; Xiao et al., 2015; Zhao et al., 2010). ILs are salts which melt at 100 °C or below, usually composed of a combination of an organic cation with an organic or inorganic anion. Their highly desirable properties which have attracted the attention of researchers include wide electrochemical window, thermal stability and low volatility. There are 10^{18} ILs that can theoretically be synthesized (Holbrey & Seddon, 1999). Furthermore, ILs are highly tunable and can be designed for a specific task, and hence they can be considered as designer solvents. These solvents have been known since 1914 or earlier but it was only after the development of air and moisture stable ILs in the 1990's (Wilkes & Zaworotko, 1992) which led to the exponential growth of the literature on ILs. ILs have been used in a plethora of applications including as extractants, electrolytes, catalysts and lubricants.

Superoxide ($O_2^{\bullet-}$) is dioxygen (O_2) with an added electron. $O_2^{\bullet-}$ is both a radical and anion and has been known as far back as 1934 (Haber & Weiss, 1934). It is a highly reactive species and reacts with most solvents, including H_2O . However, it can be stable in some solvents such as aprotic solvents, including acetonitrile (AcN), dimethyl formamide (DMF) and dimethyl sulfoxide (DMSO). It can be generated by several methods including electrochemically by reduction of O_2 or chemically by dissolution of a superoxide salt, e.g. potassium superoxide (KO_2).

Several studies have reported the generation of $O_2^{\bullet-}$ in aprotic solvents and exploited its reactivity to react with desired compounds, e.g. sulfur compounds, chlorinated hydrocarbons, carbon dioxide, vitamin K₁ (Martin & Sawyer, 1972; Oae et al., 1981; Saito et al., 1979; Sawyer et al., 1985; Takata et al., 1979). However, aprotic solvents are not environmentally friendly as they exhibit high volatility, low boiling points and have negative ecological effects. In contrast, ILs have the potential to be a 'green' replacement for aprotic solvents, to generate $O_2^{\bullet-}$ (Hayyan, 2012). Carter *et al.* (1991) reported the first study of $O_2^{\bullet-}$ generation in IL medium, 1-ethyl-3-methylimidazolium chloride mixed with $AlCl_3$. However, the $O_2^{\bullet-}$ was unstable in this IL, most likely due to impurities in the IL. Ten years later, AlNashef *et al.* (2001) successfully generated $O_2^{\bullet-}$ in 1-butyl-3-methylimidazolium hexafluorophosphate [BMIm][PF₆]. Several other studies then explored the reduction of O_2 in ILs for interest in gas sensor, batteries, and to conduct electrochemical investigations (Barnes et al., 2008; Buzzeo et al., 2003, 2004b; Evans et al., 2004; Islam & Ohsaka, 2008a; Katayama et al., 2004). However, these studies only explored the stability of $O_2^{\bullet-}$ using cyclic voltammetry (CV), which lasts up to a few minutes. In order to apply $O_2^{\bullet-}$ in solvents for industrial use, its stability for a longer period should be confirmed and studied. Hence, the stability of $O_2^{\bullet-}$ was investigated in the long term using ultraviolet-visible spectrophotometry (UV-vis) to measure the absorbance of $O_2^{\bullet-}$, which is in turn related to its concentration (Islam et al., 2009).

Sulfur in fossil fuels such as gasoline, diesel and kerosene is one of the most crucial challenges in oil refinery. In fuels, sulfur is present in the form of organic sulfur compounds, e.g. sulfides, disulfides and thiophene (TH). Upon combustion of these sulfur compounds in fuels, SO_x compounds are released, which lead to acid rain, poison catalytic converters and cause respiratory problems. Therefore, regulatory bodies are imposing increasingly stringent regulations with regard to the maximum level of sulfur

in transportation fuels. The conventional method to remove sulfur compounds, hydrodesulfurization (HDS), involves the reaction of these compounds with H₂ gas at high pressures and temperatures with the use of expensive catalysts. This method also reduces the octane rating of gasoline and releases toxic hydrogen sulfide (H₂S) gas. To reduce the sulfur content further using HDS would require even more severe conditions than those currently employed which would result in an increase in capital and operating costs. Therefore, there is an intense research effort to find an alternative means of desulfurization. Many methods have been explored including using microorganisms, extraction, adsorption and oxidation (Gui et al., 2010; He et al., 2008; Lo et al., 2003; Srivastava, 2012).

O₂^{•-} generated in ILs has already been used in reactions to replace those reported using aprotic solvents in earlier studies, e.g. destruction of chlorinated hydrocarbons (Hayyan et al., 2012d; Hayyan et al., 2012e, 2012f). Although O₂^{•-} has not been widely applied to react with sulfur compounds, reactions between O₂^{•-} and organic sulfur compounds have been reported (Oae et al., 1981; Takata et al., 1979; Chan et al., 2008). For example, disulfides, thiosulfates and sodium thiolates can be oxidized by O₂^{•-} salts dissolved in aprotic solvents such as AcN, pyridine and benzene (Oae et al., 1981; Takata et al., 1979). Chan *et al.* (2008) have reported the use of O₂^{•-} generated in imidazolium based ILs to react with sulfur compounds. However, subsequent studies have shown that O₂^{•-} is unstable in ILs with imidazolium based cations (AlNashef et al., 2010; Hayyan et al., 2013b) which were used in this study.

1.2 Problem Statement and Significance of Study

O₂^{•-} has been shown to be stable in some ILs. This was on the basis of the short term stability using CV as the analysis technique. However, CV lasts only up to a few minutes and does not give insight into the long term stability of this species in the studied solvent. Therefore, it is essential to obtain the long term stability of O₂^{•-} in a

solvent if it is to be used as media for $O_2^{\bullet-}$ reactions in industry. Recently, UV-vis spectrophotometry has been used to determine the long term stability of $O_2^{\bullet-}$ in ILs. However, it was monitored for only 2 h, using 10 min intervals. In this work, the stability of $O_2^{\bullet-}$ with ILs has been investigated for up to 24 h continuously using 1 or 2 s intervals. This is the longest period of time that $O_2^{\bullet-}$ stability has been studied with ILs and the smallest time interval used.

Desulfurization of transportation fuels is a pressing challenge, the conventional desulfurization technique, HDS, is no longer sufficient to meet the increasingly stringent sulfur level limits required. Alternative desulfurization methods including extraction, ODS, BDS and adsorption have some limitations, including high sophistication, long reaction time, economic viability and degradation of fuel. Sulfur compounds have been successfully converted using $O_2^{\bullet-}$ generated in aprotic solvents. However, the disadvantages of aprotic solvents, e.g. high volatility, low boiling point, environmental impact have limited this method from being applied as a desulfurization method. The conversion of sulfur compounds using $O_2^{\bullet-}$ generated in IL, as opposed to hazardous aprotic media, has the potential to provide an alternative desulfurization method.

1.3 Research Objectives

The objectives of this research are:

1. To test the short-term and long-term stability of $O_2^{\bullet-}$ in selected ILs.
2. To study the kinetics of $O_2^{\bullet-}$ in selected ILs and possible reaction between $O_2^{\bullet-}$ and ILs.
3. To convert selected sulfur compounds using the generated $O_2^{\bullet-}$ in selected ILs.
4. To measure the physical properties of ILs used as successful media for $O_2^{\bullet-}$ generation and stability.

1.4 Research Methodology

The specific stages of the research methodology are as listed below:

1. Background CV of tested IL is obtained with N₂ sparge at scan rate 100 mV/s.
2. O₂^{•-} is generated electrochemically by reduction of O₂, sparged in tested IL, and measured using CV technique for scan rates of 9 and 100 mV/s.
3. Long term stability of O₂^{•-} is studied using UV-vis spectrophotometry.
4. Conversion of sulfur compound experiments are carried out using chemically generated O₂^{•-} from dissolution of KO₂ in IL.
5. Sulfur compound detection and analyses are conducted using HPLC and GC/MS.
6. Physical properties of some ILs are measured, i.e. density, viscosity, surface tension and conductivity.

1.5 Outline of the Thesis

This thesis comprises of five chapters, as follows:

Chapter 1 introduces O₂^{•-} and ILs, provides the problem statement, states the research objectives, and finally the research methodology.

Chapter 2 gives a background of ILs and O₂^{•-}, including generation methods of O₂^{•-}, its applications and previous works done in relation to the generation and applications of O₂^{•-}.

Chapter 3 discusses the detailed research methodology of O₂^{•-} generation, stability and its reactions with ILs as well as the method of conversion of sulfur compounds and the follow-up chemical analyses. Materials, chemicals, equipment and analytical instruments involved in the experiments are described in this chapter.

Chapter 4 provides the obtained results and discussions.

Chapter 5 provides conclusions and recommendations for further studies.

CHAPTER TWO

LITERATURE REVIEW

2.1 Desulfurization of fuels

The desulfurization of fuels has become an area of great interest to researchers in recent years (Abin-Fuentes et al., 2013; Alonso et al., 2007a; Bosmann et al., 2001; Zhao et al., 2008). This is due to increasingly stringent regulations imposed by regulatory agencies and a decrease in the quality of extracted petroleum due to the depletion of oil reserves. Sweet, i.e. low sulfur crude reservoirs which are most easily accessible have been depleted. The extraction of sour, i.e. high sulfur crudes has become necessary due to increasing demand (Leffler, 2008; Manning et al., 1995). The sulfur compounds that must be removed from fossil fuels can be found in crude oil or may be produced from other sulfur compounds during refining stages such as cracking, desulfurization or distillation (Wauquier, 1995). The sulfur level in crude oil varies with the location from which it is extracted. Sulfur is naturally found in crude oil (0.25-4%) in the form of free elemental sulfur or organosulfur compounds (Matar & Hatch, 2001). The crude oil is then distilled into different cuts (or fractions) according to varying boiling points of components; heavier cuts contain a greater percentage of sulfur. Different groups of sulfur compound are more likely to be found in different fractions (Kulkarni & Afonso, 2010). The conventional method, HDS, is no longer sufficient to meet the increasingly stringent regulations. Therefore, alternative desulfurization technologies are necessary for producing clean fuels. Alternative desulfurization technologies currently include biodesulfurization (BDS), adsorption, extractive desulfurization (EDS) and oxidative desulfurization (ODS) (Gui et al., 2010; He et al., 2008; Lo et al., 2003). These technologies may be used as a replacement for HDS or as complementary processes in addition to HDS.

2.1.1 Hydrodesulfurization (HDS)

HDS is the conventional desulfurization process in petroleum refineries. Typical western oil refineries have at least three HDS process units to process various different feeds; see Figure 2.1 (Robinson & Dolbear, 2006). HDS was first patented by Raymond Fleck and Paul Nahin of Union Oil in 1950 and continues to be the dominant method of desulfurization in refineries (Fleck, 1950; Robinson, 2006). The process involves reaction of sulfur compounds with H_2 to form hydrocarbons and H_2S gas (Scheme 2.1) which is removed by amine washing using the Claus process. The process conditions are a temperature of 300-400 °C and pressure of 20 to 130 atm. However, heavier feeds require more severe conditions. The most common catalysts used are $CoMo/\gamma Al_2O_3$ and $NiMo/\gamma Al_2O_3$ which are activated by sulfiding (Robinson & Dolbear, 2006). The structure of this catalyst is illustrated in Figure 2.1.

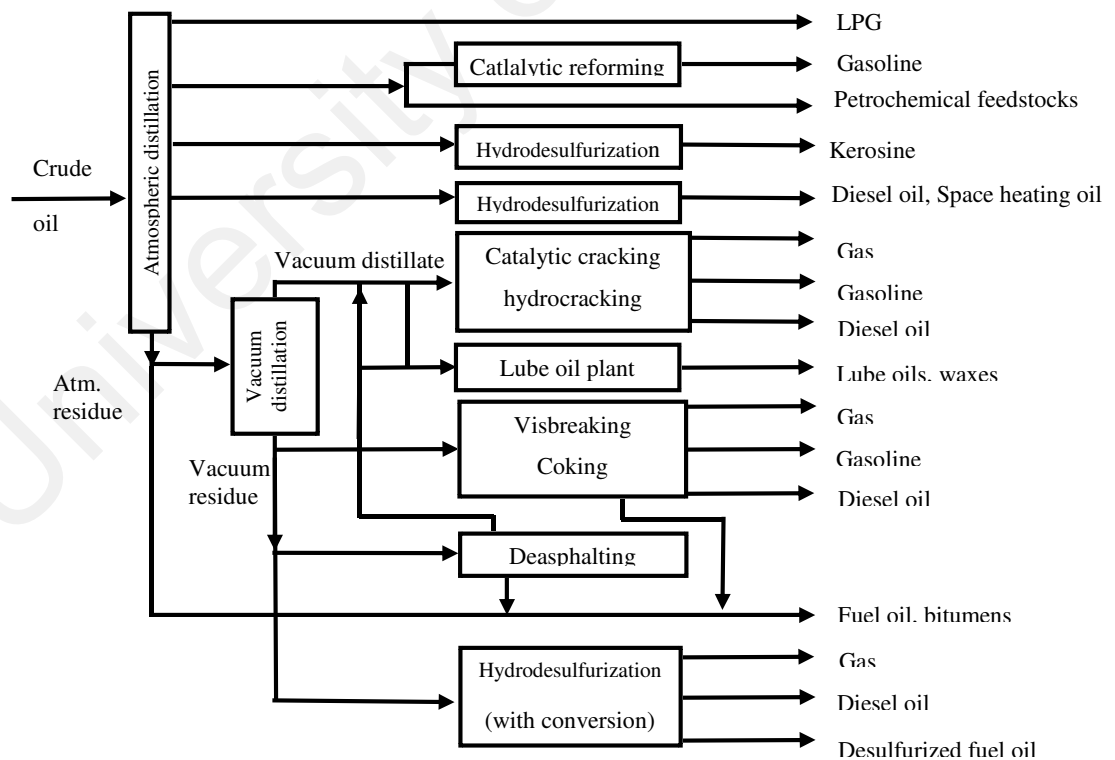
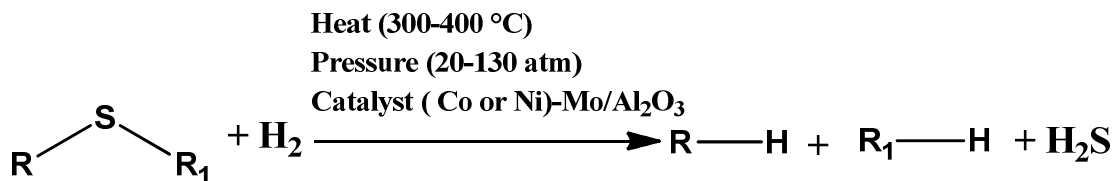


Figure 2.1: Refining flowsheet of a typical oil refinery, adapted from Wauquier (2001).



Scheme 2.1: The Conventional Desulfurization process used in refineries, hydrodesulfurization (HDS)

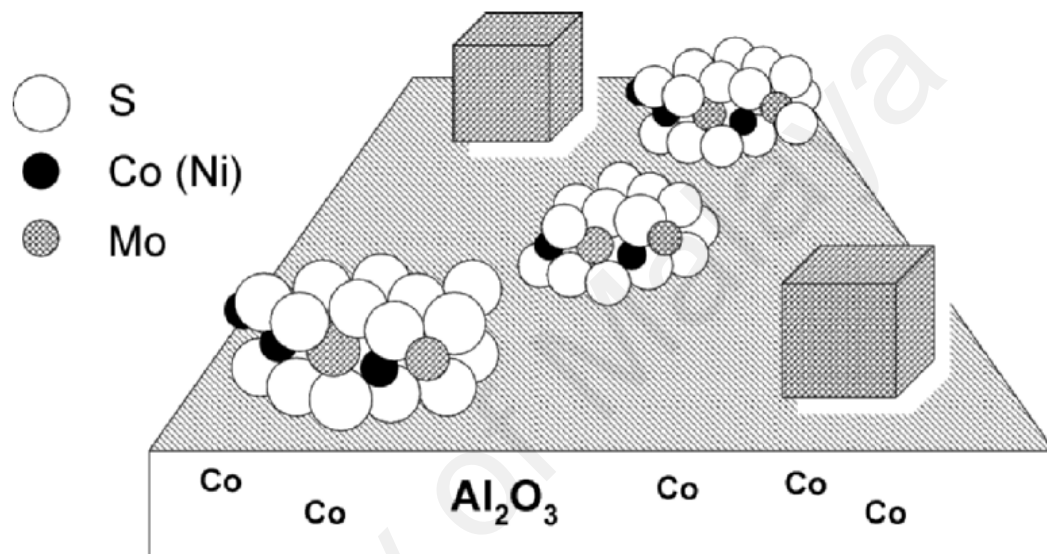
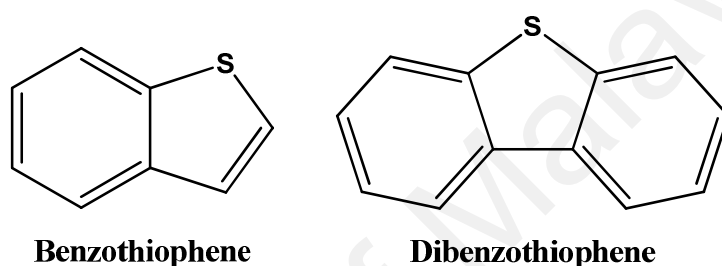


Figure 2.2: The structure of CoMo catalyst in hydrodesulfurization (Mochida & Choi, 2006)

Though increased desulfurization is possible by increasing the severity of the HDS process conditions, higher pressure leads to an increase in the saturation of olefin, i.e. alkenes which lead to a decrease in the octane rating of gasoline. Higher temperatures lead to an increase in coke formation which results in catalyst deactivation. Moreover, the severity of the process is limited by the HDS unit design (Babich & Moulijn, 2003). Sterically hindered compounds such as 4,6-dimethyldibenzothiophene react at a slow rate because the alkyl substituents on 4 and/or 6 position shield the catalyst surface from the S atom and the benzothiophene (BT) core is planar due to its aromaticity (Robinson & Dolbear, 2006). Therefore, the sterically hindered compound must first be saturated so that one or two of the 6-carbon rings are no longer aromatic; thus allowing the

molecule to twist and the catalyst surface to access the S atom (Robinson & Dolbear, 2006). As a result, HDS can efficiently remove sulfur compounds of thiols, sulfides and thiophenes (THs). In comparison, sulfur compounds such dibenzothiophene (DBT), its alkyl derivatives and benzothiophene (BT) are difficult to remove. Adapting HDS for total removal of these refractory sulfur would raise a number of problems such as increased capital and operating costs, decrease of catalyst life and consumption of more H₂ (Kulkarni & Afonso, 2010). Table 2.1 summarizes the advantages and disadvantages of HDS.



Scheme 2.2: Refractory sulfur compounds in hydrodesulfurization

Table 2.1: Summary of advantages and disadvantages of hydrodesulfurization technology (HDS)

HDS Advantages	HDS Disadvantages
Well established technology (Speight, 1999)	Requires high temperature and pressure (Srivastava, 2012)
Effective for removal of thiols, sulfides and thiophenes (Kulkarni & Afonso, 2010)	Reduces octane rating of gasoline (Kulkarni & Afonso, 2010)
	Cannot efficiently remove refractory sulfur compounds (Kulkarni & Afonso, 2010)
	Reduces octane rating of gasoline (Kulkarni & Afonso, 2010)

Though alternative methods are being intensively studied, research is also underway to improve the current HDS technology by development of better catalysts and improvement of reactor design. Other methods for improvement of HDS have also been suggested, such as removal of nitrogen compounds before HDS as nitrogen compounds have been found to deactivate the HDS catalysts.

2.1.2 Biodesulfurization (BDS)

Another alternative method of fossil fuel desulfurization is BDS. This method employs microorganisms which require sulfur to survive to eliminate sulfur in fuels. The S atom generally is found in some microorganism enzyme cofactors, amino acids and proteins. Microorganisms have been isolated which can decrease the sulfur level in fuel by consuming the sulfur in organosulfur compounds (Soleimani et al., 2007). To date, BDS has been found to occur by two pathways. In the Kodama pathway, the first attack is on a carbon atom. In the 4S pathway, the first attack is on the sulfur axis (Abro et al., 2014). BDS has attracted attention recently as a potentially green method. Several bacterial species that can desulfurize fuel have now been identified including *Pseudomonas*, *Rhodococcus spp*, *Brevibacterium*, *Gordona*, and *Arthrobacter*.

Potential benefits of BDS include lower capital and operating costs, emission of significantly less greenhouse gases, valuable byproducts and enzyme specificity, particularly for DBT and its alkyl derivatives (Srivastava, 2012).

Though BDS has many advantages, the several drawbacks of BDS prevent it from being commercialized. For example, BDS is relatively slow in comparison to chemical reactions, biomass is required in large amounts (usually 2.5 g biomass/ g sulfur) and sensitive microorganism must be kept living under the differing and sometimes severe input conditions found in refineries (Srivastava, 2012). Furthermore, the rate of desulfurization is greatly dependent on temperature, pH and dissolved oxygen concentration. These factors must be carefully controlled and monitored. One of the main reasons for not implementing BDS in the present day is that many of the biochemical pathways used by microorganisms for the removal of sulfur (Aggarwal et al., 2012) are also degradative pathways of hydrocarbons, which leads to unacceptable reduction in energy content of fuels (Lee et al., 1995). Furthermore, the process of separating oil, microbial biomass and aqueous phase are not yet well established, which

generates an uncertainty in the quality and quantity of recovered fuel (Li et al., 2009). Another limitation of this biotechnology that should be taken into consideration is the cost of culture medium used to grow the microorganisms involved (Alves & Paixão, 2014). In general, BDS is not able to decrease sulfur amount to a very low level, only to about 10–100 ppm of sulfur. This is possibly a result of higher bacterial activity at higher concentrations. Another important factor that requires attention is the competing reactions from other bacteria (Boniek et al., 2015).

Although there are several obstacles related with the actual viability of the BDS process, the search for new microbial strains to eliminate the sulfur in fossil fuels continues to be of utmost importance in biotechnological studies. Due to the discussed drawbacks of BDS, desulfurization by BDS exclusively is not likely to take place soon (Soleimani et al., 2007). Table 2.2 summarizes the advantages and disadvantages of BDS.

Table 2.2: Summary of advantages and disadvantages of biodesulfurization technology (BDS)

BDS Advantages	BDS Disadvantages
Produces less acid rain gases (Boniek et al., 2015; Izumi et al., 1994)	Sensitive microorganisms must be kept alive within the refinery environment (Srivastava, 2012)
High specificity of enzymes (Srivastava, 2012)	Cost of culture media used to grow the microorganisms involved in the bioprocess (Boniek et al., 2015; Silva et al., 2013)
Lower capital and operating Costs (Boniek et al., 2015; Guobin et al., 2006)	Separation process of oil/microbial biomass not determined (Boniek et al., 2015; Li et al., 2009; Srivastava, 2012)
High valuable by-products (Srivastava, 2012)	Very slow (Srivastava, 2012)
Remove refractory compounds under mild pressures and temperatures (Boniek et al., 2015; Caro et al., 2007)	Not very deep desulfurization achieved thus far (down to 10-100 ppm sulfur) (Kulkarni & Afonso, 2010)

2.1.3 Adsorption

An alternative option to remove sulfur from fuel is adsorption. In the non-destructive or non-reactive adsorption process, the sulfur compound is selectively adsorbed by the adsorbents without any reaction. The adsorbent is placed on a porous, unreactive substrate to increase surface area. Adsorption of sulfur compounds has been studied over adsorbents such as zinc oxide, zeolites, alumina, aluminosilicates and activated carbon (Hernández-Maldonado & Yang, 2004a; Kim et al., 2006; Li et al., 2015; Srivastava, 2012).

Some potential benefits of adsorption for desulfurization are the mild operating temperature and the low sulfur levels that could be achieved if refractory sulfur compounds are removed (Mjalli et al., 2014).

The adsorbent should be easy to regenerate and have a high and fast sulfur adsorption capacity. A vital consideration in the development of the adsorbent is selectivity as the adsorbent should adsorb the sulfur molecules in the presence of a high amount of aromatic and olefinic compounds (Song, 2003). Though adsorption can be highly efficient, regeneration of the adsorbents is a challenge. The adsorbents often require solvent washing or calcination (Hernández-Maldonado & Yang, 2004b). Many adsorbents have been reported to have a low adsorption capacity. For these adsorbents, large and multiple adsorbent beds would be required to minimize replacement and to keep the process continuous (Srivastava, 2012). Another important consideration is the treatment of the removed sulfur compounds. Table 2.3 summarizes the advantages and disadvantages of the adsorption technique.

Table 2.3: Summary of advantages and disadvantages of desulfurization by adsorption

Advantages	Disadvantages
Carried out at low temperature (Mjalli et al., 2014; Srivastava, 2012)	Few adsorbents reported with high selectivity for adsorption of refractory sulfur molecules such as 4,6-dimethyldibenzothiophene (Srivastava, 2012).
No hydrogen required (Mjalli et al., 2014; Srivastava, 2012).	Challenging to develop adsorbents which can achieve a high and fast adsorption capacity, and are also easy to regenerate (Srivastava, 2012).
Does not produce H ₂ S gas (Mjalli et al., 2014)	Many adsorbents have been reported to have low adsorption capacity for sulfur compounds. Using these adsorbents would require multiple large adsorbent beds (Srivastava, 2012).

2.1.4 Extraction

Sulfur compound extraction from fuels, extractive desulfurization (EDS) involves the use of extractant solvents to selectively remove sulfur compounds from fuels. Conventional extractants include solvents such as pyrrolidones, DMSO, DMF and AcN. EDS is carried out at mild conditions, i.e. at low pressure and temperature and does not require H₂ or catalysts (Kulkarni & Afonso, 2010). Moreover, EDS can selectively extract S compounds from fuel oils without reacting with other desired hydrocarbons. In addition, the removed sulfur compounds can be used as raw materials (Abro et al., 2014). The selectivity of the extractant is a major challenge because of the similar polarity of aromatic sulfur compounds and aromatic S-free hydrocarbons in fuel (Kulkarni & Afonso, 2010). Currently, the extractants attracting most attention in the literature are ILs (Domańska et al., 2013c; Królikowska & Karpińska, 2013; Lü et al., 2013a; Shah et al., 2013; Zawadzki et al., 2013). EDS by using ILs will be discussed further after ILs are introduced in detail in Section 2.2.

The experimental findings on EDS have found a low percent of sulfur removal, less than 50%, with a large amount of co-extraction of desired S-free hydrocarbons. A way

to increase the selectivity and amount of sulfur extracted is by oxidizing sulfur molecules before extraction. This increases their polarity and makes extraction easier due to the much increased partition coefficient of the sulfur compound in the extractant (Kulkarni & Afonso, 2010). ODS will be discussed next. Table 2.4 summarizes the advantages and disadvantages of EDS.

Table 2.4: Summary of advantages and disadvantages of desulfurization by extraction

Advantages	Disadvantages
Process occurs at low temperature and pressure (Mjalli et al., 2014)	Challenge to selectively remove sulfur compounds from fuel without extracting other s-free hydrocarbons of similar polarity (Kulkarni & Afonso, 2010)
No hydrogen required (Abro et al., 2014; Mjalli et al., 2014)	Studies on EDS report poor removal of sulfur compounds (<50%) with a high co-extraction of desired hydrocarbons from the fuel oil (Kulkarni & Afonso, 2010).
No catalyst required (Abro et al., 2014)	
Does not react with the desired fuel oils (Abro et al., 2014)	
Extracted organosulfur compounds can be used as raw materials (Abro et al., 2014)	

2.1.5 Oxidative Desulfurization (ODS)

ODS involves S compound oxidation to their corresponding sulfoxides and/or sulfones. This oxidation results in increased polarity and molecular weight, thus aiding their removal by methods such as extraction, adsorption or distillation (Srivastava, 2012). The ODS process takes place by reacting the oxidant with the fuel oil until the sulfur compounds are oxidized but before the other less reactive oil components are attacked by the oxidant. Oxidants commonly used include ozone, hydroperoxides, peroxy salts, nitrogen oxides (Pawelec et al., 2011). Early attempts of ODS used nitric acid or nitric oxide oxidants such as HNO₃ or NO/NO₂ gases (Baxendale et al., 1946;

Williams, 1928). However, it was later found that these oxidants resulted in a high amount of residues (Tam et al., 1990). The more stringent sulfur level limit in diesel then spurred reports that use hydroperoxides such as H_2O_2 and tert-butyl hydroperoxide in combination with in situ produced per-acids or a catalyst. These oxidants could efficiently produce sulfones from the oxidation of organosulfur compounds without producing large amounts of residual product (Kulkarni & Afonso, 2010). ODS is illustrated in Scheme 2.3.



Scheme 2.3: ODS reaction of organosulfur compound to corresponding sulfone

Important factors in ODS are both the oxidant and the extractive solvent. Some oxidants may result in undesired reactions with S-free hydrocarbons that decrease the quality of the fuel. An inappropriate extractant may also result in the undesired co-extraction of S-free hydrocarbons, such as aromatics and olefins (alkenes) from the liquid along with the intended sulfones (Abro et al., 2014; Ali et al., 2006).

The benefits of the ODS include mild operating conditions and its complementary chemistry to HDS. The reason for this is that HDS involves reduction by H_2 gas while ODS involves oxidation by an oxidant. In addition, conventional well known refinery equipment is used for reaction and separation. It is important to consider the regeneration of extractant or adsorbent used and waste treatment of sulfone compounds produced (Ito & van Veen, 2006). Among the different oxidants, the most popular currently is hydrogen peroxide (H_2O_2) because it is environmentally benign (Lo et al., 2003) and the oxidation/extraction step is simultaneous with high sulfur removal achieved. However, the improvements that must be made to make ODS competitive

include: (i) the H_2O_2/S ratio should be reduced (ii) the mass transfer between the polar phase and oil should be increased, and (iii) the post-treatment method for the produced sulfones should be improved (Ito & van Veen, 2006). Although the ODS processes using conventional solvents is effective, one of the key concerns is that it requires volatile organic compounds (VOCs) which are flammable and have negative environmental impact (Lo et al., 2003). For this reason, ILs were used in ODS. Currently ILs are attracting attention for use in ODS due to their various desirable properties particularly their low volatility, and their ability to act as both extractant and catalyst. ODS using ILs will be elaborated further after ILs are introduced. Table 2.5 summarizes the advantages and disadvantages of ODS.

Table 2.5: Summary of advantages and disadvantages of oxidative desulfurization (ODS)

Advantages	Disadvantages
Requires mild pressure and temperature (Kulkarni & Afonso, 2010; Srivastava, 2012)	Sulfone compound product waste management must be considered (Ito & van Veen, 2006)
Complementary chemistry to hydrodesulfurization (Kulkarni & Afonso, 2010)	Undesired side reactions by oxidant must be avoided (Abro et al., 2014; Mjalli et al., 2014; Srivastava, 2012)
Refractory S compounds which are difficult to remove by conventional HDS are easily converted by oxidation (Srivastava, 2012)	The catalytic systems reported are mostly toxic and expensive (Srivastava, 2012)
Does not use expensive hydrogen (Kulkarni & Afonso, 2010; Srivastava, 2012)	

2.2 Ionic Liquids (ILs)

In the current literature “ionic liquids” now means “liquids composed entirely of ions that are a liquid at or below 100°C” (Rogers & Seddon, 2003). Less commonly used synonyms for these materials that were used in the past are: ‘low temperature molten salt,’ ‘ionic fluid,’ ‘liquid organic salt,’ ‘room temperature molten salt,’ ‘non-aqueous ionic liquids,’ and ‘ambient temperature molten salt’ (Wilkes, 2002). It is possible, by careful choice of starting materials, to prepare ILs that are a liquid at and below room

temperature (Welton, 1999). Early work assumed all ILs had similar characteristics. However, it is presently accepted that ILs have a broad range of characteristics (Kirchner & Clare, 2009). Hence, one should avoid any generalizations for such a large class of compounds which is a common error found in the literature. ILs can be nearly anything: toxic or edible, safe or explosive, non-volatile or distillable (McCrary & Rogers, 2013). It was previously assumed that all ILs are non-volatile. However, Earle *et al.* (2006) later reported that some ILs could be vaporized and recondensed. This was a pivotal report that spurred many studies to explore and exploit this unknown possibility in the various applications of ILs. Therefore, it is often incorrectly stated in the literature that all ILs are 'green' or 'non-volatile' and it should be noted that this is not necessarily the case for all ILs as some can be highly toxic and corrosive. Most sources state that the first representative of a room temperature IL (RTIL) was synthesized and characterized in 1914 by Paul Walden though it should also be noted that some sources claim they were synthesized even earlier than this. However, it was not until the late second half of the 20th century that the potential of ILs was recognized, research efforts by Wilkes and Zaworotko (1992) led to the development of easy-to-handle air and water stable ILs. The development of these air and moisture stable ILs has been attributed to be responsible for the recent increased interest in ILs (Welton, 1999; Wilkes, 2002). A broad range of IL-based research fields has developed, which is mainly due to the fact that because of the diversity of possible IL structures, an almost unlimited number of different ILs can be synthesized. The terms "task-specific" ILs and "designer solvents" accounts for the fact that by changing the chemical structure of an IL, the physicochemical properties can be adjusted according to the boundary conditions given by the desired application (Cremer, 2013). There are, theoretically, about 10^{18} ILs that are possible to be synthesized from the different ion combinations (Holbrey & Seddon, 1999). However, one of the key concerns on the feasibility of industrial use of

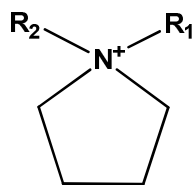
ILs is their cost. Nevertheless, on a large scale, it is possible to produce ILs at a feasible cost, 100 tons can be produced with a cost of around 10 € (RM 48) per liter (Dyson & Geldbach, 2006). However, some ILs will remain considerably more expensive than this. In most cases the IL can be regenerated and reused repeatedly which would reduce cost, making this cost relatively inexpensive.

2.2.1 Structure of ILs

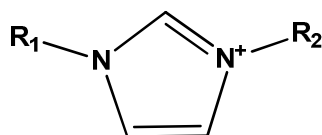
ILs comprise of cations which are organic with anions that can be either organic or inorganic. Most ILs in use are synthesized by salt metathesis reactions (Dyson & Geldbach, 2006) though there are various other methods such as acid–base neutralization (Kirchner & Clare, 2009).

2.2.1.1 Cations

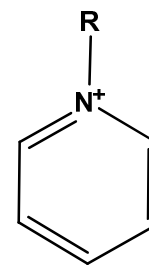
The IL cation is usually organic and asymmetrical. The cation center usually has a positively charged nitrogen or phosphorus. Examples include cations based on imidazolium, pyrrolidinium, ammonium, pyridinium, phosphonium or sulfonium, commonly completely substituted. Studies have mainly focused on ILs with asymmetric dialkylimidazolium cations. Properties of the IL, including melting point, viscosity, and solubility with solvents, are varied by modifying the cation (Dyson & Geldbach, 2006). The structures of some of the main cations studied are illustrated in Scheme 2.4 (Kirchner & Clare, 2009).



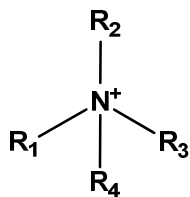
Pyrrolidinium



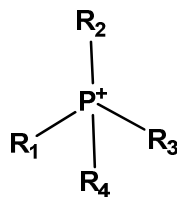
Imidazolium



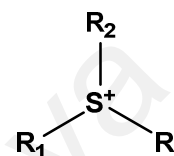
Pyridinium



Ammonium



Phosphonium

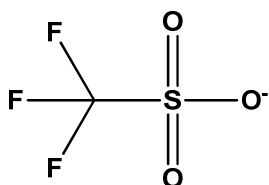


Sulfonium

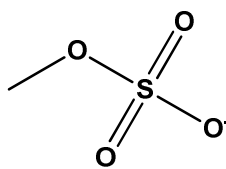
Scheme 2.4: Some of the principal cations used for ILs

2.2.1.2 Anions

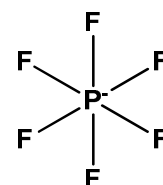
IL anions can be organic or inorganic, with a usually diffuse or protected negative charge (Kirchner & Clare, 2009). Some of the main anions studied are illustrated in Scheme 2.5 (Kirchner & Clare, 2009; Mohammad Fauzi & Amin, 2012).



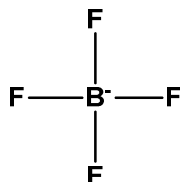
Trifluoromethanesulfonate



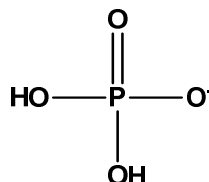
Methyl sulfate



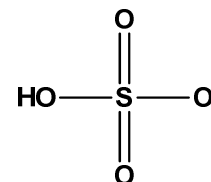
Hexafluorophosphate



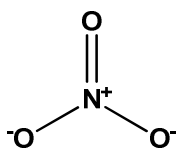
Tetrafluoroborate



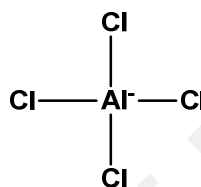
Dihydrogen phosphate



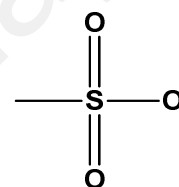
Hydrogen sulfate



Nitrate



Tetrachloroaluminate



Methane sulfonate



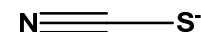
Chloride



Bromide



Iodide



Thiocyanate

Scheme 2.5: Some of the principal anions used for ILs

2.2.2 Effect of structure on physiochemical properties of ILs

IL hydrophobicity is possible to be varied by changing the cation and anion. Cations with longer alkyl chains have higher hydrophobicity. Hydrophobicity is also controlled by the anion. For instance, ILs with fluorinated anions such as hexafluorophosphate $[\text{PF}_6]^-$ and tetrafluoroborate $[\text{BF}_4]^-$ are much more hydrophobic than those with halide ions, e.g. Cl^- , Br^- in ILs with identical cations. ILs with bis(trifluoromethylsulfonyl)imide $[\text{TFSI}]^-$ anion are very hydrophobic. Water and other solvent immiscibility of ILs can be advantageous in phase separation but this would also

merit environmental concerns due to possible unintended release into the environment (Cremer, 2013).

While changing the ion backbone, i.e. the cationic headgroup/charged moiety of the cation can achieve pronounced alterations in the physicochemical properties of an IL. Fine tuning of the resultant IL is usually achieved by changing the length of the alkyl chains attached on the part of the cation which is ionic (Dyson & Geldbach, 2006).

2.2.3 Toxicity of ILs and Impact on the Environment

The toxicological and environmental properties of ILs are attracting increasing interest as ILs have become more popular and are being used in larger quantities and may be applied in the pharmaceutical or food industry. As mentioned earlier, ILs are commonly generalized as being environmentally friendly, non-toxic and 'green', this is not true for all ILs. Many ILs are more toxic than traditional organic solvents. Some ILs can be corrosive or poisonous. However, a major benefit of ILs is their non-volatility or low volatility, therefore they will not be ingested by inhalation like VOCs. Therefore, with necessary safety precautions, their exposure to humans could be low enough to not pose a serious health risk (Dyson & Geldbach, 2006). ILs with anions containing fluoride including $[\text{BF}_4]^-$ and $[\text{PF}_6]^-$ cannot be incinerated which could be an issue for their use on a large scale (Wasserscheid & Welton, 2008). A complete life cycle analysis of ILs should be considered when determining if they can be considered as green solvents. Key considerations for the life cycle analysis of ILs are: raw materials, waste treatment of chemicals and energy consumption for production. In IL synthesis, the selection of cation, anion and solvents has a significant effect on toxicity and economics. An area of increasing interest to avoid potential toxicity is by using ions of known toxicity. Moreover, biodegradation is another significant issue that should be considered in the future use of IL in industry (Wasserscheid & Welton, 2008). Although no vapor emission of solvents is highly desired in industry, it must also be considered

that water soluble ILs may potentially be released to the environment via wastewater (Freemantle, 2010).

2.2.4 Impurities

Impurities in ILs such as traces of H₂O, acids, halide ions, residual solvents and unreacted VOCs arising from the synthesis of the ILs may significantly affect the physical, spectroscopic and chemical characteristics of the liquids. One of the major challenges in IL synthesis is purity. Low levels of mainly halide or H₂O impurities could have a pronounced impact on the result of reactions (Dyson & Geldbach, 2006). Ideally, ILs should be clear and odorless. If there are no functional groups, they should be colorless. However, colorless ILs are not necessarily pure as there can be some colorless impurities such as halide contaminants. Hydrophilic ILs with anions such as [OTf]⁻ or [BF₄]⁻ are expected to contain some residual halides. Though halide contaminants are easier to extract from hydrophobic ILs, ILs with [PF₆]⁻, and to a lesser extent [BF₄]⁻ anions by contact with H₂O can form hydrogen fluoride (Wasserscheid & Welton, 2008).

Without drying techniques and handling in a moisture free environment, H₂O is always present in ILs. Even a hydrophobic IL such as 1-butyl-3-methyl-imidazolium bis(trifluoromethylsulfonyl)imide absorbs approximately 1.4 mass % H₂O at saturation, which is substantial in terms of molar amount. H₂O in ILs may be critical for some applications, but more negligible for others. Furthermore, H₂O content can have a pronounced impact on the physicochemical properties and may affect catalysts dissolved in the IL (Wasserscheid & Welton, 2008).

2.2.5 ILs Applications

Due to the high stability of the cations and anions, the electrochemical window can be very wide (4.5-6 V), and consequently some voltammetric peaks, which are normally out of the range of traditional solvents, may be observed. This has been exploited in

many electrodeposition studies of some metals and semi-conductors which were not possible to electrodeposit previously (Villagrán et al., 2006). ILs have been the focus of many works to replace conventional organic solvents as media for reactions due to their low volatility and wide liquid temperature range. The physical properties of the ILs may be adjusted systematically by simply varying the anion and functionality on the cation, making them a useful and tunable solvent for industry.

ILs are also used in many electrochemical applications including in solar cells, lithium batteries and capacitors (Silvester et al., 2008). ILs are attractive as electrolytes in gas sensors due to their wide electrochemical windows, high thermal stability, low-volatility and high conductivity (Buzzeo et al., 2004a; Huang et al., 2010; O'Mahony et al., 2008). The ability to sense gases in the atmosphere is of huge importance in a variety of fields. In particular, when the gas is toxic and harmful to the environment, the detection of trace amounts of gas is vital to prevent danger to human health (Silvester et al., 2008).

2.2.6 Desulfurization of Fuels using ILs

As discussed in Section 2.1, successful accomplishment of fuels with a low sulfur level is a challenging and important goal to achieve, considering the depletion of crude oil reserves with low sulfur contents. ILs have great potential to help achieve this goal (Kulkarni & Afonso, 2010). ILs have been used in fuel desulfurization in both EDS and ODS.

EDS initially employed molecular solvents as extractants, such as pyrimidinone, imidazolidone, DMSO and polyalkylene glycol but have now been mainly focused on ILs (Abro et al., 2014). Figure 2.3 shows the EDS process using ILs and Table 2.6 below summarizes the studies used for EDS using ILs. ILs are good extractants because they generally have a higher density than organic liquids and H₂O hence exist as a separate phase. Moisture sensitivity of an IL is an important factor as small polar

molecules such as H₂O have been reported to compete with organic sulfur compounds for absorption, resulting in a decrease in absorption efficiency (Zhang et al., 2004c).

An especially attractive feature of ILs is that they can be designed through the selection of cation and anion to perform selective extraction of the desired molecule. The first report on EDS by using ILs was reported by Bosmann *et al.* (2001).

Generally, the ideal IL for EDS should have these features (Eber et al., 2004):

- 1) High partition coefficient, i.e. ratio of S-concentration in the IL compared to in the oil.
- 2) Easy to regenerate.
- 3) Completely insoluble in oil.
- 4) Very selective in the extraction of sulfur compound, with no or very little extraction of other desired compounds from the fuel.
- 5) Highly thermally and chemically stable, green and affordable.

ILs can be regenerated by these two methods (Zhang et al., 2004c):

- i) By washing the IL with water. Water can repel aromatic sulfur compounds from the ILs. This is because H₂O is a small, strongly polar molecule and hence has a stronger interaction with ILs than aromatic compounds. The method is only possible for water-insensitive ILs.
- ii) Distillation is also a possible method within the IL temperature stability range.

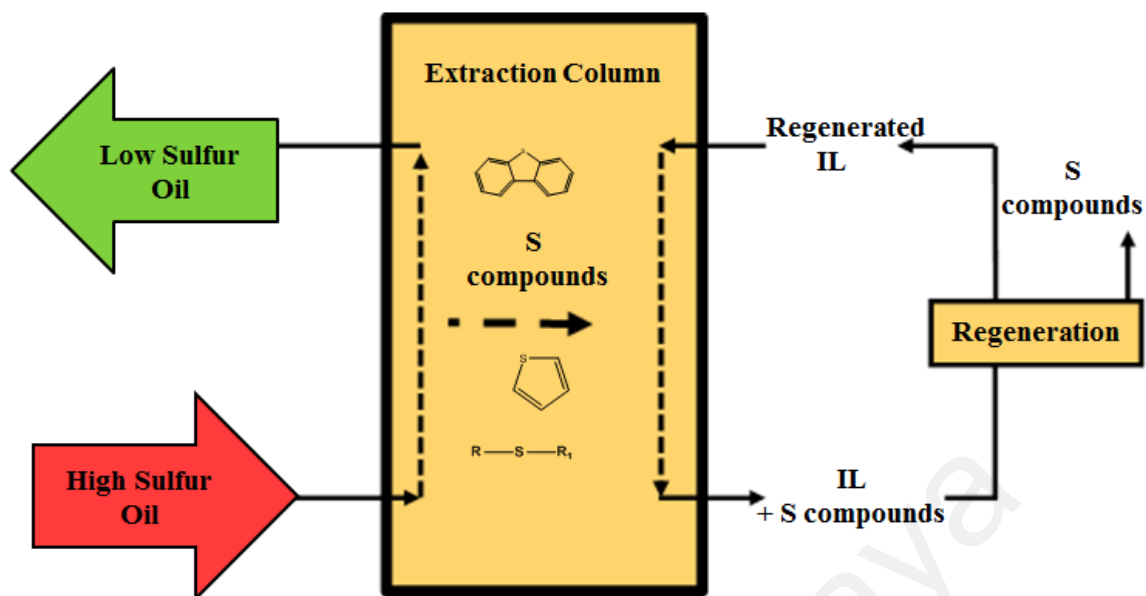


Figure 2.3: Extractive desulfurization (EDS) using ionic liquids

Table 2.6: Summary of ILs used for extractive desulfurization (EDS) of sulfur compounds.

Sulfur Compound	IL	Reference
Thiophene	1-benzyl-3-methylimidazolium bis(trifluoromethylsulfonyl)imide)	(Rogošić et al., 2016)
Thiophene	1-hexyl-3-methylimidazolium thiocyanate 1-octyl-3-methylimidazolium thiocyanate	(Mafi et al., 2016)
Thiophene	1-ethyl 3-methylimidazoliumacetate 1-ethyl-3-methylimidazoliummethylsulphate 1-ethyl-3-methylimidazoliummethylsulphonate	(Blahut & Dohnal, 2011)
Thiophene	1-butyl-1-methylpyrrolidiniumdicyanamide	(Domańska et al., 2011a)
Thiophene	1-butyl-1-methylpyrrolidiniumtetracyanoborate	(Anantharaj & Banerjee, 2011b)
Thiophene	1-ethyl-3-methylimidazoliumthiocyanate	(Verdía et al., 2011)
Thiophene	1-Ethyl-3,5-dimethyl-2-pentylpyridiniumbis(trifluoromethane-sulfonyl)imide 1-Butyl-3,5-dimethyl-2-pentylpyridiniumbis(trifluoromethane-sulfonyl)imide [1B ³ M ⁵ M ² PPy][NTf ₂]	(Marciniak, 2011)
Thiophene	1-(3-hydroxypropyl)pyridiniumbis(trifluoromethylsulfonyl)amide	(Acree et al., 2011)
Thiophene	methyl(tributyl)ammoniumbis(trifluoromethylsulfonyl)imide octyl(trimethyl)ammoniumbis(trifluoromethylsulfonyl)imide decyl(trimethyl)ammoniumbis(trifluoromethylsulfonyl)imide tetraoctylammoniumbis(trifluoromethylsulfonyl)imide	(Marciniak & Karczemna, 2011)

Table 2.6, continued

	1-butyl-3-methyl-imidazolium2-(2-methoxyethoxy)ethylsulphate	
	1-ethyl-3-methyl-imidazoliumtrifluoroacetate	
	1-ethyl-3-methyl-imidazolium trifluoromethanesulfonate	
	1-butyl-3-methyl-imidazoliumtrifluoromethanesulfonate	
	1-butyl-1-methyl-pyrrolidiniumtrifluoromethanesulfonate	
Thiophene	1-butyl-3-methyl-pyridiniumtrifluoromethanesulfonate	(Hansmeier et al., 2011)
	1-hexyloxymethyl-3-methyl-imidazoliumbis(trifluoromethylsulfonyl)-amide	
	1,3-dihexyloxymethyl-imidazoliumbis(trifluoromethylsulfonyl)-amide	
	1-(3-hydroxypropyl)pyridinium is(trifluoromethylsulfonyl)-amide	
	1-(3-hydroxypropyl)pyridiniumtrifluorotris(perfluoroethyl)phosphate	
Thiophene	1-ethyl-3-methylimidazoliumtetracyanoborate	(Paduszyński & Domańska, 2011)
Thiophene	1-butyl-1-methylpiperidiniumbis(trifluoromethylsulfonyl)imide	(Domańska & Królikowski, 2011)
Thiophene	N-hexyl-3-methylpyridiniumtosylate (p-toluenesulfonate),	(Anantharaj & Banerjee, 2011c)
	1-butyl-1-methylpyrrolidiniumtetrafluoroborate	
	1-butyl-1-methylpyrrolidiniumhexafluoro-phosphate	
Thiophene	1-butyl-4-methylpyridiniumtetrafluoroborate	(Domańska et al., 2011b)
	1-butyl-4-methylpyridiniumhexafluorophosphate	
	1-benzyl-3-methylimidazoliumtetrafluoroborate	
Thiophene	4-(2-methoxyethyl)-4-methylmorpholiniumtrifluorotris(perfluoroethyl)phosphate	(Domańska & Królikowski, 2012)
Thiophene	1-ethyl-3-methylimidazoliummethanesulfonate	(Marciniak & Królikowski, 2012a)
	{(4-(2-methoxyethyl)-4-methylmorpholiniumtrifluorotris(perfluoroethyl) phosphate	
Thiophene	1-(2-methoxyethyl)-1-methylpiperidiniumtrifluorotris(perfluoroethyl) phosphate	(Marciniak & Wlazło, 2012a)
	1-(2-methoxyethyl)-1-methylpyrrolidiniumtrifluorotris(perfluoroethyl)phosphate)	
Thiophene	1-(2-methoxyethyl)-1-methylpiperidiniumbis(trifluoromethylsulfonyl)-amide	(Marciniak & Królikowski, 2012b)
	(4-(2-methoxyethyl)-4-methylmorpholiniumbis(trifluoromethylsulfonyl)-amide	
Thiophene	1-(2-methoxyethyl)-1-methylpiperidiniumbis(trifluoromethylsulfonyl)-amide	(Królikowska et al., 2012)
	1-(2-methoxyethyl)-1-methylpyrrolidiniumbis(trifluoromethylsulfonyl)-amide)	
Thiophene	N-hexylisoquinoliniumthiocyanate	(Marciniak & Wlazło, 2012b)
Thiophene	4-(2-methoxyethyl)-4-methylmorpholiniumbis(trifluoromethylsulfonyl)-amide	(Domańska et al., 2012b)
Thiophene	1-hexyl-3-methylimidazoliumtetracyanoborate	(Batista et al., 2012)
Thiophene	1-(2-hydroxyethyl)-3-methylimidazoliumtrifluorotris(perfluoroethyl)phosphate	(Królikowska & Karpińska, 2013)
Thiophene	N-octylisoquinoliniumthiocyanate	(Domańska et al., 2013b)
Thiophene	1-butyl-1-methylpyrrolidiniumtris(pentafluoroethyl)trifluorophosphate	(Lü et al., 2013a)
Thiophene	1-butyl-3-methylimidazolium	(Shah et al., 2013)
	1-Ethyl 3-methylimidazoliumacetate	
Thiophene	1-ethyl-3-methylimidazoliumethylsulfate	(Anantharaj & Banerjee, 2013)
	1-ethyl-3-methylimidazoliummethylsulfonate	
Thiophene	1-Ethyl-3-methylimidazolium-based IL with acetate ethylsulfate , and methyl sulfonate	(Królikowska et al., 2013)
Thiophene	N-hexylisoquinoliniumthiocyanate	(Lü et al., 2013b)

Table 2.6, continued

Thiophene	1-butyl-3-methylimidazoliumtrifluoromethanesulfonate	(Domańska et al., 2013c)
Thiophene	1-butyl-1-methylpyrrolidiniumtris(pentafluoroethyl)trifluorophosphate, 1-butyl-1-methylpyrrolidiniumtetracyanoborate 1-butyl-1-methylpyrrolidiniumtricyanomethanide	(Nejad et al., 2013)
Thiophene	1-butyl-3-methylimidazolium4,5-dicyano-2-(trifluoromethyl)imidazolidine 1-butyl-3-methylpyridinium4,5-dicyano-2-(trifluoromethyl)imidazolidine	(Królikowski et al., 2013)
Thiophene	1-(2-methoxyethyl)-1-ethylpyrrolidinium trifluorotris(perfluoroethyl)phosphate	(Rodríguez-Cabo et al., 2013)
Thiophene	1-ethyl-3-methylimidazolium bis(trifluoromethylsulfonyl)imide	(Marciniak & Wlazło, 2013b)
Thiophene	1-(2-methoxyethyl)-1-methylpiperidinium trifluorotris(perfluoroethyl)phosphate	(Blahut & Dohnal, 2013)
Thiophene	1-butyl-1-methylpyrrolidinium tetracyanoborate 1-butyl-1-methylpyrrolidinium bis(oxalato)borate	(Domańska et al., 2013a)
Thiophene	1-hexyl-1-methylpyrrolidiniumbis(trifluoromethylsulfonyl)imide 1-octyl-1-methylpyrrolidiniumbis(trifluoromethylsulfonyl)imide 1-decyl-1-methylpyrrolidiniumbis(trifluoromethylsulfonyl)imide.	(Lü et al., 2012)
Thiophene	1,3,4,6,7,8-hexahydro-1-methyl-2H-pyrimido[1,2-a]pyrimidine bis(pentafluoroethyl)sulfonylimide	(Wang et al., 2012)
Thiophene	1-butyl-1-methylpyrrolidiniumtris(pentafluoroethyl)trifluorophosphate	(Domańska et al.)
Thiophene	N-octylisoquinolinium bis(trifluoromethylsulfonyl)imide	(Rodríguez-Cabo et al., 2012)
Thiophene	1-hexyl-2,4-dimethylpyridiniumbis(trifluoromethylsulfonyl)imide 1-hexyl-3,5-dimethylpyridiniumbis(trifluoromethylsulfonyl)imide	(Anantharaj & Banerjee, 2011a)
Thiophene	1-ethyl-3-methylimidazoliumthiocyanate tris-(2-hydroxyethyl)-methylammonium-ethylsulfate 1,3-Dimethylimidazoliummethylphosphonate	(De Oliveira & Aznar, 2011)
Thiophene	1-butyl-1-methylpiperidiniumthiocyanate	(Varma et al., 2011)
Thiophene	1-ethyl-3-methylimidazoliummethanesulfonate	(Domańska & Marciniak, 2010)
Thiophene	1-decyl-3-methylimidazoliumtetracyanoborate	(Rodríguez et al., 2010)
Thiophene	1-ethyl-3-methylimidazoliumbis(trifluoromethanesulfonyl)imide	(Domańska & Królikowski, 2010a)
Thiophene	1-butyl-3-methylimidazoliumtosylate (p-toluenesulfonate)	(Asumana et al., 2010)
Thiophene	1-hexyl-3-methylimidazoliumthiocyanate	(Francisco et al., 2010)
Thiophene	1-hexyl-3,5-dimethylpyridiniumbis[trifluoromethylsulfonyl]imide}	(Domańska & Królikowska, 2010)
Thiophene	1-butyl-4-methylpyridiniumthiocyanate 1-butyl-1-methylpyrrolidiniumthiocyanate	(Arce et al., 2010)
Thiophene	1-hexyl-3,5-dimethylpyridiniumbis(trifluoromethyl sulfonyl)imide	(Domańska & Patuszyński, 2010a)
Thiophene	tri- <i>iso</i> -butylmethylphosphonium <p>-toluenesulfonate</p>	(Marciniak & Wlazło, 2010)
Thiophene	1-(3-hydroxypropyl)pyridiniumtrifluorotris(perfluoroethyl)phosphate	(Revelli et al., 2010)
Thiophene	1-butyl-3-methylimidazoliumtetrafluoroborate 1,3-dimethylimidazoliummethylphosphonate 1-butyl-3-methylimidazoliumthiocyanate	(Domańska & Królikowski, 2010b)

Table 2.6, continued

Thiophene	1-butyl-3-methylimidazoliumtosylate(p-toluenesulfonate)	(Nefedieva et al., 2010)
Thiophene	1-butyl-3-methyl-pyridiniumtrifluoromethanesulfonate	(Domańska et al., 2010b)
Thiophene	N-butylquinoliniumbis{(trifluoromethyl)sulfonyl} imide	(Abai et al., 2010)
Thiophene	1-hexyloxymethyl-3-methyl-imidazoliumbis(trifluoromethylsulfonyl)-imide 1,3-dihexyloxymethyl-imidazoliumbis(trifluoromethylsulfonyl)-imide	(Domańska & Marciniak, 2009b)
Thiophene	4-methyl-N-butyl-pyridiniumbis(trifluoromethylsulfonyl)-imide	(Domańska et al., 2009a)
Thiophene	N-butyl-4-methylpyridiniumtosylate (p-toluenesulfonate) N-butyl-3-methylpyridiniumtosylate N-hexyl-3-methylpyridiniumtosylate N-butyl-4-methylpyridiniumbis{(trifluoromethyl)sulfonyl}imide 1,4-dimethylpyridiniumtosylate 2,4,6-collidinetosylate	(Domańska & Marciniak, 2009c)
Thiophene	1-ethyl-3-methylimidazoliumthiocyanate 1-butyl-3-methylimidazoliumthiocyanate 1-hexyl-3-methylimidazoliumthiocyanate triethylsulphoniumbis(trifluoromethylsulfonyl)imide	
Thiophene	1-butyl-3-methylimidazoliumhexafluorophosphate 1-butyl-3-methylimidazoliumtetrafluoroborate	(Gao et al., 2008)
Thiophene	1-ethyl-3-methyl-imidazolium-ethylsulfate 1-ethyl-3-methyl-imidazolium-ethylsulfate	(Domańska & Marciniak, 2008)
Thiophene	1-butyl-3-methylimidazoliumtrifluoromethanesulfonate	(Mochizuki & Sugawara, 2008)
Thiophene	1-ethyl-3-methylimidazoliumethylsulfate	(Liu et al., 2008)
Thiophene	1-methyl-3-octylimidazoliumbis[trifluoromethylsulfonyl]imide	(Zhang et al., 2007)
Thiophene	1-methyl-3-octylimidazoliumtetrafluoroborate, [C ₈ mim][BF ₄] 1-butyronitrile-3-methylimidazoliumbis(trifluoromethylsulfonyl)imidate 1-butyronitrile-2,3-dimethylimidazoliumbis(trifluoromethylsulfonyl)imidate 1-butyronitrile-3-methylimidazoliumdicyanamide 1-butyronitrile-2,3-dimethylimidazoliumdicyanamide 1-butyl-3-methylimidazoliumpalmitate 1-butyl-3-methylimidazoliumstearate	(Alonso et al., 2007b)
Thiophene	1-methyl-3-octylimidazoliumtetrafluoroborate	(Nie et al., 2007)
Thiophene	triethylsulphoniumbis(trifluoromethylsulfonyl)imide	(Gao et al., 2009a)
Thiophene	1-butyl-3-methylimidazoliumthiocyanate	(Domańska et al., 2009b)
Thiophene	1-butyl-1-methylpyrrolidiniumtrifluoromethanesulfonate	(Sobota et al., 2009)
Thiophene	1-ethyl-3-methylimidazoliumnitrate	(Gao et al., 2009b)
Thiophene	1-butyl-3-methylimidazoliumthiocyanate	(Domańska et al., 2009b)
Thiophene	1-butyl-1-methylpyrrolidiniumtrifluoromethanesulfonate	(Sobota et al., 2009)
Thiophene	1-ethyl-3-methylimidazoliumnitrate	(Gao et al., 2009b)
Dibenzothiophene	2-[2-(dimethylamino)ethoxy]ethanolpropionate 3-(dimethylamino)-propanenitrilepropionate)	(Nejad et al., 2012)

Table 2.6, continued

	1-butyl-3-methylimidazoliumtetrafluoroborate	
	1-butyl-3-methylimidazoliumhexafluorophosphate	
	1-butyl-3-	
	methylimidazoliumtris(pentafluoroethyl)trifluorophosphate	
	1-butyl-3-methylimidazoliummethylsulfate	
	1-butyl-3-methylimidazoliumdicyanamide	
	1-butyl-3-methylimidazoliumbis(trifluoromethylsulfonyl)imide	
	1-butyl-3-methylimidazoliumchloride	
Dibenzothiophene	1-butyl-3-methylimidazoliumoctylsulfate	(Acree Jr et al., 2012)
	1-butyl-3-methylimidazoliumhydrogensulfate	
	1-butyl-3-methylimidazoliumthiocyanate	
	1-butyl-3-methylimidazoliumacetate	
	1-butyl-3-methylimidazoliumtrifluoromethanesulfonate	
	1-ethyl-3-methylimidazoliumdiethylphosphate	
	1-ethyl-3-methylimidazoliumtetrafluoroborate	
	1-ethyl-3-methylimidazolium <i>p</i> -toluenesulfonate	
	1-hexyl-3-methylimidazoliumbis(trifluoromethylsulfonyl)imide	
	1-hexyl-3-methylimidazoliumtetrafluoroborate	
	Tributylmethylammonium methylcarbonate	
Dibenzothiophene	N -methyl-2-hydroxyethylammoniumacetate	(Chen et al., 2012)
	N -methyl-2-hydroxyethylammoniumbutanoate	
	N -methyl-2-hydroxyethylammoniumhexanoate	
Dibenzothiophene	1-ethyl-3-methylimidazoliumdiethylphosphate	(Domaníška & Królikowska, 2011)
	1-ethyl-3-methylimidazoliummethylsulfate	
Dibenzothiophene	S-Butyl-thiuroniumbis{(trifluoromethyl)sulfonyl}imide	
	S-Butyl-N,N'-	
	dimethylthiuroniumbis{(trifluoromethyl)sulfonyl}imide	(Li et al., 2010)
	S-Butyl-N,N'-	
	diethylthiuroniumbis{(trifluoromethyl)sulfonyl}imide	
Dibenzothiophene	1,3-dimethylimidazolium-methylsulfate	
	1-ethyl-3-methylimidazolium-ethylsulfate	
	1-ethyl-3-methylimidazoliummethylsulfate	(Alonso et al., 2008d)
	1-ethyl-3-ethylimidazoliummethylsulfate	
	1-butyl-3-methylimidazoliummethylsulfate	
	1-butyl-3-ethylimidazoliummethylsulfate	
Dibenzothiophene	1-butyl-pyridinium tetrafluoroborate	(Enayati & Faghihian, 2015)
Benzothiophene	1-ethyl-3-methylimidazoliummethylsulphate	(Blahut et al., 2010)
	1-ethyl-3-methylimidazoliumacetate	
Dibenzothiophene		
Benzothiophene		
4,6-		
ibenzothiophene	N-butyl-N-methylpiperidinium tetrachloroferrate	(Jiang et al., 2015)
Thiophene	triisobutyl(methyl)phosphonium <i>p</i> -toluenesulfonate (Cyphos ® IL 106)	
Dibenzothiophene	tetrabutylphosphonium methanesulfonate	(Ahmed et al., 2015a)
Benzothiophene	1-butyl-1-methylpyrrolidinium bis(trifluoromethylsulfonyl)imide	
	1-hexyl-1-methylpyrrolidinium bis(trifluoromethylsulfonyl)imide	
1-Propanethiol		
1-Butanethiol		
1-Pentanethiol		
Thiophene		
2-	1-butyl-3-methylimidazolium tetrachloroaluminate	
Methylthiophene	1-octyl-3-methylimidazolium tetrafluoroborate,	(Nejad & Beigi, 2015)
3-		
Methylthiophene		
Benzothiophene		
Dimethyl disulfide	N-methyl-N-methylimidazolium dimethyl phosphate	
	N-ethyl-N-methylimidazolium diethyl phosphate	(Tian et al., 2014)
	N-butyl-N-methylimidazolium dibutyl phosphate	

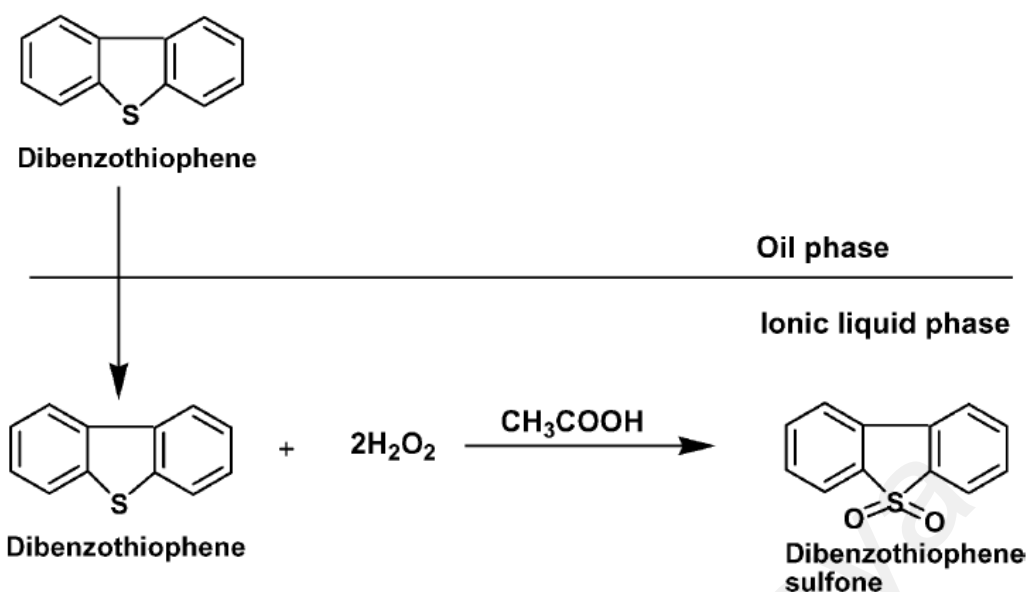
Table 2.6, continued

Dibenzothiophene Benzothiophene 4,6- Dimethyldibenzot hiophene	Anhydrous FeCl ₃ and 1-methyl-3-octylimidazoliumchloride system	(Zawadzki et al., 2013)
Thiophene Benzothiophene	1-butyl-1-methylpyrrolidinium trifluoromethanesulfonate 1-butyl-1-methylpyrrolidinium tricyanomethanide 1-hexyl-3-methylimidazolium tetracyanoborate	(Domańska et al., 2014)
Thiophene Dibenzothiophene	1-butyl-3-methylimidazolium chloride/ZnCl ₂	(Chen et al., 2014)
Thiophene Benzothiophene	1-ethyl-3-methylimidazoliumtricyanomethanide	(Marciniak & Wlazło, 2013a)
Thiophene Benzothiophene	butyl-methyl-imidazoliumoctylsulfate ethyl-methyl-imidazolium ethylsulfate	(Marciniak & Wlazło, 2013c)
Thiophene Dibenzothiophene	3-butyl-4-methylthiazoliumdicyanamide 3-butyl-4-methylthiazoliumthiocyanate 3-butyl-4-methylthiazoliumhexafluorophosphate 3-butyl-4-methylthiazoliumtetrafluoroborate	(Domańska et al., 2012a)
Thiophene Dibenzothiophene	1-ethyl-3-methylimidazoliumdicyanamide	(Kêdra-Królik et al., 2011)
Thiophene Dibenzothiophene	1-butyl-3-methylimidazoliumdicyanamide 1-ethyl-3-methylimidazoliumdicyanamide ethylated tetrahydrothiopheniumdicyanamide ethyldimethylsulfoniumdicyanamide	(Domańska & Paduszyński, 2010b)
Thiophene Dibenzothiophene	1-methyl-3-octylimidazoliumtetrafluoroborate	(Alonso et al., 2007c)
Benzothiophene Thiophene 2- Methylthiophene 3- Methylthiophene, 1-Propanthiol 1-Butanthiol 1-Pentanthiol	1-octyl-3-methylimidazoliumtetrafluoroborate 1-butyl-3-methylimidazoliumhexafluorophosphate,	(Gao et al., 2012)
Thiophene Benzothiophene Dibenzothiophene 4,6- Dimethyldibenzot hiophene	1-butyl-3,5-dimethylpyridiniumtetrafluoroborate 1-hexyl-3,5-dimethylpyridiniumtetrafluoroborate 1-octyl-3,5-dimethylpyridiniumtetrafluoroborate	(Wilfred et al., 2012)
Dibenzothiophene Diphenylsulfide Diphenyldisulfide ,	1-methyl-3-methylimidazoliummethylsulfate	(Wlazło & Marciniak, 2012)
4-Methyl- Dibenzothiophene	1-ethyl-3-methylimidazoliumdiethylphosphate 1-ethyl-3-methylimidazoliumethylsulfate	(Marciniak & Wlazło, 2010)
Dibenzothiophene Benzothiophene 4,6- Dimethyldibenzot hiophene	1-butyl-3-methyl-imidazoliumchloride-FeCl ₃ 1-butyl-3-methyl-imidazoliumchloride-ZnCl ₂ 1-butyl-3-methylimidazoliumchloride-SnCl ₂ T ₄ Cl/FeCl ₃ (where T ₄ Cl = methyl tributyl ammonium chloride), D ₁₀ Cl/FeCl ₃ (where D ₁₀ Cl = didecyl dimethyl ammonium chloride) Et ₃ NHCl/FeCl ₃ (where Et ₃ NHCl = triethylammoniumchloride)	(Domańska et al., 2010a)
Benzothiophene Dibenzothiophene	1-methyl-3-butylimidazoliumtetrafluoroborate 1-methyl-3-octylimidazoliumtetrafluoroborate (Effect of cobalt(II), nickel(II), iron(III), iron(II) and copper(I) additives were investigated)	(Domańska & Marciniak, 2009a)
Thiophene Benzothiophene Dibenzothiophene 4,6- Dibenzothiophene	1-octyl-3-methylpyridiniumtetrafluoroborate 1-hexyl-3-methylpyridiniumtetrafluoroborate 1-butyl-3-methylpyridiniumtetrafluoroborate	(Domańska & Laskowska, 2009)

2.2.7 Desulfurization of Fuels using ILs by ODS

As discussed, ILs have many benefits over conventional solvents. However, the limitation of EDS by using ILs is that the partition coefficient tends to result in the co-extraction of aromatic compounds in the fuel which are desired. Therefore, various types of ILs exhibited low efficiency for sulfur removal. As a result, researchers investigated the use of an oxidant with ILs to enhance selectivity and efficiency (Kulkarni & Afonso, 2010). In ODS ILs can serve as the extractant (Jiang et al., 2014), catalyst (Yu et al., 2014) or both extractant and catalyst (Chen et al., 2015). The major factors to be studied in the ODS/extraction efficiency are the effects of the amount of IL and oxidant, reaction time and temperature, and the recycling of IL (Fang et al., 2014).

The first work involving ODS using an IL was reported by Lo *et al.* (2003). In this report, an environmentally benign oxidation system of H₂O₂ and AcOH, and an IL as extraction solvent were used. A model light oil of tetradecane with DBT was used. The ILs selected as solvent, namely [BMIm][PF₆] and [BMIm][BF₄], were both immiscible with light oils. DBT was extracted from the model light oil phase into the IL phase and subsequently oxidized in the IL phase, shown in Scheme 2.6. The authors attributed the difference in the desulfurization efficiency of the two ILs to the miscibility of ILs with water. The water-immiscible IL of [BMIm][PF₆] achieved a higher desulfurization efficiency than water-soluble [BMIm][BF₄]. This is because it provided a medium which resulted in a higher rate of reaction. DBT oxidation was found to be inversely proportional to the concentration of H₂O (Lo et al., 2003). Within 6 h, DBT sulfone product was present in the IL phase but not in the oil phase. This can be attributed to the high polarity of the IL.



Scheme 2.6: Oxidation of DBT using H₂O₂ and AcOH in oil/IL system (Kulkarni & Afonso, 2010).

The DBT was extracted from the oil at 99%, with initial S content of 758 ppm. Mere extraction of DBT using the same IL of [BMIm][PF₆] showed only 47% extraction. This report demonstrated that chemical oxidation combined with extraction using a water-immiscible IL can, in one step, almost completely desulfurize light oil. This system was also used on actual light oil. In [BMIm][PF₆] after 10 h, sulfur level was decreased from 8040 to 1300 ppm. In addition, the Lo *et al.* (2003) also regenerated and reused the ILs four times with no change in the desulfurization yield achieved. These positive results encouraged researchers to improve this process by exploring the effect of different catalysts and ILs. H₂O₂ is usually the preferred oxidant not only due to its high oxygen content but also because of its environmental compatibility (Lü *et al.*, 2014). However, it was found that excess H₂O₂ is required. This might be due to two possible reasons: some catalysts would cause the decomposition of H₂O₂, leading to the low utilization of the oxidant or an excess amount of H₂O₂ could promote the equilibrium reaction and enhance the desulfurization efficiency. Therefore, for economic reasons, different catalysts have been studied and designed to decrease the amount of H₂O₂ required (Xiong *et al.*, 2015).

The most popular catalysts employed are polyoxometalates (POMs). POMs are a family of anionic metal oxides such as tungsten, niobium, molybdenum and vanadium. These metal oxides exhibit attractive characteristics of tenability of composition, size, shape, redox potential and acid-base properties. The reaction of POMs with H₂O₂ can increase the rate of the ODS process (Zhang et al., 2015). Thus, many research groups have studied the use of POM catalysts and POM-based ILs in ODS in attempts to combine the benefits of ILs and functional POMs (Julião et al., 2015; Xiong et al., 2015; Zhang et al., 2014). Although most POM-based ILs are efficient in ODS, a practical drawback for industrial applications is their liquid nature, which would lead to problems in separation and regeneration. To overcome this, many groups have made efforts to immobilize the ILs on a solid support (Zhang et al., 2015).

TH is difficult to oxidize compared to other sulfur compounds such as BT and DBT, this is mainly due to its aromaticity and low electron density on its sulfur atom (Zhang et al., 2012). Nevertheless, some groups have studied the oxidation of TH and TH derivatives using ILs (Lin et al., 2012b; Zhang et al., 2012; Zhao et al., 2008). Zhao *et al.* (2008) used H₂O₂/acetic acid system and using a quaternary ammonium coordinated IL of (C₄H₉)₄NBr·2C₆H₁₁NO as an effective catalyst for the removal of TH. TH could be oxidized to greater polar sulfoxide, sulfone, and SO₄²⁻, which can be extracted easily by the water phase. Lin *et al.* (2012b) used molecular oxygen as oxidant, under visible light irradiation using the visible-light responsive photocatalyst BiVO₄ co-loaded with an ultra-low loading of Pt and RuO₂, the results achieved over 99% conversion of TH oxidation. The sulfur in sulfur-containing substrates can be oxidized to SO₃ for T, 2-MT and 2,5-DMT, and partially oxidized to the corresponding sulfones for BT and DBT. Zhang *et al.* (2012) used H₂O₂ oxidant, Brønsted acidic ILs (BAILs) and ODS catalyst composed of tungstate compounds to effectively catalyze the oxidation of and TH, 2-MTH, 3-MTH, 2,5-dimethylthiophene, 2,3,5-trimethylthiophene and BT. The sulfur

atom of thiophene is oxidized to SO_4^{2-} . The authors reported the BAILs which play a triple role in ODS as extractant, reaction media and as a catalyst.

2.3 Superoxide Ion ($\text{O}_2^{\bullet-}$)

Neutral O_2 upon the addition of a single electron results in the $\text{O}_2^{\bullet-}$, Eq 2.1 (Haber & Weiss, 1934). $\text{O}_2^{\bullet-}$ is considered to be both a radical, denoted by the dot sign (\bullet) as well as an anion, charge of -1 (Daniels, 2002; Huang et al., 2009).



$\text{O}_2^{\bullet-}$ has been known as far back as 1934, when researchers suggested that $\text{O}_2^{\bullet-}$ is produced in H_2O_2 degradation and in ferrous ions oxidation by O_2 in aqueous solutions. Early interest in $\text{O}_2^{\bullet-}$ was attracted due to the invention of a breathing device in which KO_2 , combined with catalysts, could generate O_2 from CO_2 . In 1969, two reports began the great interest in $\text{O}_2^{\bullet-}$ (Knowles et al., 1969; McCord & Fridovich, 1969). These reports detected $\text{O}_2^{\bullet-}$ using Electron Spin Resonance, ESR, in an enzymatic reaction in which O_2 was involved (Knowles et al., 1969), and found metalloproteins which catalyzed $\text{O}_2^{\bullet-}$ disproportionation, i.e. “superoxide dismutases”, SODs (McCord & Fridovich, 1969). SODs were concluded to be used to protect living cells from the toxicity of $\text{O}_2^{\bullet-}$. The discovery that $\text{O}_2^{\bullet-}$ was a vital intermediate in aerobic organism spurred great interest and many studies on $\text{O}_2^{\bullet-}$ reactivity (AlNashef, 2004). $\text{O}_2^{\bullet-}$ was not intensively studied until 1970-1975 when techniques for $\text{O}_2^{\bullet-}$ investigation were developed: electrochemical reduction of O_2 , aqueous solution pulse radiolysis and flash photolysis, and the use of KO_2 -crown ether solutions in aprotic media (Daniels, 2002).

2.3.1 Superoxide Salts

Solid superoxide is possible in the form of metal superoxide salts or organic compounds such as tetraalkylammonium superoxides (Bovard, 1960). The difficulty of

formation of the superoxide salt usually increased with the atomic weight of the metal (Bovard, 1960; White & Paris, 1981). The most commonly used superoxide salt is KO_2 which is a solid under room conditions. It is manufactured by atomizing molten potassium into dry air (Bovard, 1960). A yellow fluffy material is formed which is later compacted and crushed to the chosen particle size (White & Paris, 1981). Sodium superoxide, NaO_2 , costs about ten times as much as KO_2 . For this reason, together with the fact that KO_2 is well characterized, often makes KO_2 the best choice for applications (Krawietz et al., 1998). The oxidation of potassium usually forms mixtures of peroxide and superoxide phases though the oxide has also been reported (White & Paris, 1981).

From the group 2 elements, calcium superoxide [$\text{Ca}(\text{O}_2)_2$] can also be formed. However, the utilization of $\text{Ca}(\text{O}_2)_2$ is limited by the fact that it cannot be prepared in high purities. The lack of success in producing pure $\text{Ca}(\text{O}_2)_2$ is attributed to its instability. The maximum possible purity that can be obtained for $\text{Ca}(\text{O}_2)_2$ by the equimolar disproportionation reaction is 58.4% by weight. The attempted scale-up of the process to produce commercial amounts of the superoxide was frustrated by lower product purity (Bovard, 1960; Elliott et al., 2014).

The most common use for superoxide salts is in O_2 regeneration apparatus for mining, firefighting and in space. During operation, the user exhales into a mouthpiece. The exhaled breath then travels through the exhalation duct and enters a canister containing KO_2 . The exhaled CO_2 and H_2O vapor are absorbed and replacement O_2 is released (Huang et al., 2009).

2.3.2 Superoxide in Aprotic Solvents

The electrochemical behavior of O_2 in traditional aqueous and organic solvents has been well investigated. These studies have shown that reduction of this molecule is a complex process. The electroreduction of O_2 is an important reaction in many

applications, including the electrosynthesis of ROS, fuel cells and metal-air batteries (Evans et al., 2004).

The electrogenerated nucleophilic and strong Brønsted base $O_2^{\bullet-}$ species is highly reactive in protic solvents and will rapidly and spontaneously disproportionate (Huang et al., 2009).

Disproportionation of the radical anion $O_2^{\bullet-}$ occurs in the following two steps: Eq 2.2 followed by Eq 2.3 (Rogers et al., 2009):



However, when not exposed to a proton source, such as in aprotic solvents, the $O_2^{\bullet-}$ species does not react. Reversible voltammetry O_2 electroreduction has been achieved in common aprotic solvents such as AcN, DMF and DMSO, as well as in less conventionally used aprotic solvents, e.g. propylene carbonate and acetone (AlNashef, 2004; Huang et al., 2009). In aprotic media a reversible, one-electron reduction produces the $O_2^{\bullet-}$ ion, as shown in Eq 2.4 (Barnes et al., 2008; Evans et al., 2004; Huang et al., 2009).



$O_2^{\bullet-}$ ion can be formed directly from dissolution of superoxide salts such as KO_2 in solvents, or electrochemically by reduction O_2 , usually at a potential of -1.0 V vs SCE (Barnes et al., 2008).

The $O_2^{\bullet-}$ species is known to readily react with H_2O and readily disproportionates in H_2O to O_2 and hydroperoxide, Eq 2.5 (AlNashef, 2004; Barnes et al., 2008; Buzzeo et al., 2004b; Pozo-Gonzalo et al., 2013; Sawyer & Valentine, 1981).



2.4 Generation of $O_2^{\bullet-}$ in ILs

2.4.1 Stability of $O_2^{\bullet-}$ in ILs

2.4.1.1 Short Term Stability of $O_2^{\bullet-}$ in ILs

Recently, ILs have been extensively studied as media in which to conduct electrochemical investigations due to their attractive properties, including high conductivity, high thermal stability, low volatility and wide electrochemical potential windows (Carter et al., 1991; Huang et al., 2009). They have also attracted interest as electrolytes in gas sensors. Hence, the reduction of O_2 in ILs has been investigated by many groups (Buzzeo et al., 2004a; Huang et al., 2010; O'Mahony et al., 2008).

The CV of an electrochemically active species is a popular analysis method as it provides information on the redox behavior of the species and the kinetics of reactions at the surface of the electrode. In addition, CV can also provide an insight into reaction products intermediates (Henze, 2008).

Most studies used the electrochemical generation of $O_2^{\bullet-}$ by the electroreduction of pure O_2 (AlNashef et al., 2001; Evans et al., 2004; Pozo-Gonzalo et al., 2013). However, Randström *et al.* (2007) generated $O_2^{\bullet-}$ by reducing air at 20 °C and observed a reduction peak which was about one-tenth of the reduction peak current reported by Katayama *et al.* (2005) who reduced pure O_2 at 25 °C. This ratio is plausible when taking into account the lower concentration of O_2 in air, as opposed to pure O_2 , and the lower temperature of the experiment which results in a lower diffusion coefficient. In many of these CV of O_2 studies, the mechanism was explored by fitting experimental data with simulation models.

The first report exploring the reduction of O_2 in IL was published by Carter *et al.* (1991) and involved the voltammetry of O_2 gas in 1-ethyl-3-methylimidazolium chloride/aluminum chloride using a 3 mm diameter glassy carbon (GC) electrode (Carter et al., 1991; Evans et al., 2004). A single reduction peak was observed, with no

oxidation peak (Figure 2.4) and interpreted to be due to the reduction of O_2 to $O_2^{\bullet-}$ which then reacts quickly and irreversibly with protic impurities in the IL, Eq 2.6 (AlNashef et al., 2001).

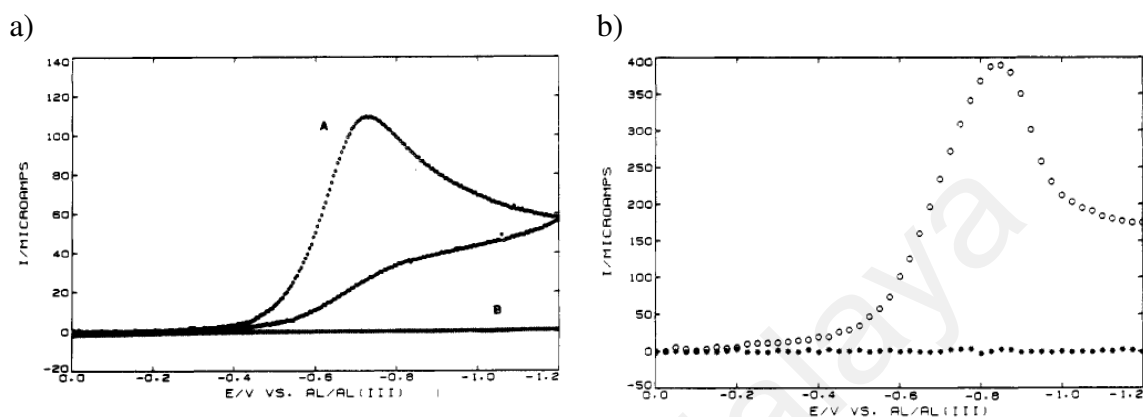


Figure 2.4: The first reported voltammetry of dioxygen in IL, a) Cyclic staircase voltammogram and b) Normal pulse voltammogram, a single cathodic peak was observed (Carter et al., 1991).

In 2001, AlNashef and coworkers investigated the electroreduction of O_2 dissolved in two ILs respectively, 1,2-dimethyl-3-*n*-butylimidazolium and 1-methyl-3-*n*-butylimidazolium cations, with anion of $[PF_6]$, using a GC macroelectrode. In 1,2-dimethyl-3-*n*-butylimidazolium hexafluorophosphate, a reduction peak was observed with no reverse oxidation peak. This was also attributed to the reaction of $O_2^{\bullet-}$ with impurities endemic in the IL. On the other hand, the electrogenerated $O_2^{\bullet-}$ oxidation was observed by CV in 1-methyl-3-*n*-butylimidazolium hexafluorophosphate, indicating its stability, Figure 2.5. Subsequently, O_2 reduction was carried out in ILs containing cations based on ammonium, morpholinium, pyrrolidinium, sulfonium, pyridinium, imidazolium and phosphonium (Evans et al., 2004; Hayyan et al., 2011; Katayama et al., 2005; Pozo-Gonzalo et al., 2013; Zigah et al., 2009).

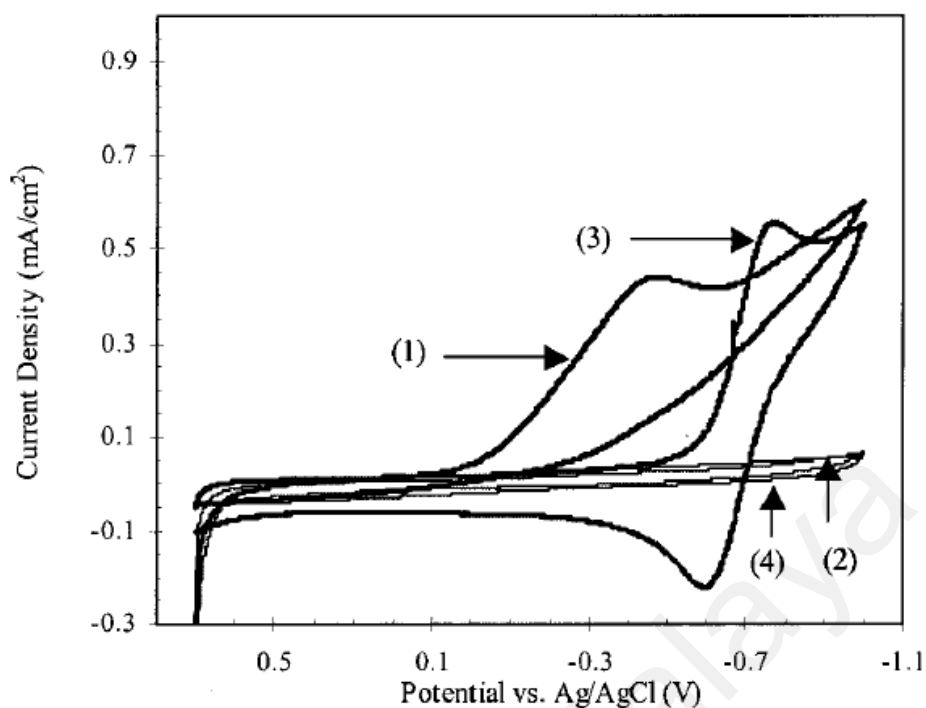


Figure 2.5: The first report of stable $O_2^{\bullet-}$ in ILs. CVs at 37°C of an IL in which $O_2^{\bullet-}$ is stable (3) [BMIm][PF₆] and unstable (1) 1,2-dimethyl-3-n-butylimidazolium hexafluorophosphate. (2) and (4) are the background voltammograms of the ILs with Nitrogen The working electrode was glassy carbon and the reference electrode was Ag/AgCl(AlNashef et al., 2001).

The type of working electrode used in CV of O_2 is an important factor in the voltammetry. Table 2.7 illustrates the effect of working electrode on the formal potential of $O_2/O_2^{\bullet-}$ redox couple in different aprotic solvents. The working electrodes that have been used for the CV of O_2 in ILs include GC, Pt, Au and HMDE. The separation between the reductive and oxidative peaks, ΔE_p , is highly dependent on the material of the working electrode. Broader voltammetry was obtained using a Pt electrode in comparison to GC and Au, in the order GC < Au < Pt. This may be due to possible product adsorption or coupled chemical reaction on Pt (Rogers et al., 2009 ; Zhang et al., 2004a).

Table 2.7: O₂/O₂^{•-} formal potentials for different electrode materials (Song & Zhang, 2008).

Solvent	Formal potentials at electrodes (V) vs. NHE			
	C	Pt	Au	Hg
AcN	-0.63	-0.65	-0.65	0.63
Py	-0.64	-0.65	-0.63	-
DMF	-0.62	-0.62	-0.64	-
DMSO	-0.54	-0.78	-0.55	-

The formal potential value becomes more positive as solvation energy increases (Song & Zhang, 2008). The degree of solvation of negatively charged O₂^{•-} increases with the acceptor number of the solvent. Therefore, as the solvent acceptor number increases, the O₂/O₂^{•-} redox potential becomes more positive. The acceptor numbers of H₂O, DMF, DMSO and AcN are 54.8, 16.0, 19.3 and 19.3 respectively (Gutmann, 1978). Table 2.8 lists the O₂/O₂^{•-} redox potential, O₂ diffusion coefficient (D_{O₂}) concentration of O₂ (C_{O₂}) and formal potential, E⁰ at scan rate of 0.1V/s in various solvents.

Table 2.8: O₂/O₂^{•-} redox potential in varying solvents (1 atm O₂) (Song & Zhang, 2008).

Solvent	C _{O₂} (mM)	D _{O₂} × 10 ⁵ (cm ² s ⁻¹)	E ⁰ (V) vs. NHE
H ₂ O	1.00	2.10	-0.16
DMSO	2.10	2.10	-0.54
DMF	4.80	5.00	-0.62
Py	4.90	5.70	-0.62
MeCN	8.10	7.20	-0.63
Quinoline	1.50	1.80	-0.63
EMIBF ₄	1.10	1.70	-0.61
PMIBF ₄	1.00	1.30	-0.58
BMIBF ₄	1.10	1.20	-0.62
[BMIm][PF ₆]	3.60	0.22	-0.64

Evans *et al.* (2004) observed different voltammograms for the IL *n*-hexyltriethylammonium bis(trifluoromethylsulfonyl)imide using working electrodes of GC, Pt, and Au, at scan rate of 0.5 V/s, the authors noticed that the background current obtained using the GC electrode was much larger than that obtained when using the Au or Pt electrodes. This large current began to swamp the current peak of interest.

In a relevant study, Rogers *et al.* (2009) noticed that the voltammetry on the Pt electrode was broader compared to Au. ΔE_p between the reduction and oxidation peaks was also greater for Pt (≈ 0.530 V on Pt, ≈ 0.270 V on Au). This might be a reflection of faster electrode kinetics on Au compared to Pt. Zhang *et al.* (2004a) suggested that the more broad voltammetry on Pt compared to Au may be due to the reversible chemical adsorption of the $O_2^{\bullet-}$ species on the Pt electrode.

In addition to working electrode, another important factor which affects voltammetry is temperature. Huang *et al.* (2009) investigated the influence of temperature on the voltammetry of ILs and found that the ΔE_p in all the ILs was reduced at higher temperatures suggesting more rapid electrode kinetics.

The cation has been reported to have the dominant effect on voltammetric behavior of O_2 reduction in IL. This was suggested by Huang *et al.* (2009) who studied the CV for the reduction of O_2 (Au vs Ag). Upon variation of the cation with a fixed anion of $[TFSI]^-$, limiting currents were different in the four ILs with varying cations of $[BMIm]^+$, *N*-butyl-*N*-methylpyrrolidinium, 1-butyl-2,3-methylimidazolium, and *n*-hexyltriethylammonium. Conversely, upon variation of the anion with a fixed cation of $[BMIm]^+$, little variation in limiting currents was observed when using anions of $[TFSI]^-$, $[PF_6]^-$ and $[BF_4]^-$. This revealed that the nature of the cation has a substantial influence on the voltammetric behavior whereas the anion did not significantly influence voltammetric behavior.

Neutral O_2 undergoes faster diffusion in the IL, which results in more steady-state-like behavior, whereas the charged radical anion $O_2^{\bullet-}$ undergoes slower diffusion which leads to a more transient reverse peak (Buzzeo et al., 2003; Evans et al., 2004; Huang et al., 2009). The diffusion of $O_2^{\bullet-}$ is most likely affected by the Coulombic interaction with the organic cations of the IL (Katayama et al., 2005). The strong interaction between $O_2^{\bullet-}$ and the cation could hinder the species more than neutral O_2 . The mass transport and the diffusion coefficient of the $O_2^{\bullet-}$ may be affected by this. In ILs, the diffusion coefficient of $O_2^{\bullet-}$ is usually 1/30 to 1/50 smaller than the diffusion coefficient of O_2 (Pozo-Gonzalo et al., 2013; Silvester et al., 2008), this is in contrast just three in the aprotic solvent AcN (Silvester et al., 2008).

2.4.1.2 Long Term Stability of $O_2^{\bullet-}$ in ILs

The majority of studies conducted on ILs have utilized CV which lasts less than a few minutes, or even a few seconds. Hence it can be considered a short-term stability test. However, this does not give an insight into the stability of $O_2^{\bullet-}$ for a longer time which is vital for exploring the practicality of using ILs as media for $O_2^{\bullet-}$ generation (Islam et al., 2009). AlNashef *et al.* (2010) and Islam *et al.* (2009) used UV-vis spectrophotometry to explore the long-term stability of $O_2^{\bullet-}$ in imidazolium based ILs. The absorbance of the peak is related to its concentration, Figure 2.6.

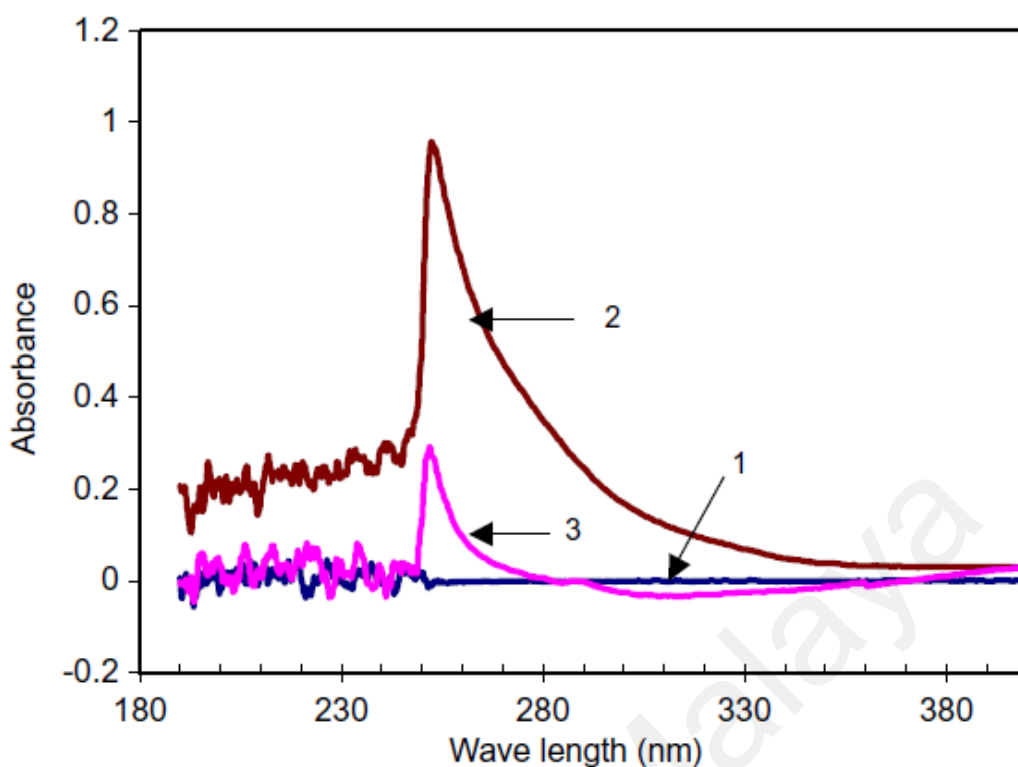


Figure 2.6: Long term stability of [BMIm][PF₆] measured by UV-vis, maximum absorbance is proportional to O₂^{•-} concentration (AlNashef et al., 2001).

Following these studies, Hayyan and co-workers explored the long term and short term stability of O₂^{•-} with many ILs comprising of cations based on piperidinium, pyrrolidinium, phosphonium, morpholinium, ammonium, and sulfonium paired with different anions (Hayyan et al., 2012d; Hayyan et al., 2012f). In order to use O₂^{•-} in various applications, the kinetics and stability of O₂^{•-} in ILs are necessary to be studied as most industrial applications require a particular period of time to utilize the reaction ingredients (Hayyan et al., 2012f). Table 2.9 lists all the studies to date which have investigated the generation of O₂^{•-} in ILs, and the techniques used.

Table 2.9: Summary of studied ILs for O₂^{•-} generation.

IL	Generation Method	Detection method	Reference
1,2-dimethyl-3- <i>n</i> -butylimidazolium hexafluorophosphate	Electrochemical	CV	(Katayama et al., 2004)
1,2-dimethyl-3-propylimidazolium bis(trifluoromethylsulfonyl)imide	Electrochemical	CV	(Katayama et al., 2004) (Evans et al., 2004) (Katayama et al., 2005)
<i>N</i> -butyl- <i>N</i> -methylpyrrolidinium bis(trifluoromethylsulfonyl)imide	Electrochemical	CV	(Randström et al., 2007) (Villagrán et al., 2006) (Huang et al., 2009) (Silvester et al., 2008)
1-butyl-2,3-methylimidazolium bis(trifluoromethylsulfonyl)imide	Electrochemical	CV	(Barnes et al., 2008) (Rogers et al., 2009) (Huang et al., 2009) (René et al., 2009)
1-butyl-3-methylimidazolium bis(trifluoromethylsulfonyl)imide	Electrochemical	CV	(Huang et al., 2009) (Ghilane et al., 2007) (AlNashef et al., 2001) (AlNashef et al., 2002) (Silvester et al., 2008)
1-butyl-3-methylimidazolium hexafluorophosphate	Electrochemical	CV	(Huang et al., 2009) (Buzzeo et al., 2003)
1-ethyl-3-methylimidazolium bis(trifluoromethylsulfonyl)imide	Electrochemical	CV	(Katayama et al., 2004) (Buzzeo et al., 2004b) (Villagrán et al., 2006) (Carter et al., 1991)

Table 2.9, continued

IL	Generation Method	Detection method	Reference
1-ethyl-3-methylimidazolium chloride mixed with AlCl ₃	Electrochemical	CV	(Zhang et al., 2004a)
1-ethyl-3-methylimidazolium tetrafluoroborate	Electrochemical	CV	(Islam et al., 2005a) (Islam & Ohsaka, 2008a) (Ding, 2009) (Zhang et al., 2004a)
1- <i>n</i> -butyl-3-methylimidazolium tetrafluoroborate	Electrochemical	CV	(Islam et al., 2005a) (Huang et al., 2009) (Zhao et al., 2010) (Ding, 2009) (Tang et al., 2005) (Zhang et al., 2004a)
1- <i>n</i> -propyl-3-methylimidazolium tetrafluoroborate	Electrochemical	CV	(Ding, 2009) (Martiz et al., 2004)
trimethylbutylammonium bis(trifluoromethylsulfonyl)imide	Electrochemical	CV	(Martiz et al., 2004)
[C ₅ H ₅ N+C ₈ F ₁₈][TFSI]	Electrochemical	CV	(Martiz et al., 2004)
[C ₅ H ₅ N+C ₁₈ H ₃₈].[TFSI]	Electrochemical	CV	(Martiz et al., 2004)
[C ₅ H ₅ N+C ₈ H ₁₈] [TFSI]	Electrochemical	CV	(Martiz et al., 2004)
[NC(CH ₂) ₄] ₄ N ⁺ ·[TFSI]	Electrochemical	CV	(Buzzeo et al., 2003)

Table 2.9, continued

IL	Generation Method	Detection method	Reference
<i>n</i> -hexyltriethylammonium bis(trifluoromethylsulfonyl)imide	Electrochemical	CV	(Buzzeo et al., 2004b) (Evans et al., 2004) (Rogers et al., 2009) (Huang et al., 2009) (Katayama et al., 2004)
trimethyl- <i>n</i> -hexylammonium bis(trifluoromethylsulfonyl)imide	Electrochemical	CV	(Zigah et al., 2009) (Katayama et al., 2004)
triethylbutylammonium bis(trifluoromethylsulfonyl)imide	Electrochemical	CV	(Ghilane et al., 2007) (Evans et al., 2004)
tris(<i>n</i> -hexyl)tetradecylphosphonium trifluorotris (pentafluoroethyl) phosphate	Electrochemical	CV	(Huang et al., 2010) (Evans et al., 2004)
tris(<i>n</i> -hexyl)tetradecylphosphonium bis(trifluoromethylsulfonyl)imide	Electrochemical	CV	(Laoire et al., 2009)
Tetrabutylammonium hexafluorophosphate [TBA][PF ₆] /AcN	Electrochemical	CV	(Laoire et al., 2009)
Lithium hexafluorophosphate (LiPF ₆) /AcN	Electrochemical	CV	(Laoire et al., 2009)
tetrabutylammonium perchlorate (TBAClO ₄) /AcN	Electrochemical	CV	(Laoire et al., 2009)
potassium hexafluorophosphate (KPF ₆) /AcN	Electrochemical	CV	(Laoire et al., 2009)
Sodium hexafluorophosphate (NaPF ₆) /AcN	Electrochemical	CV	(Hayyan et al., 2012d)
<i>N</i> -hexylpyridinium bis(trifluoromethylsulfonyl)imide	Electrochemical/ Chemical	CV/ UV-vis	(Hayyan et al., 2012d)
<i>N</i> -methoxyethyl- <i>N</i> -methylmorpholinium bis(trifluoromethylsulfonyl)imide	Electrochemical/ Chemical	CV/ UV-vis	(Hayyan et al., 2012d)
<i>N</i> -ethyl- <i>N,N</i> -dimethyl-2-methoxyethylammonium bis(trifluoromethylsulfonyl)imide	Electrochemical/ Chemical	CV/ UV-vis	(Hayyan et al., 2012d)
triethylsulfonium bis(trifluoromethylsulfonyl)imide	Electrochemical/ Chemical	CV/ UV-vis	(Hayyan et al., 2011)

Table 2.9, continued

IL	Generation Method	Detection method	Reference
N-(3-Hydroxypropyl)pyridinium bis(trifluoromethylsulfonyl)imide	Electrochemical	CV	(Hayyan et al., 2011)
[1-(3-methoxypropyl)-1-methylpiperidinium bis(trifluoromethylsulfonyl)imide	Electrochemical	CV	(Hayyan et al., 2011)
1-hexyl-1-methyl-pyrrolidinium bis(trifluoromethylsulfonyl)imide	Electrochemical	CV	(Hayyan et al., 2012f)
1-(3-methoxypropyl)-1-methylpiperidinium bis(trifluoromethylsulfonyl)imide	Electrochemical/ Chemical	CV/ UV-vis	(Hayyan et al., 2012f)
1-hexyl-1-methyl-pyrrolidinium bis(trifluoromethylsulfonyl)imide	Electrochemical/ Chemical	CV/ UV-vis	(Hayyan et al., 2012f)
triethyl (tetradecyl)phosphonium bis(trifluoromethylsulfonyl)imide	Electrochemical/ Chemical	CV/ UV-vis	(Hayyan et al., 2012e)
1-butyl-1-methylpyrrolidinium trifluoroacetate	Electrochemical/ Chemical	CV/ UV-vis	(AlNashef et al., 2010)
1-butyl-3-methylimidazolium hexafluorophosphate	Chemical	UV-vis	(AlNashef et al., 2010)
1-ethyl-3-methylimidazolium ethylsulfate	Chemical	UV-vis	(Hayyan et al., 2012b)
1-(2-methoxyethyl)-1-methylpiperidinium tris(pentafluoroethyl)trifluorophosphate	Electrochemical/ Chemical	CV/ UV-vis	(Hayyan et al., 2012b)
triethyl(tetradecyl)phosphonium tris(pentafluoroethyl)trifluorophosphate	Electrochemical/ Chemical	CV/ UV-vis	(Hayyan et al., 2013b)
1-butyl-3-methylimidazolium trifluoromethanesulfonate	Electrochemical/	CV	(Hayyan et al., 2013b)
1-butyl-1-methylpyrrolidinium bis(trifluoromethylsulfonyl)imide	Electrochemical/ Chemical	CV/ RREV/ UV-vis	(Hayyan et al., 2012c) (Schwenke et al., 2015)
1-butyl-1-methylpyrrolidinium trifluoromethanesulfonate	Chemical/ electrochemical	UV-vis / CV	(Herranz et al., 2012) (Hayyan et al., 2012c)

Table 2.9, continued

IL	Generation Method	Detection method	Reference
1-butyl-2,3-dimethylimidazolium trifluoromethanesulfonate	Chemical/ electrochemical	UV-vis / CV	(Hayyan et al., 2015b)
N-butyl-3-methylpyridinium dicyanamide	Chemical	UV-vis	(Hayyan et al., 2015b)
N-hexylpyridinium bis(trifluoromethylsulfonyl)imide	Chemical	UV-vis	(Hayyan et al., 2015b)
N-(3-hydroxypropyl)pyridinium bis(trifluoromethylsulfonyl)imide	Chemical	UV-vis	(Hayyan et al., 2015b)
N-butyl-3-methylpyridinium methylsulfate	Chemical	UV-vis	(Hayyan et al., 2015b)
1,3-Dimethylimidazolium methylsulfate	Chemical	UV-vis	(Hayyan et al., 2015b)
1-Butyl-2,3-dimethylimidazolium trifluoromethylsulfonate	Chemical	UV-vis	(Hayyan et al., 2015b)
1-Ethyl-3-methylimidazolium methylsulfate	Chemical	UV-vis	(Hayyan et al., 2015b)
1-Butyl-1-methylpyrrolidinium dicyanamide	Chemical	UV-vis	(Hayyan et al., 2015b)
1-Butyl-1-methylpyrrolidinium trifluoromethanesulfonate	Chemical	UV-vis	(Hayyan et al., 2015b)
1-(3-Methoxypropyl)-1-methylpiperidinium bis(trifluoromethylsulfonyl)imide	Chemical	UV-vis	(Hayyan et al., 2015b)
1-(2-Methoxyethyl)-1-methylpiperidinium tris(pentafluoroethyl)trifluorophosphate	Chemical	UV-vis	(Hayyan et al., 2015b)
1-Butyl-1-methylpyrrolidinium trifluoroacetate	Chemical	UV-vis	(Hayyan et al., 2015b)
1-Butyl-1-methylpyrrolidinium bis(trifluoromethylsulfonyl)imide	Chemical	UV-vis	(Hayyan et al., 2015b)

Table 2.9, continued

IL	Generation Method	Detection method	Reference
1-Hexyl-1-methyl-pyrrolidinium bis(trifluoromethylsulfonyl)imide	Chemical	UV-vis	(Hayyan et al., 2015b)
1-Ethyl-3-methylimidazolium bis(trifluoromethylsulfonyl)imide	Chemical	UV-vis	(Hayyan et al., 2015b)
Trihexyl(tetradecyl)phosphonium bis(trifluoromethylsulfonyl)imide	Chemical	UV-vis	(Hayyan et al., 2015b)
Trihexyl(tetradecyl)phosphonium tris(pentafluoroethyl)trifluorophosphate	Chemical	UV-vis	(Hayyan et al., 2015b)
N-methoxyethyl-N-methylmorpholinium bis(trifluoromethylsulfonyl)imide	Chemical	UV-vis	(Hayyan et al., 2015b)
N-ethyl-N,N-dimethyl-2-methoxyethylammonium bis(trifluoromethylsulfonyl)imide	Chemical	UV-vis	(Hayyan et al., 2015b)
Triethylsulfonium bis(trifluoromethylsulfonyl)imide	Chemical	UV-vis	(Hayyan et al., 2015b)
Trihexyl(tetradecyl)phosphonium tris(pentafluoroethyl)trifluorophosphate	Chemical	UV-vis	(Hayyan et al., 2015b)
N-methoxyethyl-N-methylmorpholinium bis(trifluoromethylsulfonyl)imide	Chemical	UV-vis	(Hayyan et al., 2015b)
N-ethyl-N,N-dimethyl-2-methoxyethylammonium bis(trifluoromethylsulfonyl)imide	Chemical	UV-vis	(Hayyan et al., 2015b)
Triethylsulfonium bis(trifluoromethylsulfonyl)imide	Chemical	UV-vis	(Hayyan et al., 2011)
trihexyl(tetradecyl)phosphonium chloride	Chemical	UV-vis	(Ahmed et al., 2015b)
trihexyl(tetradecyl)phosphonium bromide	Chemical	UV-vis	(Ahmed et al., 2015b)
trihexyl(tetradecyl)phosphonium Bis (2,4,4-trimethylpentyl)phosphinate	Chemical	UV-vis	(Ahmed et al., 2015b)

Table 2.9, continued

IL	Generation Method	Detection method	Reference
trihexyl(tetradecyl)phosphonium dicyanamide	Chemical	UV-vis	(Ahmed et al., 2015b)
trihexyl(tetradecyl)phosphonium tosylate	Chemical	UV-vis	(Buzzeo et al., 2004b)

University of Malaya

2.4.2 Destruction of Chlorinated Hydrocarbons Using O₂^{•-}

The disposal of chlorine and bromine containing waste from industry is of growing concern. Traditionally, there are various techniques to degrade these CHCs, including electrochemical, photochemical, biological and chemical oxidation, as well as incineration. However, these methods have several drawbacks such as high consumption of energy, emission of toxic by product gases (including acid gas e.g. HCl or halogen gas e.g. Cl₂), lack of economic viability, and complexity (Hayyan et al., 2012d). Hayyan and coworkers successfully used O₂^{•-} generated chemically by dissolving KO₂ in ILs for the destruction of dichlorophenol (Hayyan et al., 2012f), chlorobenzenes (Hayyan et al., 2012e) and hexachloroethane (Hayyan et al., 2012d). The authors conducted these experiments under atmospheric pressure, room temperature and with destruction of greater than 90%. The authors attributed this to the nucleophilic substitution of O₂^{•-} with chlorine atoms. Table 2.10 summarizes the chlorinated hydrocarbons destroyed, IL used and destruction percentage achieved.

Table 2.10: Destruction of chlorinated hydrocarbons using O₂^{•-} generated in ionic liquids.

CHC	IL	Destruction percentage	Ref
2,4-Dichlorophenol (DCP)	N- Methoxyethyl-N-methylmorpholinium bis(trifluoromethylsulfonyl)imide [MO1,1O2][TFSI]	>98%	(Hayyan et al., 2012f)
1,2-Dichlorobenzene (DCB)	1-(3-Methoxypropyl)-1-methylpiperidinium bis (trifluoromethylsulfonyl) imide, [MOPMPip][TFSI]	>82%	(Hayyan et al., 2012f).
1,2-Dichlorobenzene (DCB)	1-Hexyl-1-methyl-pyrrolidinium bis trifluoromethylsulfonyl)imide, [HMPYrr][TFSI]	>96.7%	(Hayyan et al., 2012f).
1,2-Dichlorobenzene(DC B)	1-(3-Methoxypropyl)-1-methylpiperidinium bis(trifluoromethylsulfonyl)imide, [MOPMPip][TFSI]	>90%	(Hayyan et al., 2012e).
1,3-Dichlorobenzene (1,3-DCB)	1-Hexyl-1-methyl-pyrrolidinium bis(trifluoromethylsulfonyl)imide, [HMPYrr][TFSI]		
1,3,5-Trichlorobenzene(TC B) Penta-chlorobenzene (PCB)			
Hexachlorobenzene (HCB)			
Hexachloroethane	1-butyl-1-methylpyrrolidinium trifluoroacetate [BMPYrr][TFA]	>98%	(Hayyan et al., 2012e)

2.4.3 Conversion of Sulfur Compounds Using $O_2^{\bullet-}$

Although $O_2^{\bullet-}$ has not been extensively studied as an oxidant in ODS, reactions of sulfur compounds with $O_2^{\bullet-}$ have been reported (Chan, 2010; Oae et al., 1981; Takata et al., 1979). Oae *et al.* (1981) found that disulfide, thiosulfinate, sodium sulfonate, sodium thiolate, thiol and thiosulfonate were readily oxidized to sulfinic and sulfonic acids. The $O_2^{\bullet-}$ was generated by dissolving KO_2 salt in solvent with the aid of 18-crown-6-ether under mild conditions (Chan, 2010; Oae et al., 1981). The reactivity was found to increase in the following order: disulfide \approx sodium thiolate \approx sodium sulfonate $<$ thiosulfonate $<$ thiosulfinate. Higher polarity solvents such as pyridine and AcN produced more favorable results than benzene, and larger amounts of crown ether increased the rate of reaction. The reaction was attributed to be due to $O_2^{\bullet-}$ nucleophilic attack and electron transfer (Oae et al., 1981; Takata et al., 1979). Sulfur compounds which are more complex, including thiouracils, thioureas and thioamides could be oxidized with $O_2^{\bullet-}$ to form amides or other corresponding hydrocarbons, as well as inorganic sulfate or elemental sulfur (Chan, 2010).

Regarding the use of $O_2^{\bullet-}$ generated in ILs for ODS, Chan *et al.* (2008) used KO_2 dissolved in [BMIm][PF₆] to react with sulfur compounds. However, it was later proven in other studies that $O_2^{\bullet-}$ reacts with imidazolium-based cations of ILs to form 2-imidazolones (AlNashef et al., 2010; Hayyan et al., 2013). Therefore, $O_2^{\bullet-}$ is not stable in this class of ILs. The author made no mention of drying the ILs before dissolution of the salt, which is an important precaution in chemical generation of $O_2^{\bullet-}$ in a solvent as $O_2^{\bullet-}$ reacts with H_2O to form H_2O_2 . Therefore, it is possible this desulfurization was caused by H_2O_2 formed from reaction of superoxide salt with H_2O in the IL, and not by $O_2^{\bullet-}$.

Ahmed *et al.* (2015b) employed KO_2 as oxidant in the ODS of DBT and TH in ILs. DBT appeared to be unreactive to the $O_2^{\bullet-}$ while TH showed up to 15% conversion after

2 h. This difference in reactivity explained to be caused by the difference in electron densities of the S atoms in in the two molecules, and the nucleophilicity of $O_2^{\bullet-}$. The IL used in the ODS also showed an effect on TH conversion, with longer alkyl chain length causing higher conversion. TH conversion was found to depend on the IL in the following order: Cyphos® IL 104 i.e. trihexyl(tetradecyl)phosphonium bis(2,4,4-trimethylpentyl)phosphinate, 15% > 1-hexyl-1-methylpyrrolidinium bis(trifluoromethylsulfonyl)imide, 8% > 1-buty-1-methylpyrrolidinium bis(trifluoromethylsulfonyl)imide [BMPyrr][TFSI], 7%.

University of Malaya

CHAPTER THREE

EXPERIMENTAL METHODOLOGY

3.1 Instruments, Accessories, Gases, Chemicals and Ionic Liquids Used

3.1.1 Instruments

1. Potentiostat/ Galvanostat (PAR Model 263A)
2. HPLC (Shimadzu)
3. GC/MS (Agilent 7890A GC WITH 5975 C MSD)
4. UV-vis spectrophotometer (PerkinElmer- Lambda 35)
5. PH Meter (Trans Instruments BP 3001)
6. Conductivity Meter (Trans instruments BC3020)
7. Density meter (Mettler Toledo DM40)
8. Viscometer (Brookfield)
9. Tensiometer (KSV Sigma 702)
10. FTIR spectrometer (Bruker tensor 27)

3.1.2 Equipment

1. Glove box (Pure Lab^{HE} GP-1)
2. Ultra-sonic cleaner (SASTEC)
3. Vacuum oven (Mettmert VO500)
4. Hotplates from Fisher Scientific (SASTEC and WiseStire)
5. Digital balance (Mettler Toledo AG204)
6. Refrigerator (TOCHIBA GR-R72MD)
7. Water circulator (Protech Model 631D)

3.1.3 Accessories

3.1.3.1 Electrodes

- a) Glassy carbon macro-electrode (BASi, 3 mm)
- b) Platinum macro-electrode (BASi, 3 mm)
- c) Ag/AgCl reference electrode (BASi, 5.7 mm)

3.1.3.2 Polishing Kit (BASi PK-4)

- a) Base Plates: heavy glass plates
- b) Substrates: brown texmet/alumina pad
- c) Polishing Suspension: 0.05 μm alumina polish

3.1.4 Gases

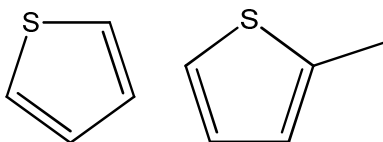
- Ultra-high pure O_2 (MOX)
- Ultra-high pure N_2 (MOX)
- Helium/ Argon (MOX)

3.1.5 Chemicals

1. Potassium superoxide (Sigma Aldrich, 99.9%)
2. Dimethyl sulfoxide (Fisher Scientific, 99.98%)
3. Diethyl ether (UNIVAR, 99%)
4. Acetonitrile (UNICHROM/Merck, HPLC grade 99.9%)
5. Isopropanol (R&M Chemicals GC Assay 99.7%)
6. Methanol (R&M Chemicals GC Assay 99.8%)
7. Distilled water
8. Deionized water

3.1.6 Sulfur Compounds

The studied sulfur compounds were purchased from Merck. The structures are shown in Scheme 3.1.



Thiophene 2-Methylthiophene

Scheme 3.1: Structures of sulfur compounds used.

Table 3.1: Sulfur compounds used in this work.

Sulfur Compound	Abbrev.	Company & purity
Thiophene	TH	Merck 99%
2-Methylthiophene	2-MTH	Merck 99%

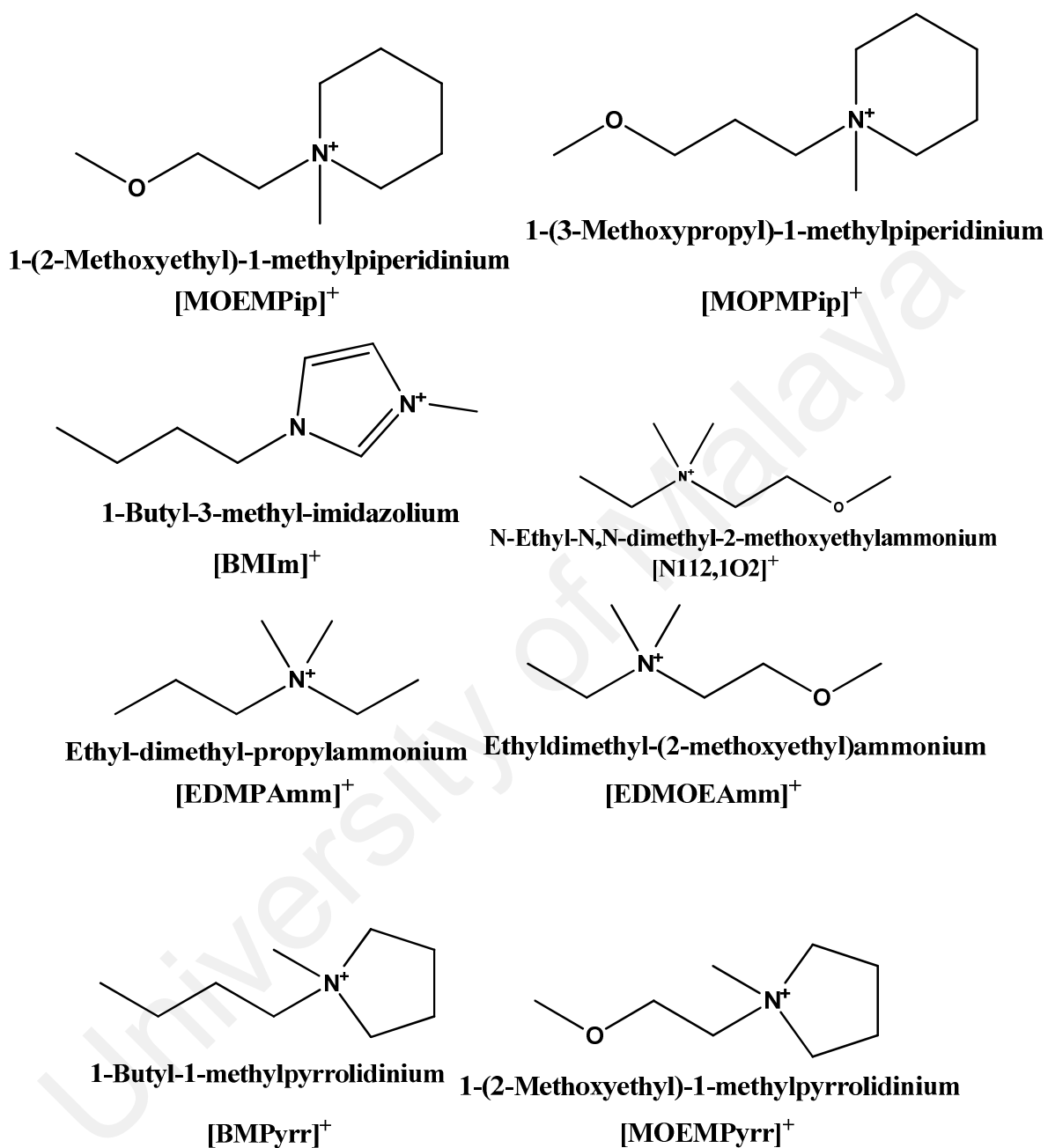
3.1.7 Ionic Liquids

The ILs used in this work were of synthesis grade (Merck). Table 3.2 lists the IL formulas, abbreviations, molecular weights, pH and densities. Scheme 3.2 and Scheme 3.3 illustrate the cation and anion structures of these ILs respectively.

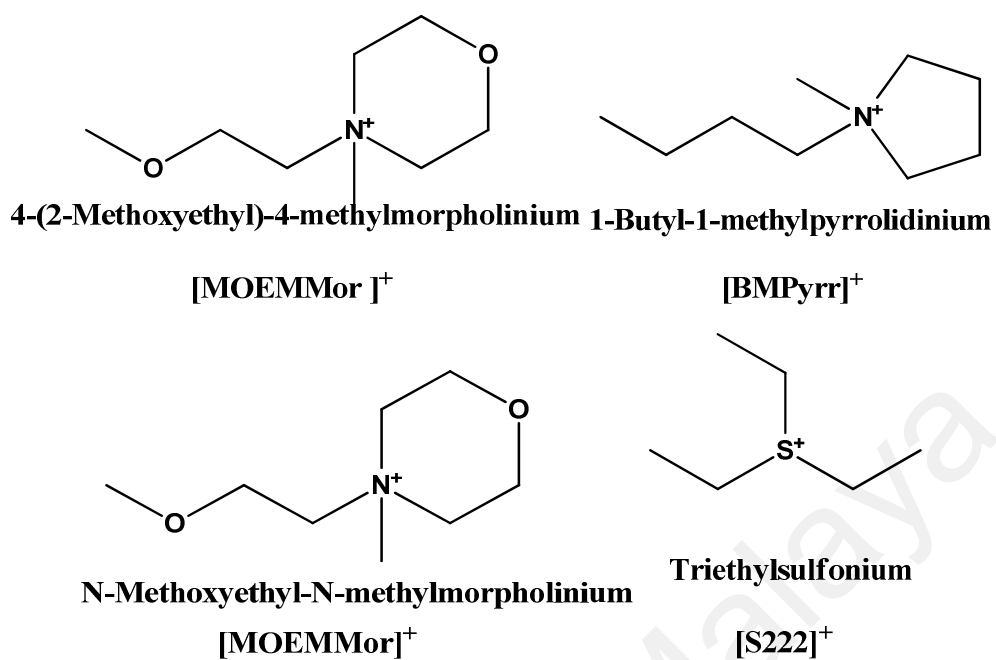
University of Malaya

Table 3.2: Ionic liquids specifications.

IL	Abbreviation	pH at 20 °C	Density at 20 °C (g/cm ³)	M.Wt. (gm/mol)	Formula	Assay (%)	Water (%)	Halides (%)
1-(2-Methoxyethyl)-1-methylpiperidinium tris(pentafluoroethyl)trifluorophosphate	[MOEMPip][TPTP]	5	-	603.27	C ₁₅ H ₂₀ F ₁₈ NOP	≥ 99.0	≤ 0.01	≤ 0.01
1-(2-Methoxyethyl)-1-methylpiperidinium bis(trifluoromethylsulfonyl)imide	[MOEMPip][TFSI]	5	1.45	452.44	C ₁₂ H ₂₂ F ₆ N ₂ O ₅ S ₂	-	-	-
1-(3-Methoxypropyl)-1-methylpiperidinium bis(trifluoromethylsulfonyl)imide	[MOPMPip][TFSI]	6	1.41	452.44	C ₁₂ H ₂₂ F ₆ N ₂ O ₅ S ₂	-	-	-
1-Butyl-3-methyl-imidazolium octylsulfate	[BMIm][OctSO ₄]	2 - 3	1.07	348.5	C ₁₆ H ₃₂ N ₂ O ₄ S	≥ 98.0	≤ 1.0	≤ 0.1
1-Butyl-3-methylimidazolium hexafluorophosphate	[BMIm][PF ₆]	-	1.38	284.19	C ₈ H ₁₅ F ₆ N ₂ P	≥ 98.0	≤ 1.0	≤ 0.1
N-Ethyl-N,N-dimethyl-2-methoxyethylammonium bis(trifluoromethylsulfonyl)imide	[N112,1O2][TFSI]	5	1.43	412.37	C ₈ H ₁₈ F ₆ N ₂ O ₅ S ₂	≥ 98.0	≤ 1.0	≤ 0.1
Ethyl-dimethyl-propylammonium bis(trifluoromethylsulfonyl)imide	[EDMPAmm][TFSI]	-	1.41	396.37	C ₉ H ₁₈ F ₆ N ₂ O ₄ S ₂	≥ 98.0	≤ 1.0	≤ 0.1
Ethyl-dimethyl-(2-methoxyethyl)ammonium tris(pentafluoroethyl)trifluorophosphate	[EDMOEAmm][TPTP]	-	-	577.23	C ₁₃ H ₁₈ F ₁₈ NOP	≥ 99.0	≤ 0.01	≤ 0.01
1-Butyl-1-methylpyrrolidinium bis(trifluoromethylsulfonyl)imide	[BMPyrr][TFSI]	5	1.4	422.41	C ₁₁ H ₂₀ F ₆ N ₂ O ₄ S ₂	≥ 98.0	≤ 1.0	≤ 0.1
1-Butyl-1-methylpyrrolidinium tetracyanoborate	[BMPyrr][B(CN) ₄]	3	0.98	257.15	C ₁₃ H ₂₀ BN ₅	-	-	-
1-(2-Methoxyethyl)-1-methylpyrrolidinium bis(trifluoromethylsulfonyl)imide	[MOEMPyrr][TFSI]	5	1.46	424.38	C ₁₀ H ₁₈ F ₆ N ₂ O ₅ S ₂	≥ 98.0	≤ 1.0	≤ 0.1
1-(2-Methoxyethyl)-1-methylpyrrolidinium tris(pentafluoroethyl)trifluorophosphate	[MOEMPyrr][TPTP]	5	-	589.24	C ₁₄ H ₁₈ F ₁₈ NOP	≥ 99.0	≤ 0.01	≤ 0.01
4-(2-Methoxyethyl)-4-methylmorpholinium tris(pentafluoroethyl)trifluorophosphate	[MOEMMor][TPTP]	5	-	605.24	C ₁₄ H ₁₈ F ₁₈ NO ₂ P	≥ 99.0	≤ 0.01	≤ 0.01
N-Methoxyethyl-N-methylmorpholinium bis(trifluoromethylsulfonyl)imide	[MOEMMor][TFSI]	5	1.51	440.38	C ₁₀ H ₁₈ F ₆ N ₂ O ₆ S ₂	≥ 98.0	≤ 1.0	≤ 0.1
Triethylsulfonium bis(trifluoromethylsulfonyl)imide	[S222][TFSI]	-	1.46	399.40	C ₈ H ₁₅ F ₆ NO ₄ S ₃	≥ 98.0	≤ 1.0	≤ 0.1

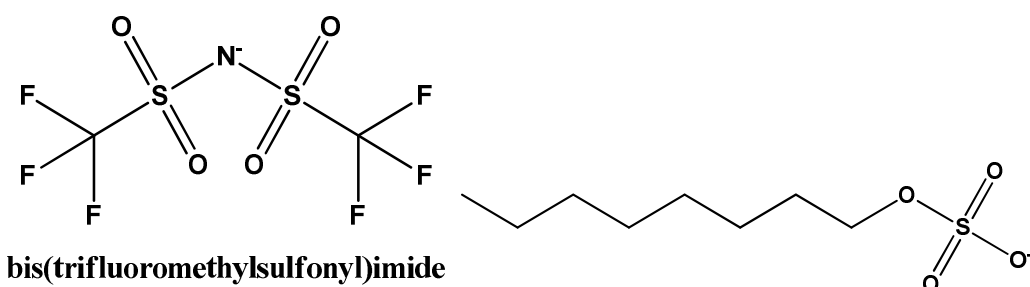


Scheme 3.2: Structures of cations



Scheme 3.2, continued

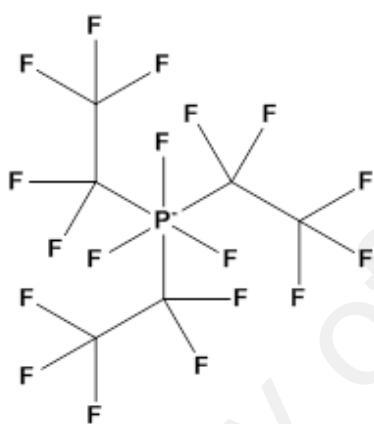
University of Malaya



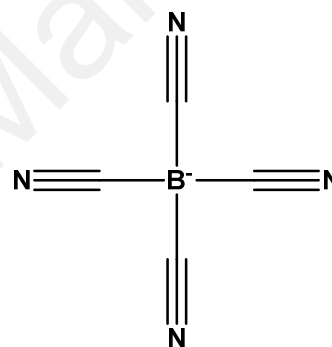
[TFSI]⁻

octylsulfate

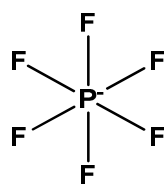
[OctSO₄]⁺



[TPTP]⁻



[B(CN)₄]⁻



[PF₆]⁻

Scheme 3.3: Structures of anions

3.2 Experimental Procedures

3.2.1 Preparation for Experiments

3.2.1.1 Drying of ILs

Prior to all experiments, the ILs were vacuum dried overnight at 60 °C. They dried to eliminate the volatile impurities and moisture since the moisture negatively affects the generation of $O_2^{\bullet-}$. It is essential to remove these electrochemically active molecules prior to voltammetric measurements (O'Mahony et al., 2008; Ohno, 2005; Zhao et al., 2010).

3.2.1.2 Acidity of ILs

The IL pH was first measured using pH strips (Merck). If the IL was acidic then a very small amount of KO_2 (0.0005-0.001 g), was added to approximately 5 g of the IL until the pH became 7. This small amount of KO_2 can neutralize the IL without having an effect on the IL electrochemical behavior.

3.2.2 Electrochemical Generation of Superoxide Ion

3.2.2.1 Cleansing of the Electrochemical Cell

The electrochemical cell and its cover were cleaned using isopropanol and dried. Connection clips to the electrodes were cleaned by removing the corroded layer on the connecting part to prevent potential and current overload during the experiments.

3.2.2.2 Polishing of Electrodes

The working electrode and counter electrode were polished using alumina solution (BASi) followed by sonication for 10 min in distilled water prior to use. This was to remove impurities on the electrode surface which may have been formed from previous experiments.

3.2.2.3 Electrochemical Procedure

The electrochemical analysis technique selected was CV as this technique is widely used to obtain useful information on O_2 reduction and $O_2^{\bullet-}$ reactions (Bard & Faulkner, 2001). The electrochemistry experiments were performed using a potentiostat/galvanostat (PAR EG&G 263A) connected to a computer with data acquisition software. The one compartment cell used was covered with a Teflon cap containing 4 holes to accommodate for i) working electrode (glassy carbon (GC) macro-electrode (BASi, 3 mm diam)) ii) counter electrode (Platinum) iii) reference electrode (Ag/AgCl (BASi)) and iv) gas sparging tube.

The content of the reference electrode was separated by a filtering material of glass frit, to avoid contamination of the investigated IL (Ohno, 2005).

The electrochemical experiments were conducted in a glove box with an atmosphere of helium or argon. Prior to the CV of O_2 , a background CV was obtained after O_2 is purged from the IL by bubbling with dry N_2 .

The IL was then bubbled with O_2 for a minimum of 30 min to ensure the IL was saturated with O_2 (AlNashef et al., 2001; Buzzeo et al., 2004a; Buzzeo et al., 2003; Ding, 2009). To further confirm equilibrium was reached, CVs were conducted at different time intervals until the cathodic peak current was a constant value. O_2 was bubbled briefly between CV runs to ensure the IL was saturated with O_2 . N_2 or O_2 bubbling was discontinued when running the CV scan.

3.2.3 Chemical Generation of $O_2^{\bullet-}$

Initially, pH strips were used to measure the IL pH. If the IL was acidic, small amounts of KO_2 were added to the IL until the pH increased to 7. DMSO (Fisher, 99.98%) and tested IL were dried overnight at 60 °C. The chemical generation of $O_2^{\bullet-}$ was achieved via

addition of KO_2 to DMSO under vigorous stirring (Islam et al., 2009; Oritani et al., 2004). A known quantity of IL was then added to the DMSO containing $\text{O}_2^{\bullet-}$ to monitor the concentration of $\text{O}_2^{\bullet-}$ with time. A UV-vis spectrophotometer (Perkin-Elmer, Lambda 35) was used to obtain the absorption spectrum of the sample. The software timedrive program was then used to measure the absorbance at the wavelength of $\text{O}_2^{\bullet-}$ absorbance every 1 or 2 s for a certain period of time. The reference solution used was DMSO.

3.2.3.1 Calibration of $\text{O}_2^{\bullet-}$ in DMSO Using UV-vis Spectrophotometer

A weighed amount of KO_2 was dissolved in a sealed vial containing dried quantity of DMSO by using a magnetic stirrer. DMSO was poured into another vial as the blank. Height of the peak corresponding to the $\text{O}_2^{\bullet-}$ was determined by running the UV-vis spectrophotometer.

3.2.4 Conversion of Sulfur Compound

Firstly, a known amount of sulfur compound and IL were added to a vial. The mixture was stirred by using the magnetic stirrer for about half an hour. After the mixture reached equilibrium, a sample was withdrawn and diluted with AcN and then analyzed using High Performance Liquid Chromatography (HPLC), as shown in Table 3.3. KO_2 was then gradually added to the IL/sulfur compound mixture under vigorous stirring. Prior to KO_2 addition and after addition, HPLC samples were obtained by withdrawing 0.1 g of IL-sulfur and adding it to 1 g of AcN (UNICHROM, HPLC grade 99.9%). This procedure of adding more KO_2 and taking HPLC samples was repeated until sulfur compound peak did not change or was not detected. Finally, the solution was extracted with DEE (UNIVAR, 99.9%) and then analyzed by GC/MS to identify the unknown products formed by conversion process.

Table 3.3: HPLC specifications and analytical conditions.

Analytical Instruments	
Shimadzu HPLC System	Liquid chromatograph LC-10AD _{VP} System controller SCL-10A _{VP} UV-vis Detector SPD-10A _{VP} Auto injector SIL-10AD _{VP} Column oven CTO-10AS _{VP} Degasser DGU-14A Shimadzu LC solution software
Column	Size: 4.6 x 150 mm, 5 μ m Description: Eclipse Plus C18 Agilent
Guard column	Agilent Zorbax reliance cartridge
Analytical Conditions	
Mobile phase	AcN:Deionized Water (75:25%), HPLC grade
Flow rate	1 ml/min, low pressure gradient
Wavelength	254 nm
Column Temperature	30 °C
Injection Volume	5 μ l

3.2.5 Physical Properties

Physical properties were measured at various temperatures (25 °C, 30 °C, 40 °C, 50 °C, 60 °C, 70 °C and 80 °C) controlled by using a jacketed vessel and water circulator. Conductivity was measured using conductivity Meter (Trans instruments BC3020) calibrated using standard conductivity solutions. Density was obtained using Mettler Toledo DM40 density meter. Viscosity was determined using Brookfield viscometer. Surface tension was obtained using KSV Sigma 702 Tensiometer.

3.2.6 GC/MS Analysis

For the chemical analysis, 1 μ l of the sample was injected into Agilent Gas system 7890A with 5975C inert MSD . A HP-5ms Agilent column (30 m length x 0.250 mm i.d., 0.25 micron film thickness) was used and helium was employed as the carrier gas with flux 1 ml/ min using splitless mode. Oven temperature was held at 30 °C for 10 min and increased to 300 °C by a rate of 10 °C/min followed by isothermal period of 20 min. Injector

temperature was set to 250 °C. Compounds were identified by reference library NIST11 and by comparison of fragmentation patterns with literature data, as shown in Table 3.4.

Table 3.4: GC/MS specifications and analytical conditions.

Analytical Instruments	
Agilent GC/MS System	GC 7890A MSD 5975C Autosampler 7693
Column	Size: 30 m (length) x 0.250 mm (i.d.) x 0.25 Micron (Film thickness) Description: HP-5ms Agilent
Analytical Conditions	
Injection Temp.	250 °C
Interface Temp	280 °C
Carrier Gas	Helium
Column inlet pressure	6.48 psi
Column flow	1 ml/min
Carrier flow	44 ml/min
Injection Volume	1 µl
Mode	Splitless
MS Libraries	NIST11

3.2.7 Solubilities of Sulfur Compounds in ILs

The solubility of sulfur compound in an IL was measured at room temperature by adding an excess amount of the sulfur compound to the IL under vigorous stirring. The mixture was allowed to settle until separated into two phases. After reaching equilibrium, a sample was carefully withdrawn from the saturated IL phase and diluted with AcN, AcN (UNICHROM, HPLC grade 99.9%) and then analyzed by HPLC using the same analysis conditions shown in Table 3.3.

CHAPTER FOUR

RESULTS AND DISCUSSION

4.1 Superoxide Ion Generation

4.1.1 Electrochemical Generation of $O_2^{\bullet-}$

4.1.1.1 Cyclic Voltammetry (Short Term Stability Test)

CVs for the reduction of O_2 in 14 ILs are carried out at scan rates of 9 and 100 mV/s, as shown in Figures A1-A14 (Appendix A). Figure 4.1 below shows the CV obtained for [EDMPAmm][TFSI].

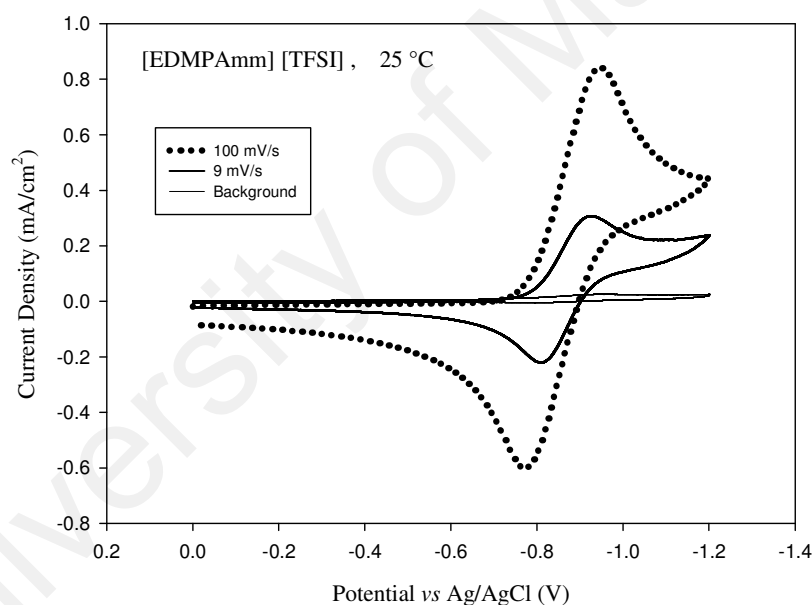


Figure 4.1: CVs in [EDMPAmm][TFSI] after sparging with oxygen and nitrogen (background) at 25 °C for scan rates of 9 and 100 mV/s.

Table 4.1 lists the ILs used in which CVs are conducted to generate $O_2^{\bullet-}$ and to study its short term stability. A background scan of the IL purged with N_2 was first taken at 100 mV/s before O_2 was bubbled in the IL. The purpose of this background scan was to ensure there were no electroactive impurities in the IL that can be reduced/oxidized within the

scanned potential range and hence interfered with the signal. The absence of peaks in the background CV confirmed the ILs were stable to electrochemical decomposition in the scanned potential range and there were no electroactive impurities.

Table 4.1: List of ILs in which CV was used to electrochemically generate $O_2^{\bullet-}$ from reduction of O_2 .

IL	IL
[MOEMPip][TPTP]	[BMPyrr][TFSI]
[MOEMPip][TFSI]	[BMPyrr][B(CN) ₄]
[MOPMPip][TFSI]	[MOEMPyrr][TFSI]
[BMIm][OctSO ₄]	[MOEMPyrr][TPTP]
[N112,1O2][TFSI]	[MOEMMor][TPTP]
[EDMPAmm][TFSI]	[MOEMMor][TFSI]
[EDMOEAmm][TPTP]	[S222][TFSI]

ILs were vacuum dried prior to use and the experiment was conducted in a glove box with strict moisture control in order to avoid absorption of moisture from the environment. This is because $O_2^{\bullet-}$ reacts readily with H_2O by the reaction shown in Eq 2.5 (Pozo-Gonzalo et al., 2013). The presence of H_2O in the IL can also significantly reduce the viscosity of the IL. This change in viscosity has an effect on the diffusion coefficient of O_2 and electrogenerated species by changing the mass transport of these species in the electrolyte (Pozo-Gonzalo et al., 2013). It has been suggested that the diffusion behaviors of O_2 and $O_2^{\bullet-}$ are highly influenced by the physical properties of IL. However, the mechanism of O_2 reduction did not differ between conventional solvents and ILs (Silvester et al., 2008).

H₂O molecules in ILs are difficult to be removed completely. This is because H₂O has a very different structure when dissolved in ILs than in its pure form. H₂O molecules in ILs are structurally associated with the ions of the ILs (Cammarata et al., 2001; Köddermann et al., 2006).

All the studied ILs were acidic without pretreatment and were neutralized by adding a small amount of KO₂. The addition of a small amount of KO₂ to the IL reacts with impurities and protons which would also react with O₂^{•-} (Marklund, 1976; Rogers et al., 2009). Numerous studies found the reduction of O₂ to be a complex process, which is sensitive to the solvent employed, especially its acidity (Dilimon et al., 2010; Sawyer & Seo, 1977; Strbac & Adžić, 1996). It is important to stress that impurities in an IL may considerably influence the results of O₂^{•-} stability in the IL by reacting with this species. Thus, the purity of the IL under investigation is an important factor to consider. For example, O₂^{•-} may appear to be unstable to the IL when in fact the reaction occurs with the existing impurities. Table 3.2 lists the specifications of the ILs studied and their purity. Most likely, the first work on O₂^{•-} generation in IL could not eliminate protic impurities in the IL which reacted with O₂^{•-}, resulting in unstable generation of O₂^{•-} (Carter et al., 1991). Using CV, AlNashef *et al.* (2001) observed O₂^{•-} was stable in [BMIm][PF₆] but unstable in [BDMIm][PF₆]. The acidity of these ILs is similar and it is also doubtful the additional methyl group in [BDMIm][PF₆] caused this instability. Therefore, the authors attributed the instability of O₂^{•-} to reaction with impurities in the IL. Impurities in ILs may also explain the inconsistency in the literature on O₂^{•-} stability of ILs with phosphonium based cations. Some research groups (Evans et al., 2004; Hayyan et al., 2012f) found that O₂^{•-} was unstable in phosphonium based ILs, while others reported it was stable (Ahmed et al., 2015b; Pozo-Gonzalo et al., 2013). This discrepancy is again likely due to impurities in the

IL. In a relevant study, Schwenke *et al.* (2015) also explained that the impurities in as-received tetraglyme without any pretreatment were the reason for the apparent instability of the glymes that other studies had related to a direct reaction of the glymes with $O_2^{\bullet-}$. In order to complete the CV, the potential was swept from a position of zero voltage down to a potential after the reduction peak (approximately ± 1 V vs. Ag/AgCl) and back to zero voltage. Figure 4.2 shows both the forward reduction peak and the backward oxidation peak in the IL after sparging with O_2 . The presence of the backward peak confirms that the generated $O_2^{\bullet-}$ is stable within the time limits of the experiments.

When the voltage is reduced, a reduction peak is formed, indicating the reduction of O_2 to $O_2^{\bullet-}$. When the voltage sweep is reversed and the voltage is increased, the generated $O_2^{\bullet-}$ is oxidized to O_2 . If the $O_2^{\bullet-}$ generated in the reduction peak reacts with the IL after being produced, it would not be available to be oxidized, and hence no oxidation peak would be observed. Thus, a backward oxidation peak indicates $O_2^{\bullet-}$ is stable in the IL. Generally, the lower the ratio of the oxidation peak is compared to the reduction peak, the more unstable $O_2^{\bullet-}$ to the IL. The absence of an oxidation peak would indicate that $O_2^{\bullet-}$ has reacted irreversibly in the IL and is unstable in this IL. This indicated $O_2^{\bullet-}$ instability in CV may be presumed to be due to $O_2^{\bullet-}$ reaction with i) the IL cation, ii) impurities in the IL or iii) electrochemical decomposition products of the IL, if the O_2 reduction potential is close to the EW limit of the IL.

The CVs for all tested ILs were asymmetrical, which was in line with the one-electron reduction of O_2 to $O_2^{\bullet-}$, which was then oxidized according to Eq 2.4. The oxidation peak on the reverse scan indicates the generated $O_2^{\bullet-}$ is stable between the time it is formed and the oxidation potential is applied, see Figure 4.2.

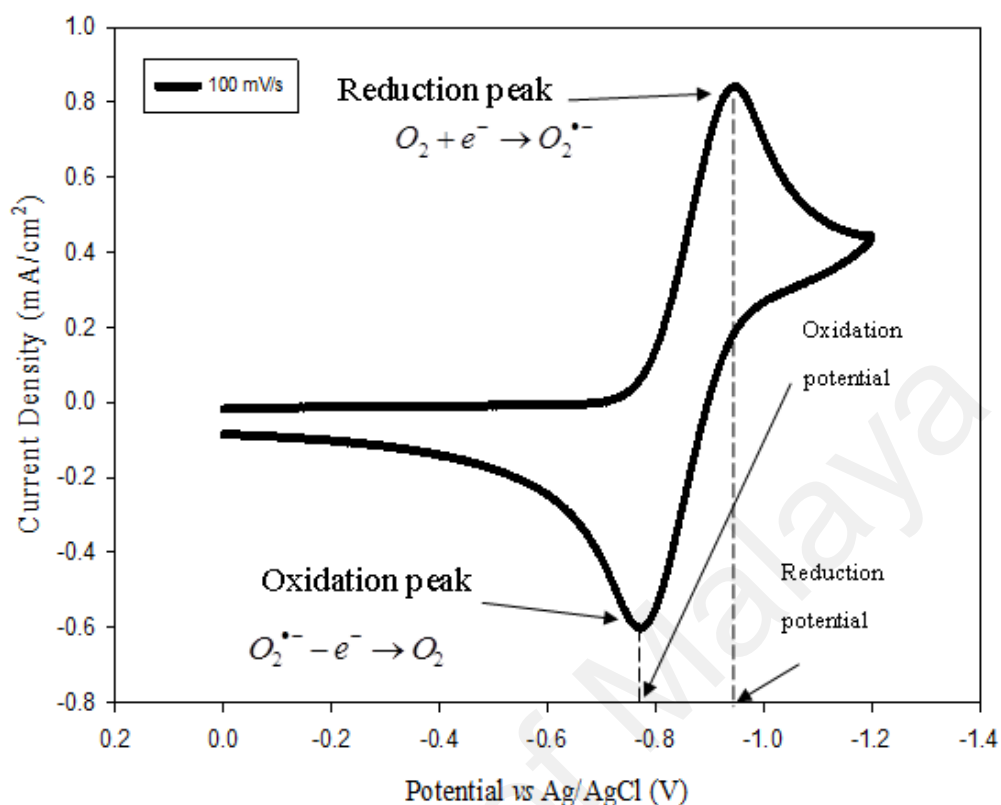


Figure 4.2: Cyclic voltammetry of O₂ in [EDMPAm][TFSI] at scan rate of 100 mV/s.

The cathodic and anodic peaks occurred at different peak potentials and currents for all the ILs studied. This difference in voltammograms is due to the variance in solubility and diffusion of O₂/O₂^{•-} in the ILs because of difference in ILs structures. The reduction potential of O₂ to produce O₂^{•-} generation was ±(-1) V in all the ILs. This is in line with the findings of other research groups (Evans et al., 2004; Huang et al., 2009). The O₂/O₂^{•-} redox potential is most affected by the degree of solvation of O₂^{•-}, as the solvation energy of neutral O₂ is not likely to be affected by the media (Sawyer, 1991).

It was observed that some of the CVs obtained in this work have small additional peaks or humps other than those corresponding to the O₂/O₂^{•-} couple. This was observed in [MOEMPip][TFSI] and [N112,1O2][TFSI], and could be due to an unknown trace

impurity or the adsorption of the IL cations on the electrode surface. Evans *et al.* (2004) observed a slight peak at a potential before the potential corresponding to O₂ reduction. The authors assigned this small pre-wave to an impurity in the IL, which was not able to be eliminated by Ar purging or vacuum drying. These small peaks were also observed by Islam *et al.* (2005b) who observed a small peak when conducting the CV of O₂ in ILs. The same group explained that cathodic peaks observed in O₂ and Ar saturated [EMIm][BF₄] could be a result of the adsorption of [EMIm]⁺ cations on the electrode surface (Islam *et al.*, 2005a). The authors explained this cation adsorption was presumably via the cation alkyl on the electrode surface. Islam and Ohsaka (2008b) also attributed electrode adsorption of [BMI]⁺ via its n-butyl chain to the slight peak obtained.

(a) *Reversibility*

The presence of a cathodic and anodic peak in all the acquired CVs indicates that O₂ reduction is reversible in all the tested ILs. For a totally irreversible processes, no anodic peak would be observed as the reduction product is not available to be reoxidized. It was then deciphered if the redox process is reversible or quasi-reversible. For a reversible redox process the following conditions must be met (Henze, 2008):

- i) ΔE_p value (Eq 4.1) should be close to 57 for a reversible reaction at 25 °C (Mabbott, 1983).

$$\Delta E_p = E_{\text{Pox}} - E_{\text{Pred}} = \frac{57}{n} \text{ mV} \tag{4.1}$$

Where ΔE_p is the potential peak separation, i.e. between reduction and oxidation peak in mV. E_{Pox} is the potential at the oxidation peak (mV), E_{Pred} is the potential of the reduction peak (mV) and n is the number of electrons transferred ($n=1$ in the case of the O₂/O₂ redox couple).

- ii) The potential of the current peak should not change with scan rate.

iii) The oxidation and reduction peaks should have equal heights.

Table 4.2 shows the anodic and cathodic peak potentials and current densities, the ratio of anodic/cathodic current density, peak potential separation, and formal potential for all ILs (Excluding [BMIm][OctSO₄], [EDMOEAmm][TPTP] and [MOEMPip][TFSI]). The results for [BMIm][OctSO₄] are shown in Table 4.4. The values for [EDMOEAmm][TPTP] and [MOEMPip][TFSI] could not be calculated due to interferences in the peaks. From the results shown in Table 4.2, it is determined that for all the studied ILs, the process cannot be considered reversible due to the following reasons:

- i) ΔE_p values are not close to 57 mV
- ii) The potential of the reduction and oxidation peaks shifted with scan rate.
- iii) The anodic and cathodic peak currents are not equal for the respective scan rate, i.e. $j_p^a / j_p^c \neq 1$.

However, the process is also not irreversible because an oxidation peak is obtained for all the ILs. Therefore, it can be considered as a quasi-reversible process. This is in agreement with the conclusion reported for the CV of O₂ in aprotic solvent systems (Sawyer, 1991) and in ILs such as [BMPyrr][TFSI] and trimethyl-*n*-hexylammonium bis(trifluoromethylsulfonyl)imide (Katayama et al., 2004).

Table 4.2: CVs of O₂ in ILs studied in this work (Excluding [BMIm][OctSO₄], [EDMOEAm][TPTP] and [MOEMPip][TFSI])

	Scan Rate :100 mV/s					Scan Rate : 9 mV/s				
	Peak Potential (V)	Peak Current density (mA/cm ²)	j_p^a / j_p^c	ΔE_p (V)	E^0 vs Ag/AgCl (V)	Peak Potential (V)	Current density (mA/cm ²)	j_p^a / j_p^c	ΔE_p (V)	E^0 vs Ag/AgCl (V)
[BMPyrr][B(CN) ₄]										
Reduction Peak	-0.91	0.81	0.68	0.17	-0.83	-0.87	0.28	0.73	0.10	-0.82
Oxidation Peak	-0.74	-0.55				-0.77	-0.20			
[MOEMPyrr][TFSI]										
Reduction Peak	-0.96	0.81	0.42	0.22	-0.85	-0.89	0.26	0.63	0.11	-0.83
Oxidation Peak	-0.74	-0.34				-0.78	-0.16			
[MOEMPyrr][TPTP]										
Reduction Peak	-0.96	0.64	0.68	0.20	-0.86	-0.95	0.36	0.62	0.16	-0.87
Oxidation Peak	-0.76	-0.43				-0.79	-0.22			
[BMPyrr][TFSI]										
Reduction Peak	-0.97	1.08	0.44	0.22	-0.86	-0.92	0.33	0.34	0.12	-0.86
Oxidation Peak	-0.75	-0.48				-0.80	-0.11			
[MOEMMor][TFSI]										
Reduction Peak	-0.91	0.48	0.48	0.27	-0.77	-0.84	0.17	0.43	0.15	-0.77
Oxidation Peak	-0.63	-0.23				-0.69	-0.07			
[S222][TFSI]										
Reduction Peak	-0.98	1.16	0.36	0.22	-0.87	-0.95	0.47	0.09	0.16	-0.87
Oxidation Peak	-0.76	-0.42				-0.79	-0.04			

Table 4.2, continued

	Scan Rate :100 mV/s					Scan Rate : 9 mV/s				
	Peak Potential (V)	Peak Current density (mA/cm ²)	j_p^a / j_p^c	ΔE_p (V)	E^0 vs Ag/AgCl (V)	Peak Potential (V)	Current density (mA/cm ²)	j_p^a / j_p^c	ΔE_p (V)	E^0 vs Ag/AgCl (V)
[EDMPAmm][TFSI]										
Reduction Peak	-0.94	0.84				-0.92	0.31			
Oxidation Peak	-0.77	-0.60	0.71	0.17	-0.86	-0.81	-0.22	0.72	0.11	-0.87
MOPMPiP][TFSI]										
Reduction Peak	-1.20	0.54				-1.05	0.21			
Oxidation Peak	-0.62	-0.19	0.34	0.59	-0.91	-0.75	-0.05	0.24	0.30	-0.90
[N112,1O2][TFSI]										
Reduction Peak	-0.94	1.03				-0.90	0.37			
Oxidation Peak	-0.72	-0.52	0.51	0.23	-0.83	-0.76	-0.16	0.45	0.14	-0.83
[MOEMPip][TPTP]										
Reduction Peak	-1.32	0.82				-1.14	0.30			
Oxidation Peak	-0.74	-0.52	0.63	0.58	-1.03	-0.88	-0.19	0.64	0.27	-1.01

j_p^a / j_p^c = ratio of anodic current density to cathodic one

ΔE_p = Peak potential separation (separation between the oxidative and reductive peaks)

E^0 vs Ag/AgCl (V) = Formal potential (($E_{pred} + E_{pox}$)/ 2)

(b) CV of Imidazolium Based IL

The CV obtained for the imidazolium based IL, [BMIm][OctSO₄], is shown in Figure 4.3. For scan rate of 9 mV/s, a reduction peak occurs at -0.83 mV/s, with a current density of 0.22 mA/cm². The oxidation peak occurs at -0.41 mV/s, with a current density of -0.08 mA/cm². For scan rate of 100 mV/s, a single reduction peak occurs at -1.51 mV/s with a current density of 1.11 mA/cm². The results suggest that O₂^{•-} is stable in the short term in [BMIm][OctSO₄].

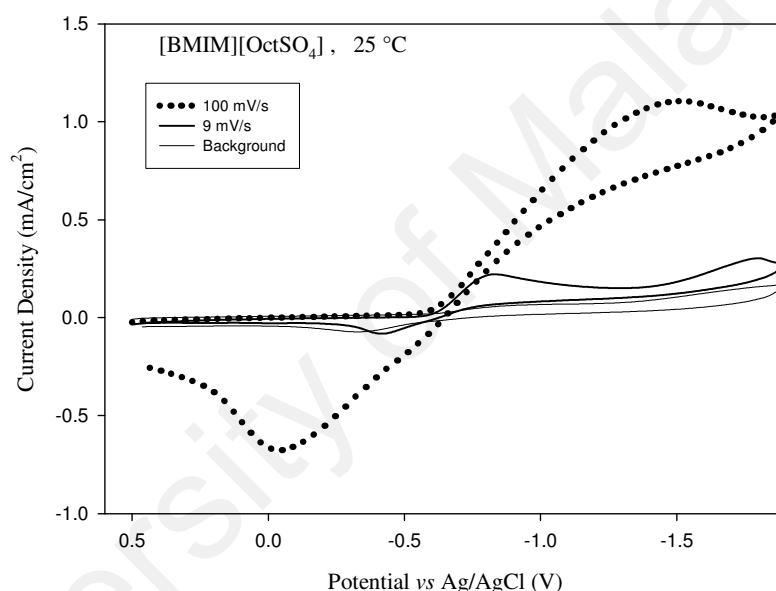


Figure 4.3: CVs in [BMIm][OctSO₄] after sparging with oxygen and nitrogen (background) at 25 °C for scan rates of 9 and 100 mV/s.

Several studies reported the voltammetry of the imidazolium based cation which is reported in this work, [BMIm]⁺, but with other anions as shown in Table 4.3 (AlNashef et al., 2001; AlNashef et al., 2002; Ghilane et al., 2007; Huang et al., 2009; Silvester et al., 2008; Hayyan et al., 2013b). However, some of these studies cannot be compared with this work to decipher the effect of anion on the CV as the CVs were conducted using a different working electrode such as Au or Pt (Buzzeo et al., 2003; Huang et al., 2009; Silvester et al., 2008) or using a different scan rate. The effect of working electrode substrate on CV and the scan rate prevents a fair comparison with these results.

Table 4.3: The CV of 1-butyl-3-methylimidazolium ILs with different anions.

IL	Reference
1-butyl-3-methylimidazolium	(Huang et al., 2009)
bis(trifluoromethylsulfonyl)imide	(Ghilane et al., 2007) (AlNashef et al., 2001)
1-butyl-3-methylimidazolium hexafluorophosphate	(AlNashef et al., 2002) (Silvester et al., 2008) (Huang et al., 2009)
1-butyl-3-methylimidazolium trifluoromethanesulfonate	(Hayyan et al., 2013b)

On the other hand, Hayyan *et al.* (2013b) and AlNashef *et al.* (2001) used the same GC working electrode and reference electrode as in this work. Therefore, for a scan rate of 100 mV/s, the results of [BMIm][OctSO₄] can be compared with [BMIm][PF₆] of AlNashef *et al.* (2001). At scan rate of 9 mV/s, the result can be compared with [BMIm]⁺ paired with trifluoromethanesulfonate, [TfO]⁻, of Hayyan *et al.* (2013b). The comparison between the CV of these ILs with the CV for [BMIm][OctSO₄] in this work is illustrated in Table 4.4.

At a scan rate of 100 mV/s, the O₂^{•-} reduction peak in [OctSO₄]⁻ occurs at a much more negative potential than in [PF₆]⁻ (AlNashef *et al.*, 2001). The current density produced at this reduction peak is also much greater in [OctSO₄]⁻ than in [PF₆]⁻. The values for ratio of oxidation/reduction peak current densities are close for both ILs, 0.6 for [OctSO₄]⁻ compared to 0.5 for [PF₆]⁻. The peak separation for [OctSO₄]⁻ is more than four times the separation found for [PF₆]⁻.

At scan rate of 9 mV/s, [OctSO₄]⁻ produced a similar oxidation and reduction peak potential compared to [TfO]⁻ (Hayyan *et al.*, 2013b). However, the separation between

oxidation and reduction peak potentials in $[\text{OctSO}_4]^-$ was three times the separation found for $[\text{TfO}]^-$.

Table 4.4: Comparison of redox peaks for ILs with 1-butyl-3-methylimidazolium cation and different anions. Working electrode, GC, reference electrode Ag/AgCl

Anion and scan rate	$\text{O}_2^{\bullet-}$ potential peak	Peak Potential (V)	Current density (mA/cm ²)	j_p^a / j_p^c	ΔE_p (V)	E^0 vs Ag/AgCl (V)	Ref
$[\text{OctSO}_4]^-$ 100 mV/s	Reduction Peak	-1.51	1.11	0.61	1.47	-0.78	This work
	Oxidation Peak	-0.05	-0.68				
$[\text{PF}_6]^-$ 100 mV/s	Reduction Peak	-0.86	0.34	0.50	0.32	-0.7	(AlNashef et al., 2001)
	Oxidation Peak	-0.54	-0.17				
$[\text{OctSO}_4]^-$ 9 mV/s	Reduction Peak	-0.83	0.22	0.37	0.42	-0.62	This work
	Oxidation Peak	-0.413	-0.08				
$[\text{TfO}]^-$ 9 mV/s	Reduction Peak	-0.70	0.34	0.26	0.15	-0.63	(Hayyan et al., 2013b)
	Oxidation Peak	-0.55	-0.09				

$$j_p^a / j_p^c = \text{ratio of anodic current density to cathodic one}$$

ΔE_p = Peak potential separation (separation between the oxidative and reductive peaks)

E^0 vs Ag/AgCl (V) = Formal potential $((E_{pred} + E_{pox})/2)$

(c) CV of Ammonium Based ILs

For the CV of $[\text{EDMPAmm}][\text{TFSI}]$ (Figure 4.1), the ratio of the current density of the anodic peak to cathodic peak is 0.7 at a slow scan rate of 9 mV/s, suggesting that $\text{O}_2^{\bullet-}$ is very stable in $[\text{EDMPAmm}][\text{TFSI}]$. The high stability may be expected for ammonium based ILs as $\text{O}_2^{\bullet-}$ can form an ionic salt of tetramethylammonium superoxide, $(\text{CH}_3)_4\text{NO}_2$ (Sawyer & Valentine, 1981).

The CV of $[\text{EDMOEAm}][\text{TPTP}]$ scanned from 0 to -1.2 V is shown in Figure 4.4. An interesting observation was made in that the current density of the oxidation peak was

much greater than the current density of the reduction peak. For the redox of $O_2/O_2^{\bullet-}$, the oxidation the current density should be the same or less. It was also noticed that the current density increased after the $O_2^{\bullet-}$ reduction peak.

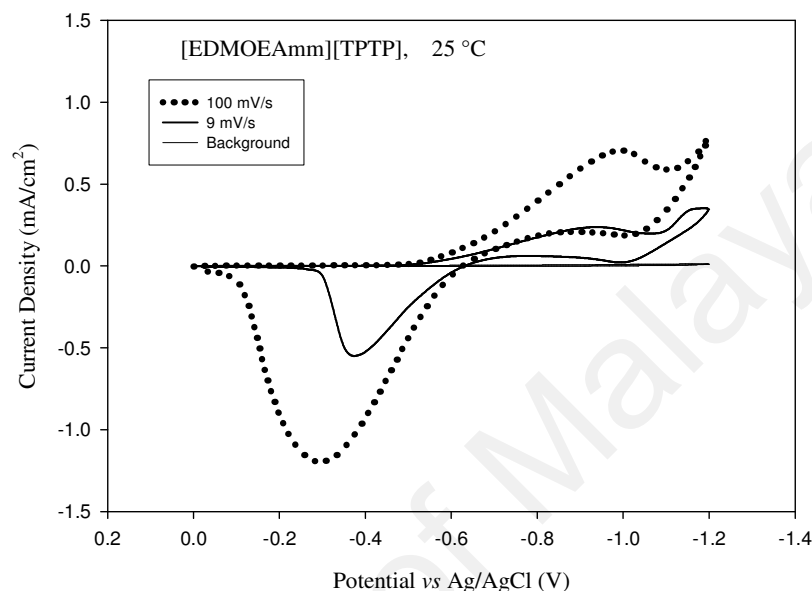


Figure 4.4: CVs in [EDMOEAmm][TPTP] (0 to -1.2 V), after sparging with oxygen and nitrogen (background) at 25 °C for scan rates of 9 and 100 mV/s.

The IL was then purged with N_2 to remove O_2 and no peak was observed for the background scan. This suggested that the disturbance was not caused by an impurity but by a species that was produced from the reduction of O_2 . To further investigate, the range of potential scanned was widened to a scan of 0.2 to -1.7 V, as shown in Figure 4.5. As can be seen in Figure 4.5, for a scan rate of 100 mV/s at an extended range, a second cathodic peak (b) occurs at -1.27 V. It was also observed that a small second anodic peak (c) was formed at -0.98 V. This second anodic peak was not present when the IL was scanned from 0 to -1.2 V.

The following explanation is suggested: at scan rate 100 mV/s, two reduction peaks were obtained because at the first peak (a) O_2 was reduced to $O_2^{\bullet-}$ at -1.04 V, Eq 2.1. Subsequently, a second peak (b) was obtained at -1.27 V due to $O_2^{\bullet-}$ further reduction to

O_2^{2-} (i.e. peroxide anion), Eq 4.2. This further reduction of $O_2^{\bullet-}$ to O_2^{2-} is in accordance with Sawyer and Roberts using DMSO as a medium for $O_2^{\bullet-}$ generation with Au and Hg as electrodes (Sawyer & Roberts Jr, 1966). When the scan was reversed, an anodic peak (c) was observed when O_2^{2-} was oxidized to $O_2^{\bullet-}$ at -0.98 V, Eq 4.3. Subsequently, another anodic peak (d) was observed when $O_2^{\bullet-}$ was further oxidized to O_2 at -0.33 V, Eq 4.4. The unexpected large oxidation peak observed in Figure 4.4 can be explained by the reaction of produced O_2^{2-} and undissolved O_2 in the IL to form two $O_2^{\bullet-}$ species, Eq 4.5. Therefore, the sources of $O_2^{\bullet-}$ oxidized at peak (d) were from (1) $O_2^{\bullet-}$ which was not further reduced to O_2^{2-} , 2) $O_2^{\bullet-}$ formed from the one-electron oxidation of O_2^{2-} and 3) $O_2^{\bullet-}$ formed from the reaction of O_2^{2-} with O_2 .

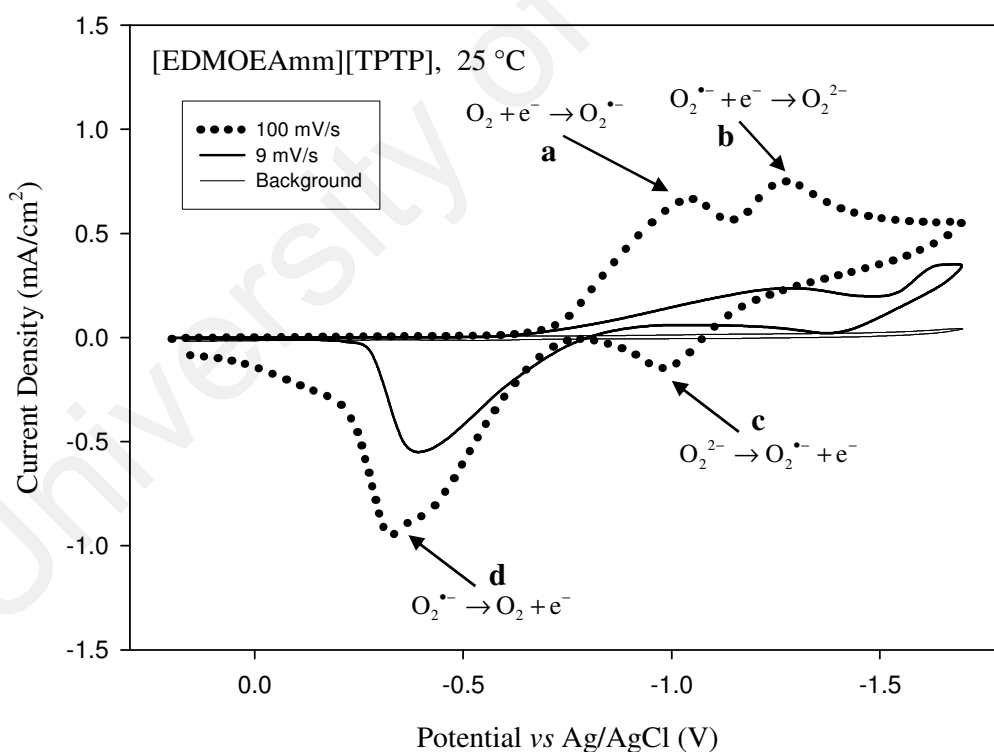


Figure 4.5: CVs in [EDMOEAm][TPTP] (0.2 to -1.7 V), after sparging with oxygen and nitrogen (background) at 25 °C for scan rates of 9 and 100 mV/s.



Katayama *et al.* (2004) observed similar results for electroreduction of O_2 in trimethyl-*n*-hexylammonium bis(trifluoromethylsulfonyl)imide (Au working electrode, scan rate of 50 mV/s). Similarly, two cathodic peaks are detected, as illustrated in Figure 4.6. However, on the reverse scan, a secondary anodic peak corresponding to O_2^{2-} oxidation to $\text{O}_2^{\bullet-}$ was not observed. Similarly, an anodic peak corresponding to O_2^{2-} oxidation to O_2 was also not observed in DMSO (Katayama *et al.*, 2004; Sawyer & Roberts Jr, 1966). Katayama observed a broad anodic peak superimposed on the $\text{O}_2^{\bullet-}$ oxidation peak which was ascribed to O_2^{2-} oxidation to O_2 , Eq 4.6. However, this peak was not observed in the present work. Katayama *et al.* (2004) reported similar results for [BMPyrr][TFSI]. Therefore, this is not exclusive to ammonium cation based ILs. Of the studied ILs in this work, the large oxidation peak was only identified for [EDMOEAm][TPTP].



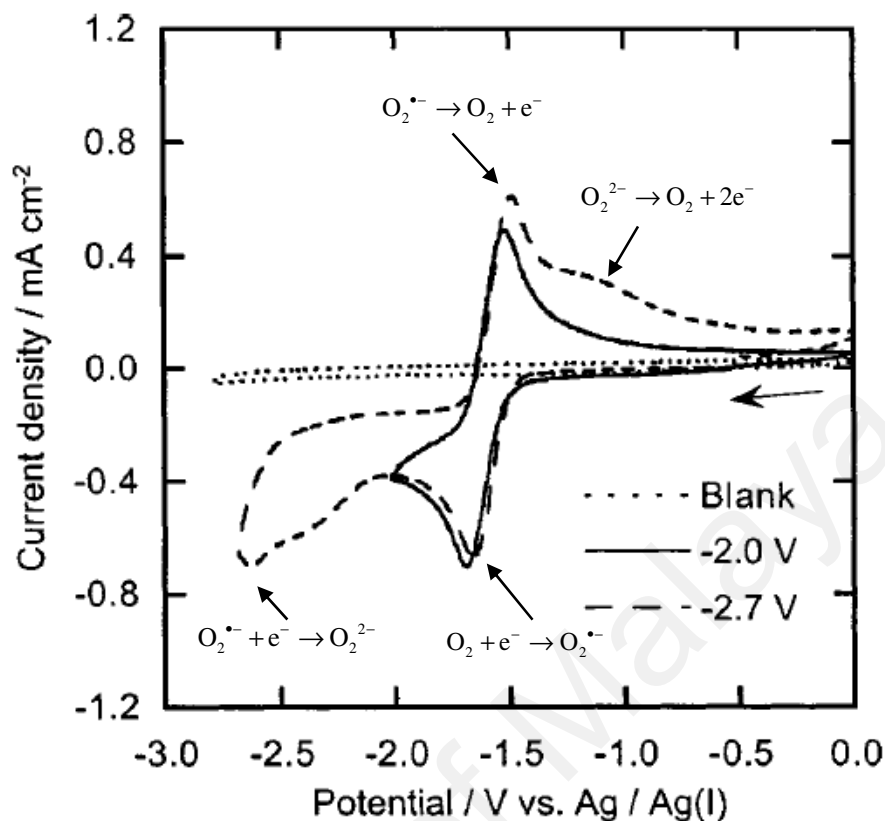


Figure 4.6: CVs of a Au electrode in in trimethyl-n-hexylammonium bis(trifluoromethylsulfonyl)imide [TMHA][TFSI] before and after saturation with O_2 at 25 °C. Scan rate 50 mV/s (IUPAC voltammogram convention) (Katayama et al., 2004).

(d) *CV of Pyrrolidinium Based ILs*

The CV for [BMPyrr][TFSI] is as shown in Figure 4.7. At a scan rate of 9 mV/s, the reduction peak is formed at -0.92 V with a current density 0.33 mA/cm² and oxidation peak occurs at -0.80 V with a current density -0.11 mA/cm². At a scan rate of 100 mv/s, the reduction peak is formed at -0.97 V with a current density 1.08 mA/cm² and the oxidation peak occurs at -0.75 V with a current density -0.48 mA/cm². The formal redox potential was -0.86 V. This indicates $O_2^{\bullet-}$ is stable in this IL. Similar results were obtained by Katayama and coworkers. They studied the electrochemical behavior of $O_2/O_2^{\bullet-}$ in this IL using Au and Pt disk-macroelectrode as working electrodes at a scan rate of 50 mV/s, see Figure 4.8 (Katayama et al., 2004; Katayama et al., 2005).

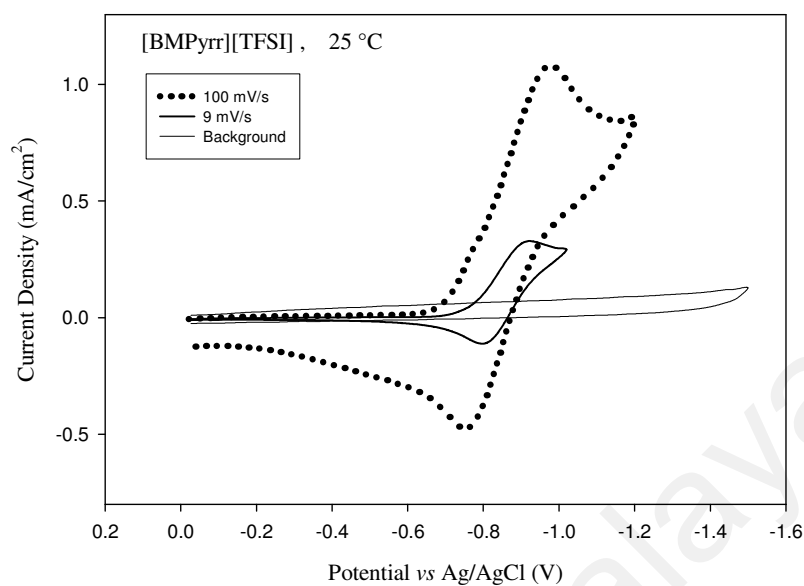


Figure 4.7: CVs in [BMPyrr][TFSI], after sparging with oxygen and nitrogen (background) at 25 °C for scan rates of 9 and 100 mV/s.

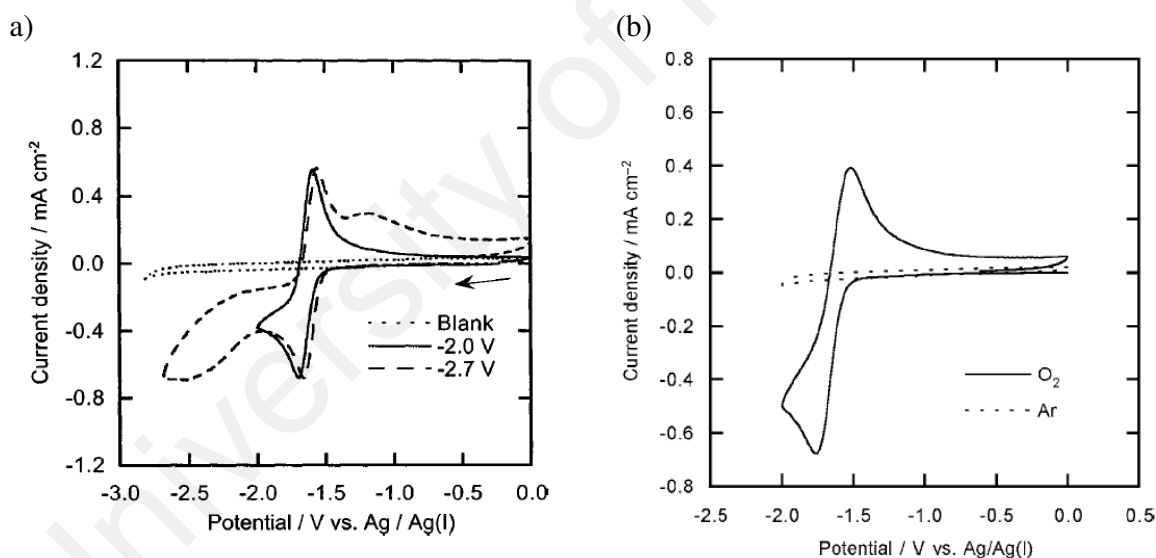


Figure 4.8: CVs of O₂ in [BMPyrr][TFSI] at 25 °C using scan rate of 50 mV/s. a) Au electrode (Katayama et al., 2004) and b) Pt electrode (Katayama et al., 2005)

(e) CV of Sulfonium Based ILs

The sulfonium based IL, [S222][TFSI], Figure 4.9, appears to be most reactive as O₂^{•-} is unstable with almost no oxidation peak at scan rate of 9 mV/s. The ratio of current density of oxidation peak/current density of reduction peak is by far the lowest at 0.09 for 9 mV/s

and 0.36 for 100 mV/s, even though it is difficult to make quantitative evaluations with CV (Katayama et al., 2004). Further analysis is required to elucidate $O_2^{\bullet-}$ stability using long term stability test.

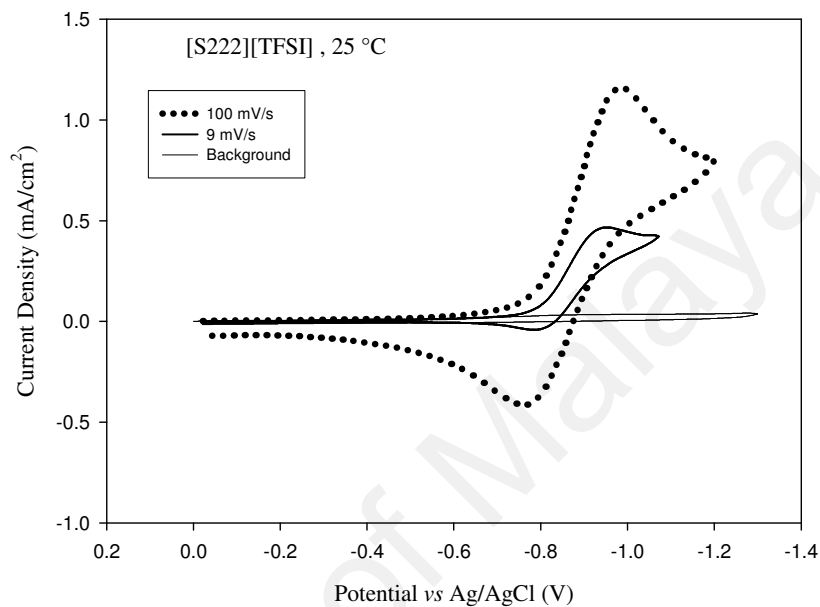


Figure 4.9: CVs in [S222][TFSI], after sparging with oxygen and nitrogen (background) at 25 °C for scan rates of 9 and 100 mV/s.

4.1.2 Chemical Generation of $O_2^{\bullet-}$

In this work, chemical generation of $O_2^{\bullet-}$ was achieved via dissolution of KO_2 in the ILs. To study the long term stability of $O_2^{\bullet-}$, ILs with different cation and anion combinations were introduced to DMSO with generated $O_2^{\bullet-}$. The decrease in concentration of $O_2^{\bullet-}$ was then monitored.

4.1.2.1 Long Term Stability of $O_2^{\bullet-}$

In order to investigate the long term stability of $O_2^{\bullet-}$ in ILs, 15 ILs with different cation and anion combinations were introduced to $O_2^{\bullet-}$ generated in DMSO, Table 4.5. The decreasing absorbance of $O_2^{\bullet-}$ was then monitored every 1-2 s using UV-vis in order to determine the stability and kinetics of the $O_2^{\bullet-}$ in the presence of the IL. The change of superoxide absorbance peak with time obtained for these ILs is shown in Figures B1-B15 (Appendix B). To the best of my knowledge, this was the first time that this precise time interval was used. Previous studies have monitored the absorbance of $O_2^{\bullet-}$ by scanning the absorbance spectra at larger intervals such as 10 min (Ahmed et al., 2015b). Recently, Schwenke *et al.* (2015) used 1 min as the minimum time interval for only the first 30 min of the reaction, then the time interval was increased to every 5 min and finally every 30 min, until the reaction had taken place for 20 h. It is expected that using this precise time interval of 1-2 s would provide more reliable and accurate results, especially for rapid reactions. In addition to the precise time interval, in this work the reaction was monitored for a long period of time of up to 24 h. By contrast, the majority of previous studies monitored the reaction for only up to 2 h, with only one recent study following the reaction up to 20 h.

Table 4.5: Examined ILs as media for the long term stability of $O_2^{\bullet-}$.

IL	IL
[MOEMPip][TPTP]	[BMPyrr][TFSI]
[MOEMPip][TFSI]	[BMPyrr][B(CN) ₄]
[MOPMPip][TFSI]	[MOEMPyrr][TFSI]
[BMIm][OctSO ₄]	[MOEMPyrr][TPTP]
[BMIm][PF ₆]	[MOEMMor][TPTP]
[N112,1O2][TFSI]	[MOEMMor][TFSI]
[EDMPAmm][TFSI]	[S222][TFSI]
[EDMOEAmm][TPTP]	

As elaborated in Section 2.3.3, there are many superoxide salts such as NaO₂, CsO₂, RbO₂ and KO₂. The superoxide salt KO₂ was selected as it is the most stable, economical and commercially available. There are many aprotic solvents in which $O_2^{\bullet-}$ is stable such as AcN, DMF and acetone. The aprotic solvent DMSO was selected as KO₂ is insoluble in most aprotic organic solvents but is slightly soluble in DMSO (Kim et al., 1979) and DMSO can dissolve the highest amount of KO₂ without reaction compared with other aprotic solvents (Schwenke et al., 2013). The concentration of $O_2^{\bullet-}$ in DMSO can be obtained using UV-vis as $O_2^{\bullet-}$ absorbs UV-light, with maximum absorbance at wavelengths of 250–275 nm (Hayyan et al., 2012f; Schwenke et al., 2013).

The concentration of $O_2^{\bullet-}$ can be obtained from the absorbance. It was found that the Beer-Lambert law was valid as the relationship between absorbance and concentration showed a good fit with linear regression. The relationship obtained from this calibration is concentration (M or mol/l) = 0.00132 A, R² = 0.986.

Eq 4.7 describes the Beer-Lambert Law, which is the principal law in spectrometry (Casas & Sordo, 2011).

$$A = a \cdot b \cdot c$$

4.7

Where A is the absorbance of a solution, c is the concentration of the absorbing species and b is the path-length of the radiation in the absorbing medium. When the concentration c is in mol L⁻¹ and b is in cm, then the constant a is expressed in L mol⁻¹ cm⁻¹. In this case, it is given the symbol ϵ and is known the molar extinction coefficient or molar absorptivity (Casas & Sordo, 2011).

Maximum absorbance peaks of O₂^{•-} at approximately 260 ± 10 nm were observed for the studied ILs. It can be seen from the plots of absorbance vs time shown in Figs B1-B15 (Appendix B) that morpholinium [Mor]⁺, ammonium [Amm]⁺, piperidinium [Pip]⁺ and pyrrolidinium [Pyr]⁺ based ILs are more stable than imidazolium [Im]⁺ and sulfonium [S]⁺ based ILs as there was a drastic drop in absorbance for the latter two ILs. For imidazolium based ILs, the reaction lasted less than 1 h, while only up to 30 s for the sulfonium based IL.

Figure 4.10 shows the decrease of peak height of O₂^{•-} with time in the DMSO/IL solutions for three ILs: [BMPyr][TFSI], [N112,1O2][TFSI] and [MOPMPip][TFSI]. From the plots, it can be observed that O₂^{•-} is more stable with [N112,1O2][TFSI] than [MOPMPip][TFSI] and [BMPyr][TFSI] as the absorbance decreases at a slower rate.

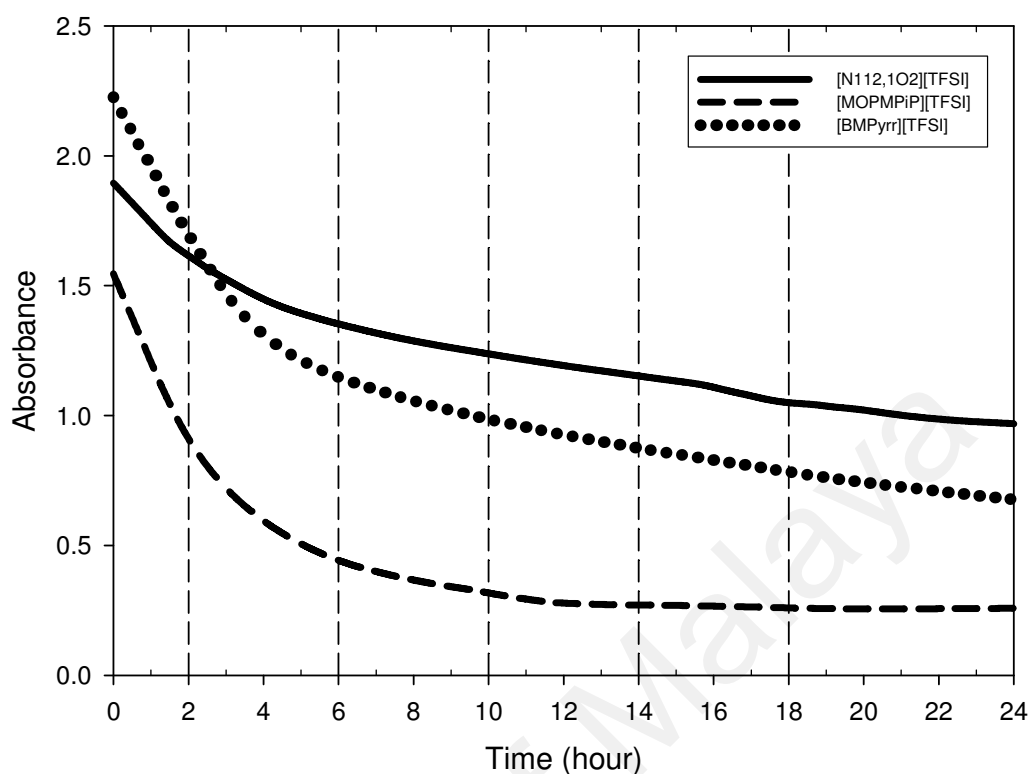


Figure 4.10: The change of $O_2^{\bullet-}$ absorbance peak with time for [BMPyrr][TFSI], [N112,1O2][TFSI] and [MOPMPip][TFSI] in DMSO.

4.1.2.2 Kinetics Study

Assuming the added IL into DMSO was in large excess compared to $O_2^{\bullet-}$, the effect of IL concentration was negligible and the reaction may follow the pseudo 1st order reaction (Hayyan et al., 2015b). This assumption is in line with AlNashef *et al.* (2010) and Islam *et al.* (2009). However, other studies (Afanas'ev, 1989; Mohammad et al., 2001; Sawyer, 1991) suggested both pseudo 1st and 2nd order reactions and determined rate constants of k_1 and k_2 for $O_2^{\bullet-}$ with various reactants. The derivation of the equations used to obtain the pseudo 1st order and pseudo 2nd order models is shown in Appendix C.

It was found that for all the ILs studied, the reaction showed a good fit when the reaction time was divided into smaller 2 to 6 h zones before reaching steady state, as opposed to considering the overall reaction time. Figure 4.11 shows the plot of $\ln(\text{concentration in mol/l})$ vs time for pseudo 1st order model and $(1/\text{concentration in mol/l})$ vs time for pseudo

2nd order model. The more linear these graphs are, the better the agreement with the respective model. As can be seen there is a good fit in the beginning of the reaction but, as the reaction progresses, the line deviates from the linear trend. Most studies monitored the reaction for the first 2 h and hence a good fit was obtained (Ahmed et al., 2015b; Hayyan et al., 2015b). However, these results showed this good fit is not constant for the overall reaction time if the reaction time is extended.

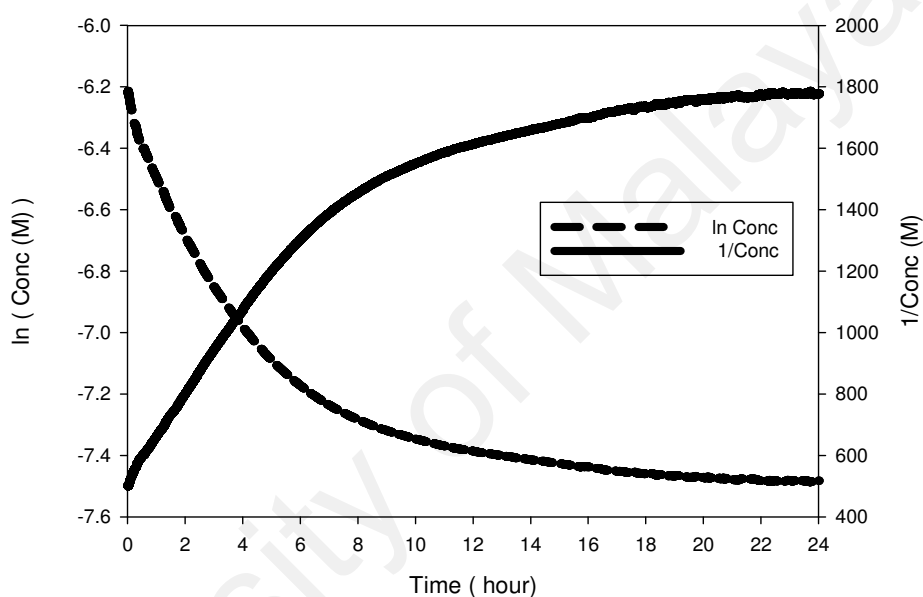


Figure 4.11: The change of O₂^{•-} ln(concentration) and 1/ concentration with time for [MOEMPyrr][TPTP] in DMSO.

Table 4.6: Rate constant of O₂^{•-} in DMSO containing [MOEMPyrr][TPTP]

[MOEMPyrr] [TPTP]	0-2 h	2-6 h	6-10 h	10-14 h	14-18 h	18-24 h	Overall
k ₁ (s ⁻¹)	6.022×10 ⁻⁵	3.342×10 ⁻⁵	1.174×10 ⁻⁵	ss	ss	ss	2.851×10 ⁻⁵ (0-10 h)
R ²	0.987	0.988	0.979	ss	ss	ss	0.922
k ₂ (M ⁻¹ s ⁻¹)	3.933×10 ⁻²	3.514×10 ⁻²	1.686×10 ⁻²	ss	ss	ss	2.958×10 ⁻² (0-10 h)
R ²	0.996	0.997	0.985	ss	ss	ss	0.973

k₁, pseudo 1st order rate constant. k₂, pseudo 2nd order rate constant, ss= steady state

The following points were observed from the analysis of the rate constants of the ILs at different zones:

- i) Overall marginally higher R^2 for k_2 than k_1 in the first 2 h.
- ii) The value of k_1 and k_2 generally decreases with time.
- iii) R^2 for overall reaction time usually lower than when divided into zones

In order to quantify the rate stability, the value of k_2 for the first 2 h of reaction was used. This is because overall there is a marginally higher R^2 for k_2 than for k_1 in first 2 h.

Table 4.7 lists the ILs in order of decreasing stability, i.e. increasing value of k_2 . It should be noted that for reactions that achieved steady state before 2 h, i.e. imidazolium and sulfonium based ILs, the reaction was only considered until steady state was achieved.

Table 4.7: Pseudo 2nd order rate constants (k_2 in $M^{-1} s^{-1}$) for reaction of $O_2^{\bullet-}$ with ILs in DMSO, in order of decreasing stability of $O_2^{\bullet-}$

IL	0-2 h	R ²
N-Methoxyethyl-N-methyl morpholinium bis(trifluoromethylsulfonyl)imide	4.732×10^{-3}	0.984
4-(2-Methoxyethyl)-4-methyl morpholinium tris(pentafluoroethyl)trifluorophosphate	7.770×10^{-3}	0.999
Ethyl-dimethyl-propyl ammonium bis(trifluoromethylsulfonyl) imide	1.06×10^{-2}	0.947
N-Ethyl-N,N-dimethyl-2-methoxyethyl ammonium bis(trifluoromethylsulfonyl)imide	1.17×10^{-2}	0.940
Ethyldimethyl-(2-methoxyethyl) ammonium tris(pentafluoroethyl)trifluoroshosphate	1.317×10^{-2}	0.965
1-Butyl-1-methyl pyrrolidinium bis (trifluoromethylsulfonyl) imide	1.87×10^{-2}	0.987
1-(2-Methoxyethyl)-1-methyl piperidinium bis(trifluoromethylsulfonyl)imide	2.804×10^{-2}	0.996
1-(2-Methoxyethyl)-1-methyl pyrrolidinium bis(trifluoromethylsulfonyl)imide	3.37×10^{-2}	0.987
1-(2-Methoxyethyl)-1-methyl piperidinium tris(pentafluoroethyl)trifluorophosphate	3.859×10^{-2}	0.995
1-(2-Methoxyethyl)-1-methyl pyrrolidinium tris(pentafluoroethyl)trifluorophosphate	3.93×10^{-2}	0.996
1-Butyl-1-methyl pyrrolidinium tetracyanoborate	4.36×10^{-2}	0.998
1-(3-Methoxypropyl)-1-methyl piperidinium bis(trifluoromethylsulfonyl)imide	5.36×10^{-2}	0.995
1-Butyl-3-methyl imidazolium hexafluorophosphate	$2.86 \times 10^{-1} *$	0.981
1-Butyl-3-methyl- imidazolium octylsulfate	$8.54 \times 10^{-1} *$	0.990
Triethyl sulfonium bis(trifluoromethylsulfonyl)imide	$3.547 *$	0.949

*Imidazolium 0-20 min, sulfonium 0-30 s

The stability is mainly dominated by the type of cation with the following with stability decreasing in the order morpholinium > ammonium > piperidinium \approx pyrrolidinium >> imidazolium >> sulfonium. This is in line with the trend observed by Hayyan *et al.* (2015b). It can be noticed that the anions did not have a substantial influence on $O_2^{\bullet-}$ stability in the presence ILs. This is expected as $O_2^{\bullet-}$ is regarded as radical anion; thus, its tendency to react with the cations is highly possible.

In this work, no clear trend was observed with anions. Though it has been suggested that the anions may affect $O_2^{\bullet-}$ stability because of their role in the hydrophobicity of ILs, as $O_2^{\bullet-}$ is highly reactive with H_2O (Cremer, 2013). However, numerous precautions were taken to avoid the exposure of the ILs to air, e.g. vacuum drying and sealing the cuvette to avoid absorption of moisture from the atmosphere into the liquid during the experiment.

(a) UV-vis of Ammonium Based ILs

$O_2^{\bullet-}$ showed high stability with the ammonium based ILs, namely [N112,1O2][TFSI], [EDMPAmm][TFSI] and [EDMOEAmm][TPTP]. These ILs were some of the most stable ILs investigated in this work, after the morpholinium based ILs. The reaction between $O_2^{\bullet-}$ and all the ammonium based ILs reached steady state after 18 h. Table 4.8 shows the calculated rate constant of $O_2^{\bullet-}$ in DMSO containing ammonium based ILs. The values of k_1 were in the order of 10^{-6} to $10^{-5} s^{-1}$ while k_2 values were in the order of 10^{-3} to $10^{-2} M^{-1}s^{-1}$. The results shown in Table 4.8 confirm that ammonium ILs have high stability. This is in accordance with those reported by Laoire *et al.* (2009) who explored the O_2 reduction in solvents of AcN with $[PF_6]^-$ anion, with cations of tetrabutylammonium $[TBAm]^{+}$, K^{+} , Na^{+} and Li^{+} . The authors found that cations in the electrolyte have a significant effect on the reduction mechanism of O_2 . The large cations of $[TBAm]^{+}$ salts resulted in a reversible $O_2/O_2^{\bullet-}$ redox couple whereas smaller Li^{+} , K^{+} , and Na^{+} cations displayed irreversible one-electron reduction of O_2 to LiO_2 , KO_2 , NaO_2 , respectively. The authors attributed this difference in $O_2^{\bullet-}$ reversibility to the difference in the charge density on the cation surfaces. When cation size increases ($Li^{+} < K^{+} < Na^{+} < TBAm^{+}$), the charge density, i.e. charge per unit volume, decreases. This results in weaker interactions with $O_2^{\bullet-}$. Li^{+} and Na^{+} cations have a higher charge density and thus have higher Lewis acidity. As a result, Li^{+} and Na^{+} form ionic bonds with oxides. This ionic compound precipitates on

the electrode surface and covers the electrode surface, causing passivation. In contrast, the [TBAm]⁺ salt solutions had a high stability of O₂•⁻ due to the formation of the [TBAm]⁺⋯O₂•⁻ complex (Hayyan et al., 2012d; Laoire et al., 2010). This stability is also anticipated because O₂•⁻ forms an ionic salt by pairing with the ammonium cation, resulting in tetramethylammonium superoxide (Sawyer & Valentine, 1981).

Table 4.8: Rate constant of O₂•⁻ in DMSO containing ammonium based ILs.

IL		0-2 h	2-6 h	6-10 h	10-14 h	14-18 h	18-24 h	Overall
[N112,1O2][TFSI]	k ₁ s ⁻¹	2.700 ×10 ⁻⁵	1.269 ×10 ⁻⁵	6.155 ×10 ⁻⁶	4.888 ×10 ⁻⁶	7.244 ×10 ⁻⁶	ss	7.507 ×10 ⁻⁶
	R ²	0.930	0.967	0.981	0.978	0.915	ss	0.930
	k ₂ M ⁻¹ s ⁻¹	1.171 ×10 ⁻²	6.569 ×10 ⁻³	3.620 ×10 ⁻³	3.109 ×10 ⁻³	5.008 ×10 ⁻³	ss	4.276 ×10 ⁻³
	R ²	0.940	0.973	0.983	0.978	0.910	ss	0.963
[EDMPAm][TFSI]	k ₁ s ⁻¹	2.509 ×10 ⁻⁵	4.794 ×10 ⁻⁶	5.628 ×10 ⁻⁶	4.213 ×10 ⁻⁶	6.484 ×10 ⁻⁶	ss	5.385 ×10 ⁻⁶
	R ²	0.949	0.800	0.957	0.928	0.872	ss	0.961
	k ₂ M ⁻¹ s ⁻¹	1.059 ×10 ⁻²	2.240 ×10 ⁻³	2.850 ×10 ⁻³	2.289 ×10 ⁻³	3.764 ×10 ⁻³	ss	2.734 ×10 ⁻³
	R ²	0.947	0.800	0.958	0.929	0.867	ss	0.974
[EDMOEAm][TPTP]	k ₁ s ⁻¹	2.526 ×10 ⁻⁵	2.144 ×10 ⁻⁵	1.272 ×10 ⁻⁵	8.922 ×10 ⁻⁶	6.380 ×10 ⁻⁶	ss	1.313 ×10 ⁻⁵
	R ²	0.962	0.996	0.996	0.998	0.999	ss	0.946
	k ₂ M ⁻¹ s ⁻¹	1.317 ×10 ⁻²	1.460 ×10 ⁻²	1.103 ×10 ⁻²	9.040 ×10 ⁻³	7.210 ×10 ⁻³	ss	1.085 ×10 ⁻²
	R ²	0.965	0.999	0.998	0.999	0.999	ss	0.985

(b) UV-vis of Pyrrolidinium Based ILs

The O₂•⁻ in DMSO containing pyrrolidinium ILs, namely [BMPyrr][B(CN)₄], [MOEMPyrr][TFSI] [MOEMPyrr][TPTP] and [BMPyrr][TFSI] were stable, with similar

stability as in the DMSO containing piperidinium based ILs. [BMPyrr][B(CN)₄], [MOEMPyrr][TFSI] and [MOEMPyrr][TPTP] reached steady state after 10 h while [BMPyrr][TFSI] took over 24 h to reach steady state. Table 4.9 shows the calculated rate constant of O₂^{•-} in DMSO containing pyrrolidinium based ILs. The values of k₁ were in the order of 10⁻⁶ to 10⁻⁵ s⁻¹ and k₂ values were in the order of 10⁻² M⁻¹s⁻¹.

Table 4.9: Rate constant of O₂^{•-} in DMSO containing pyrrolidinium based ILs.

IL		0-2 h	2- 6 h	6 -10 h	10- 14 h	14- 18 h	18 -24 h	Overall
[MOEMPyrr][TFSI]	k ₁ s ⁻¹	4.990 ×10 ⁻⁵	3.663 ×10 ⁻⁵	1.598 ×10 ⁻⁵	ss	ss	ss	3.071 ×10 ⁻⁵
	R ²	0.984	0.992	0.987	ss	ss	ss	0.956
	k ₂ M ⁻¹ s ⁻¹	3.365 ×10 ⁻²	3.901 ×10 ⁻²	2.455 ×10 ⁻²	ss	ss	ss	3.370 ×10 ⁻²
	R ²	0.987	0.999	0.993	ss	ss	ss	0.992
[BMPyrr][B(CN) ₄]	k ₁ s ⁻¹	6.641 ×10 ⁻⁵	4.794 ×10 ⁻⁵	2.246 ×10 ⁻⁵	ss	ss	ss	4.143 ×10 ⁻⁵
	R ²	0.998	0.997	0.980	ss	ss	ss	0.964
	k ₂ M ⁻¹ s ⁻¹	4.355 ×10 ⁻²	5.740 ×10 ⁻²	4.423 ×10 ⁻²	ss	ss	ss	5.282 ×10 ⁻²
	R ²	0.998	0.999	0.990	ss	ss	ss	0.997
[MOEMPyrr][TPTP]	k ₁ s ⁻¹	6.022 ×10 ⁻⁵	3.342 ×10 ⁻⁵	1.174 ×10 ⁻⁵	ss	ss	ss	2.851 ×10 ⁻⁵
	R ²	0.987	0.988	0.979	ss	ss	ss	0.922
	k ₂ M ⁻¹ s ⁻¹	3.933 ×10 ⁻²	3.514 ×10 ⁻²	1.686 ×10 ⁻²	ss	ss	ss	2.958 ×10 ⁻²
	R ²	0.996	0.997	0.985	ss	ss	ss	0.973
[BMPyrr][TFSI]	k ₁ s ⁻¹	2.921 ×10 ⁻⁵	2.123 ×10 ⁻⁵	1.655 ×10 ⁻⁵	1.340 ×10 ⁻⁵	1.238 ×10 ⁻⁵	9.885 ×10 ⁻⁶	1.477 ×10 ⁻⁵
	R ²	0.991	0.995	0.999	0.978	0.997	0.978	0.981
	k ₂ M ⁻¹ s ⁻¹	1.868 ×10 ⁻²	1.764 ×10 ⁻²	1.791 ×10 ⁻²	1.793 ×10 ⁻²	1.996 ×10 ⁻²	1.955 ×10 ⁻²	1.882 ×10 ⁻²
	R ²	0.987	0.998	0.999	0.970	0.998	0.984	0.998

Schwenke *et al.* (2015) used the same IL studied in this work, i.e. [BMPyrr][TFSI], for use as electrolyte in Li-O₂ cells as it has attracted considerable attention due to its electrochemical and chemical stability. The pseudo 1st order rate constant obtained in their study, using the UV-vis method was 0.16-1.64×10⁻³ min⁻¹ (0.266 to 2.73 ×10⁻⁵ s⁻¹) for 18 h. This is in fair agreement with the value obtained in the present work, 1.477×10⁻⁵ s⁻¹ for 24 h.

(c) *UV-vis of Imidazolium Based ILs*

O₂^{•-} showed low stability with the imidazolium based ILs, namely [BMIm][OctSO₄] and [BMIm][PF₆]. These ILs were the most unstable ILs investigated in this work after the sulfonium based IL [S222][TFSI]. The reaction between O₂^{•-} and the imidazolium based ILs reached steady state after only 1 h. For this reason, the reaction is divided into smaller zones of 0-20 min and 20-60 min. The calculated rate constants are shown in Table 4.10. The calculated values of k₁ and k₂ are in the order 10⁻⁵ to 10⁻⁴ s⁻¹ and 10⁻² to 10⁻¹ M⁻¹s⁻¹, respectively. The value of R² is higher when considering only the first 20 min of reaction as opposed to the overall reaction time.

Table 4.10: Rate constant of O₂^{•-} in DMSO containing imidazolium based ILs.

IL		0-20 min	20-60 min	overall 0-1 h
[BMIm][OctSO ₄]	k ₁ s ⁻¹	5.805×10 ⁻⁴	5.466×10 ⁻⁵	1.670×10 ⁻⁴
	R ²	0.970	0.823	0.724
	k ₂ M ⁻¹ s ⁻¹	8.542×10 ⁻¹	1.177×10 ⁻¹	2.969×10 ⁻¹
	R ²	0.990	0.837	0.786
[BMIm][PF ₆]	k ₁ s ⁻¹	4.016×10 ⁻⁴	3.879×10 ⁻⁵	1.138×10 ⁻⁴
	R ²	0.963	0.853	0.724
	k ₂ M ⁻¹ s ⁻¹	2.859×10 ⁻¹	3.590×10 ⁻²	9.213×10 ⁻²
	R ²	0.981	0.864	0.771

Islam *et al.* (2009) reported the pseudo 1st order rate constant of the reaction for 1-*n*-butyl-2,3-dimethylimidazolium tetrafluoroborate, which was approximately estimated to be $2.5 \times 10^{-3} \text{ s}^{-1}$. In this work, the pseudo 1st order rate constants were $4.02 \times 10^{-4} \text{ s}^{-1}$ for [BMIm][PF₆] and $5.81 \times 10^{-4} \text{ s}^{-1}$ for [BMIm][OctSO₄], which are inconsistent with their reported value. The rate constant was smaller than that reported by Islam *et al.* (2009) but larger than that reported by Hayyan *et al.* (2015) who found imidazolium ILs namely 1-butyl-2,3-dimethylimidazolium trifluoromethylsulfonate, 1-ethyl-3-methylimidazolium bis(trifluoromethylsulfonyl)imide, 1-ethyl-3-methylimidazolium methylsulfate and 1,3-dimethylimidazolium methylsulfate to have k_1 and k_2 of $\times 10^{-5}$ and 10^{-2} order, respectively. The R² values reported by Hayyan *et al.* (2015) for these ILs ranged from 0.238 to 0.688 and were lower than in the present work. The pseudo 1st order rate constant calculated by Islam *et al.* (2009) was reported as a rough estimate.

The results showed that O₂^{•-} was unstable in [BMIm][OctSO₄] for a long term even though the CV results found O₂^{•-} to be stable for the short term. This shows the importance of the long term stability test. The instability of the imidazolium based ILs is expected as nucleophilic species, such as OH⁻ and CN⁻ have been found to attack many imidazolium based cations (Salerno *et al.*, 1997). O₂^{•-} has been found to be a strong nucleophile in aprotic media (Sawyer, 1991). Recent studies reported that O₂^{•-} reacts with imidazolium-based ILs to produce the corresponding alkyl-2-imidazolones in excellent purity and high yield. These products are useful for various applications and have are used in pharmacology and chemotherapy (AlNashef *et al.*, 2010; Hayyan *et al.*, 2013b).

(d) *UV-vis of Sulfonium based ILs*

The O₂^{•-} was found to be by far the least stable in the presence of the IL [S222][TFSI]. The pseudo 1st and 2nd order rate constants of [S222][TFSI] were 3 orders of magnitude

larger than the most stable ILs, [MOEMMor][TFSI]. Furthermore, the reaction only lasted 30 s before reaching the steady state. It was found that the reaction occurred rapidly, with the following rate constants: k_1 $2.645 \times 10^{-3} \text{ s}^{-1}$ with R^2 0.944 and k_2 $3.547 \text{ M}^{-1} \text{ s}^{-1}$ with R^2 0.949. Hayyan (2012) noticed that the R^2 of fitting of this ILs was low, e.g. $R^2 = 0.233$ for 2nd order in [S222][TFSI]. This was attributed to the rapid reaction of $\text{O}_2^{\bullet-}$ with IL after the addition of IL to DMSO containing $\text{O}_2^{\bullet-}$, thus making the determination of rate constant difficult. However, as the time interval used in this work for this IL was 1 s, the decrease in concentration could be accurately monitored to obtain a good fit for both models, R^2 0.949 for 2nd order rate constant. It should be noted that the long term stability result of $\text{O}_2^{\bullet-}$ with [S222][TFSI] was inconsistent with the stability result obtained by the CV technique. The CV technique or short term stability test suggested a stable generated $\text{O}_2^{\bullet-}$ by the presence of the anodic peak on the reverse scan, as shown in Figure 4.9. Clearly, this shows the need and usefulness to study the long-term stability of $\text{O}_2^{\bullet-}$ for industrial applications.

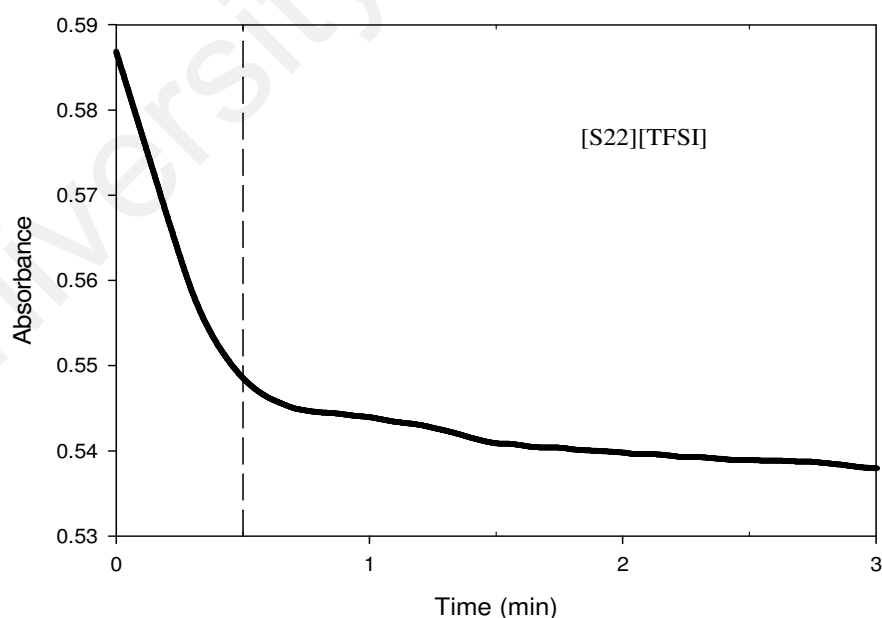


Figure 4.12: The change of $\text{O}_2^{\bullet-}$ absorbance peak with time for [S222][TFSI] in DMSO.

4.2 Conversion of Sulfur compounds by $O_2^{\bullet-}$

In terms of the selection of the ILs to be used in the conversion process of sulfur compounds, ILs based on pyrrolidinium, piperidinium, morpholinium and ammonium cations were chosen as they possess the highest stability of $O_2^{\bullet-}$. In contrast, the imidazolium and sulfonium based ILs were not selected as the results from the short term and long term stability investigations strongly indicated that $O_2^{\bullet-}$ generated in these ILs is unstable, making them unsuitable as media for $O_2^{\bullet-}$ reactions.

4.2.1.1 Conversion of Thiophene by $O_2^{\bullet-}$

Table 4.11 shows the conversion percentage of TH by $O_2^{\bullet-}$ in [BMPyrr][TFSI], [MOEMMor][TFSI], [MOEMPip][TPTP], [MOEMMor][TPTP] and [EDMPAmm][TFSI]. The TH/ KO_2 molar ratio was 1:22, which is close to that reported by Chan *et al.* (2008). The conversion of TH using $O_2^{\bullet-}$ in the studied ILs followed the order of [MOEMMor][TPTP] > [MOEMMor][TFSI] > [EDMPAmm][TFSI] > [MOEMPip][TPTP] > [BMPyrr][TFSI]. This is in accordance with the stability of $O_2^{\bullet-}$ in these ILs in the absence of TH. It is clear from the tabulated results that the extent of conversion of sulfur compound is dependent on the used IL; see Table 4.11. Hence, it can be deduced that ILs do not only behave as media for the generation of $O_2^{\bullet-}$ but they also have catalytic activity to accelerate the reaction rate between $O_2^{\bullet-}$ and the substrate being converted. Figure 4.13 shows HPLC chromatograms of TH in [EDMPAmm][TFSI] before and after KO_2 addition.

Table 4.11: Conversion of TH by $O_2^{\bullet-}$ at RT.

<i>IL</i>	<i>Conversion%</i>
[BMPyrr][TFSI]	35
[MOEMMor][TFSI]	92
[MOEMPip][TPTP]	80
[MOEMMor][TPTP]	97
[EDMPAmm][TFSI]	86

KO₂/sulfur molar ratio 22:1

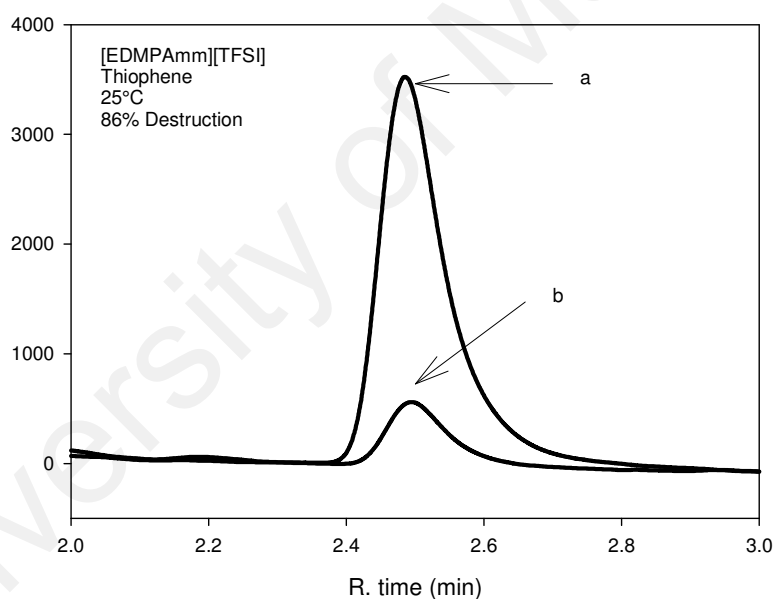


Figure 4.13: HPLC chromatograms of TH in [EDMPAmm][TFSI] (a) before KO₂ addition (b) after KO₂ addition.

In a previous study, Chan *et al.* (2008) used KO₂ dissolved in [BMIm][PF₆] to react with sulfur compounds. Although they investigated the use of KO₂ for the conversion of selected sulfur compounds, there are several main differences between their work and the present work, as can be seen in Table 4.12. The IL used by Chan *et al.* (2008), [BMIm][PF₆], was

not an appropriate medium for the generation of a stable $O_2^{\bullet-}$ whether in terms of the cation or the anion. It has been proven that imidazolium cation reacts with $O_2^{\bullet-}$ to produce the corresponding 2-imidazolone (AlNashef et al., 2010; Hayyan et al., 2013b). In addition, $[PF_6]^-$ anion produces hydrofluoric acid when it is in contact with H_2O (Pereiro et al., 2007). Therefore, it can be assumed that Chan *et al.* (2008) achieved good results using KO_2 in comparison to H_2O_2 due to the in situ generation of H_2O_2 from $O_2^{\bullet-}$. The in situ generated H_2O_2 has a purity of 100% in comparison to the studied H_2O_2 with a purity of 30% (as reported by the Chan group). This explains how 7 mmol of KO_2 gave similar sulfur removal to 44 mmol of H_2O_2 , and the ratio of sulfur/ KO_2 was 1:28 in comparison to sulfur/ H_2O_2 with a ratio 1:180, giving > 98% sulfur removal under the same conditions.

Table 4.12: Experimental conditions comparison between Chan *et al.* (2008) and this study.

Conditions	Chan <i>et al.</i> (2008)	Present work
Temperature	70 °C	Different temperature range from RT-100 °C
IL	[BMIm][PF ₆]	[BMPyrr][TFSI] [MOEMMor][TFSI] [MOEMPip][TPTP] [MOEMMor][TPTP] [EDMPAm][TFSI]
Supporting agent	Tetraoctyl-ammonium fluoride Glacial acetic acid	None
Studied Sulfur compounds	BT, DBT	TH, 2-MTH
Experimental mixture	Sulfur compound+mineral oil+ KO_2 +glacial acetic acid+IL+tetraoctyl-ammonium fluoride	Sulfur compound+IL+ KO_2

Recently, Ahmed *et al.* (2015b) studied the conversion of sulfur compounds by $O_2^{\bullet-}$ generated in ILs. However, the maximum conversion percentage achieved was only 15% for TH using trihexyl(tetradecyl)phosphonium bis(2,4,4-trimethylpentyl)phosphinate. In contrast, the conversion percentage achieved in the present study was much higher (i.e., 99%). This can be attributed to the increase of KO_2 solubility in ILs by increasing temperature. For instance, it was noticed that KO_2 dissolution in [BMPyrr][TFSI] was very slow at room temperature even though the released $O_2^{\bullet-}$ has a fair stability.

4.2.1.2 Conversion of 2-Methylthiophene by $O_2^{\bullet-}$

It was also found that the conversion of TH is higher than that of 2-MTH for all ILs (Table 4.13). This is in accordance with that reported by Ahmed *et al.* (2015b) that lower electron density on the S atom makes the sulfur compound more prone to being attacked by the negatively charged $O_2^{\bullet-}$ nucleophile since the S atom in TH has a lower electron density, 5.596, than the S atom in 2-MTH, 5.706 (Otsuki *et al.*, 2000). It is important to note the significance of this relationship between reactivity with $O_2^{\bullet-}$ and electron density on the S atom as it opposes the trend observed when conducting ODS using H_2O_2 . Previous studies, that used H_2O_2 as an oxidant, reported the order of reactivity for the sulfur compounds to be the same as the electron density of these compounds (García-Gutiérrez *et al.*, 2006; Tian *et al.*, 2015). Hence, sulfur compounds that are more difficult to be converted using H_2O_2 (Lin *et al.*, 2012a) are in fact more readily converted by $O_2^{\bullet-}$. For instance, Otsuki *et al.* (2000) reported that TH and TH derivatives could not be oxidized at 50 °C when using H_2O_2 due to the lower electron densities on the sulfur atoms. However, when using the present $O_2^{\bullet-}$ in IL system, the oxidation of TH and TH derivative was easily carried out even at room temperature.

Table 4.13: Conversion of 2-MTH by $O_2^{\bullet-}$ at RT.

IL	Conversion %
[BMPyrr][TFSI]	20
[MOEMMor][TFSI]	53
[EDMPAmm][TFSI]	41

4.2.1.3 Effect of Temperature on Conversion of Thiophene and 2-Methylthiophene by $O_2^{\bullet-}$

Table 4.14 shows the effect of temperature on the TH and 2-MTH conversion. [BMPyrr][TFSI] and [MOEMMor][TFSI] were selected for this purpose as they have the same anion of [TFSI]⁻. Remarkably, the percentage of conversion for both sulfur compounds was significantly enhanced with temperature increase. This can be attributed to the increase of solubility of KO_2 in the ILs. For instance, the conversion of TH in [BMPyrr][TFSI] was only 35% at room temperature due to the low solubility of KO_2 in this IL. However, the conversion process was improved after temperature increase up to 81% at 70 °C. At 100 °C, 92% of conversion was achieved for 2-MTH in [BMPyrr][TFSI] while only 20% conversion was achieved at room temperature. In contrast, 92% TH conversion was reported in [MOEMMor][TFSI] at room temperature and 99% of TH could be converted at 70 °C; Figure 4.14. The 2-MTH conversion in [MOEMMor][TFSI] increased from 53% at room temperature to 96% at 100 °C; see Figure 4.15. This clearly shows that temperature is a significant parameter for the conversion process. Again, the temperature increase is expected to accelerate the dissolution rate of superoxide salts in the IL. In addition, higher amounts of these salts will be dissolved.

Table 4.14: Conversion of TH and 2-MTH by O₂^{•-} at different temperatures.

Temp. (°C)	TH Conversion %	2-MTH Conversion %	TH Conversion %	2-MTH Conversion %
	[BMPyrr] [TFSI]	[BMPyrr] [TFSI]	[MOEMMor] [TFSI]	[MOEMMor] [TFSI]
	RT*	35	20	92
40	40	31	93	65
50	65	59	94	70
60	70	62	96	74
70	81	75	99	83
80	-	85	-	89
90	-	89	-	91
100	-	92	-	96

*RT: room temperature

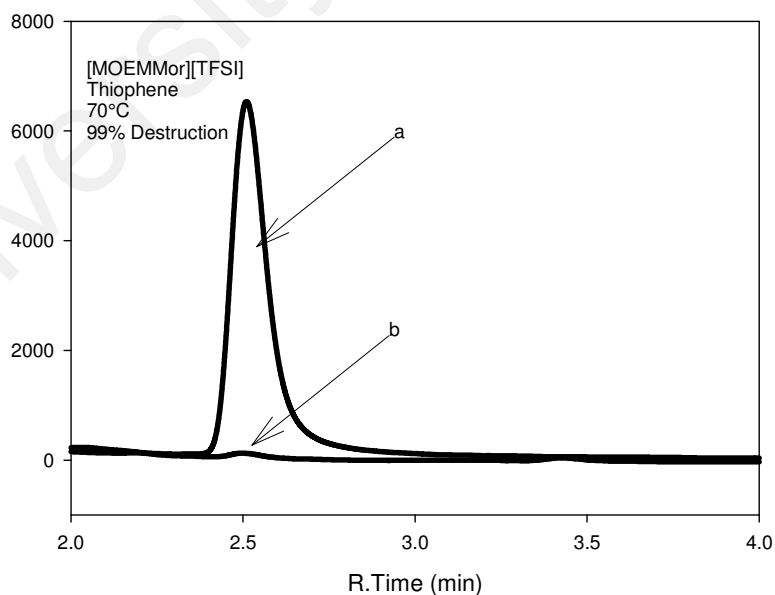


Figure 4.14: HPLC chromatograms of TH in [MOEMMor][TFSI] (a) before KO₂ addition (b) after KO₂ addition.

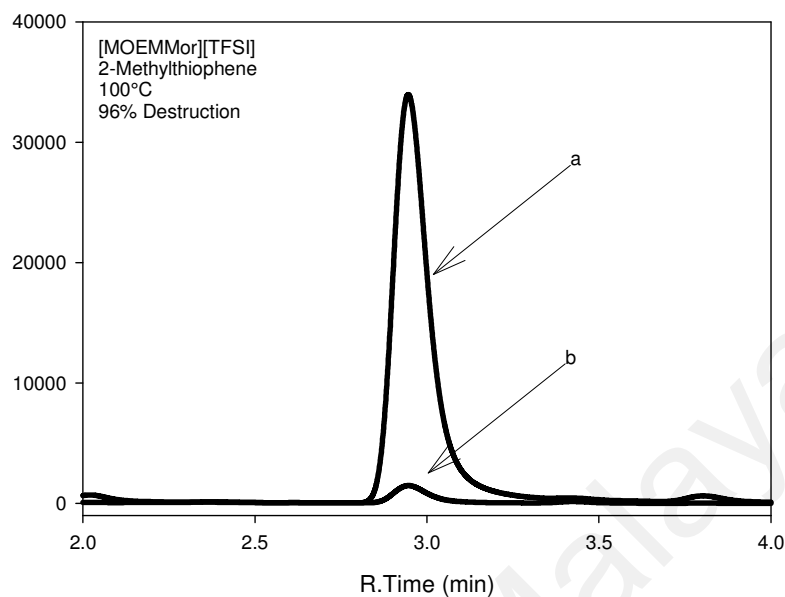


Figure 4.15: HPLC chromatograms of 2-MTH in [MOEMMor][TFSI] (a) before KO₂ addition (b) after KO₂ addition.

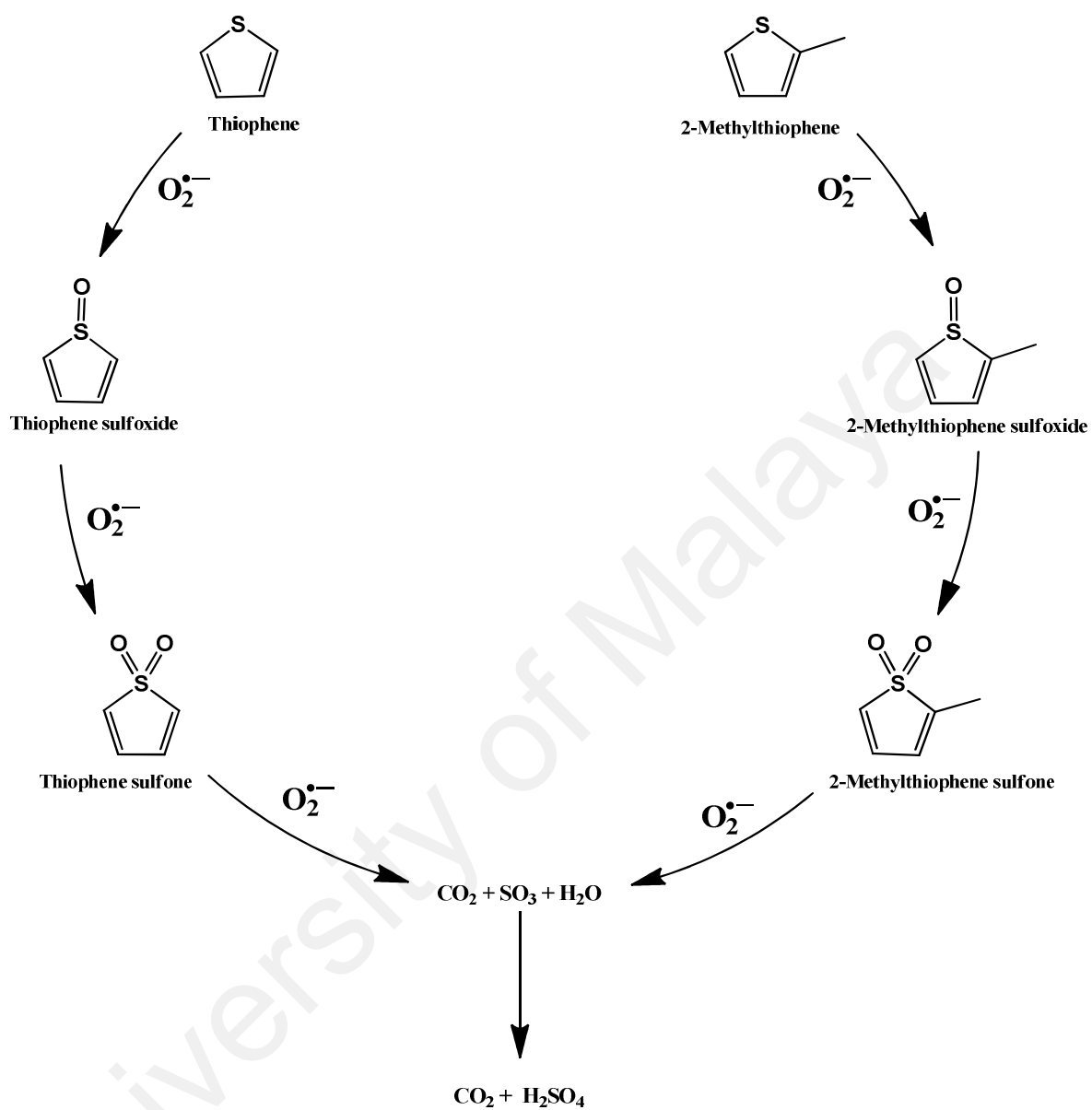
4.2.1.4 Mechanism of Reaction

There were no products detected using HPLC and GC/MS which may lead to the conclusion that these products are either gaseous or unstable. Therefore, in order to identify the reaction products, an aqueous solution of BaCl₂ was added to the mixture of IL sulfur compound KO₂. A white precipitate was formed, indicating the presence of SO₄²⁻ (Daintith, 2009). On the basis of this analysis, the mechanism as shown in Scheme 4.1 is proposed. In summary, when using the IL as a solvent, TH and 2-MTH are oxidized by O₂^{•-} to the corresponding sulfoxide, which is further oxidized to the corresponding sulfone, and then oxidized to SO₃, CO₂ and H₂O. Subsequently, SO₃ reacts with H₂O to form H₂SO₄. The final products of the reaction, CO₂ and H₂SO₄, can easily be removed, unlike the initial organic compound which requires a complicated process for separation. This was in agreement with Lin *et al.* (2012a) who reported that the intermediate of TH and its

derivatives 2-MTH and 2,5-dimethylthiophene after oxidation were unstable and easily further oxidized to SO_3 . In contrast, for benzothiophene and its derivatives benzothiophene and dibenzothiophene, it was observed that the corresponding sulfones were relatively stable and were identified to be the main products (Lin et al., 2012a).

In order to ensure that the decrease in concentration of S compound was not due to the reaction with the IL or due to evaporation, controlled experiments were conducted by carrying out the process under the same reaction conditions but without the addition of KO_2 . The analyses of the samples before and after the process using HPLC and GC/MS showed that the concentration of the sulfur compound did not change. In addition, no byproducts were detected. This indicated that there was no reaction between the IL and sulfur compound, and hence the decrease in the S compound concentration can be ascribed to the reaction with KO_2 . Furthermore, based on the GC/MS analysis of samples with KO_2 after the reaction, there was also no detectable byproduct.

Since the $\text{O}_2^{\bullet-}$ is a radical anion, the design of the process should avoid exposure of the system to contaminants that may affect the reaction. For example, precautions must be taken to avoid exposure to moisture as $\text{O}_2^{\bullet-}$ readily disproportionates with H_2O (Eq 2.5). In addition, $\text{O}_2^{\bullet-}$ also nucleophilically attacks the carbon in CO_2 to ultimately form the peroxodicarbonate ion, $\text{C}_2\text{O}_6^{2-}$ (Buzzeo et al., 2004b). However, CO_2 in air is about 360 ppm by volume, 0.00036 vol % (Brimblecombe, 1996) which will not significantly affect the reaction.



Scheme 4.1: The proposed reaction mechanism between TH and 2-MTH with $O_2^{\bullet-}$, respectively.

4.2.2 Solubilities of Sulfur Compounds in ILs

In order to further investigate the feasibility of using the ILs in desulfurization, the solubility of sulfur compounds were studied in four ILs: [BMPyrr][TFSI], [MOEMMor][TFSI], [MOEMPip][TPTP] and [MOEMMor][TPTP].

Table 4.15 shows the solubilities of TH and 2-MTH in the ILs. The cation and anion structures and their size are important parameters that affect the solubility of aromatic compounds (Zhang & Zhang, 2002a). In general, the solubility of TH in the ILs was higher (except in [MOEMPip][TPTP]) in comparison to 2-MTH. This is in accordance with other studies which reported a methyl group markedly reduced the solubility of aromatic compounds in ILs (Zhang et al., 2004b; Zhang & Zhang, 2002a, 2002b). However, it is important to conduct studies on the extraction of sulfur compounds from diesel feed using these ILs.

Table 4.15: Solubilities of the sulfur compounds in ILs.

IL	TH	MTH
	wt%	wt%
[BMPyrr][TFSI]	51.28	43.32
[MOEMMor][TFSI]	50.16	32.03
[MOEMPip][TPTP]	47.43	48.53
[MOEMMor][TPTP]	43.66	31.87

4.3 Physical Properties of ILs

Scaling up of a chemical process, including the sizing of reactor and determination of energy requirements requires knowledge of the physical properties of the ILs. The high electrostatic interactions between the ions of ILs give their characteristic physicochemical properties which distinguish them from conventional organic solvents (Tokuda et al., 2005). Several of their physical properties, such as density and viscosity can be easily tuned or tailored by variation of cation and anion (Domańska, 2006; Govinda et al., 2013; Regueira et al., 2012). The determination and understanding of these fundamental physical and transport properties is indispensable for process design (Muhammad et al., 2008). Furthermore, the collection of a large data bank for thermophysical properties of various ILs is essential, not only for product process design but also for the development of predictive methods and the design of ILs (Królikowska et al., 2014).

Some ILs that possess high stability of $O_2^{\bullet-}$, namely [MOEMMor][TFSI], [EDMPAmm][TFSI], [MOEMPyrr][TFSI], [MOEMPip][TFSI] and [N112,1O2][TFSI] were selected to investigate their thermophysical properties. The selected ILs share same anion, [TFSI]⁻; thus the effect of cation structure was examined. The important physical properties such as the density, conductivity, viscosity and surface tension were obtained as a function of temperature and in the temperature range of 25 to 80 °C (298.15 to 353.15 K). Measurements were obtained at 25 °C, 30 °C, 40 °C, 50 °C, 60 °C, 70 °C and 80 °C.

4.3.1.1 Density

Figure 4.16 shows the temperature dependence of density (ρ) for the five [TFSI]-anion-based ILs. The densities decreased in the order [MOEMMor][TFSI] > [MOEMPyrr][TFSI] > [MOEMPip][TFSI] > [N112,1O2][TFSI] > [EDMPAmm][TFSI]. At 298.15 K, the values of density were 1.50 g cm⁻³ for [MOEMMor][TFSI], 1.45 g cm⁻³ for [MOEMPyrr][TFSI],

1.43 g cm⁻³ for [MOEMPip][TFSI], 1.42 g cm⁻³ for [N112,1O2][TFSI] and 1.40 g cm⁻³ for [EDMPAmm][TFSI]. At room temperature, the density of the ILs was higher than that of H₂O, which is 0.997 g cm⁻³ (Hall & Hoff, 2011). The densities obtained did not show a relationship with molecular weight of the cation but depended on the structure of the cation. Seki *et al.* (2010) also found density did not show a relationship with the molecular weight of the cation.

The rate of decrease in density with temperature was similar for all samples and the slope of dp/dT varied from 9.09 to 10.26×10⁻⁴ g cm⁻³ K⁻¹. This was in accordance with literature values (8.8 to 10.6×10⁻⁴ g cm⁻³ K⁻¹) for 1-alkyl-3-methylimidazolium and 1,3-dialkylimidazolium ILs containing the same [TFSI] anion (Tao *et al.*, 2014; Tokuda *et al.*, 2005; Zheng *et al.*, 2011).

The value of density at 298.15 K for [MOEMPyrr][TFSI], 1.45 g cm⁻³, was in agreement to that reported by Zhou *et al.* (2006) and Regueira *et al.* (2012). For [MOEMPyrr][TFSI], the values obtained at 313.15 K and 333.15 K were identical to those reported by Regueira *et al.* (2012), 1.439 g cm⁻³ at 313.15 K and 1.421 g cm⁻³ at 333.15 K. However, it should be mentioned here that the density as a function of wide range of temperature was not investigated before.

The density of [N112,1O2] at 298 K, 1.41 g cm⁻³, was slightly lower than reported by Zhou *et al.* (2006), i.e. 1.45 g cm⁻³.

Generally, in a narrow range of temperature, density ρ (g cm⁻³) is expressed as in, Eq 4.8 (Seki *et al.*, 2010):

$$\rho = b - aT \quad 4.8$$

Where fitting parameters a and b are related to the coefficient of volume expansion in $\text{g cm}^{-3}\text{K}^{-1}$ and extrapolated density at 0 K in g cm^{-3} , respectively and T is temperature in K (Seki et al., 2010). Calculated values of a and b are listed in Table 4.16.

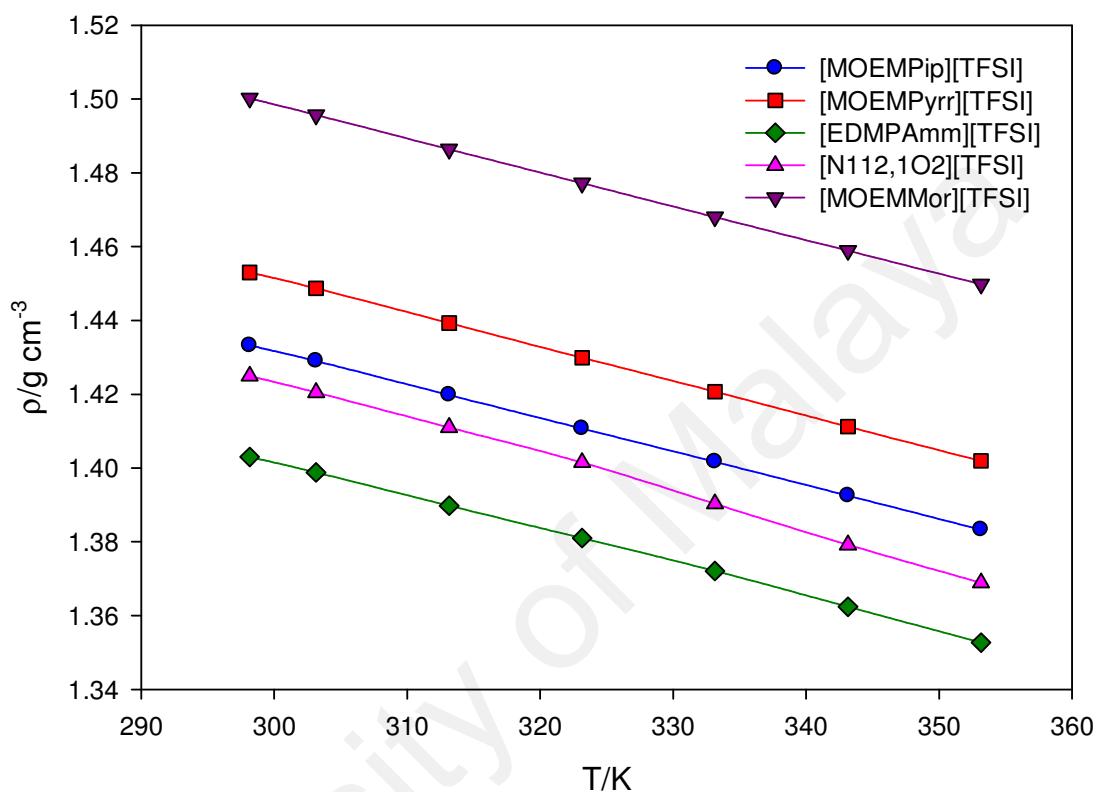


Figure 4.16: Densities of ILs as a function of temperature.

Table 4.16: Calculated parameters for a and b of density of [TFSI]-based ILs using Eq 4.8.

IL	a	b	R^2
	$\text{g cm}^{-3}\text{K}^{-1} \times 10^4$	g cm^{-3}	
[EDMPAmm][TFSI]	9.12	1.675	0.99952
[MOEMPip][TFSI]	9.09	1.704	0.99996
[MOEMPyrr][TFSI]	9.32	1.731	0.99996
[N112,1O2][TFSI]	10.3	1.732	0.99866
[MOEMMor][TFSI]	9.18	1.774	0.99999

4.3.1.2 Viscosity

The viscosity η is a macroscopic property of ILs, which occurs due to microscopic interactions such as van der Waals, columbic and hydrogen bonding (Bhattacharjee et al., 2015). Viscosity is thought to be affected by the size and shape of the IL ions. It affects ionic conductivity and mass transport phenomena, thereby restricting their suitability for particular applications (Bhattacharjee et al., 2015; Seki et al., 2010). The viscosity of some ILs is frequently significantly higher than that of conventional organic fluids commonly used in industry. High viscosity could be unfavorable for some industrial applications due to its negative impact on processes such as stirring, pumping and mass transfer operations (Aparicio et al., 2010). In numerous applications such as fuel cell, synthetic solvents and field-effect transistors, high viscosity is a serious problem (Seki et al., 2010). However, large viscosities can be favorable for other applications, such as lubrication (Aparicio et al., 2010).

Figure 4.17 depicts the viscosities of the ILs as a function of temperature. It can be seen that at room temperature, the IL with the morpholinium based cation [MOEMMor]⁺ showed a profoundly greater viscosity compared to the other ILs. At room temperature, the [MOEMMor]⁺ based IL showed a dramatically higher viscosity (257.6 mPa s) than the other cations based ILs which had similar viscosities in the range of 52.19 mPa s [MOEMPyrr] to 69.89 mPa s [MOEMPip]. The values obtained for the ammonium based ILs were similar at 59.39 mPa s [N112,1O2] and 58.79 mPa s [EDMPAmm]. However, at higher temperatures, the difference in viscosities between [MOEMMor] and the other ILs was less significant. The observed decrease in viscosity with temperature is expected. This is due to the increase in the average speed of the species in the liquid, which decreases the intermolecular forces and hence the fluid resistance to flow (Hayyan et al., 2012a). At room temperature, the IL viscosities were much higher than that of H₂O which is 0.8901 mPa s

(Hall & Hoff, 2011). Like density, the viscosities obtained did not depend on molecular weight of the cation but instead depended on the cation structure, as was found by Seki *et al.* (2010).

At 298 K, the viscosity obtained for [MOEMPyrr], 52.19 mPa s, was in agreement to that reported by Zhou *et al.* (2006), i.e. 53 mPa s. However, the value for [EDMPAmm], 58.79 mPa s, was much less than that reported by McFarlane *et al.* (2000), i.e. 83 mPa s.

The viscosities of the studied ILs were fitted using the Arrhenius model as shown below, Eq 4.9 (Hayyan *et al.*, 2015a):

$$\eta = \eta_0 e^{\left[\frac{-E_\eta}{RT}\right]} \quad 4.9$$

Where T is temperature (K), R is gas constant ($\text{J mol}^{-1}\text{K}^{-1}$), E_η is activation energy (Pa L mol^{-1}), η_0 is pre-exponential constant (mPa s) and η is viscosity (mPa s). A good regression of the experimental data with the Arrhenius model is shown by the linear trend of $\ln(\text{viscosity})$ as a function of $\ln(1/T)$, the R^2 values are ranged from 0.975 to 0.998, Figure 4.18. Calculated values of $-(E_\eta/R)$ and η_0 are listed in Table 4.17.

Table 4.17: Calculated parameters for $-(E_\eta/R)$ and η_0 of viscosity of [TFSI]-based ILs using 4.9

IL	$-(E_\eta/R)$ K	η_0 mPa s	R^2
[MOEMMor][TFSI]	4379.80	1.07×10^{-4}	0.9974
[EDMPAmm] [TFSI]	2835.30	4.45×10^{-3}	0.9975
[MOEMPip][TFSI]	3164.90	1.61×10^{-3}	0.9837
[N112,1O2][TFSI]	2951.40	2.76×10^{-3}	0.9749
[MOEMPyrr][TFSI]	2627.70	7.80×10^{-3}	0.9981

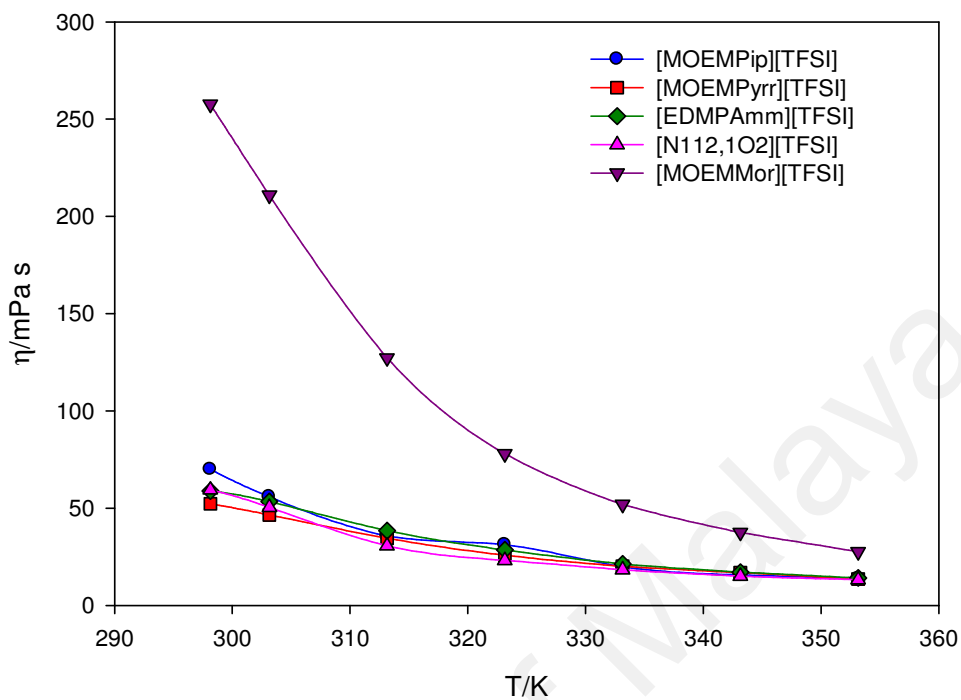


Figure 4.17: Viscosities of ILs as a function of temperature

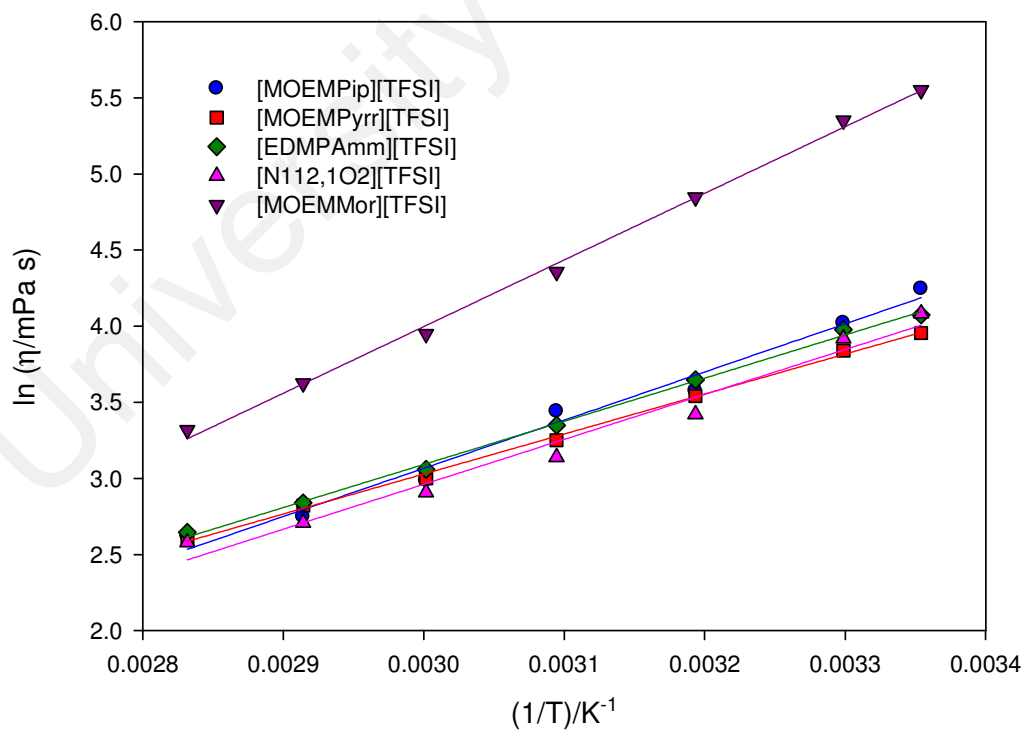


Figure 4.18: $\ln(\eta)$ of ILs as a function of $(1/T)$ temperature

4.3.1.3 Conductivity

Though ILs are totally comprised of ions, not all of the ions are available to participate in conduction processes. The resulting conductivity (γ) is dependent on the nature and structure of the IL (MacFarlane et al., 2009). Figure 4.19 illustrates the conductivities of the samples as a function of temperature. It can be seen the morpholinium cation displays the poorest conductivity at all temperatures. This is expected as it also shows the highest viscosity which affects conductivity (Bhattacharjee et al., 2015). This low conductivity and high viscosity of morpholinium based ILs was also obtained by Yeon *et al.* (2005) for *N*-(2-hydroxyethyl)-*N*-methyl morpholinium based ILs [HEMMor][BF₄] and [HEMMor][TFSI].

Generally, the conductivity increased at a faster rate at higher temperatures, except for [MOEMPyrr]⁺ in which it decreases at a slower rate at higher temperature. Conductivity decreases in the order [MOEMPyrr] (3.45 mS cm⁻¹) > [N112,1O2] (2.88 mS cm⁻¹) > [EDMPAmm] (2.48 mS cm⁻¹) > [MOEMPip] (2.09 mS cm⁻¹) > [MOEMMor] (0.653 mS cm⁻¹). This order of conductivity was maintained at all temperatures with the exception of 80 °C at which the conductivities of the ammonium based ILs were almost identical.

The conductivity of [MOEMPyrr]⁺ at 298.15 K (3.45 mS cm⁻¹) was similar but slightly lower than that reported by Zhou *et al.* (2006) which was 3.7 mS cm⁻¹. The value for [N112,1O2]⁺ (2.88 mS cm⁻¹) was also slightly lower than the value of 3.1 mS cm⁻¹ reported by Zhou *et al.* (2005). The value obtained for [EDMPAmm] (2.48 mS cm⁻¹) was double the result reported by McFarlane *et al.* (2000) which was 1.2 mS cm⁻¹.

The Arrhenius equation was used to fit the behavior as shown below in Eq 4.10 (Hayyan et al., 2015a)

$$\gamma = \gamma_0 e^{\left[\frac{E_\gamma}{RT} \right]} \quad 4.10$$

Where γ the conductivity in (mS cm^{-1}), γ_0 is a constant (mS cm^{-1}), E_γ is the activation energy of conductivity (Pa L mol^{-1}) and R is the gas constant ($\text{J mol}^{-1} \text{K}^{-1}$). The data showed a good fit with the Arrhenius model (Figure 4.20), with R^2 range from 0.973 to 0.991. Calculated values of $-(E_\gamma/R)$ and γ_0 are listed in Table 4.18.

Table 4.18: Calculated parameters for $-(E_\gamma/R)$ and γ_0 of conductivity of [TFSI]-based ILs using Eq 4.9

IL	$-(E_\gamma/R)$ K	γ_0 mS cm^{-1}	R^2
[MOEMPip][TFSI]	1930.60	1353.70	0.9901
[MOEMPyrr][TFSI]	1292.10	281.63	0.9733
[EDMPAmm][TFSI]	1687.80	705.85	0.9770
[N112,1O2][TFSI]	1478.80	404.12	0.9893
[MOEMMor][TFSI]	3042.10	17483.28	0.9910

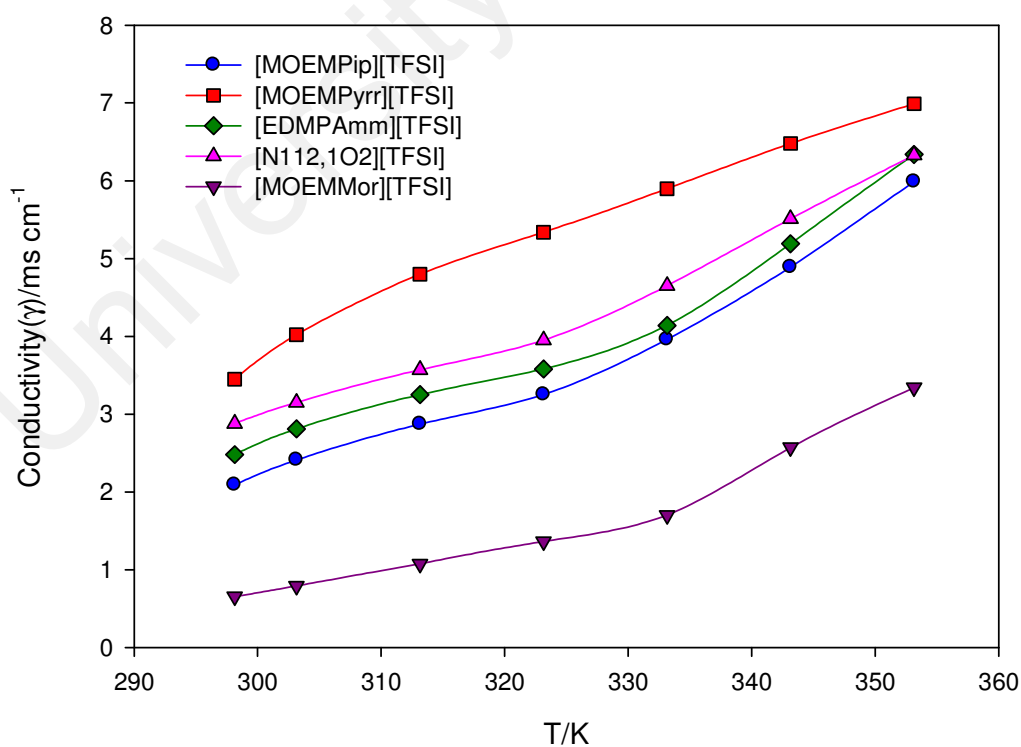


Figure 4.19: Conductivities (γ) of ILs as a function of temperature

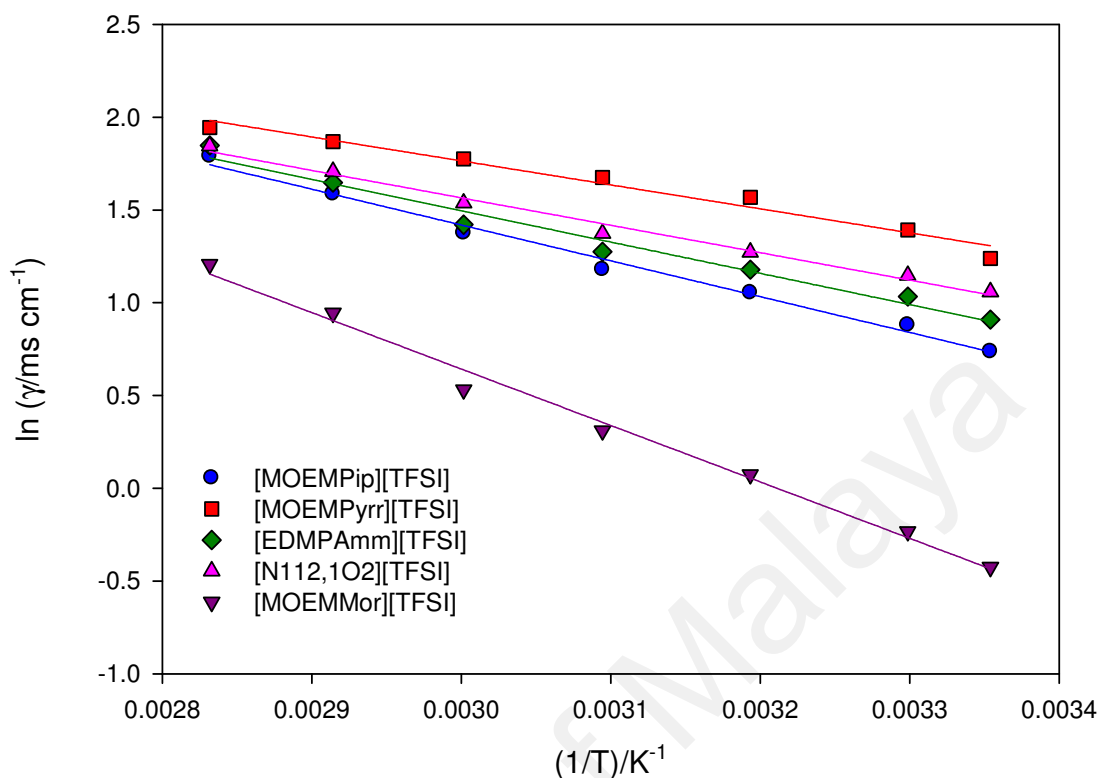


Figure 4.20: \ln (conductivity, γ) of ILs as a function of $(1/T)$ temperature

4.3.1.4 Surface Tension

Surface tension (σ) is an important physical property which is defined as the force to close a cut of unit length in the surface of a liquid (Tariq et al., 2012). Thermodynamically, surface tension is defined as the change of surface free enthalpy G per area A ($\sigma = \delta G/\delta A$) (Kolbeck et al., 2010). The determination of surface tension of ILs is a way to indirectly determine important information on the interactions between the IL ions (Tariq et al., 2012). Surface tension occurs as a result of the molecular orientation at the surface as well as intermolecular interactions in the bulk cohesive energy (Kolbeck et al., 2010). Other studies have shown that ILs with the $[\text{TFSI}]^-$ anion generally exhibit lower surface tension values than other anions (Tariq et al., 2012).

Figure 4.21 depicts the obtained surface tension of the ILs. At room temperature, surface tension of the ILs is less than that of H₂O, 71.98 mN m⁻¹ (Hall & Hoff, 2011) and decreases in the order at 50.14 [MOEMMor] > 49.22 [MOEMPyr] > 47.56 [N112,1O2] > 46.56 [EDMPAmm] > 44.65 mN m⁻¹ [MOEMPip]. The surface tension decreased with temperature following a linear trend, at higher temperatures of 60 to 80 °C the surface tension of the ammonium based ILs [N112,1O2]⁺ and [EDMPAmm]⁺ was very similar. The surface tensions of the ILs at room temperature were also less than those reported for glucose or fruit sugar based DESs, 70 to 76 mN m⁻¹ (Hayyan et al., 2012a; Hayyan et al., 2013a).

The surface tension–temperature relationship was fitted linearly for all ILs according to the following relationship, Eq 4.11:

$$\sigma = b - aT \quad 4.11$$

Where, σ is surface tension (mN m⁻¹) and T is temperature (K). While a (mN m⁻¹ K⁻¹) and b (mN m⁻¹) are constants that vary according to the type of IL. Table 4.19 shows the values of surface tension parameters a and b for Eq 4.11. The obtained linear trend is expected as surface tension is known to decrease linearly with temperature between freezing to boiling temperature though it vanishes non-linearly close to the critical point (Ghatee et al., 2010). The magnitude of the slope of the temperature dependence of surface tension, i.e. surface entropy, can be used to characterize fluids in terms of the molecular energetics and surface microstructure (Ghatee et al., 2010; Tariq et al., 2012).

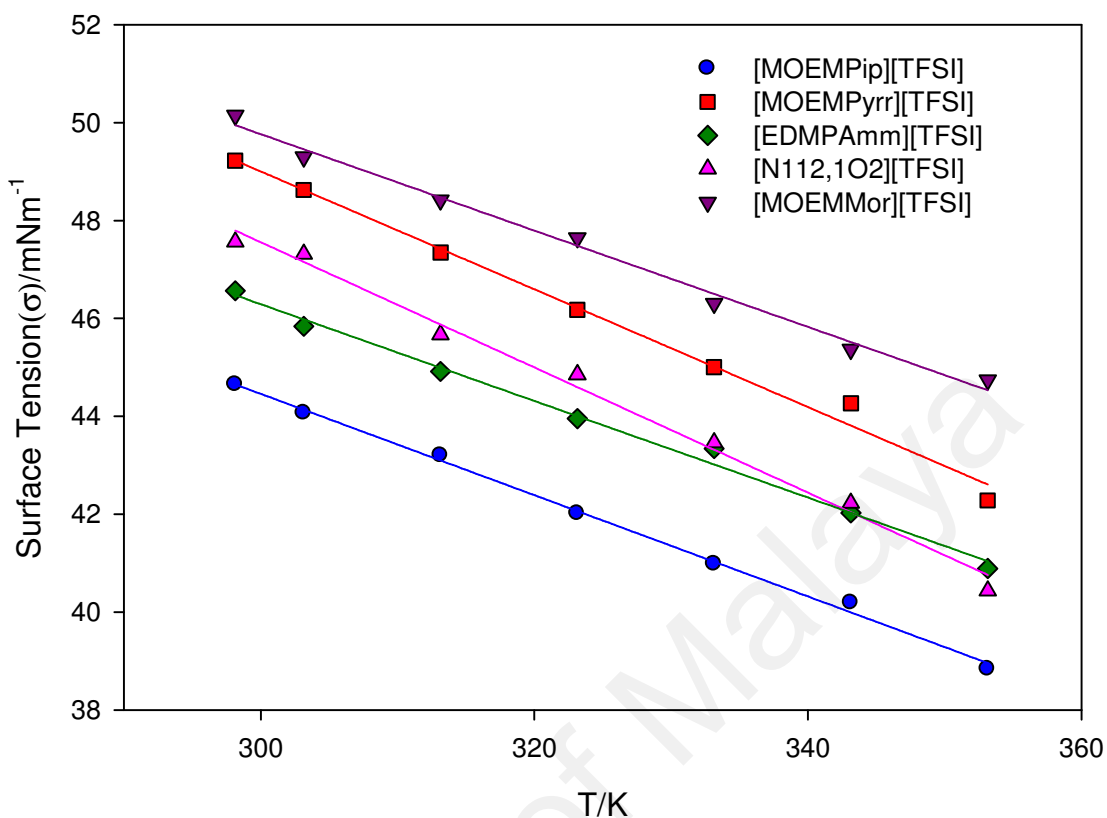


Figure 4.21: Surface tensions (σ) of ILs as a function of temperature

Table 4.19: Calculated parameters for a and b of surface tension [TFSI]-based ILs using Eq 4.11.

IL	a	b	R ²
	mN m ⁻¹ K ⁻¹ × 10 ²	mN m ⁻¹	
[EDMPAmm][TFSI]	9.88	75.918	0.993
[MOEMPip][TFSI]	10.35	75.495	0.997
[MOEMPyrr][TFSI]	12.03	85.101	0.991
[N112,1O2][TFSI]	12.03	85.101	0.992
[MOEMMor][TFSI]	9.85	79.305	0.992

CHAPTER FIVE

CONCLUSIONS AND RECOMMENDATIONS

5.1 Conclusions

The generation and stability of $O_2^{\bullet-}$ with 15 ILs were investigated. The ILs investigated comprised of cations based on morpholinium, ammonium, imidazolium, piperidinium, pyrrolidinium and sulfonium, paired with anions of $[TFSI]^-$, $[OctSO_4]^-$, $[B(CN)_4]^-$ and $[TPTP]^-$. CV and UV-vis spectrophotometry tests were conducted to investigate the respective short and long term stability of $O_2^{\bullet-}$. From the stability of $O_2^{\bullet-}$ results, five ILs were selected as media to carry out reactions with dissolved sulfur compounds, namely TH and 2-MTH. The solubility of TH and 2-MTH was determined in four ILs. Furthermore, the physical properties of five ILs, exhibiting stability of $O_2^{\bullet-}$, were determined. Physical properties of density, viscosity, conductivity and surface tension were obtained for the five ILs in the temperature range of 25 to 80 °C (298.15 to 353.15 K).

To study short term stability of $O_2^{\bullet-}$ with ILs, $O_2^{\bullet-}$ was generated electrochemically by reduction of O_2 . CV of O_2 dissolved in IL was conducted in 14 ILs, namely $[MOEMPip][TPTP]$, $[BMPyrr][TFSI]$, $[MOEMPip][TFSI]$, $[BMPyrr][B(CN)_4]$, $[MOPMPip][TFSI]$, $[MOEMPyrr][TFSI]$, $[BMIm][OctSO_4]$, $[MOEMPyrr][TPTP]$, $[N112,1O2][TFSI]$, $[MOEMMor][TPTP]$, $[EDMPAmm][TFSI]$, $[MOEMMor][TFSI]$, $[EDMOEAmm][TPTP]$ and $[S222][TFSI]$. The reduction and oxidation peaks were observed in all ILs corresponding to the reversible reduction of O_2 to form $O_2^{\bullet-}$ and the short term stability of $O_2^{\bullet-}$ in these ILs. The process was determined to be quasi reversible in all ILs due to the following reasons: i) peak potential separation values, ΔE_p , were not close to 57 mV ii) the potential of the reduction and oxidation peaks shifted with scan rate

iii) The anodic and cathodic peak currents were not equal for the respective scan rate, i.e. the ratio of anodic and cathodic peak currents, j_p^a / j_p^c , was less than 1.

It was observed that some of the CVs obtained in this work had small additional peaks or humps which were not assigned to the $O_2/O_2^{\bullet-}$ couple. This was observed in [MOEMPip][TFSI] and [N112,1O2][TFSI]. These peaks were attributed to unknown trace impurities or the adsorption of the IL cations on the electrode surface. For [EDMOEAm][TPTP], the oxidation peak produced was larger than the reduction peak, the potential range was extended to further investigate. It was concluded that the large oxidation peak was caused by the reaction of O_2^{2-} ions with undissolved O_2 in the IL to produce two ions of $O_2^{\bullet-}$. These O_2^{2-} ions were produced by the further reduction of $O_2^{\bullet-}$. The small oxidation peak obtained for [S222][TFSI] at 9 mV/s, with j_p^a / j_p^c of only 0.09 suggested $O_2^{\bullet-}$ might be unstable in this IL.

Following the short term stability of $O_2^{\bullet-}$ investigation, the long term stability was investigated. Superoxide ion was generated chemically by dissolving KO_2 in DMSO. The rate constants based on pseudo 1st and 2nd order reactions between the IL and $O_2^{\bullet-}$ generated in DMSO were determined. It was found that the reaction had overall marginally higher R^2 for k_2 than k_1 in first 2 h. The value of k_1 and k_2 generally decreased with time. R^2 for the overall reaction time was usually lower than when divided into zones. The values of k_1 ranged from 7.049×10^{-6} to $2.645 \times 10^{-3} \text{ s}^{-1}$. The values of k_2 ranged from 4.732×10^{-3} to $3.547 \text{ M}^{-1} \text{ s}^{-1}$. In order to rate stability, the IL stability was sorted in order of decreasing k_2 in the first 2 h. The stability was found to be primarily influenced by the cation structure. The stability of $O_2^{\bullet-}$ decreased following the addition of IL in the following order: morpholinium > ammonium > piperidinium \approx pyrrolidinium \gg Imidazolium \gg sulfonium. The results indicated that $O_2^{\bullet-}$ was unstable with [S222][TFSI], k_2 of $3.547 \text{ M}^{-1} \text{ s}^{-1}$, R^2

0.949 and imidazolium based ILs [BMIm][OctSO₄] and [BMIm][PF₆] with k_2 of $8.54 \times 10^{-1} \text{ M}^{-1} \text{ s}^{-1}$, R^2 0.99 and $2.86 \times 10^{-1} \text{ M}^{-1} \text{ s}^{-1}$, R^2 0.981 respectively. This was explained by the reaction of O₂^{•-} with the IL cation. In contrast, the most stable IL [MOEMMor][TFSI] had k_2 of 4.732×10^{-3} , R^2 0.984. The most unstable IL [S222][TFSI] reached steady state after only 30s while [BMIm][OctSO₄] and [BMIm][PF₆] reached steady state after 1 h. In contrast the other ILs which were considered stable in the long term took over 10 h to reach steady state.

Superoxide ion was then used to convert sulfur compounds (i.e. TH and 2-MTH) using ILs which exhibited O₂^{•-} stability as reaction media. Five ILs were selected, namely [BMPyrr][TFSI], [MOEMMor][TFSI], [MOEMPip][TPTP], [MOEMMor][TPTP] and [EDMPAmm][TFSI]. The sulfur compound conversion was achieved through chemical generation of O₂^{•-} by addition of KO₂ to the IL with dissolved sulfur compound. The mixture before and after addition of KO₂ was analyzed using HPLC and GC/MS. At room temperature, TH was converted in the following order: [MOEMMor][TPTP] 97% > [MOEMMor][TFSI] 92% > [EDMPAmm][TFSI] 86% > [MOEMPip][TPTP] 80% > [BMPyrr][TFSI] 35%. This is in accordance with the stability of O₂^{•-} in these ILs in the absence of TH. The 2-MTH was then converted using [MOEMMor][TFSI], [EDMPAmm][TFSI] and [BMPyrr][TFSI]. The conversion was in the following order: [MOEMMor][TFSI] 53% > [EDMPAmm][TFSI] 41% > [BMPyrr][TFSI] 20%. However, the conversion obtained for 2-MTH was lower than TH. This was explained by the lower electron density on the S atom for TH, which makes TH more prone to being attacked by the negatively charged O₂^{•-} nucleophile.

It is noteworthy that the extent of both TH and 2-MTH conversion was dependent on the structure of the used IL. Hence, ILs not only behaved as media for the generation of O₂^{•-},

but also had catalytic activity to accelerate the reaction rate between $O_2^{\bullet-}$ and the substrate being converted.

The effect of temperature on the reaction was then studied by increasing the temperature of the reaction, up to 70 °C for TH and up to 100 °C 2-MTH, taking into consideration their boiling points. The conversion of TH and 2-MTH was studied using [BMPyrr][TFSI] and [MOEMMor][TFSI]. The percentage of conversion for both sulfur compounds was significantly enhanced with temperature increase. This was attributed to the solubility increase of KO_2 in the ILs. The maximum conversion for TH was at 70 °C [BMPyrr][TFSI] 81% and [MOEMMor][TFSI] 99%. For 2-MTH, at 100 °C conversion was [BMPyrr][TFSI] 92% and [MOEMMor][TFSI] 96%.

On the basis of HPLC and GC/MS analysis, a reaction mechanism was proposed. The reaction mechanism is as follows: when using the IL as a medium, the sulfur compound was oxidized by $O_2^{\bullet-}$ to the corresponding sulfoxide, which was further oxidized to the corresponding sulfone, and then oxidized to SO_3 , CO_2 , and H_2O . Subsequently, SO_3 reacts with H_2O to form H_2SO_4 . In order to further investigate the feasibility of using the ILs in desulfurization, the solubility of sulfur compounds were studied in four ILs: [BMPyrr][TFSI], [MOEMMor][TFSI], [MOEMPip][TPTP] and [MOEMMor][TPTP]. In general, the solubility of TH in the ILs was higher (except in [MOEMPip][TPTP]) in comparison to 2-MTH.

The thermophysical properties, which are vital for process scale up, were studied. Five ILs paired with $[TFSI]^-$, namely [MOEMPip][TFSI], [MOEMPyrr][TFSI], [MOEMMor][TFSI], [N112,1O2][TFSI] and [EDMPAmm][TFSI] were selected. The physical properties of density, viscosity, conductivity and surface tension were determined at various temperatures of 25 °C, 30 °C, 40 °C, 50 °C, 60 °C, 70 °C and 80 °C. All ILs

exhibited Arrhenius behavior for conductivity and viscosity. Surface tension and density followed a linear trend. [MOEMMor][TFSI] was notable with the highest density, viscosity and surface tension.

5.2 Recommendations

The investigation found the feasibility of using $O_2^{\bullet-}$ as desulfurization agent to convert sulfur compounds with high conversion percentage obtained. In addition, the products formed can easily be removed. However, there is still room to explore the stability of $O_2^{\bullet-}$ with other types of ILs. In addition, there are other factors, for industrial implementation which should be considered, such as $O_2^{\bullet-}$ stability, sulfur solubility, cost of ILs and their physicochemical properties with toxicological profile.

The following points are recommended for further studies:

- i. There is a need to extend the investigation on the stability of $O_2^{\bullet-}$ with sulfonium cation based IL and then to identify the product of this reaction. Unlike imidazolium based ILs, the reaction between $O_2^{\bullet-}$ and sulfonium ILs has not been well studied.
- ii. The solubility of KO_2 in ILs requires more attention as higher solubility of KO_2 salt will result in more $O_2^{\bullet-}$ species being available for reaction. Hence, the reaction can take place with less reaction time and moderate temperature.
- iii. Low cost ionic liquid analogues known deep eutectic solvents (DESs) should be explored as media for $O_2^{\bullet-}$ reactions.
- iv. The reaction between $O_2^{\bullet-}$ and other sulfur compounds such as sulfides, benzothiophene and dibenzothiophene should be studied

References

- Abai, M., Holbrey, J. D., Rogers, R. D., & Srinivasan, G. (2010). Ionic liquid S-alkylthiuronium salts. *New Journal of Chemistry*, 34(9), 1981-1993.
- Abin-Fuentes, A., Mohamed, M. E.-S., Wang, D. I., & Prather, K. L. (2013). Exploring the mechanism of biocatalyst inhibition in microbial desulfurization. *Applied and environmental microbiology*, 79(24), 7807-7817.
- Abro, R., Abdeltawab, A. A., Al-Deyab, S. S., Yu, G., Qazi, A. B., Gao, S., & Chen, X. (2014). A review of extractive desulfurization of fuel oils using ionic liquids. *RSC Advances*, 4(67), 35302-35317.
- Acree Jr, W. E., Baker, G. A., Revelli, A. L., Moise, J. C., & Mutelet, F. (2012). Activity coefficients at infinite dilution for organic compounds dissolved in 1-alkyl-1-methylpyrrolidinium bis(trifluoromethylsulfonyl)imide ionic liquids having six-, eight-, and ten-carbon alkyl chains. *Journal of Chemical and Engineering Data*, 57(12), 3510-3518.
- Acree, W. E., Baker, G. A., Mutelet, F., & Moise, J. C. (2011). Partition coefficients of organic compounds in four new tetraalkylammonium bis(trifluoromethylsulfonyl)imide ionic liquids using inverse gas chromatography. *Journal of Chemical and Engineering Data*, 56(9), 3688-3697.
- Afanas'ev, I. B. (1989). *Superoxide Ion Chemistry and Biological Implications*: Taylor & Francis.
- Aggarwal, S., Karimi, I. A., Kilbane II, J. J., & Lee, D. Y. (2012). Roles of sulfite oxidoreductase and sulfite reductase in improving desulfurization by *Rhodococcus erythropolis*. *Molecular BioSystems*, 8(10), 2724-2732.
- Ahmed, O. U., Mjalli, F. S., Al-Wahaibi, T., Al-Wahaibi, Y., & AlNashef, I. M. (2015a). Optimum Performance of Extractive Desulfurization of Liquid Fuels Using Phosphonium and Pyrrolidinium-Based Ionic Liquids. *Industrial & Engineering Chemistry Research*, 54(25), 6540-6550.
- Ahmed, O. U., Mjalli, F. S., Al Wahaibi, T., Al-Waheibi, Y. M., & AlNashef, I. M. (2015b). Stability of Superoxide Ion in Phosphonium-Based Ionic Liquids. *Industrial and Engineering Chemistry Research*, 54(7), 2074-2080.
- Ali, M. F., Al-Malki, A., El-Ali, B., Martinie, G., & Siddiqui, M. N. (2006). Deep desulphurization of gasoline and diesel fuels using non-hydrogen consuming techniques. *Fuel*, 85(10-11), 1354-1363.
- AlNashef, I. M. (2004). *Electrochemistry Superoxide Ion In Room Temperature Ionic Liquids And Its Applications Green Engineering* (Doctor of Philosophy), University of South Carolina 2004.

- AlNashef, I. M., Hashim, M. A., Mjalli, F. S., Ali, M. Q. A. H., & Hayyan, M. (2010). A novel method for the synthesis of 2-imidazolones. *Tetrahedron Letters*, 51(15), 1976-1978.
- AlNashef, I. M., Leonard, M. L., Kittle, M. C., Matthews, M. A., & Weidner, J. W. (2001). Electrochemical generation of superoxide in room-temperature ionic liquids. *Electrochemical and Solid-State Letters*, 4(11), D16-D18.
- AlNashef, I. M., Leonard, M. L., Matthews, M. A., & Weidner, J. W. (2002). Superoxide Electrochemistry in an Ionic Liquid. *Industrial & Engineering Chemistry Research*, 41(18), 4475-4478.
- Alonso, L., Arce, A., Francisco, M., Rodríguez, O., & Soto, A. (2007a). Gasoline desulfurization using extraction with [C8mim][BF₄] ionic liquid. *AIChE Journal*, 53(12), 3108-3115.
- Alonso, L., Arce, A., Francisco, M., Rodríguez, O., & Soto, A. (2007b). Liquid-liquid equilibria for systems composed by 1-methyl-3-octylimidazolium tetrafluoroborate ionic liquid, thiophene, and n-hexane or cyclohexane. *Journal of Chemical and Engineering Data*, 52(5), 1729-1732.
- Alonso, L., Arce, A., Francisco, M., & Soto, A. (2007c). Measurement and correlation of liquid-liquid equilibria of two imidazolium ionic liquids with thiophene and methylcyclohexane. *Journal of Chemical and Engineering Data*, 52(6), 2409-2412.
- Alonso, L., Arce, A., Francisco, M., & Soto, A. (2008a). (Liquid + liquid) equilibria of [C8mim][NTf₂] ionic liquid with a sulfur-component and hydrocarbons. *Journal of Chemical Thermodynamics*, 40(2), 265-270.
- Alonso, L., Arce, A., Francisco, M., & Soto, A. (2008b). Phase behaviour of 1-methyl-3-octylimidazolium bis[trifluoromethylsulfonyl]imide with thiophene and aliphatic hydrocarbons: The influence of n-alkane chain length. *Fluid Phase Equilibria*, 263(2), 176-181.
- Alonso, L., Arce, A., Francisco, M., & Soto, A. (2008c). Solvent extraction of thiophene from n-alkanes (C₇, C₁₂, and C₁₆) using the ionic liquid [C8mim][BF₄]. *Journal of Chemical Thermodynamics*, 40(6), 966-972.
- Alonso, L., Arce, A., Francisco, M., & Soto, A. (2008d). Thiophene separation from aliphatic hydrocarbons using the 1-ethyl-3-methylimidazolium ethylsulfate ionic liquid. *Fluid Phase Equilibria*, 270(1-2), 97-102.
- Alves, L., & Paixão, S. (2014). Enhancement of Dibenzothiophene Desulfurization by *Gordonia* alkanivorans Strain 1B Using Sugar Beet Molasses as Alternative Carbon Source. *Applied Biochemistry and Biotechnology*, 172(6), 3297-3305.
- Anantharaj, R., & Banerjee, T. (2011a). Liquid-liquid equilibria for quaternary systems of imidazolium based ionic liquid+thiophene+pyridine+iso-octane at 298.15K:

- Experiments and quantum chemical predictions. *Fluid Phase Equilibria*, 312(1), 20-30.
- Anantharaj, R., & Banerjee, T. (2011b). Phase behaviour of 1-ethyl-3-methylimidazolium thiocyanate ionic liquid with catalytic deactivated compounds and water at several temperatures: Experiments and theoretical predictions. *International Journal of Chemical Engineering*.
- Anantharaj, R., & Banerjee, T. (2011c). Quantum chemical studies on the simultaneous interaction of thiophene and pyridine with ionic liquid. *AIChE Journal*, 57(3), 749-764.
- Anantharaj, R., & Banerjee, T. (2013). Liquid-liquid equilibrium studies on the removal of thiophene and pyridine from pentane using imidazolium-based ionic liquids. *Journal of Chemical and Engineering Data*, 58(4), 829-837.
- Aparicio, S., Atilhan, M., & Karadas, F. (2010). Thermophysical Properties of Pure Ionic Liquids: Review of Present Situation. *Industrial & Engineering Chemistry Research*, 49(20), 9580-9595.
- Arce, A., Francisco, M., & Soto, A. (2010). Evaluation of the polysubstituted pyridinium ionic liquid [hmpy][Ntf₂] as a suitable solvent for desulfurization: Phase equilibria. *Journal of Chemical Thermodynamics*, 42(6), 712-718.
- Arnaut, L. G., Formosinho, S. J., & Burrows, H. (2006). *Chemical Kinetics: From Molecular Structure to Chemical Reactivity*: Elsevier Science.
- Asumana, C., Yu, G., Li, X., Zhao, J., Liu, G., & Chen, X. (2010). Extractive desulfurization of fuel oils with low-viscosity dicyanamide-based ionic liquids. *Green Chemistry*, 12(11), 2030-2037.
- Babich, I. V., & Moulijn, J. A. (2003). Science and technology of novel processes for deep desulfurization of oil refinery streams: a review☆. *Fuel*, 82(6), 607-631.
- Bard, A. J., & Faulkner, L. R. (2001). *Electrochemical methods: fundamentals and applications (2 ed.)* (2 ed.): Wiley New York.
- Barnes, A. S., Rogers, E. I., Streeter, I., Aldous, L., Hardacre, C., Wildgoose, G. G., & Compton, R. G. (2008). Unusual Voltammetry of the Reduction of O₂ in [C₄dmim][N(Tf)₂] Reveals a Strong Interaction of O₂^{•-} with the [C₄dmim]⁺ Cation. *The Journal of Physical Chemistry C*, 112(35), 13709-13715.
- Batista, M. L. S., Tome, L. I. N., Neves, C. M. S. S., Rocha, E. M., Gomes, J. R. B., & Coutinho, J. A. P. (2012). The origin of the LCST on the liquid-liquid equilibrium of thiophene with ionic liquids. *Journal of Physical Chemistry B*, 116(20), 5985-5992.

- Baxendale, J. H., Evans, M. G., & Park, C. S. (1946). The mechanism and kinetics of the initiation of polymerisation by systems containing hydrogen peroxide. *Transactions of the Faraday Society*, 42(0), 155-169.
- Bhattacharjee, A., Coutinho, J. P., Freire, M., & Carvalho, P. (2015). Thermophysical Properties of Two Ammonium-Based Protic Ionic Liquids. *Journal of Solution Chemistry*, 44(3-4), 703-717.
- Blahut, A., & Dohnal, V. (2011). Interactions of volatile organic compounds with the ionic liquid 1-butyl-1-methylpyrrolidinium dicyanamide. *Journal of Chemical and Engineering Data*, 56(12), 4909-4918.
- Blahut, A., & Dohnal, V. (2013). Interactions of volatile organic compounds with the ionic liquids 1-butyl-1-methylpyrrolidinium tetracyanoborate and 1-butyl-1-methylpyrrolidinium bis(oxalato)borate. *Journal of Chemical Thermodynamics*, 57, 344-354.
- Blahut, A., Sobota, M., Dohnal, V., & Vrbka, P. (2010). Activity coefficients at infinite dilution of organic solutes in the ionic liquid 1-ethyl-3-methylimidazolium methanesulfonate. *Fluid Phase Equilibria*, 299(2), 198-206.
- Boniek, D., Figueiredo, D., dos Santos, A., & de Resende Stoianoff, M. (2015). Biodesulfurization: a mini review about the immediate search for the future technology. *Clean Technologies and Environmental Policy*, 17(1), 29-37.
- Bosmann, A., Datsevich, L., Jess, A., Lauter, A., Schmitz, C., & Wasserscheid, P. (2001). Deep desulfurization of diesel fuel by extraction with ionic liquids. *Chemical Communications*(23), 2494-2495.
- Bösmann, A., Datsevich, L., Jess, A., Lauter, A., Schmitz, C., & Wasserscheid, P. (2001). Deep desulfurization of diesel fuel by extraction with ionic liquids. *Chemical Communications*(23), 2494-2495.
- Bovard, R. M. (1960). Oxygen Sources for Space Flights. *Aerospace medicine*, 31, 407-412.
- Brimblecombe, P. (1996). *Air Composition and Chemistry*: Cambridge University Press.
- Buzzeo, M. C., Hardacre, C., & Compton, R. G. (2004a). Use of Room Temperature Ionic Liquids in Gas Sensor Design. *Analytical Chemistry*, 76(15), 4583-4588.
- Buzzeo, M. C., Klymenko, O. V., Wadhawan, J. D., Hardacre, C., Seddon, K. R., & Compton, R. G. (2003). Voltammetry of oxygen in the room-temperature ionic liquids 1-ethyl-3-methylimidazolium bis((trifluoromethyl) sulfonyl) imide and hexyltriethylammonium bis((trifluoromethyl) sulfonyl) imide: One-electron reduction to form superoxide. Steady-state and transient behavior in the same cyclic voltammogram resulting from widely different diffusion coefficients of oxygen and superoxide. *The Journal of Physical Chemistry A*, 107(42), 8872-8878.

- Buzzeo, M. C., Klymenko, O. V., Wadhawan, J. D., Hardacre, C., Seddon, K. R., & Compton, R. G. (2004b). Kinetic Analysis of the Reaction between Electrogenerated Superoxide and Carbon Dioxide in the Room Temperature Ionic Liquids 1-Ethyl-3-methylimidazolium Bis(trifluoromethylsulfonyl)imide and Hexyltriethylammonium Bis(trifluoromethylsulfonyl)imide. *The Journal of Physical Chemistry B*, 108(12), 3947-3954.
- Cammarata, L., Kazarian, S. G., Salter, P. A., & Welton, T. (2001). Molecular states of water in room temperature ionic liquids. *Physical Chemistry Chemical Physics*, 3(23), 5192-5200.
- Caro, A., Boltes, K., Letón, P., & García-Calvo, E. (2007). Dibenzothiophene biodesulfurization in resting cell conditions by aerobic bacteria. *Biochemical engineering journal*, 35(2), 191-197.
- Carter, M. T., Hussey, C. L., Strubinger, S. K. D., & Osteryoung, R. A. (1991). Electrochemical reduction of dioxygen in room-temperature imidazolium chloride-aluminum chloride molten salts. *Inorganic Chemistry*, 30(5), 1149-1151.
- Casas, J. S., & Sordo, J. (2011). *Lead: Chemistry, analytical aspects, environmental impact and health effects*: Elsevier Science.
- Cassol, C. C., Umpierre, A. P., Ebeling, G., Ferrera, B., Chiaro, S. S. X., & Dupont, J. (2007). On the extraction of aromatic compounds from hydrocarbons by imidazolium ionic liquids. *International Journal of Molecular Sciences*, 8(7), 593-605.
- Chan, N. Y. (2010). *Superoxide Radical And UV Irradiation In Ultrasound Assisted Oxidative Desulfurization (UAOD): A Potential Alternative For Greener Fuels*. (Doctor of Philosophy), University Of Southern California.
- Chan, N. Y., Lin, T.-Y., & Yen, T. F. (2008). Superoxides: Alternative Oxidants for the Oxidative Desulfurization Process. *Energy & Fuels*, 22(5), 3326-3328.
- Chen, X., Guan, Y., Abdeltawab, A. A., Al-Deyab, S. S., Yuan, X., Wang, C., & Yu, G. (2015). Using functional acidic ionic liquids as both extractant and catalyst in oxidative desulfurization of diesel fuel: An investigation of real feedstock. *Fuel*, 146, 6-12.
- Chen, X., Liu, G., Yuan, S., Asumana, C., Wang, W., & Yu, G. (2012). Extractive Desulfurization of Fuel Oils with Thiazolium-Based Ionic Liquids. *Separation Science and Technology*, 47(6), 819-826.
- Chen, X., Yuan, S., Abdeltawab, A. A., Al-Deyab, S. S., Zhang, J., Yu, L., & Yu, G. (2014). Extractive desulfurization and denitrogenation of fuels using functional acidic ionic liquids. *Separation and Purification Technology*, 133, 187-193.

- Chu, X., Hu, Y., Li, J., Liang, Q., Liu, Y., Zhang, X., . . . Yue, W. (2008). Desulfurization of Diesel Fuel by Extraction with [BF₄]-based Ionic Liquids. *Chinese Journal of Chemical Engineering*, 16(6), 881-884.
- Cremer, T. (2013). *Ionic Liquid Bulk and Interface Properties: Electronic Interaction, Molecular Orientation and Growth Characteristics*: Springer.
- Daintith, J. (2009). *The Facts on File Dictionary of Inorganic Chemistry*: Facts On File, Incorporated.
- Daniels, S. L. (2002). "On the ionization of air for removal of noxious effluvia" (Air ionization of indoor environments for control of volatile and particulate contaminants with nonthermal plasmas generated by dielectric-barrier discharge). *Ieee Transactions on Plasma Science*, 30(4), 1471-1481.
- De Oliveira, L. H., Álvarez, V. H., & Aznar, M. (2012). Liquid-liquid equilibrium in N -methyl-2-hydroxyethylammonium acetate, butanoate, or hexanoate Ionic Liquids + dibenzothiophene + n dodecane systems at 298.2 K and atmospheric pressure. *Journal of Chemical and Engineering Data*, 57(3), 744-750.
- De Oliveira, L. H., & Aznar, M. (2011). Phase Equilibria in Ionic Liquids + Dibenzothiophene + n-Dodecane Systems. *Industrial and Engineering Chemistry Research*, 50(4), 2289-2295.
- Dharaskar, S. A., Wasewar, K. L., Varma, M. N., & Shende, D. Z. (2015). Imidazolium ionic liquid as energy efficient solvent for desulfurization of liquid fuel. *Separation and Purification Technology*, 155, 101-109.
- Dharaskar, S. A., Wasewar, K. L., Varma, M. N., Shende, D. Z., & Yoo, C. K. (2014). Extractive Desulfurization of Liquid Fuels by Energy Efficient Green Thiazolium based Ionic Liquids. *Industrial & Engineering Chemistry Research*, 53(51), 19845-19854.
- Dilimon, V., Narayanan, N. V., & Sampath, S. (2010). Electrochemical reduction of oxygen on gold and boron-doped diamond electrodes in ambient temperature, molten acetamide-urea-ammonium nitrate eutectic melt. *Electrochimica Acta*, 55(20), 5930-5937.
- Ding, K. (2009). The Electrocatalysis of Multi-walled Carbon Nanotubes (MWCNTs) for Oxygen Reduction Reaction (ORR) in Room Temperature Ionic Liquids (RTILs). *Portugaliae Electrochimica Acta*, 27(2), 165-175.
- Domańska, U., & Królikowska, M. (2011). Measurements of activity coefficients at infinite dilution for organic solutes and water in the ionic liquid 1-butyl-1-methylpiperidinium thiocyanate. *Journal of Chemical and Engineering Data*, 56(1), 124-129.
- Domańska, U. (2006). Thermophysical properties and thermodynamic phase behavior of ionic liquids. *Thermochimica Acta*, 448(1), 19-30.

- Domańska, U., Królikowski, M., & Acree Jr, W. E. (2011a). Thermodynamics and activity coefficients at infinite dilution measurements for organic solutes and water in the ionic liquid 1-butyl-1-methylpyrrolidinium tetracyanoborate. *Journal of Chemical Thermodynamics*, 43(12), 1810-1817.
- Domańska, U., & Królikowska, M. (2010). Measurements of activity coefficients at infinite dilution in solvent mixtures with thiocyanate-based ionic liquids using glc technique. *Journal of Physical Chemistry B*, 114(25), 8460-8466.
- Domańska, U., & Królikowski, M. (2010a). Determination of activity coefficients at infinite dilution of 35 solutes in the ionic liquid, 1-butyl-3-methylimidazolium tosylate, using gas-liquid chromatography. *Journal of Chemical and Engineering Data*, 55(11), 4817-4822.
- Domańska, U., & Królikowski, M. (2010b). Phase equilibria study of the binary systems (1-butyl-3-methylimidazolium tosylate ionic liquid + water, or organic solvent). *Journal of Chemical Thermodynamics*, 42(3), 355-362.
- Domańska, U., & Królikowski, M. (2011). Thermodynamics and activity coefficients at infinite dilution measurements for organic solutes and water in the ionic liquid N-hexyl-3-methylpyridinium tosylate. *Journal of Physical Chemistry B*, 115(22), 7397-7404.
- Domańska, U., & Królikowski, M. (2012). Measurements of activity coefficients at infinite dilution for organic solutes and water in the ionic liquid 1-ethyl-3-methylimidazolium methanesulfonate. *Journal of Chemical Thermodynamics*, 54, 20-27.
- Domańska, U., Królikowski, M., Acree Jr, W. E., & Baker, G. A. (2013a). Physicochemical properties and activity coefficients at infinite dilution for organic solutes and water in a novel bicyclic guanidinium superbases-derived protic ionic liquid. *Journal of Chemical Thermodynamics*, 58, 62-69.
- Domańska, U., Królikowski, M., & Ślesińska, K. (2009a). Phase equilibria study of the binary systems (ionic liquid + thiophene): Desulphurization process. *Journal of Chemical Thermodynamics*, 41(11), 1303-1311.
- Domańska, U., & Laskowska, M. (2009). Measurements of activity coefficients at infinite dilution of aliphatic and aromatic hydrocarbons, alcohols, thiophene, tetrahydrofuran, MTBE, and water in ionic liquid [BMIM][SCN] using GLC. *Journal of Chemical Thermodynamics*, 41(5), 645-650.
- Domańska, U., Lukoshko, E. V., & Królikowski, M. (2012a). Measurements of activity coefficients at infinite dilution for organic solutes and water in the ionic liquid 1-butyl-1-methylpyrrolidinium tris(pentafluoroethyl)trifluorophosphate ([BMPYR][FAP]). *Chemical Engineering Journal*, 183, 261-270.

- Domańska, U., Lukoshko, E. V., & Królikowski, M. (2013b). Phase behaviour of ionic liquid 1-butyl-1-methylpyrrolidinium tris(pentafluoroethyl)trifluorophosphate with alcohols, water and aromatic hydrocarbons. *Fluid Phase Equilibria*, 345, 18-22.
- Domańska, U., Lukoshko, E. V., & Królikowski, M. (2013c). Separation of thiophene from heptane with ionic liquids. *Journal of Chemical Thermodynamics*, 61, 126-131.
- Domańska, U., Lukoshko, E. V., & Wlazło, M. (2012b). Measurements of activity coefficients at infinite dilution for organic solutes and water in the ionic liquid 1-hexyl-3-methylimidazolium tetracyanoborate. *Journal of Chemical Thermodynamics*, 47, 389-396.
- Domańska, U., & Marciniak, A. (2008). Activity coefficients at infinite dilution measurements for organic solutes and water in the ionic liquid 1-butyl-3-methylimidazolium trifluoromethanesulfonate. *Journal of Physical Chemistry B*, 112(35), 11100-11105.
- Domańska, U., & Marciniak, A. (2009a). Activity coefficients at infinite dilution measurements for organic solutes and water in the 1-hexyloxymethyl-3-methylimidazolium and 1,3-dihexyloxymethyl-imidazolium bis(trifluoromethylsulfonyl)-imide ionic liquids-The cation influence. *Fluid Phase Equilibria*, 286(2), 154-161.
- Domańska, U., & Marciniak, A. (2009b). Activity coefficients at infinite dilution measurements for organic solutes and water in the ionic liquid 4-methyl-N-butylpyridinium bis(trifluoromethylsulfonyl)-imide. *Journal of Chemical Thermodynamics*, 41(12), 1350-1355.
- Domańska, U., & Marciniak, A. (2009c). Activity coefficients at infinite dilution measurements for organic solutes and water in the ionic liquid triethylsulphonium bis(trifluoromethylsulfonyl)imide. *Journal of Chemical Thermodynamics*, 41(6), 754-758.
- Domańska, U., & Marciniak, A. (2010). Physicochemical properties and activity coefficients at infinite dilution for organic solutes and water in the ionic liquid 1-decyl-3-methylimidazolium tetracyanoborate. *Journal of Physical Chemistry B*, 114(49), 16542-16547.
- Domańska, U., Marciniak, A., Królikowska, M., & Arasimowicz, M. (2010a). Activity coefficients at infinite dilution measurements for organic solutes and water in the ionic liquid 1-hexyl-3-methylimidazolium thiocyanate. *Journal of Chemical and Engineering Data*, 55(7), 2532-2536.
- Domańska, U., & Patuszyński, K. (2010a). Gas-liquid chromatography measurements of activity coefficients at infinite dilution of various organic solutes and water in triisobutylmethylphosphonium tosylate ionic liquid. *Journal of Chemical Thermodynamics*, 42(6), 707-711.
- Domańska, U., & Patuszyński, K. (2010b). Measurements of activity coefficients at infinite dilution of organic solutes and water in 1-propyl-1-methylpiperidinium

- bis{(trifluoromethyl) sulfonyl}imide ionic liquid using g.l.c. *Journal of Chemical Thermodynamics*, 42(11), 1361-1366.
- Domańska, U., Redhi, G. G., & Marciniak, A. (2009b). Activity coefficients at infinite dilution measurements for organic solutes and water in the ionic liquid 1-butyl-1-methylpyrrolidinium trifluoromethanesulfonate using GLC. *Fluid Phase Equilibria*, 278(1-2), 97-102.
- Domańska, U., Walczak, K., & Królikowski, M. (2014). Extraction desulfurization process of fuels with ionic liquids. *The Journal of Chemical Thermodynamics*, 77, 40-45.
- Domańska, U., Zawadzki, M., Królikowska, M., Marc Tshibangu, M., Ramjugernath, D., & Letcher, T. M. (2011b). Measurements of activity coefficients at infinite dilution of organic compounds and water in isoquinolinium-based ionic liquid [C8iQuin][NTf2] using GLC. *Journal of Chemical Thermodynamics*, 43(3), 499-504.
- Domańska, U., Zawadzki, M., Królikowski, M., & Lewandowska, A. (2012c). Phase equilibria study of binary and ternary mixtures of {N-octylisoquinolinium bis{(trifluoromethyl)sulfonyl}imide+hydrocarbon, or an alcohol, or water}. *Chemical Engineering Journal*, 181-182, 63-71.
- Domańska, U., Zawadzki, M., Marc Tshibangu, M., Ramjugernath, D., & Letcher, T. M. (2010b). Phase equilibria study of {N-butylquinolinium bis{(trifluoromethyl) sulfonyl}imide + aromatic hydrocarbons, or an alcohol} binary systems. *Journal of Chemical Thermodynamics*, 42(9), 1180-1186.
- Dyson, P. J., & Geldbach, T. J. (2006). *Metal Catalysed Reactions in Ionic Liquids*: Springer.
- Earle, M. J., Esperanca, J. M. S. S., Gilea, M. A., Canongia Lopes, J. N., Rebelo, L. P. N., Magee, J. W., . . . Widegren, J. A. (2006). The distillation and volatility of ionic liquids. *Nature*, 439(7078), 831-834.
- Elliott, A., Kshirsager, G., Noehren, W., & Kuper, C. (2014).
- Enayati, M., & Faghihian, H. (2015). N-butyl-pyridinium tetrafluoroborate as a highly efficient ionic liquid for removal of dibenzothiophene from organic solutions. *Journal of Fuel Chemistry and Technology*, 43(2), 195-201.
- Eßer, J., Wasserscheid, P., & Jess, A. (2004). Deep desulfurization of oil refinery streams by extraction with ionic liquids. *Green Chemistry*, 6(7), 316-322.
- Evans, R. G., Klymenko, O. V., Saddoughi, S. A., Hardacre, C., & Compton, R. G. (2004). Electroreduction of oxygen in a series of room temperature ionic liquids composed of group 15-centered cations and anions. *The Journal of Physical Chemistry B*, 108(23), 7878-7886.

- Fang, D., Wang, Q., Liu, Y., Xia, L., & Zang, S. (2014). High-Efficient Oxidation–Extraction Desulfurization Process by Ionic Liquid 1-Butyl-3-methyl-imidazolium Trifluoroacetic Acid. *Energy & Fuels*, 28(10), 6677-6682.
- Fleck, R. N., Nahin, Paul G. (1950). United States Patent No.
- Francisco, M., Arce, A., & Soto, A. (2010). Ionic liquids on desulfurization of fuel oils. *Fluid Phase Equilibria*, 294(1-2), 39-48.
- Freemantle, M. (2010). *An introduction to ionic liquids*: Royal Society of Chemistry.
- Gao, H., Guo, C., Xing, J., & Liu, H. (2012). Deep Desulfurization of Diesel Oil with Extraction Using Pyridinium-Based Ionic Liquids. *Separation Science and Technology*, 47(2), 325-330.
- Gao, H., Li, Y., Wu, Y., Luo, M., Li, Q., Xing, J., & Liu, H. (2009a). Extractive desulfurization of fuel using 3-methylpyridinium-based ionic liquids. *Energy and Fuels*, 23(5), 2690-2694.
- Gao, H., Luo, M., Xing, J., Wu, Y., Li, Y., Li, W., . . . Liu, H. (2008). Desulfurization of fuel by extraction with pyridinium-based ionic liquids. *Industrial and Engineering Chemistry Research*, 47(21), 8384-8388.
- Gao, H., Xing, J., Li, Y., Li, W., Liu, Q., & Liu, H. (2009b). Desulfurization of diesel fuel by extraction with lewis-acidic ionic liquid. *Separation Science and Technology*, 44(4), 971-982.
- García-Gutiérrez, J. L., Fuentes, G. A., Hernández-Terán, M. E., Murrieta, F., Navarrete, J., & Jiménez-Cruz, F. (2006). Ultra-deep oxidative desulfurization of diesel fuel with H₂O₂ catalyzed under mild conditions by polymolybdates supported on Al₂O₃. *Applied Catalysis A*, 305(1), 15-20.
- Ghatee, M. H., Zare, M., Zolghadr, A. R., & Moosavi, F. (2010). Temperature dependence of viscosity and relation with the surface tension of ionic liquids. *Fluid Phase Equilibria*, 291(2), 188-194.
- Ghilane, J., Lagrost, C., & Hapiot, P. (2007). Scanning Electrochemical Microscopy in Unusual Solvents: Inequality of Diffusion Coefficients Problem. *Analytical Chemistry*, 79(19), 7383-7391.
- Govinda, V., Madhusudhana Reddy, P., Bahadur, I., Attri, P., Venkatesu, P., & Venkateswarlu, P. (2013). Effect of anion variation on the thermophysical properties of triethylammonium based protic ionic liquids with polar solvent. *Thermochimica Acta*, 556, 75-88.
- Gui, J., Liu, D., Sun, Z., Liu, D., Min, D., Song, B., & Peng, X. (2010). Deep oxidative desulfurization with task-specific ionic liquids: An experimental and computational study. *Journal of Molecular Catalysis A: Chemical*, 331(1-2), 64-70.

- Guobin, S., Huaiying, Z., Jianmin, X., Guo, C., Wangliang, L., & Huizhou, L. (2006). Biodesulfurization of hydrodesulfurized diesel oil with *Pseudomonas delafieldii* R-8 from high density culture. *Biochemical engineering journal*, 27(3), 305-309.
- Gutmann, V. (1978). *The donor-acceptor approach to molecular interactions*: Plenum Press.
- Haber, F., & Weiss, J. (1934). *The catalytic decomposition of hydrogen peroxide by iron salts*. Paper presented at the Proceedings of the Royal Society of London A: Mathematical, Physical and Engineering Sciences.
- Hall, C., & Hoff, W. D. (2011). *Water Transport in Brick, Stone and Concrete*: Taylor & Francis.
- Hansmeier, A. R., Meindersma, G. W., & De Haan, A. B. (2011). Desulfurization and denitrogenation of gasoline and diesel fuels by means of ionic liquids. *Green Chemistry*, 13(7), 1907-1913.
- Hayyan, A., Mjalli, F. S., AlNashef, I. M., Al-Wahaibi, T., Al-Wahaibi, Y. M., & Hashim, M. A. (2012a). Fruit sugar-based deep eutectic solvents and their physical properties. *Thermochimica Acta*, 541, 70-75.
- Hayyan, A., Mjalli, F. S., AlNashef, I. M., Al-Wahaibi, Y. M., Al-Wahaibi, T., & Hashim, M. A. (2013a). Glucose-based deep eutectic solvents: Physical properties. *Journal of Molecular Liquids*, 178, 137-141.
- Hayyan, M. (2012). *Generation of superoxide ion in ionic liquids and its application in the destruction of hazardous materials*. (Doctor of Philosophy), University of Malaya Kuala Lumpur.
- Hayyan, M., Aissaoui, T., Hashim, M. A., AlSaadi, M. A., & Hayyan, A. (2015a). Triethylene glycol based deep eutectic solvents and their physical properties. *Journal of the Taiwan Institute of Chemical Engineers*, 50, 24-30.
- Hayyan, M., Hashim, M. A., & AlNashef, I. M. (2015b). Kinetics of superoxide ion in dimethyl sulfoxide containing ionic liquids. *Ionics*, 21(3), 719-728.
- Hayyan, M., Mjalli, F. S., AlNashef, I. M., & Hashim, M. A. (2012b). Generation and stability of superoxide ion in tris(pentafluoroethyl)trifluorophosphate anion-based ionic liquids. *Journal of Fluorine Chemistry*, 142, 83-89.
- Hayyan, M., Mjalli, F. S., AlNashef, I. M., & Hashim, M. A. (2012c). Stability and Kinetics of Generated Superoxide Ion in Trifluoromethanesulfonate Anion-Based Ionic Liquids. *International Journal of Electrochemical Science*, 7(10), 9658-9667.
- Hayyan, M., Mjalli, F. S., Hashim, M. A., & AlNashef, I. M. (2011). Electrochemical Generation of Superoxide Ion in Ionic Liquid 1-(3-Methoxypropyl)-1-Methylpiperidinium Bis (Trifluoromethylsulfonyl) Imide. *Conference on Advanced Materials and Nanotechnology (Caman 2009)*, 17.

- Hayyan, M., Mjalli, F. S., Hashim, M. A., & AlNashef, I. M. (2012d). Generation of Superoxide Ion in Pyridinium, Morpholinium, Ammonium, and Sulfonium-Based Ionic Liquids and the Application in the Destruction of Toxic Chlorinated Phenols. *Industrial & Engineering Chemistry Research*, 51(32), 10546-10556.
- Hayyan, M., Mjalli, F. S., Hashim, M. A., & AlNashef, I. M. (2013b). An investigation of the reaction between 1-butyl-3-methylimidazolium trifluoromethanesulfonate and superoxide ion. *Journal of Molecular Liquids*, 181, 44-50.
- Hayyan, M., Mjalli, F. S., Hashim, M. A., AlNashef, I. M., Al-Zahrani, S. M., & Chooi, K. L. (2012e). Generation of superoxide ion in 1-butyl-1-methylpyrrolidinium trifluoroacetate and its application in the destruction of chloroethanes. *Journal of Molecular Liquids*, 167, 28-33.
- Hayyan, M., Mjalli, F. S., Hashim, M. A., AlNashef, I. M., Al-Zahrani, S. M., & Chooi, K. L. (2012f). Long term stability of superoxide ion in piperidinium, pyrrolidinium and phosphonium cations-based ionic liquids and its utilization in the destruction of chlorobenzenes. *Journal of Electroanalytical Chemistry*, 664, 26-32.
- Hayyan, M., Mjalli, F. S., Hashim, M. A., AlNashef, I. M., & Tan, X. M. (2011). Electrochemical reduction of dioxygen in bis (trifluoromethylsulfonyl) imide based ionic liquids. *Journal of Electroanalytical Chemistry*, 657(1), 150-157.
- He, L., Li, H., Zhu, W., Guo, J., Jiang, X., Lu, J., & Yan, Y. (2008). Deep Oxidative Desulfurization of Fuels Using Peroxophosphomolybdate Catalysts in Ionic Liquids. *Industrial & Engineering Chemistry Research*, 47(18), 6890-6895.
- Henze, G. (2008). Analytical Voltammetry and Polarography *Handbook of Analytical Techniques* (pp. 785-825): Wiley-VCH Verlag GmbH.
- Hernández-Maldonado, A. J., & Yang, R. T. (2004a). Desulfurization of Diesel Fuels by Adsorption via π -Complexation with Vapor-Phase Exchanged Cu(I)-Y Zeolites. *Journal of the American Chemical Society*, 126(4), 992-993.
- Hernández-Maldonado, A. J., & Yang, R. T. (2004b). New sorbents for desulfurization of diesel fuels via π -complexation. *AIChE Journal*, 50(4), 791-801.
- Herranz, J., Garsuch, A., & Gasteiger, H. A. (2012). Using rotating ring disc electrode voltammetry to quantify the superoxide radical stability of aprotic Li-Air battery electrolytes. *The Journal of Physical Chemistry C*, 116(36), 19084-19094.
- Holbrey, J. D., López-Martin, I., Rothenberg, G., Seddon, K. R., Silvero, G., & Zheng, X. (2008). Desulfurisation of oils using ionic liquids: Selection of cationic and anionic components to enhance extraction efficiency. *Green Chemistry*, 10(1), 87-92.
- Holbrey, J. D., & Seddon, K. R. (1999). Ionic Liquids. *Clean Products and Processes*, 1(4), 223-236.

- Huang, C., Chen, B., Zhang, J., Liu, Z., & Li, Y. (2004). Desulfurization of gasoline by extraction with new ionic liquids. *Energy and Fuels*, 18(6), 1862-1864.
- Huang, X.-J., Aldous, L., O'Mahony, A. M., del Campo, F. J., & Compton, R. G. (2010). Toward Membrane-Free Amperometric Gas Sensors: A Microelectrode Array Approach. *Analytical Chemistry*, 82(12), 5238-5245.
- Huang, X.-J., Rogers, E. I., Hardacre, C., & Compton, R. G. (2009). The reduction of oxygen in various room temperature ionic liquids in the temperature range 293–318 K: Exploring the applicability of the Stokes–Einstein relationship in room temperature ionic liquids. *The Journal of Physical Chemistry B*, 113(26), 8953-8959.
- Islam, M. M., Ferdousi, B. N., Okajima, T., & Ohsaka, T. (2005a). A catalytic activity of a mercury electrode towards dioxygen reduction in room-temperature ionic liquids. *Electrochemistry Communications*, 7(7), 789-795.
- Islam, M. M., Imase, T., Okajima, T., Takahashi, M., Niikura, Y., Kawashima, N., . . . Ohsaka, T. (2009). Stability of superoxide ion in imidazolium cation-based room-temperature ionic liquids. *The Journal of Physical Chemistry A*, 113(5), 912-916.
- Islam, M. M., & Ohsaka, T. (2008a). Roles of Ion Pairing on Electroreduction of Dioxygen in Imidazolium-Cation-Based Room-Temperature Ionic Liquid. *The Journal of Physical Chemistry C*, 112(4), 1269-1275.
- Islam, M. M., & Ohsaka, T. (2008b). Two-electron quasi-reversible reduction of dioxygen at HMDE in ionic liquids: Observation of cathodic maximum and inverted peak. *Journal of Electroanalytical Chemistry*, 623(2), 147-154.
- Islam, M. M., Saha, M. S., Okajima, T., & Ohsaka, T. (2005b). Current oscillatory phenomena based on electrogenerated superoxide ion at the HMDE in dimethylsulfoxide. *Journal of Electroanalytical Chemistry*, 577(1), 145-154.
- Ito, E., & van Veen, J. A. R. (2006). On novel processes for removing sulphur from refinery streams. *Catalysis Today*, 116(4), 446-460.
- Izumi, Y., Ohshiro, T., Ogino, H., Hine, Y., & Shimao, M. (1994). Selective desulfurization of dibenzothiophene by *Rhodococcus erythropolis* D-1. *Applied and environmental microbiology*, 60(1), 223-226.
- Jian-long, W., Zhao, D. s., Zhou, E. p., & Dong, Z. (2007). Desulfurization of gasoline by extraction with N-alkyl-pyridinium-based ionic liquids. *Ranliao Huaxue Xuebao/Journal of Fuel Chemistry and Technology*, 35(3), 293-296.
- Jiang, W., Zhu, W., Chang, Y., Chao, Y., Yin, S., Liu, H., . . . Li, H. (2014). Ionic liquid extraction and catalytic oxidative desulfurization of fuels using dialkylpiperidinium tetrachloroferrates catalysts. *Chemical Engineering Journal*, 250, 48-54.

- Jiang, W., Zhu, W., Li, H., Wang, X., Yin, S., Chang, Y., & Li, H. (2015). Temperature-responsive ionic liquid extraction and separation of the aromatic sulfur compounds. *Fuel*, *140*, 590-596.
- Julião, D., Gomes, A. C., Pillinger, M., Cunha-Silva, L., de Castro, B., Gonçalves, I. S., & Balula, S. S. (2015). Desulfurization of model diesel by extraction/oxidation using a zinc-substituted polyoxometalate as catalyst under homogeneous and heterogeneous (MIL-101(Cr) encapsulated) conditions. *Fuel Processing Technology*, *131*(0), 78-86.
- Katayama, Y., Onodera, H., Yamagata, M., & Miura, T. (2004). Electrochemical reduction of oxygen in some hydrophobic room-temperature molten salt systems. *Journal of the Electrochemical Society*, *151*(1), A59-A63.
- Katayama, Y., Sekiguchi, K., Yamagata, M., & Miura, T. (2005). Electrochemical behavior of oxygen/superoxide ion couple in 1-butyl-1-methylpyrrolidinium bis(trifluoromethylsulfonyl) imide room-temperature molten salt. *Journal of the Electrochemical Society*, *152*(8), E247-E250.
- Kêdra-Królik, K., Fabrice, M., & Jaubert, J. N. (2011). Extraction of thiophene or pyridine from n-heptane using ionic liquids. gasoline and diesel desulfurization. *Industrial and Engineering Chemistry Research*, *50*(4), 2296-2306.
- Kim, J. H., Ma, X., Zhou, A., & Song, C. (2006). Ultra-deep desulfurization and denitrogenation of diesel fuel by selective adsorption over three different adsorbents: A study on adsorptive selectivity and mechanism. *Catalysis Today*, *111*(1-2), 74-83.
- Kim, S., DiCosimo, R., & San Filippo, J. (1979). Spectrometric and chemical characterization of superoxide. *Analytical Chemistry*, *51*(6), 679-681.
- Kirchner, B., & Clare, B. (2009). *Ionic Liquids*: Springer.
- Knowles, P., Gibson, J., Pick, F., & Bray, R. (1969). Electron-spin-resonance evidence for enzymic reduction of oxygen to a free radical, the superoxide ion. *Biochem. J*, *111*, 53-58.
- Ko, N. H., Lee, J. S., Huh, E. S., Lee, H., Jung, K. D., Kim, H. S., & Cheong, M. (2008). Extractive desulfurization using Fe-containing ionic liquids. *Energy and Fuels*, *22*(3), 1687-1690.
- Köddermann, T., Wertz, C., Heintz, A., & Ludwig, R. (2006). The Association of Water in Ionic Liquids: A Reliable Measure of Polarity. *Angewandte Chemie International Edition*, *45*(22), 3697-3702.
- Kolbeck, C., Lehmann, J., Lovelock, K. R. J., Cremer, T., Paape, N., Wasserscheid, P., . . . Steinrück, H. P. (2010). Density and Surface Tension of Ionic Liquids. *The Journal of Physical Chemistry B*, *114*(51), 17025-17036.

- Krawietz, T. R., Murray, D. K., & Haw, J. F. (1998). Alkali Metal Oxides, Peroxides, and Superoxides: A Multinuclear MAS NMR Study. *The Journal of Physical Chemistry A*, 102(45), 8779-8785.
- Królikowska, M., & Karpińska, M. (2013). Phase equilibria study of the (N-octylisoquinolinium thiocyanate ionic liquid + aliphatic and aromatic hydrocarbon, or thiophene) binary systems. *Journal of Chemical Thermodynamics*, 63, 128-134.
- Królikowska, M., Karpińska, M., & Królikowski, M. (2013). Measurements of activity coefficients at infinite dilution for organic solutes and water in N-hexylisoquinolinium thiocyanate, [HiQuin][SCN] using GLC. *Journal of Chemical Thermodynamics*, 62, 1-7.
- Królikowska, M., Karpińska, M., & Zawadzki, M. (2012). Phase equilibria study of the binary systems (N-hexylisoquinolinium thiocyanate ionic liquid + organic solvent or water). *Journal of Physical Chemistry B*, 116(14), 4292-4299.
- Królikowska, M., Lipiński, P., & Maik, D. (2014). Density, viscosity and phase equilibria study of {ethylsulfate-based ionic liquid + water} binary systems as a function of temperature and composition. *Thermochimica Acta*, 582, 1-9.
- Królikowski, M., Walczak, K., & Domańska, U. (2013). Solvent extraction of aromatic sulfur compounds from n-heptane using the 1-ethyl-3-methylimidazolium tricyanomethanide ionic liquid. *The Journal of Chemical Thermodynamics*, 65(0), 168-173.
- Kulkarni, P. S., & Afonso, C. A. M. (2010). Deep desulfurization of diesel fuel using ionic liquids: current status and future challenges. *Green Chemistry*, 12(7), 1139-1149.
- Laoire, C. O., Mukerjee, S., Abraham, K. M., Plichta, E. J., & Hendrickson, M. A. (2009). Elucidating the Mechanism of Oxygen Reduction for Lithium-Air Battery Applications. *The Journal of Physical Chemistry C*, 113(46), 20127-20134.
- Laoire, C. O., Mukerjee, S., Abraham, K. M., Plichta, E. J., & Hendrickson, M. A. (2010). Influence of Nonaqueous Solvents on the Electrochemistry of Oxygen in the Rechargeable Lithium–Air Battery. *The Journal of Physical Chemistry C*, 114(19), 9178-9186.
- Lee, M., Senius, J., & Grossman, M. (1995). Sulfur-specific microbial desulfurization of sterically hindered analogs of dibenzothiophene. *Applied and environmental microbiology*, 61(12), 4362-4366.
- Leffler, W. L. (2008). *Petroleum Refining: In Nontechnical Language*: PennWell Corporation.
- LI, C.-j., Ran, Z., PENG, M.-q., Hao, L., Gang, Y., & Dong-sheng, X. (2015). Study on desulfurization and denitrification by modified activated carbon fibers with visible-light photocatalysis. *Journal of Fuel Chemistry and Technology*, 43(12), 1516-1522.

- Li, F. T., Liu, Y., Sun, Z. M., Chen, L. J., Zhao, D. S., Liu, R. H., & Kou, C. G. (2010). Deep extractive desulfurization of gasoline with xEt 3NHCl·FeCl₃ ionic liquids. *Energy and Fuels*, 24(8), 4285-4289.
- Li, Y.-G., Gao, H.-S., Li, W.-L., Xing, J.-M., & Liu, H.-Z. (2009). In situ magnetic separation and immobilization of dibenzothiophene-desulfurizing bacteria. *Bioresource Technology*, 100(21), 5092-5096.
- Lin, F., Wang, D., Jiang, Z., Ma, Y., Li, J., Li, R., & Li, C. (2012a). Photocatalytic oxidation of thiophene on BiVO₄ with dual co-catalysts Pt and RuO₂ under visible light irradiation using molecular oxygen as oxidant. *Energy Environ. Sci.*, 5(4), 6400-6406.
- Lin, F., Wang, D., Jiang, Z., Ma, Y., Li, J., Li, R., & Li, C. (2012b). Photocatalytic oxidation of thiophene on BiVO₄ with dual co-catalysts Pt and RuO₂ under visible light irradiation using molecular oxygen as oxidant. *Energy & Environmental Science*, 5(4), 6400-6406.
- Liu, D., Gui, J., Song, L., Zhang, X., & Sun, Z. (2008). Deep desulfurization of diesel fuel by extraction with task-specific ionic liquids. *Petroleum Science and Technology*, 26(9), 973-982.
- Lo, W. H., Yang, H. Y., & Wei, G. T. (2003). One-pot desulfurization of light oils by chemical oxidation and solvent extraction with room temperature ionic liquids. *Green Chemistry*, 5(5), 639-642.
- Lü, H., Wang, S., Deng, C., Ren, W., & Guo, B. (2014). Oxidative desulfurization of model diesel via dual activation by a protic ionic liquid. *Journal of Hazardous Materials*, 279(0), 220-225.
- Lü, R., Lin, J., & Qu, Z. (2012). Theoretical study on interactions between ionic liquids and organosulfur compounds. *Computational and Theoretical Chemistry*.
- Lü, R., Liu, D., Lu, Y., & Wang, S. (2013a). The nature of interactions between [Cu₂Cl₃]-based ionic liquid and thiophene - A theoretical study. *Journal of Saudi Chemical Society*.
- Lü, R., Qu, Z., & Lin, J. (2013b). Comparative study of interactions between thiophene\pyridine\benzene\ heptane and 1-butyl-3-methylimidazolium trifluoromethanesulfonate by density functional theory. *Journal of Molecular Liquids*, 180, 207-214.
- Mabbott, G. A. (1983). An introduction to cyclic voltammetry. *Journal of Chemical Education*, 60(9), 697.
- MacFarlane, D. R., Forsyth, M., Izgorodina, E. I., Abbott, A. P., Annat, G., & Fraser, K. (2009). On the concept of ionicity in ionic liquids. *Physical Chemistry Chemical Physics*, 11(25), 4962-4967.

- Mafi, M., Dehghani, M. R., & Mokhtarani, B. (2016). Novel liquid–liquid equilibrium data for six ternary systems containing IL, hydrocarbon and thiophene at 25 °C. *Fluid Phase Equilibria*, 412, 21-28.
- Manning, F. S., Thompson, R. E., & Thompson, R. E. (1995). *Oilfield Processing of Petroleum: Crude oil*: PennWell Corporation.
- Marciniak, A. (2011). Activity coefficients at infinite dilution and physicochemical properties for organic solutes and water in the ionic liquid 1-(3-hydroxypropyl)pyridinium bis(trifluoromethylsulfonyl)-amide. *Journal of Chemical Thermodynamics*, 43(10), 1446-1452.
- Marciniak, A., & Karczemna, E. (2011). Influence of the ionic liquid structure on thiophene solubility. *Fluid Phase Equilibria*, 307(2), 160-165.
- Marciniak, A., & Królikowski, M. (2012a). Ternary (liquid + liquid) equilibria of {trifluorotris(perfluoroethyl) phosphate based ionic liquids + thiophene + heptane}. *Journal of Chemical Thermodynamics*, 49, 154-158.
- Marciniak, A., & Królikowski, M. (2012b). Ternary liquid-liquid equilibria of bis(trifluoromethylsulfonyl)-amide based ionic liquids+thiophene+n-heptane. The influence of cation structure. *Fluid Phase Equilibria*, 321, 59-63.
- Marciniak, A., & Wlazlo, M. (2010). Activity coefficients at infinite dilution measurements for organic solutes and water in the ionic liquid 1-butyl-3-methyl-pyridinium trifluoromethanesulfonate. *Journal of Chemical and Engineering Data*, 55(9), 3208-3211.
- Marciniak, A., & Wlazło, M. (2010). Activity coefficients at infinite dilution measurements for organic solutes and water in the ionic liquid 1-(3-hydroxypropyl)pyridinium trifluorotris(perfluoroethyl)phosphate. *Journal of Physical Chemistry B*, 114(20), 6990-6994.
- Marciniak, A., & Wlazło, M. (2012a). Activity coefficients at infinite dilution and physicochemical properties for organic solutes and water in the ionic liquid 1-(2-methoxyethyl)-1- methylpiperidinium bis(trifluoromethylsulfonyl)-amide. *Journal of Chemical Thermodynamics*, 49, 137-145.
- Marciniak, A., & Wlazło, M. (2012b). Activity coefficients at infinite dilution and physicochemical properties for organic solutes and water in the ionic liquid 4-(2-methoxyethyl)-4- methylmorpholinium bis(trifluoromethylsulfonyl)-amide. *Journal of Chemical Thermodynamics*, 47, 382-388.
- Marciniak, A., & Wlazło, M. (2013a). Activity coefficients at infinite dilution and physicochemical properties for organic solutes and water in the ionic liquid 1-(2-hydroxyethyl)-3-methylimidazolium trifluorotris(perfluoroethyl)phosphate. *The Journal of Chemical Thermodynamics*, 64(0), 114-119.

- Marciniak, A., & Wlazło, M. (2013b). Activity coefficients at infinite dilution and physicochemical properties for organic solutes and water in the ionic liquid 1-(2-methoxyethyl)-1-methylpyrrolidinium trifluorotris(perfluoroethyl)phosphate. *Journal of Chemical Thermodynamics*, 57, 197-202.
- Marciniak, A., & Wlazło, M. (2013c). Activity coefficients at infinite dilution and physicochemical properties for organic solutes and water in the ionic liquid 1-(2-methoxyethyl)-1-methylpyrrolidinium trifluorotris(perfluoroethyl)phosphate. *Journal of Chemical Thermodynamics*, 60, 57-62.
- Marklund, S. (1976). Spectrophotometric study of spontaneous disproportionation of superoxide anion radical and sensitive direct assay for superoxide dismutase. *Journal of Biological Chemistry*, 251(23), 7504-7507.
- Martin, R. P., & Sawyer, D. T. (1972). Electrochemical reduction of sulfur dioxide in dimethylformamide. *Inorganic Chemistry*, 11(11), 2644-2647.
- Martiz, B., Keyrouz, R., Gmouh, S., Vaultier, M., & Jouikov, V. (2004). Superoxide-stable ionic liquids: new and efficient media for electrosynthesis of functional siloxanes. *Chemical Communications*(6), 674-675.
- Matar, S., & Hatch, L. F. (2001). *Chemistry of Petrochemical Processes*: Elsevier Science.
- McCord, J. M., & Fridovich, I. (1969). Superoxide dismutase an enzymic function for erythrocuprein (hemocuprein). *Journal of Biological Chemistry*, 244(22), 6049-6055.
- McCrary, P. D., & Rogers, R. D. (2013). 1-Ethyl-3-methylimidazolium hexafluorophosphate: from ionic liquid prototype to antitype. *Chemical Communications*, 49(54), 6011-6014.
- McFarlane, D. R., Sun, J., Golding, J., Meakin, P., & Forsyth, M. (2000). High conductivity molten salts based on the imide ion. *Electrochimica Acta*, 45(8-9), 1271-1278.
- Mjalli, F. S., Ahmed, O. U., Al-Wahaibi, T., Al-Wahaibi, Y., & AlNashef, I. M. (2014). Deep oxidative desulfurization of liquid fuels. *Reviews in Chemical Engineering*, 30(4), 337-378.
- Mochida, I., & Choi, K.-H. (2006). Current Progress in Catalysts and Catalysis for Hydrotreating. In C. Hsu & P. Robinson (Eds.), *Practical Advances in Petroleum Processing* (pp. 257-296): Springer New York.
- Mochizuki, Y., & Sugawara, K. (2008). Removal of organic sulfur from hydrocarbon resources using ionic liquids. *Energy and Fuels*, 22(5), 3303-3307.

- Mohammad Fauzi, A. H., & Amin, N. A. S. (2012). An overview of ionic liquids as solvents in biodiesel synthesis. *Renewable and Sustainable Energy Reviews*, 16(8), 5770-5786.
- Mohammad, M., Khan, A. Y., Subhani, M. S., Bibi, N., Ahmad, S., & Saleemi, S. (2001). Kinetics and electrochemical studies on superoxide. *Research on Chemical Intermediates*, 27(3), 259-267.
- Muhammad, A., Abdul Mutalib, M. I., Wilfred, C. D., Murugesan, T., & Shafeeq, A. (2008). Thermophysical properties of 1-hexyl-3-methyl imidazolium based ionic liquids with tetrafluoroborate, hexafluorophosphate and bis(trifluoromethylsulfonyl)imide anions. *The Journal of Chemical Thermodynamics*, 40(9), 1433-1438.
- Nefedieva, M., Lebedeva, O., Kultin, D., Kustov, L., Borisenkova, S., & Krasovskiy, V. (2010). Ionic liquids based on imidazolium tetrafluoroborate for the removal of aromatic sulfur-containing compounds from hydrocarbon mixtures. *Green Chemistry*, 12(2), 346-349.
- Nejad, N. F., & Beigi, A. M. (2015). Efficient desulfurization of gasoline fuel using ionic liquid extraction as a complementary process to adsorptive desulfurization. *Petroleum Science*, 12(2), 330-339.
- Nejad, N. F., Shams, E., Adibi, M., Miran Beigi, A. A., & Torkestani, S. K. (2012). Desulfurization from model of gasoline by extraction with synthesized [BF₄]⁻ and [PF₆]⁻ based ionic liquids. *Petroleum Science and Technology*, 30(15), 1619-1628.
- Nejad, N. F., Soolari, E. S., Adibi, M., Miran Beigi, A. A., & Torkestani, S. K. (2013). Imidazolium-based alkylsulfate ionic liquids and removal of sulfur content from model of gasoline. *Petroleum Science and Technology*, 31(5), 472-480.
- Nie, Y., Li, C., Meng, H., & Wang, Z. (2008). N,N-dialkylimidazolium dialkylphosphate ionic liquids: Their extractive performance for thiophene series compounds from fuel oils versus the length of alkyl group. *Fuel Processing Technology*, 89(10), 978-983.
- Nie, Y., Li, C., Sun, A., Meng, H., & Wang, Z. (2006). Extractive desulfurization of gasoline using imidazolium-based phosphoric ionic liquids. *Energy and Fuels*, 20(5), 2083-2087.
- Nie, Y., Li, C. X., & Wang, Z. H. (2007). Extractive desulfurization of fuel oil using alkylimidazole and its mixture with dialkylphosphate ionic liquids. *Industrial and Engineering Chemistry Research*, 46(15), 5108-5112.
- O'Mahony, A. M., Silvester, D. S., Aldous, L., Hardacre, C., & Compton, R. G. (2008). Effect of Water on the Electrochemical Window and Potential Limits of Room-Temperature Ionic Liquids. *Journal of Chemical & Engineering Data*, 53(12), 2884-2891.

- Oae, S., Takata, T., & Kim, Y. (1981). Reaction of Organic Sulfur Compounds with Superoxide Anion – III Oxidation of Organic Sulfur Compounds to Sulfinic and Sulfonic Acids. *Tetrahedron Letters*, 32, 37 – 44.
- Ohno, H. (2005). *Electrochemical Aspects of Ionic Liquids*: John Wiley & Sons.
- Oliveira, L. H. D., & Aznar, M. (2010). Liquid-liquid equilibrium data in ionic liquid + 4-methylthiophene + n-dodecane systems. *Industrial and Engineering Chemistry Research*, 49(19), 9462-9468.
- Oritani, T., Fukuhara, N., Okajima, T., Kitamura, F., & Ohsaka, T. (2004). Electrochemical and spectroscopic studies on electron-transfer reaction between novel water-soluble tetrazolium salts and a superoxide ion. *Inorganica Chimica Acta*, 357(2), 436-442.
- Otsuki, S., Nonaka, T., Takashima, N., Qian, W., Ishihara, A., Imai, T., & Kabe, T. (2000). Oxidative Desulfurization of Light Gas Oil and Vacuum Gas Oil by Oxidation and Solvent Extraction. *Energy and Fuels*, 14(6), 1232-1239.
- Paduszyński, K., & Domańska, U. (2011). Limiting activity coefficients and gas-liquid partition coefficients of various solutes in piperidinium ionic liquids: Measurements and LSER calculations. *Journal of Physical Chemistry B*, 115(25), 8207-8215.
- Pawelec, B., Navarro, R. M., Campos-Martin, J. M., & Fierro, J. L. G. (2011). Retracted article: Towards near zero-sulfur liquid fuels: a perspective review. *Catalysis Science & Technology*, 1(1), 23-42.
- Pereiro, A. B., Legido, J. L., & Rodríguez, A. (2007). Physical properties of ionic liquids based on 1-alkyl-3-methylimidazolium cation and hexafluorophosphate as anion and temperature dependence. *Journal of Chemical Thermodynamics*, 39(8), 1168-1175.
- Pozo-Gonzalo, C., Torriero, A. A., Forsyth, M., MacFarlane, D. R., & Howlett, P. C. (2013). Redox chemistry of the superoxide ion in a phosphonium-based ionic liquid in the presence of water. *The Journal of Physical Chemistry Letters*, 4(11), 1834-1837.
- Randström, S., Appetecchi, G. B., Lagergren, C., Moreno, A., & Passerini, S. (2007). The influence of air and its components on the cathodic stability of N-butyl-N-methylpyrrolidinium bis(trifluoromethanesulfonyl)imide. *Electrochimica Acta*, 53(4), 1837-1842.
- Regueira, T., Lugo, L., & Fernández, J. (2012). High pressure volumetric properties of 1-ethyl-3-methylimidazolium ethylsulfate and 1-(2-methoxyethyl)-1-methylpyrrolidinium bis(trifluoromethylsulfonyl)imide. *The Journal of Chemical Thermodynamics*, 48, 213-220.

- René, A., Hauchard, D., Lagrost, C., & Hapiot, P. (2009). Superoxide Protonation by Weak Acids in Imidazolium Based Ionic Liquids. *The Journal of Physical Chemistry B*, *113*(9), 2826-2831.
- Revelli, A. L., Mutelet, F., & Jaubert, J. N. (2010). Extraction of benzene or thiophene from n-Heptane using ionic liquids. NMR and thermodynamic study. *Journal of Physical Chemistry B*, *114*(13), 4600-4608.
- Robinson, P. (2006). Petroleum Processing Overview. In C. Hsu & P. Robinson (Eds.), *Practical Advances in Petroleum Processing* (pp. 1-78): Springer New York.
- Robinson, P., & Dolbear, G. (2006). Hydrotreating and Hydrocracking: Fundamentals. In C. Hsu & P. Robinson (Eds.), *Practical Advances in Petroleum Processing* (pp. 177-218, 176, 110, 123): Springer New York.
- Rodríguez-Cabo, B., Francisco, M., Soto, A., & Arce, A. (2012). Hexyl dimethylpyridinium ionic liquids for desulfurization of fuels. Effect of the position of the alkyl side chains. *Fluid Phase Equilibria*, *314*, 107-112.
- Rodríguez-Cabo, B., Soto, A., & Arce, A. (2013). Desulfurization of fuel-oils with [C2mim][NTf2]: A comparative study. *Journal of Chemical Thermodynamics*, *57*, 248-255.
- Rodríguez, H., Francisco, M., Soto, A., & Arce, A. (2010). Liquid-liquid equilibrium and interfacial tension of the ternary system heptane+thiophene+1-ethyl-3-methylimidazolium bis(trifluoromethanesulfonyl)imide. *Fluid Phase Equilibria*, *298*(2), 240-245.
- Rogers, E. I., Huang, X.-J., Dickinson, E. J. F., Hardacre, C., & Compton, R. G. (2009). Investigating the Mechanism and Electrode Kinetics of the Oxygen/Superoxide (O₂/O₂^{•-}) Couple in Various Room-Temperature Ionic Liquids at Gold and Platinum Electrodes in the Temperature Range 298–318 K. *The Journal of Physical Chemistry C*, *113*(41), 17811-17823.
- Rogers, R. D., & Seddon, K. R. (2003). Ionic liquids--solvents of the future? *Science*, *302*(5646), 792-793.
- Rogošić, M., Sander, A., Kojić, V., & Vuković, J. P. (2016). Liquid-liquid equilibria in the ternary and multicomponent systems involving hydrocarbons, thiophene or pyridine and ionic liquid (1-benzyl-3-methylimidazolium bis(trifluoromethylsulfonyl)imide). *Fluid Phase Equilibria*, *412*, 39-50.
- Saito, I., Otsuki, T., & Matsuura, T. (1979). The reaction of superoxide ion with vitamin K1 and its related compounds. *Tetrahedron Letters*, *20*(19), 1693-1696.
- Salerno, A., Ceriani, V., & Perillo, I. A. (1997). Nucleophilic addition to substituted 1H-4,5-dihydroimidazolium salts. *Journal of Heterocyclic Chemistry*, *34*(3), 709-716.
- Sawyer, D. T. (1991). *Oxygen Chemistry*: Oxford University Press, USA.

- Sawyer, D. T., Calderwood, T. S., Johlman, C. L., & Wilkins, C. L. (1985). Oxidation by superoxide ion of catechols, ascorbic acid, dihydrophenazine, and reduced flavins to their respective anion radicals. A common mechanism via a combined proton-hydrogen atom transfer. *The Journal of Organic Chemistry*, 50(9), 1409-1412.
- Sawyer, D. T., & Roberts Jr, J. L. (1966). Electrochemistry of oxygen and superoxide ion in dimethylsulfoxide at platinum, gold and mercury electrodes. *Journal of Electroanalytical Chemistry (1959)*, 12(2), 90-101.
- Sawyer, D. T., & Seo, E. T. (1977). One-electron mechanism for the electrochemical reduction of molecular oxygen. *Inorganic Chemistry*, 16(2), 499-501.
- Sawyer, D. T., & Valentine, J. S. (1981). How super is superoxide? *Accounts of Chemical Research*, 14(12), 393-400.
- Schwenke, K. U., Herranz, J., Gasteiger, H. A., & Piana, M. (2015). Reactivity of the Ionic Liquid Pyr14TFSI with Superoxide Radicals Generated from KO₂ or by Contact of O₂ with Li₇Ti₅O₁₂. *Journal of the Electrochemical Society*, 162(6), A905-A914.
- Schwenke, K. U., Meini, S., Wu, X., Gasteiger, H. A., & Piana, M. (2013). Stability of superoxide radicals in glyme solvents for non-aqueous Li-O₂ battery electrolytes. *Physical Chemistry Chemical Physics*, 15(28), 11830-11839.
- Seki, S., Kobayashi, T., Kobayashi, Y., Takei, K., Miyashiro, H., Hayamizu, K., . . . Umabayashi, Y. (2010). Effects of cation and anion on physical properties of room-temperature ionic liquids. *Journal of Molecular Liquids*, 152(1-3), 9-13.
- Shah, M. R., Anantharaj, R., Banerjee, T., & Yadav, G. D. (2013). Quaternary (liquid + liquid) equilibria for systems of imidazolium based ionic liquid + thiophene + pyridine + cyclohexane at 298.15 K: Experiments and quantum chemical predictions. *Journal of Chemical Thermodynamics*, 62, 142-150.
- Silva, T. P., Paixão, S. M., Teixeira, A. V., Roseiro, J. C., & Alves, L. (2013). Optimization of low sulfur carob pulp liquor as carbon source for fossil fuels biodesulfurization. *Journal of Chemical Technology and Biotechnology*, 88(5), 919-923.
- Silvester, D. S., Rogers, E. I., Barrosse-Antle, L. E., Broder, T. L., & Compton, R. G. (2008). The electrochemistry of simple inorganic molecules in room temperature ionic liquids. *Journal of the Brazilian Chemical Society*, 19(4), 611-620.
- Sobota, M., Dohnal, V., & Vrbka, P. (2009). Activity coefficients at infinite dilution of organic solutes in the ionic liquid 1-ethyl-3-methyl-imidazolium nitrate. *Journal of Physical Chemistry B*, 113(13), 4323-4332.
- Soleimani, M., Bassi, A., & Margaritis, A. (2007). Biodesulfurization of refractory organic sulfur compounds in fossil fuels. *Biotechnology advances*, 25(6), 570-596.

- Song, C. (2003). An overview of new approaches to deep desulfurization for ultra-clean gasoline, diesel fuel and jet fuel. *Catalysis Today*, 86(1–4), 211-263.
- Song, C., & Zhang, J. (2008). Electrocatalytic oxygen reduction reaction *PEM fuel cell electrocatalysts and catalyst layers* (pp. 89-134): Springer.
- Speight, J. G. (1999). *The Desulfurization of Heavy Oils and Residua*: Taylor & Francis.
- Srivastava, V. C. (2012). An evaluation of desulfurization technologies for sulfur removal from liquid fuels. *RSC Advances*, 2(3), 759-783.
- Strbac, S., & Adžić, R. (1996). The influence of pH on reaction pathways for O₂ reduction on the Au (100) face. *Electrochimica Acta*, 41(18), 2903-2908.
- Takata, T., Kim, Y. H., & Oae, S. (1979). Reaction of organic sulfur compounds with superoxide anion: oxidation of disulfides, thioisulfates and thioisulfonates to their sulfinic and sulfonic acids. *Tetrahedron Letters*, 20(9), 821-824.
- Tam, P. S., Kittrell, J. R., & Eldridge, J. W. (1990). Desulfurization of fuel oil by oxidation and extraction. 1. Enhancement of extraction oil yield. *Industrial & Engineering Chemistry Research*, 29(3), 321-324.
- Tang, M. C.-Y., Wong, K.-Y., & Chan, T. H. (2005). Electrosynthesis of hydrogen peroxide in room temperature ionic liquids and in situ epoxidation of alkenes. *Chemical Communications*(10), 1345-1347.
- Tao, R., Tamas, G., Xue, L., Simon, S. L., & Quitevis, E. L. (2014). Thermophysical Properties of Imidazolium-Based Ionic Liquids: The Effect of Aliphatic versus Aromatic Functionality. *Journal of Chemical & Engineering Data*, 59(9), 2717-2724.
- Tariq, M., Freire, M. G., Saramago, B., Coutinho, J. A. P., Lopes, J. N. C., & Rebelo, L. P. N. (2012). Surface tension of ionic liquids and ionic liquid solutions. *Chemical Society Reviews*, 41(2), 829-868.
- Tian, Y., Meng, X., & Shi, L. (2014). Removal of dimethyl disulfide via extraction using imidazolium-based phosphoric ionic liquids. *Fuel*, 129, 225-230.
- Tian, Y., Yao, Y., Zhi, Y., Yan, L., & Lu, S. (2015). Combined Extraction–Oxidation System for Oxidative Desulfurization (ODS) of a Model Fuel. *Energy and Fuels*, 29(2), 618-625.
- Tokuda, H., Hayamizu, K., Ishii, K., Susan, M. A. B. H., & Watanabe, M. (2005). Physicochemical Properties and Structures of Room Temperature Ionic Liquids. 2. Variation of Alkyl Chain Length in Imidazolium Cation. *The Journal of Physical Chemistry B*, 109(13), 6103-6110.
- Troy, D. B., Remington, J. P., & Beringer, P. (2006). *Remington: The Science and Practice of Pharmacy*: Lippincott Williams & Wilkins.

- Varma, N. R., Ramalingam, A., & Banerjee, T. (2011). Experiments, correlations and COSMO-RS predictions for the extraction of benzothiophene from n-hexane using imidazolium-based ionic liquids. *Chemical Engineering Journal*, 166(1), 30-39.
- Verdía, P., González, E. J., Rodríguez-Cabo, B., & Tojo, E. (2011). Synthesis and characterization of new polysubstituted pyridinium-based ionic liquids: Application as solvents on desulfurization of fuel oils. *Green Chemistry*, 13(10), 2768-2776.
- Villagrán, C., Aldous, L., Lagunas, M. C., Compton, R. G., & Hardacre, C. (2006). Electrochemistry of phenol in bis{(trifluoromethyl)sulfonyl}amide ([NTf₂]⁻) based ionic liquids. *Journal of Electroanalytical Chemistry*, 588(1), 27-31.
- Wang, J. L., Zhao, D. S., & Li, K. X. (2012). Extractive desulfurization of gasoline using ionic liquid based on CuCl. *Petroleum Science and Technology*, 30(23), 2417-2423.
- Wasserscheid, P., & Welton, T. (2008). *Ionic liquids in synthesis* (Vol. 1): Wiley Online Library.
- Wauquier, J.-P. (2001). *Petroleum Refining. Volume 2 , Separation Processes*: Editions OPHRYS.
- Wauquier, J. P. (1995). *Petroleum Refining. Volume 1, Process Flowsheets*: Atlasbooks Dist Serv.
- Welton, T. (1999). Room-temperature ionic liquids. Solvents for synthesis and catalysis. *Chemical reviews*, 99(8), 2071-2084.
- White, M. G., & Paris, D. T. (1981). Control of breathing atmospheres using alkali metal superoxides: an engineering analysis.
- Wilfred, C. D., Kiat, C. F., Man, Z., Bustam, M. A., Mutalib, M. I. M., & Phak, C. Z. (2012). Extraction of dibenzothiophene from dodecane using ionic liquids. *Fuel Processing Technology*, 93(1), 85-89.
- Wilkes, J. S. (2002). A short history of ionic liquids - from molten salts to neoteric solvents. *Green Chemistry*, 4(2), 73-80.
- Wilkes, J. S., & Zaworotko, M. J. (1992). Air and water stable 1-ethyl-3-methylimidazolium based ionic liquids. *Journal of the Chemical Society, Chemical Communications*(13), 965-967.
- Williams, B. H. (1928). The thermal decomposition of hydrogen peroxide in aqueous solutions. *Transactions of the Faraday Society*, 24(0), 245-255.
- Wlazło, M., & Marciniak, A. (2012). Activity coefficients at infinite dilution and physicochemical properties for organic solutes and water in the ionic liquid 4-(2-methoxyethyl)-4-methylmorpholinium trifluorotris(perfluoroethyl)phosphate. *Journal of Chemical Thermodynamics*, 54, 366-372.

- Xiong, J., Zhu, W., Ding, W., Yang, L., Zhang, M., Jiang, W., . . . Li, H. (2015). Hydrophobic mesoporous silica-supported heteropolyacid induced by ionic liquid as a high efficiency catalyst for the oxidative desulfurization of fuel. *RSC Advances*, 5(22), 16847-16855.
- Yeon, S.-H., Kim, K.-S., Choi, S., Lee, H., Kim, H. S., & Kim, H. (2005). Physical and electrochemical properties of 1-(2-hydroxyethyl)-3-methyl imidazolium and N-(2-hydroxyethyl)-N-methyl morpholinium ionic liquids. *Electrochimica Acta*, 50(27), 5399-5407.
- Yu, F.-L., Wang, Y.-Y., Liu, C.-Y., Xie, C.-X., & Yu, S.-T. (2014). Oxidative desulfurization of fuels catalyzed by ammonium oxidative-thermoregulated bifunctional ionic liquids. *Chemical Engineering Journal*, 255, 372-376.
- Zawadzki, M., Niedzicki, L., Wiczorek, W., & Domańska, U. (2013). Estimation of extraction properties of new imidazolidine anion based ionic liquids on the basis of activity coefficient at infinite dilution measurements. *Separation and Purification Technology*, 118(0), 242-254.
- Zhang, B., Jiang, Z., Li, J., Zhang, Y., Lin, F., Liu, Y., & Li, C. (2012). Catalytic oxidation of thiophene and its derivatives via dual activation for ultra-deep desulfurization of fuels. *Journal of Catalysis*, 287, 5-12.
- Zhang, D., Okajima, T., Matsumoto, F., & Ohsaka, T. (2004a). Electroreduction of dioxygen in 1-n-alkyl-3-methylimidazolium tetrafluoroborate room-temperature ionic liquids. *Journal of the Electrochemical Society*, 151(4), D31-D37.
- Zhang, J., Zhang, Q., Qiao, B., & Deng, Y. (2007). Solubilities of the gaseous and liquid solutes and their thermodynamics of solubilization in the novel room-temperature ionic liquids at infinite dilution by gas chromatography. *Journal of Chemical and Engineering Data*, 52(6), 2277-2283.
- Zhang, M., Zhu, W., Li, H., Xun, S., Ding, W., Liu, J., . . . Wang, Q. (2014). One-pot synthesis, characterization and desulfurization of functional mesoporous W-MCM-41 from POM-based ionic liquids. *Chemical Engineering Journal*, 243, 386-393.
- Zhang, M., Zhu, W., Xun, S., Xiong, J., Ding, W., Li, M., . . . Li, H. (2015). Enhanced Oxidative Desulfurization of Dibenzothiophene by Functional Mo-Containing Mesoporous Silica. *Chemical Engineering & Technology*, 38(1), 117-124.
- Zhang, S., Lu, X., Zhou, Q., Li, X., Zhang, X., & Li, S. (2009). *Ionic Liquids: Physicochemical Properties*: Elsevier Science.
- Zhang, S., Zhang, Q., & Zhang, Z. C. (2004b). Extractive desulfurization and denitrogenation of fuels using ionic liquids. *Industrial and Engineering Chemistry Research*, 43(2), 614-622.

- Zhang, S., Zhang, Q., & Zhang, Z. C. (2004c). Extractive desulfurization and denitrogenation of fuels using ionic liquids. *Industrial & Engineering Chemistry Research*, 43(2), 614-622.
- Zhang, S., & Zhang, Z. C. (2002a). Novel properties of ionic liquids in selective sulfur removal from fuels at room temperature. *Green Chemistry*, 4(4), 376-379.
- Zhang, S., & Zhang, Z. C. (2002b). Selective sulfur removal from fuels using ionic liquids at room temperature. *Prepr Pap Am Chem Soc Div Fuel Chem 2002b*, 47, 449-451.
- Zhao, C., Bond, A. M., Compton, R. G., O'Mahony, A. M., & Rogers, E. I. (2010). Modification and Implications of Changes in Electrochemical Responses Encountered When Undertaking Deoxygenation in Ionic Liquids. *Analytical Chemistry*, 82(9), 3856-3861.
- Zhao, D., Sun, Z., Li, F., Liu, R., & Shan, H. (2008). Oxidative Desulfurization of Thiophene Catalyzed by (C₄H₉)₄NBr·2C₆H₁₁NO Coordinated Ionic Liquid. *Energy & Fuels*, 22(5), 3065-3069.
- Zheng, W., Mohammed, A., Hines, L. G., Xiao, D., Martinez, O. J., Bartsch, R. A., . . . Quitevis, E. L. (2011). Effect of Cation Symmetry on the Morphology and Physicochemical Properties of Imidazolium Ionic Liquids. *The Journal of Physical Chemistry B*, 115(20), 6572-6584.
- Zhou, Z. B., Matsumoto, H., & Tatsumi, K. (2005). Low-Melting, Low-Viscous, Hydrophobic Ionic Liquids: Aliphatic Quaternary Ammonium Salts with Perfluoroalkyltrifluoroborates. *Chemistry-A European Journal*, 11(2), 752-766.
- Zhou, Z. B., Matsumoto, H., & Tatsumi, K. (2006). Cyclic quaternary ammonium ionic liquids with perfluoroalkyltrifluoroborates: synthesis, characterization, and properties. *Chemistry-A European Journal*, 12(8), 2196-2212.
- Zigah, D., Wang, A., Lagrost, C., & Hapiot, P. (2009). Diffusion of Molecules in Ionic Liquids/Organic Solvent Mixtures. Example of the Reversible Reduction of O₂ to Superoxide. *The Journal of Physical Chemistry B*, 113(7), 2019-2023.

LIST OF PUBLICATIONS AND PAPERS PRESENTED

Publications

- **Published**

1. Maan Hayyan, **Muna Hassan Ibrahim**, Adeeb Hayyan, Inas M. AlNashef, Mohd Ali Hashim. Facile Route for Fuel Desulfurization Using Generated Superoxide Ion in Ionic Liquids. *Industrial & Engineering Chemistry Research*, 54(49), 12263-12269, 2015 (ISI-Cited Publication) (Impact factor: 2.587, Q1).

- **In Press**

1. Maan Hayyan, **Muna Hassan Ibrahim**, Adeeb Hayyan, Mohd Ali Hashim. Investigating the Long-Term Stability and Kinetics of Superoxide Ion in Dimethyl Sulfoxide Containing Ionic Liquids and the Application of Thiophene Compound Destruction. *Brazilian Journal of Chemical Engineering* (ISI-Cited Publication) (Impact factor: 1.043, Q3).

- **Under Review**

1. **Muna Hassan Ibrahim**, Maan Hayyan, Mohd Ali Hashim, Adeeb Hayyan. The Role of Ionic Liquids in Desulfurization of Fuels: A Review. *Renewable & Sustainable Energy Reviews*. (ISI-Cited Publication) (Impact factor: 5.901, Q1).
2. **Muna Hassan Ibrahim**, Maan Hayyan, Mohd Ali Hashim, Adeeb Hayyan. Thermophysical properties of Piperidinium, Ammonium, Pyrrolidinium and Morpholinium Ionic liquids paired with Bis(trifluoromethylsulfonyl)imide anion. *Arabian Journal of Chemistry*. (ISI-Cited Publication) (Impact factor: 3.725, Q1).

- **In Preparation**

Muna Hassan Ibrahim, Maan Hayyan, Mohd Ali Hashim, Adeeb Hayyan. In Situ Generation of Peroxide Dianion Using Reduction of Dioxygen in Ionic Liquids. *Electrochemistry Communications*. (ISI-Cited Publication) (Impact factor: 4.847, Q1).

Conferences

1. **Muna Hassan Ibrahim**, Maan Hayyan, Mohd Ali Hashim, Adeeb Hayyan. Investigating the Stability of Superoxide Ion in 1-Butyl-1-methylpyrrolidinium bis(trifluoromethylsulfonyl)imide Ionic Liquid. 2nd International Conference on Purity, Utility Reaction and Environmental Research (PURE2015), 9-11 November, Kuala Lumpur, Malaysia, 2015.
2. **Muna Hassan Ibrahim**, Maan Hayyan, Mohd Ali Hashim. Investigating the Stability of Superoxide ion in Imidazolium-based Ionic Liquids, International Conference on Purity, Utility Reaction and Environmental Research-PURE2014, 19-21 December, Putrajaya, Malaysia, 2014.
3. **Muna Hassan Ibrahim**, Maan Hayyan, Mohd Ali Hashim. Potential Applications of Ionic Liquids in the Desulfurization of Fuels, International Conference on Ionic Liquids 2013 (ICIL 13), 11-13 December, Langkawi Island, Malaysia, 2013.

Exhibitions

1. BRONZE MEDAL. Mohd Ali Hashim, Maan Hayyan, Adeeb Hayyan, **Muna Hassan Ibrahim**. A Novel Desulphurization Method Using In-Situ Generated Superoxide Ion in Ionic Liquids. Malaysia Technology Expo (MTE), Putra World Trade Centre, February 2016, Malaysia

2. Ionic Liquids and Eutectic Solvents for Advanced Processing Technology of Fuel and Biofuel. BioMalaysia, Kuala Lumpur Convention Centre, 31 May 2016-02 June 2016, Malaysia.

Other Achievements and Research Interests

Conference Host/ Emcee

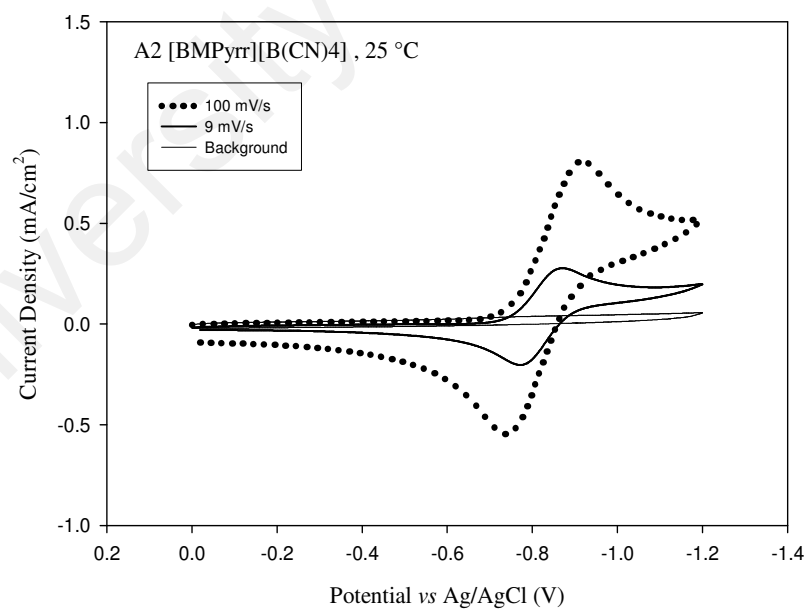
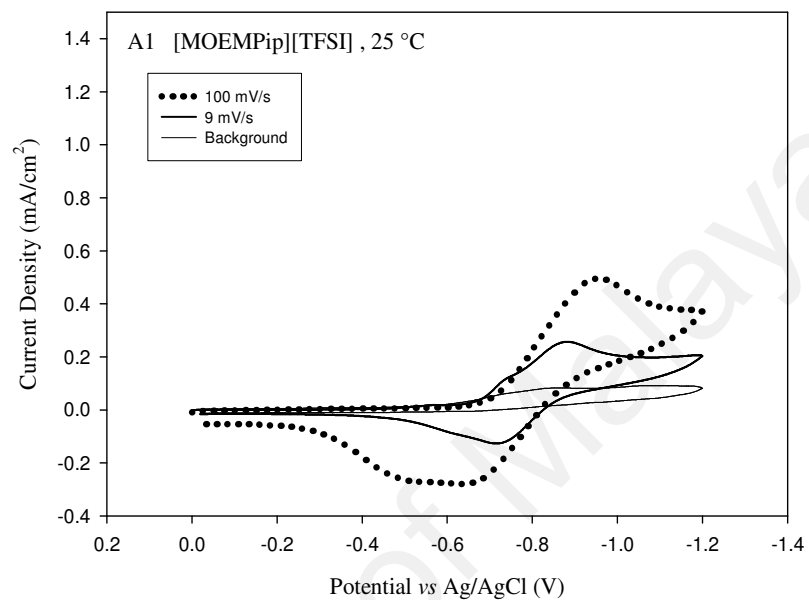
1. 2nd International Conference on Purity, Utility Reaction and Environmental Research (PURE2015), 9-11 November, Kuala Lumpur, Malaysia, 2015.
2. International Conference on Purity, Utility Reaction and Environmental Research (PURE2014), 19-21 December, Putrajaya, Malaysia, 2014.

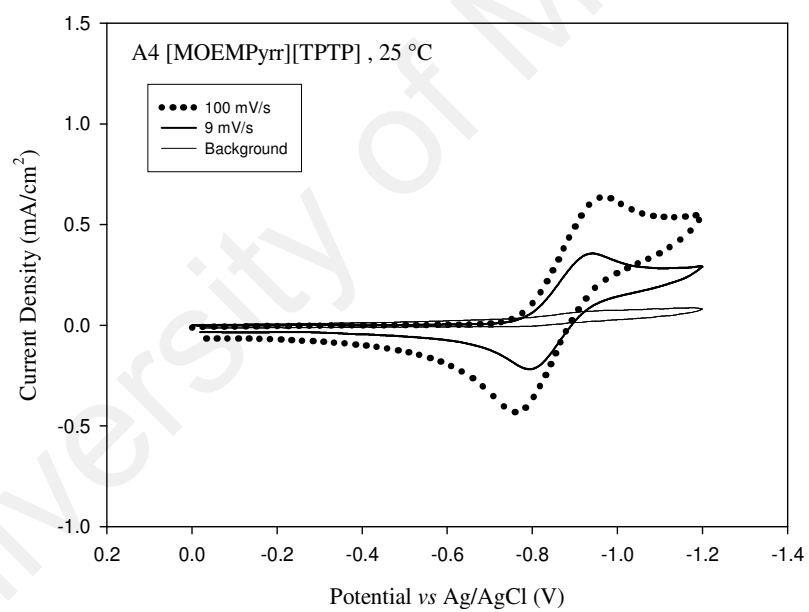
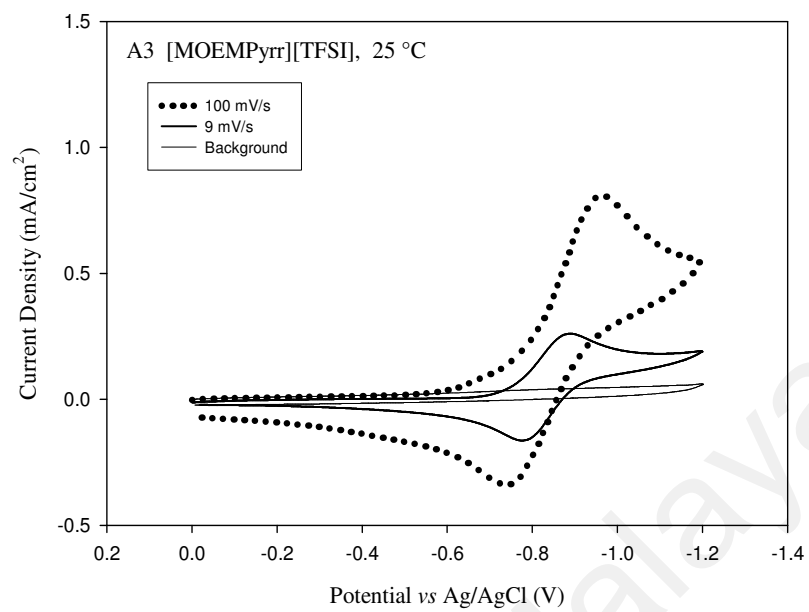
University of Malaya

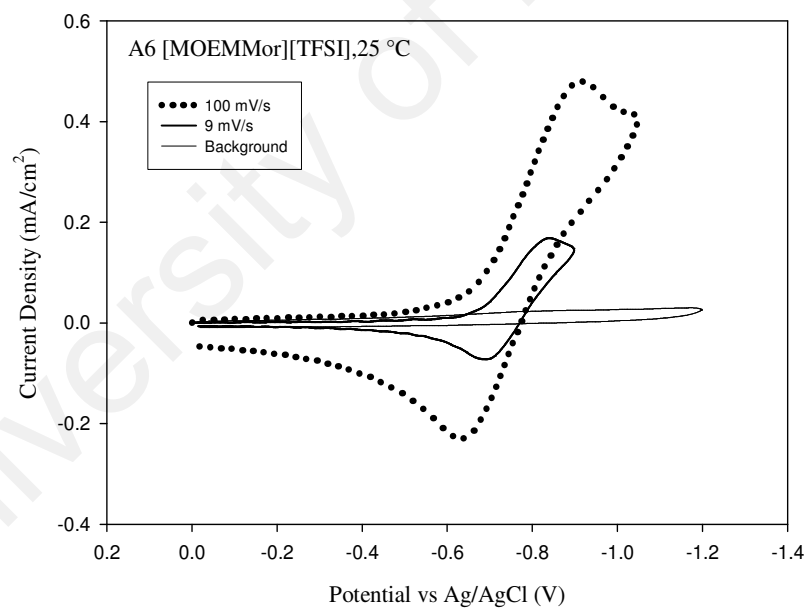
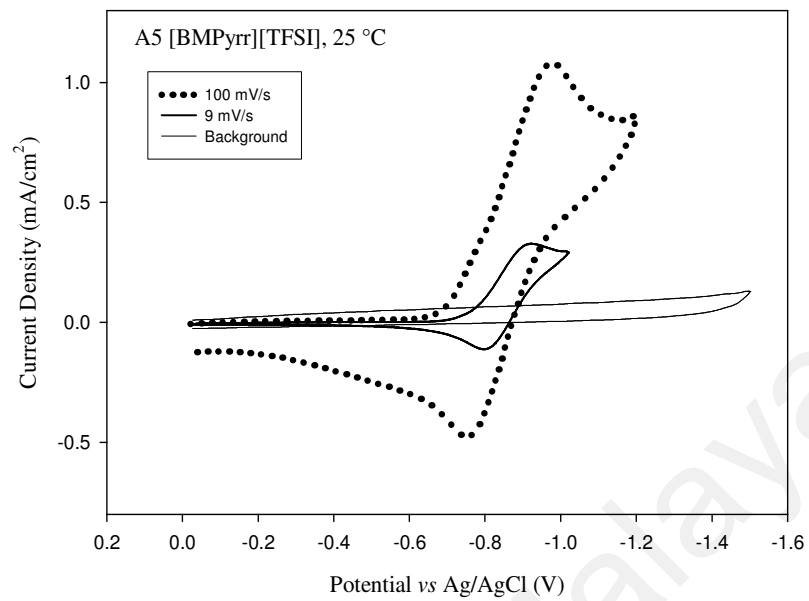
APPENDICES

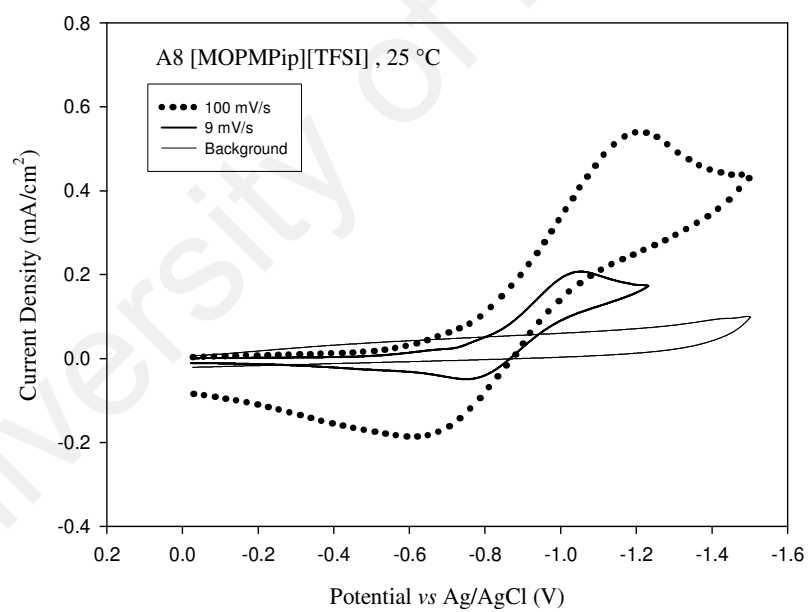
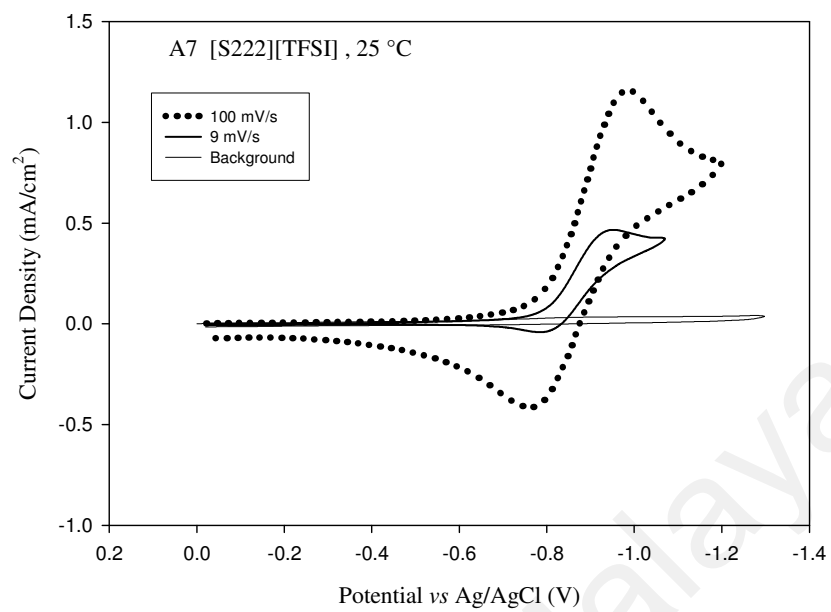
APPENDIX A

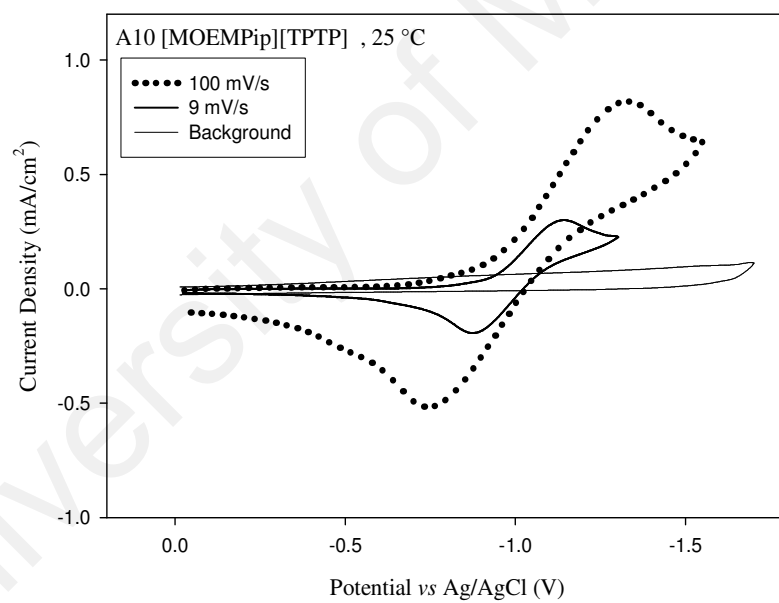
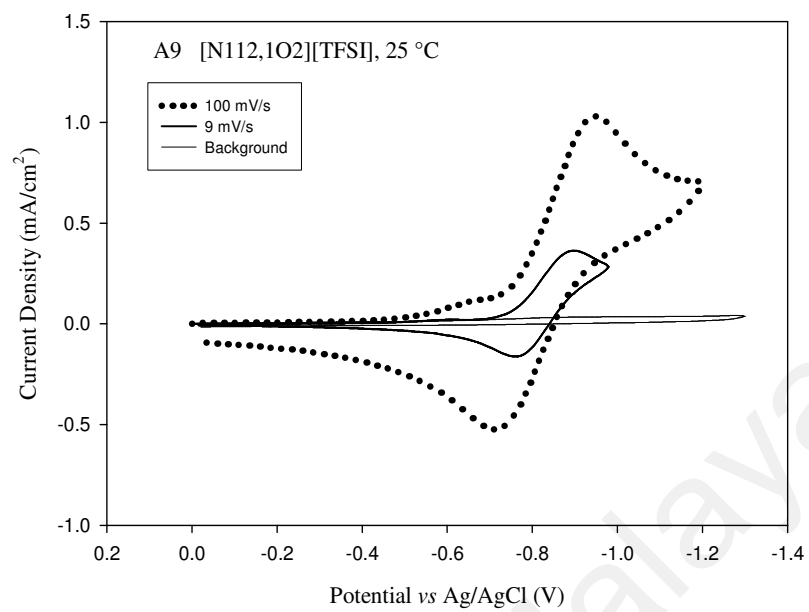
Cyclic Voltammograms of $O_2^{\bullet-}$ in ILs

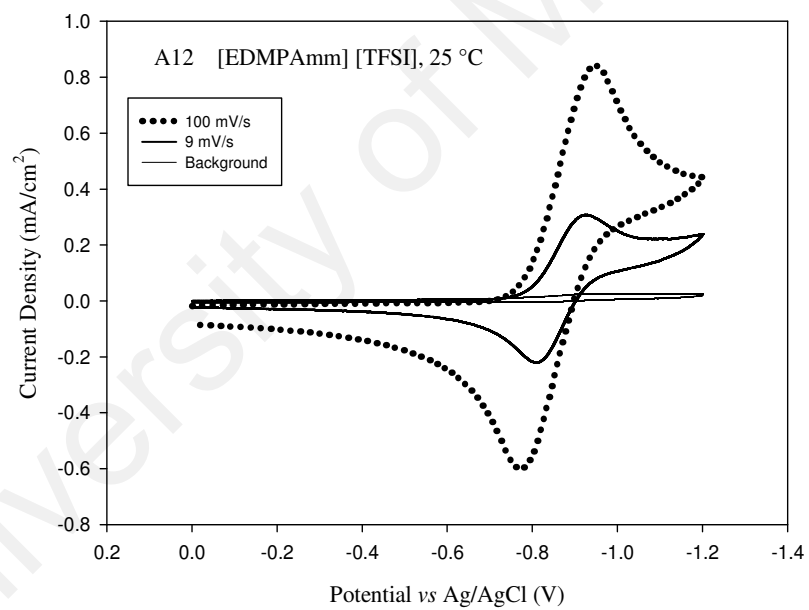
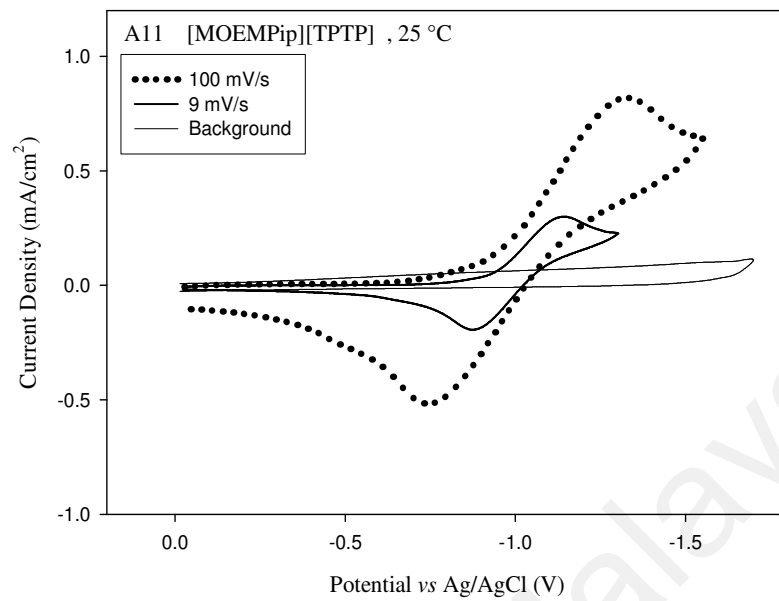


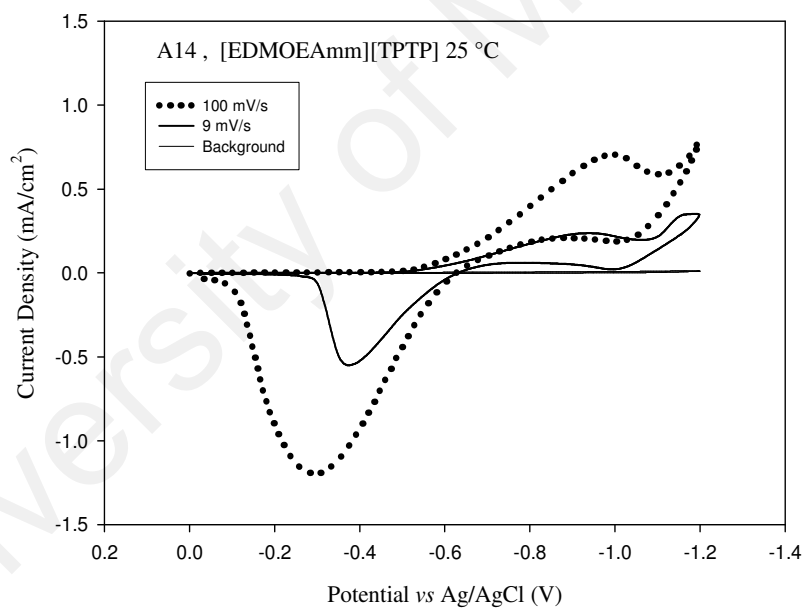
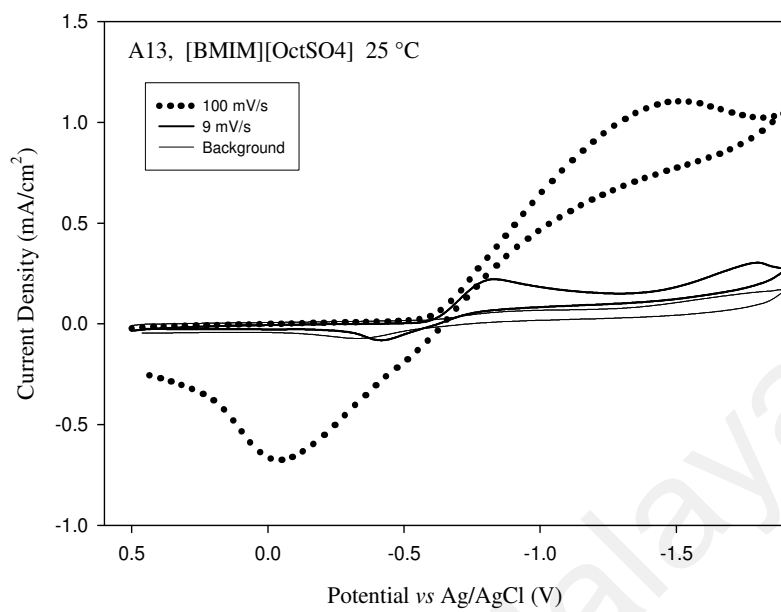


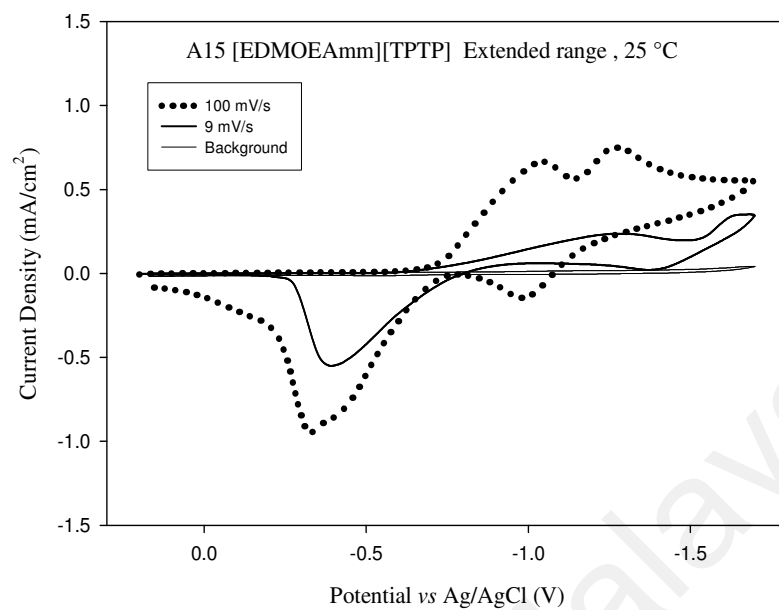










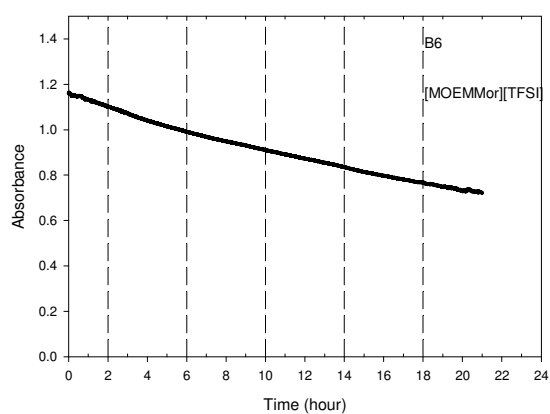
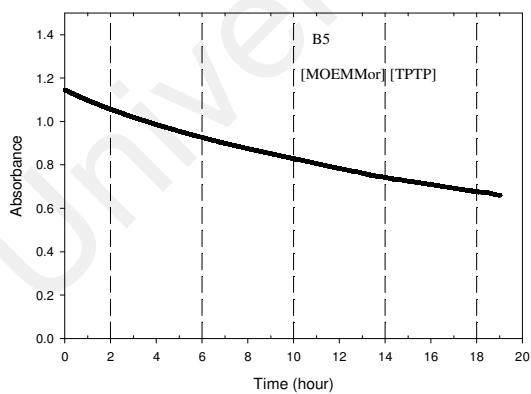
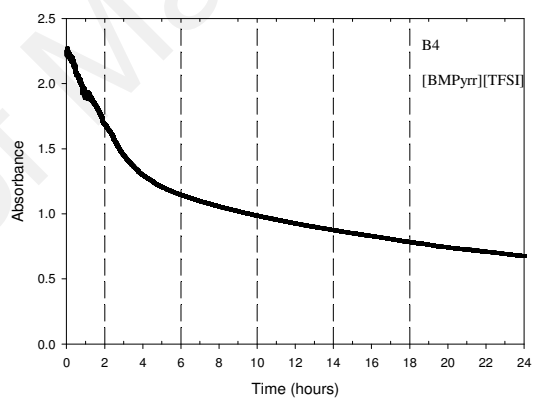
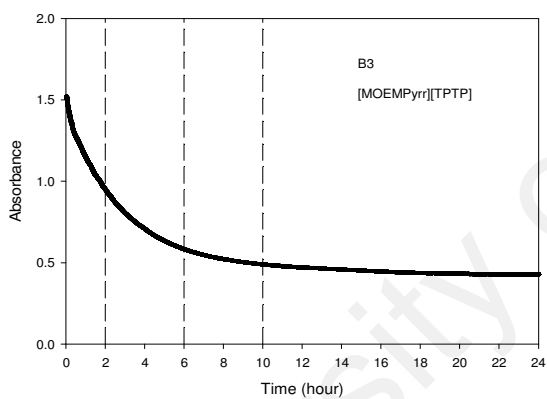
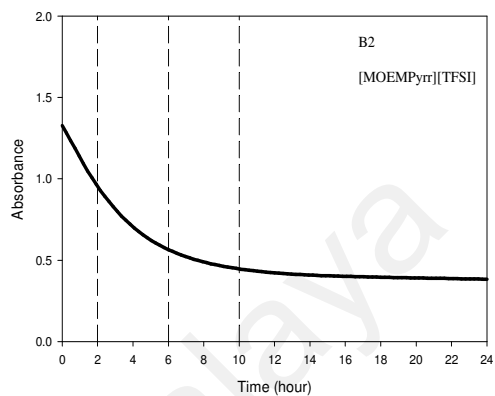
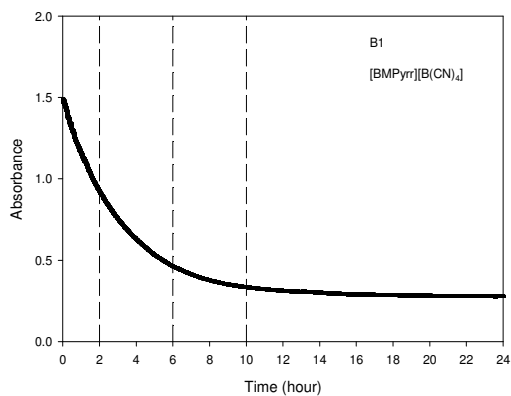


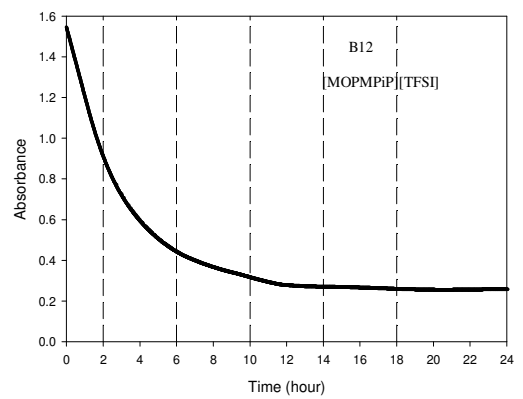
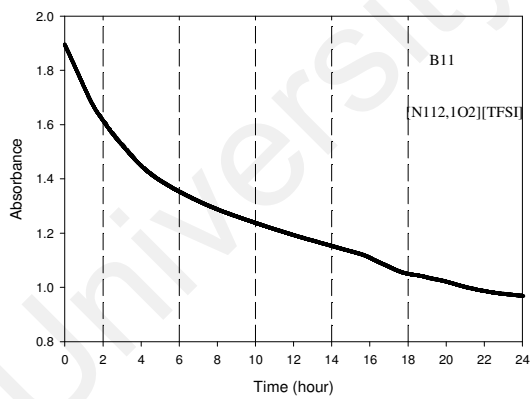
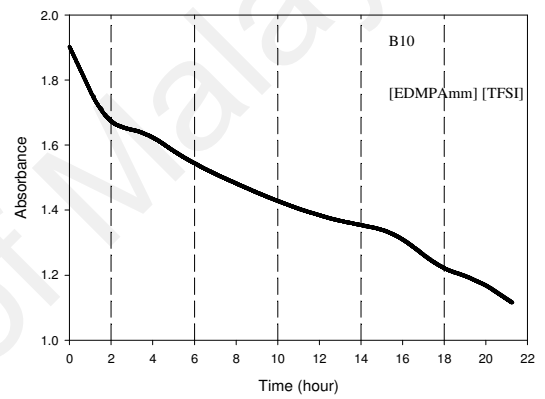
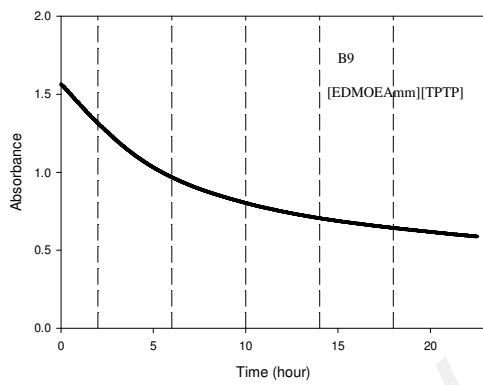
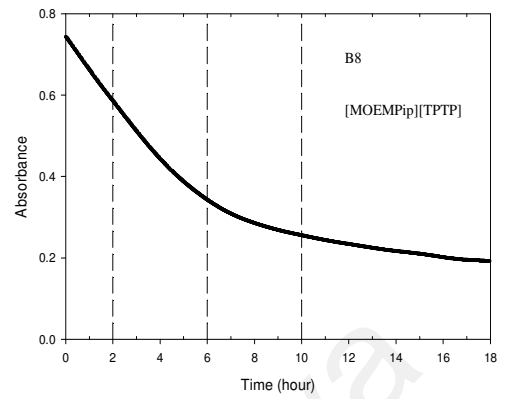
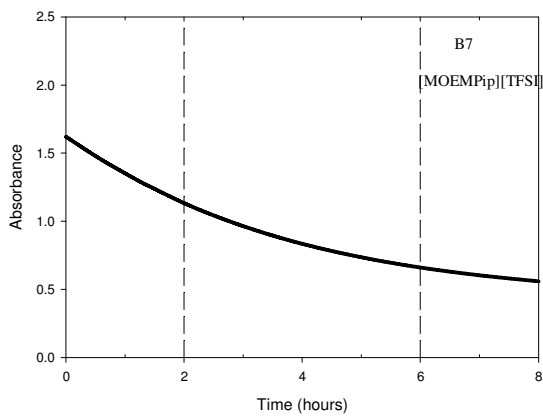
Figures A1-A15: Cyclic voltammograms of $O_2^{\bullet-}$ generation in ILs at 25 °C, and scan rates of 9 and 100 mV/s using GC macro-electrode.

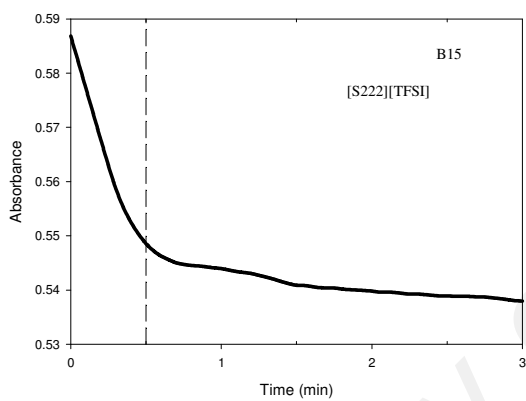
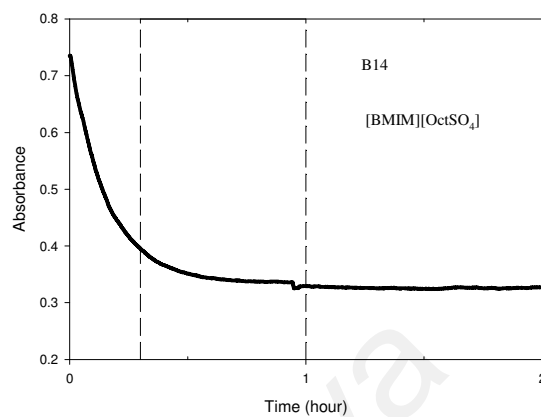
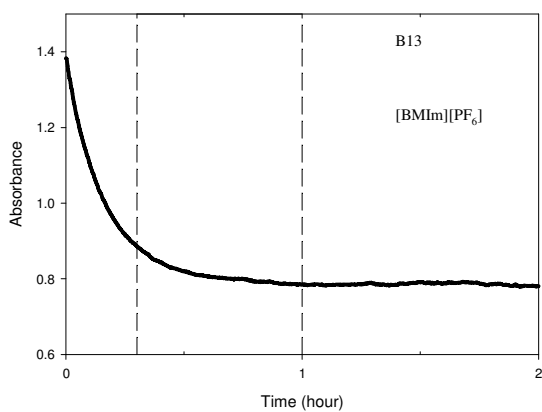
University of Malaya

APPENDIX B

The Long Term Stability Experiments of $O_2^{\bullet-}$







Figures B1-B15: The change of superoxide absorbance peak with time.

Table B.2: ILs sorted in order of stability (based on increasing k_1) in first two hours

IL	0-2 hrs* (s ⁻¹)	R ²
N-Methoxyethyl-N-methylmorpholinium bis(trifluoromethylsulfonyl)imide	7.049×10^{-6}	0.984
4-(2-Methoxyethyl)-4-methylmorpholinium tris(pentafluoroethyl)trifluorophosphate	1.124×10^{-5}	0.999
Ethyl-dimethyl-propylammonium bis(trifluoromethylsulfonyl) imide	2.51×10^{-5}	0.949
Ethyl-dimethyl-(2-methoxyethyl)ammonium tris(pentafluoroethyl)trifluorophosphate	2.526×10^{-5}	0.962
N-Ethyl-N,N-dimethyl-2-methoxyethylammonium bis(trifluoromethylsulfonyl)imide	2.70×10^{-5}	0.93
1-Butyl-1-methylpyrrolidinium bis (trifluoromethylsulfonyl) imide	2.92×10^{-5}	0.991
1-(2-Methoxyethyl)-1-methylpiperidinium tris(pentafluoroethyl)trifluorophosphate	3.360×10^{-5}	0.995
1-(2-Methoxyethyl)-1-methylpiperidinium bis(trifluoromethylsulfonyl)imide	4.985×10^{-5}	0.997
1-(2-Methoxyethyl)-1-methylpyrrolidinium bis(trifluoromethylsulfonyl)imide	4.99×10^{-5}	0.984
1-(2-Methoxyethyl)-1-methylpyrrolidinium tris(pentafluoroethyl)trifluorophosphate	6.02×10^{-5}	0.987
1-Butyl-1-methylpyrrolidinium tetracyanoborate	6.64×10^{-5}	0.998
1-(3-Methoxypropyl)-1-methylpiperidinium bis (trifluoromethylsulfonyl) imide	8.31×10^{-5}	0.999
1-Butyl-3-methylimidazolium hexafluorophosphate	4.02×10^{-4} *	0.963
1-Butyl-3-methyl-imidazolium octylsulfate	5.81×10^{-4} *	0.97
Triethylsulfonium bis(trifluoromethylsulfonyl)imide	2.645×10^{-3} *	0.944

*Imidazolium 0-20 min, sulfonium 0-30 s

Table B.3: Rate constant of O₂^{•-} in DMSO containing ILs with morpholinium based cation

IL		0-2 hrs	2- 6 h	6 -10 h	10- 14 h	1- 18 h	18 -24 h	Overall
4-(2-Methoxyethyl)-4-methylmorpholinium tris(pentafluoroethyl)trifluorophosphate	k ₁ s ⁻¹	1.124×10 ⁻⁵	9.101×10 ⁻⁶	7.653×10 ⁻⁶	7.827×10 ⁻⁶	6.454×10 ⁻⁶	ss	7.850×10 ⁻⁶
	R ²	0.999	0.999	1.000	0.999	0.998	ss	
	k ₂ M ⁻¹ s ⁻¹	7.770×10 ⁻³	7.002×10 ⁻³	6.640×10 ⁻³	7.587×10 ⁻³	6.922×10 ⁻³	ss	7.014×10 ⁻³
	R ²	0.999	0.911	0.879	0.999	0.998	ss	0.998
N-Methoxyethyl-N-methylmorpholinium bis(trifluoromethylsulfonyl)imide	k ₁ s ⁻¹	7.049×10 ⁻⁶	7.449×10 ⁻⁶	5.776×10 ⁻⁶	5.867×10 ⁻⁶	5.914×10 ⁻⁶	ss	6.218×10 ⁻⁶
	R ²	0.984	0.997	0.999	0.999	0.998	ss	0.998
	k ₂ M ⁻¹ s ⁻¹	4.732×10 ⁻³	5.418×10 ⁻³	4.619×10 ⁻³	5.107×10 ⁻³	5.625×10 ⁻³	ss	5.231×10 ⁻³
	R ²	0.984	0.998	0.999	0.999	0.998	ss	0.999

Table B.4: Rate constant of O₂^{•-} in DMSO containing ILs with piperidinium based cation

IL		0-2 h	2- 6 h	6 -10 h	10- 14 h	14- 18 h	18 -24 h	Overall
1-(2-Methoxyethyl)-1-methylpiperidinium tris(pentafluoroethyl)trifluorophosphate	k ₁ s ⁻¹	3.360×10 ⁻⁵	3.819×10 ⁻⁵	1.951×10 ⁻⁵	ss	ss	ss	3.189×10 ⁻⁵
	R ²	0.995	0.999	0.982	ss	ss	ss	0.984
	k ₂ M ⁻¹ s ⁻¹	3.859×10 ⁻²	6.554×10 ⁻²	5.103×10 ⁻²	ss	ss	ss	5.975×10 ⁻²
	R ²	0.995	0.998	0.991	ss	ss	ss	0.994
1-(3-Methoxypropyl)-1-methylpiperidinium bis(trifluoromethylsulfonyl)imide	k ₁ s ⁻¹	8.305×10 ⁻⁵	4.858×10 ⁻⁵	2.130×10 ⁻⁵	ss	ss	ss	4.280×10 ⁻⁵
	R ²	0.999	0.992	0.982	ss	ss	ss	0.942
	k ₂ M ⁻¹ s ⁻¹	5.361×10 ⁻²	6.138×10 ⁻²	4.375×10 ⁻²	ss	ss	ss	5.539×10 ⁻²
	R ²	0.995	1.000	0.985	ss	ss	ss	0.995
1-(2-Methoxyethyl)-1-methylpiperidinium bis(trifluoromethylsulfonyl)imide	k ₁ s ⁻¹	4.985×10 ⁻⁵	3.746×10 ⁻⁵	2.280×10 ⁻⁵	ss	ss	ss	3.723×10 ⁻⁵
	R ²	0.997	0.995	0.997	ss	ss	ss	0.983
	k ₂ M ⁻¹ s ⁻¹	2.804×10 ⁻²	3.362×10 ⁻²	2.857×10 ⁻²	ss	–	–	3.211×10 ⁻²
	R ²	0.996	1.000	0.999	ss	–	–	0.999

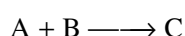
APPENDIX C Derivation of Equations Used to Obtain Pseudo 1st Order and Pseudo 2nd Order

Models

The derivation of the equations used to obtain the pseudo 1st order and pseudo 2nd order models is shown in below:

The reaction is assumed to be either 1st or 2nd order, with respect to concentration of O₂^{•-}.

If A= O₂^{•-}, B is the IL cations and C is the product



The reaction kinetics can be determined from the concentration of superoxide ions vs time graph determined from Absorbance vs time using the UV-vis

The IL was assumed to be added in excess so that its concentration can be assumed to be constant, hence the reaction may be assumed to be pseudo 1st or 2nd order (Troy et al., 2006). This is called the isolation method (Arnaut et al., 2006).

Here rate is defined as the rate of disappearance of O₂^{•-}

$$r_{C_A} = k_A C_A^a C_B^b$$

If $C_B \gg C_A$, C_B can be assumed to be constant

$$r_{C_A} = [k_A C_B^b] C_A^a$$

If $k_{obs} = [k_A C_B^b]$

$$r_{C_A} = k_{obs} C_A^a$$

The kinetics of the reaction between O₂^{•-} and the studied ILs was studied. Both the pseudo 1st order and pseudo 2nd order models were used. The reaction is assumed to be either 1st (a=1) or 2nd (a=2) order with respect to O₂^{•-}.

First order	Second Order
$r_{C_A} = k_A C_A$	$r_{C_A} = k_A C_A^2$
$\frac{dC_A}{dt} = k_A C_A$	$\frac{dC_A}{dt} = k_A C_A^2$
$\int \frac{dC_A}{dt} = \int k_A C_A$	$\int \frac{dC_A}{dt} = \int k_A C_A^2$
$\int \frac{1}{C_A} dC_A = \int k_A dt$	$\int \frac{1}{C_A^2} dC_A = \int k_A dt$
$\ln(C_A) = k_A t + C$	$-\frac{1}{C_A} = k_A t + C$
	$\frac{1}{C_A} = -k_A t + C$

The plots of $\ln(C_A) = k_A t + C$ and $\frac{1}{C_A} = -k_A t + C$ are tested, the graph with the greater R^2

value is concluded to be the most likely reaction order.